이학박사학위논문

진핵생물의 전령RNA 꼬리에 관한 전사체 수준의 연구

Transcriptome-wide studies on eukaryotic mRNA tail

2016년 8월

서울대학교 대학원

생명과학부

임재철

Abstract

Transcriptome-wide studies on eukaryotic mRNA tail

Jaechul Lim
School of Biological Sciences
The Graduate School
Seoul National University

Eukaryotic mRNA is subject to intensive post-transcriptional modifications, which critically influences mRNA stability and translatability. Newly synthesized mRNA acquires a 7-methlyguanosine cap at the 5′ end and polyadenosine tail at the 3′ end. In addition to such canonical modifications, recent studies have revealed untemplated nucleotide additions such as U-tail and G-tail, base modifications including N6-methyladenosine and pseudouridylation, and A-to-I editing, as epitranscriptomic signatures of mRNA.

To investigate RNA tailing at the genomic scale, I recently developed a method called TAIL-seq which accurately measures poly(A) tail length and 3′ end modifications. Interestingly, I discovered that mammalian cells carried median 50–100 nt of poly(A) tail and widespread uridylation and guanylation at the downstream of poly(A) tail. Moreover, U-tails were mainly found on short poly(A) tails (<~25 nt), implicating its role in mRNA turnover.

Uridylation has been observed on mRNAs in various species, yet its mechanism and significance remained unknown. By applying TAIL-seq, I identify TUT4 and TUT7 (TUT4/7), also known as ZCCHC11 and ZCCHC6, respectively, as mRNA uridylation enzymes in mammals. Uridylation readily occurs on deadenylated mRNAs in cells. Consistently, purified TUT4/7 selectively recognize and uridylate RNAs with short A tails (<~25 nt) in vitro. Moreover, PABPC1 antagonizes uridylation of polyadenylated mRNAs, contributing to the specificity for short A. In cells depleted of TUT4/7, the vast majority of

mRNAs lose the oligo-U tails, and their half-lives are extended. Suppression of mRNA decay factors leads to the accumulation of oligo-uridylated mRNAs. In line with this, microRNA induces uridylation of its targets, and TUT4/7 are required for enhanced decay of microRNA targets. My study explains the mechanism underlying selective uridylation of deadenylated mRNAs, and demonstrates a fundamental role of oligo-U-tail as a molecular mark for global mRNA decay.

Next, I report a new version of TAIL-seq (mRNA TAIL-seq or mTAIL-seq), which increases sequencing depth for mRNAs by ~1,000 fold compared to the previous version. Original version of TAIL-seq provided a various information, but its low sensitivity precluded its application to minute amounts of biological materials. With the improved method, I investigate the regulation of poly(A) tail in *Drosophila* oocytes and embryos. I find that maternal mRNAs are polyadenylated mainly during late oogenesis, prior to fertilization, and further modulated upon egg activation. Wispy, a noncanonical poly(A) polymerase, adenylates most maternal mRNAs with a few intriguing exceptions such as ribosomal protein transcripts. By comparing mTAIL-seq data to ribosome profiling data, I further find a strong coupling between poly(A) tail length and translational efficiency during egg activation. My data suggest that regulation of poly(A) tail in oocytes shapes the translatomic landscape of embryos, thereby directing the onset of animal development. By virtue of the high sensitivity, low cost, technical robustness, and broad accessibility, mTAIL-seq will be a potent tool to improve our understanding of mRNA tailing.

Taken together, I investigated mRNA tailings in eukaryotes by using sequencing methods that I develped, TAIL-seq and mTAIL-seq, and found their roles in the control of mRNA stability and translation.

Keywords: Post-transcriptional modification; High-throughput sequencing; TAIL-seq; mRNA tailing; Poly(A) tail; Uridylation; Cytoplasmic polyadenylation

Student ID: 2011-20349

Contents

List of Figures

List of Tables

List of Abbreviations

AEL	After Egg Laying
cDNA	complementary DNA
CDS	Coding Sequence
CPE	Cytoplasmic Polyadenylation Element
CPEB	CPE Binding protein
CRISPR	Clustered Regularly Interspaced Short Palindromic Repeats
DNA	Deoxyribonucleic Acid
GO	Gene Ontology
mRNA	messenger RNA
NMD	Nonsense-Mediated Decay
PABP	Poly(A) Bnding Protein
PAP	Poly(A) Polymerase
PAT	Poly(A) Tail
PCR	Polymerase Chain Reaction
RACE	Rapid Amplification of cDNA Ends
RNA	Ribonucleic Acid
rRNA	ribosomal RNA

RT	Reverse Transcription
snoRNA	small nucleolar RNA
snRNA	small nuclear RNA
TALEN	Transcription Activator-like Effector Nuclease
TE	Translational Efficiency
tRNA	transfer RNA
TUT	Terminal Uridylyl Transferase
UTP	Uridine Triphosphate
UTR	Untranslated Region

1. Introduction

1.1 Life cycle of mRNA

The fate of messenger RNAs (mRNAs) is exquisitely modulated by multiple layers of post-transcriptional regulation. In the nucleus, pre-mRNAs undergo three processing steps for their maturation: 5′ capping, splicing, and 3′ processing and polyadenylation (Figure 1.1). Once mRNAs are exported to the cytoplasm, mRNAs are associated with cytoplasmic poly(A) binding proteins (PABPCs) and translational machinery to produce proteins (Figure 1.1) (Norbury, 2013; Weill et al., 2012). During the process, transcripts failed to become functionally competent are targeted to surveillance system (Houseley & Tollervey, 2009). For instance, as a quality control mechanism, nonsense-mediated decay (NMD) eliminates prematurely terminated mRNAs to prevent an unproductive translation (Schoenberg & Maquat, 2012). After translation is finished, the bulk of mRNAs are subject to the first step of decay initiated by poly(A) tail shortening, called deadenylation (Figure 1.1) (Garneau et al., 2007). If the length of poly(A) tails decreases to a certain threshold, either of two decay pathways – the 5′-3′ or the 3′-5′ pathway which are not mutually exclusive – is activated to degrade transcripts (Figure 1.1) (Garneau et al., 2007).

1.2 mRNA tailing in eukaryotes

The 3′ termini of nascent mRNAs are generated by endonucleolytic cleavage (Norbury, 2013). Soon afterwards, the poly(A) tails are processively added by canonical poly(A) polymerase (PAP) and associated with poly(A) binding proteins (PABPs), which is known to stabilize mRNA and facilitate translation (Figure 1.1) (Weill et al., 2012). In addition to the canonical PAP, many noncanonical PAPs have been reported to carry out nontemplated nucleotide additions (uridylation or adenylation) which affect mRNA turnover and translation (Table 1.1) (Martin & Keller, 2007; Norbury, 2013).

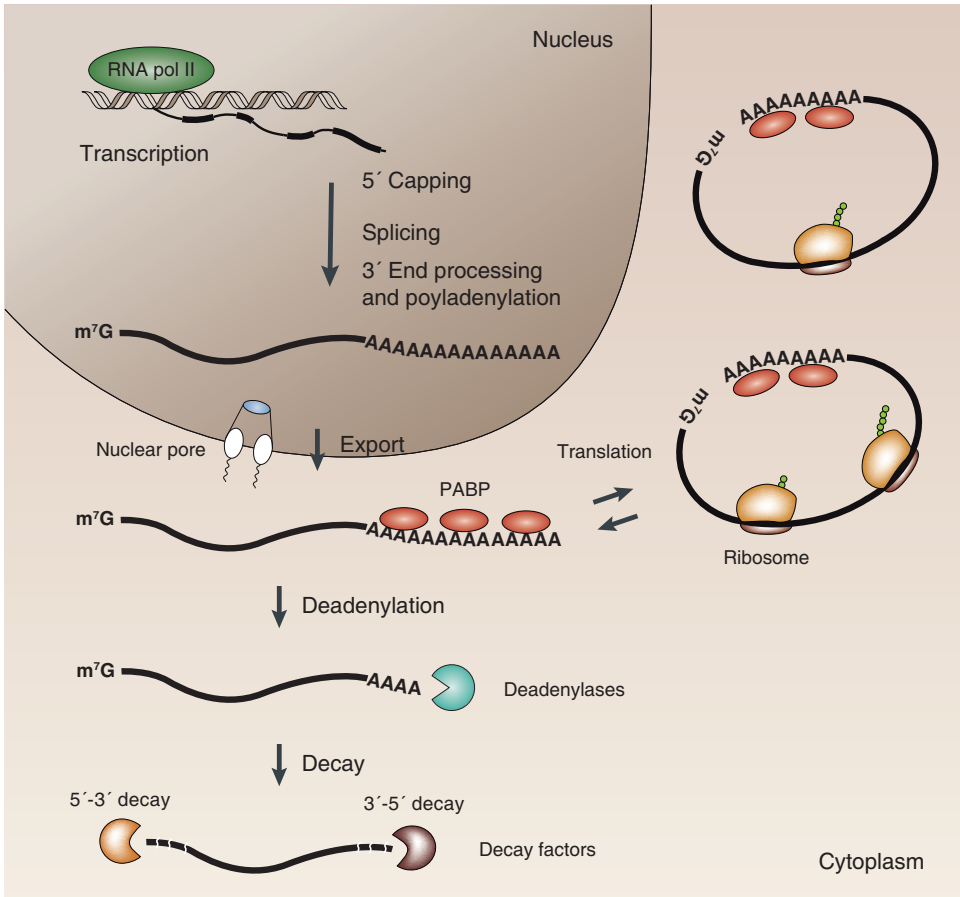

Figure 1.1 Life cycle of mRNA.

	Species	Enzyme	Reference
Poly(A)$^+$ mRNAs	*S. pombe*	Cid1	(Rissland et al., 2007; Rissland & Norbury, 2009)
	A. thaliana	URT1	(Sement et al., 2013)
	A. nidulans	CutA and CutB*	(Morozov et al., 2010, 2012)
	mammals	unknown	
Poly(A)$^-$ mRNAs (histone mRNA)	*H. sapiens*	TUT4 (TUT1/3)	(Mullen & Marzluff, 2008; Schmidt et al., 2011; Su et al., 2013)
miRNA-directed cleavage products	*A. thaliana*	HESO1	(Shen & Goodman, 2004; Ren et al., 2014)
	M. musculus	unknown	(Shen & Goodman, 2004)

Table 1.1 mRNA uridylating enzymes in eukaryotes. *Mixed tailing with C and U.

In fission yeast, Cid1 has been described as the first terminal uridylyl transferase (TUT) which attaches U residues to poly(A) tails of several mRNAs (Rissland et al., 2007; Rissland & Norbury, 2009). Similarly, a homolog of Cid1, URT1 in *Arabidopsis* was reported to uridylate decapped mRNAs (Sement et al., 2013). In *Aspergillus nidulans*, CutA and CutB, noncanonical PAPs, catalyze mixed tailing with cytidines and uridines (Morozov et al., 2010, 2012). Uridylation was also found on human replication-dependent histone mRNAs that lack a poly(A) tail (Mullen & Marzluff, 2008). For histone mRNAs, TUT1 (also known as MTPAP/PAPD1) and TUT3 (also known as PAPD5/TRF4-2) were initially reported (Mullen & Marzluff, 2008), but recent studies revealed that TUT4 (also known as ZCCHC11) is a responsible enzyme for uridylation of histone mRNAs (Schmidt et al., 2011; Su et al., 2013). Enzymes that carry out uridylation of poly(A)$^+$ mRNAs in mammals have been uncharacterized yet.

Apart from poly(A) tailed mRNAs, miRNA-directed cleavage products (5′ fragments) in plants and mammalian cells were also known to be uridylated (Shen & Goodman, 2004). In plants, HESO1 (HEN1 suppressor 1), which is a miRNA nucleotidyl transferase, uridylates cleaved products to facilitate their degradation (Ren et al., 2014). An enzyme for uridylation of mammalian 5′ fragments remains elusive.

In *Xenopus*, *Drosophila*, and mouse, elongation of A-tails, called cytoplasmic polyadenylation has been extensively studied(Mendez & Richter, 2001; Richter, 2007; Salles et al., 1994). A noncanonical PAP, TUT2 (also known as GLD-2/PAPD4) adds long adenosine tail to deadenylated mRNAs stored in the cytoplasm (Kwak et al., 2004; Norbury, 2013). In neurons, oocytes and early embryos where new transcription is limited, deadenylated mRNAs are not degraded, but reused upon stimulation by cytoplasmic polyadenylation (D'Ambrogio et al., 2013; Weill et al., 2012).

1.3 TAIL-seq: Transcriptome-wide determination of poly(A) tail length and 3′ end modification

Technically, transcriptome-wide investigation of the 3′ extremity of mRNA (3′-terminome) has been infeasible because of difficulties associated with sequencing homopolymers. Deep

sequencing technologies have not been able to read homopolymers of longer than ~30 nt, although Illumina sequencing chemistry deals with homopolymeric sequences relatively well (Bragg et al., 2013). Even in Illumina sequencer, however, fluorescent signals from T stretches (which corresponds to the poly(A) tail in reverse orientation) tend to accumulate over cycle because of incomplete cleavage of T fluorophore (Ledergerber & Dessimoz, 2011). So, it was difficult to discern non-poly(T) sequences following poly(T), according to standard base calling algorithm. In addition, another global approach, microarray combined with differential elution from oligo(dT) column, has been often used to estimate the ratio of long and short poly(A) tails, however the resolution and accuracy were highly limited (Cui et al., 2013; Du & Richter, 2005; Meijer et al., 2007; Novoa et al., 2010). Therefore, current knowledge is restricted to studies from individual genes which were carried by low-throughput methodologies such as northern blotting and RT-PCR (Norbury, 2013; Salles et al., 1999).

Moreover, in practice, detection of 3′ termini of mRNA was hampered by relative scarcity of mRNA. Highly abundant non-coding RNAs such as rRNAs and snRNAs overwhelm cDNA library unless poly(A)$^+$ mRNAs are selectively enriched. Although the enrichment of mRNAs using poly(A) tail is a conventional way, it is not suitable for detecting 3′-terminome because oligo(dT) pull-down introduces bias towards long poly(A) tail and splint ligation can preclude the non-A sequences at the very 3′ end of poly(A) tail. So, despite the importance, the information of actual sequences of 3′ end remains obscure.

Overcoming the challenges, I recently developed a sequencing technique named TAIL-seq to determine the 3′ end sequences of transcriptome in collaboration with Dr. Hyeshik Chang (Chang et al., 2014b). TAIL-seq has several main features compared to the common RNA-seq. First, TAIL-seq removes rRNAs and small non-coding RNAs (<200 nt) by rRNA depletion and size fractionation, respectively (Figure 1.2[1]). Enrichment of mRNAs by oligo(dT) is not used in TAIL-seq. Second, the 3′ adaptor is directly ligated to RNAs before RNA fragmentation to preserve the sequence information of 3′ end. Third, 3′ adaptor ligated RNAs are partially digested by RNase T1 which cleaves selectively after G residues. Fourth, two biotin residues in the 3′ adaptor enable a streptavidin purification

[1]Chang, H., Lim, J., Ha, M., & Kim, V. N. (2014b). Tail-seq: Genome-wide determination of poly(a) tail length and 3' end modifications. Mol Cell, 53(6), 1044–52.

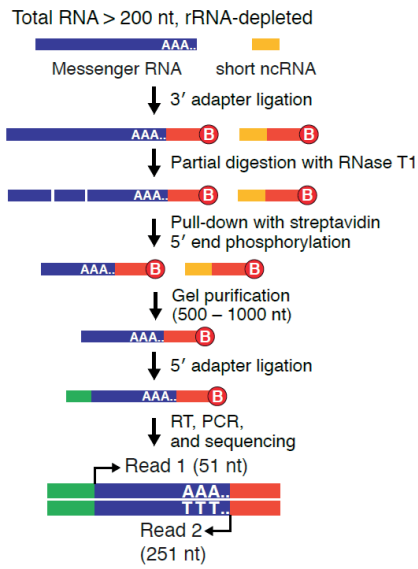

Figure 1.2 Experimental procedure of TAIL-seq.

of the 3′-most fragments. Fifth, the 3′ adaptor contains 15 nt of random sequences which improve sequencing performance by diversifying sequence composition in initial cycles of read 2. The degenerate sequences also serve as a duplication filter to eliminate PCR amplification artifacts. Sixth, TAIL-seq library is sequenced on Illumina platform in paired-end to yield 51 nt from the 5′ end (read 1), which is used to identify the transcript and 231 nt from the 3′ end (read 2), used for 3′ end sequence determination. Seventh, Dr. Hyeshik Chang developed a new algorithm that is specialized in detecting signal transition between poly(T) and non-T sequences (Figure 1.3[2]). Looking at the raw images from the sequencer, he noticed that the signal from T homopolymers decreases while non-T signals increase once the cycle reaches non-T region. He adopted a machine learning algorithm to detect the position of transition from T stretches (poly[A] tail) to heterogeneous sequences (3′ UTR) and precisely measured poly(A) tail length.

TAIL-seq is the first method that provides global measurement of poly(A) length and 3′ end modification of mRNAs (Chang et al., 2014b). In designing the TAIL-seq, I intended to be as comprehensive as possible, which allowed us to cover the complex 3′

[2]Chang, H., Lim, J., Ha, M., & Kim, V. N. (2014b). Tail-seq: Genome-wide determination of poly(a) tail length and 3' end modifications. Mol Cell, 53(6), 1044–52.

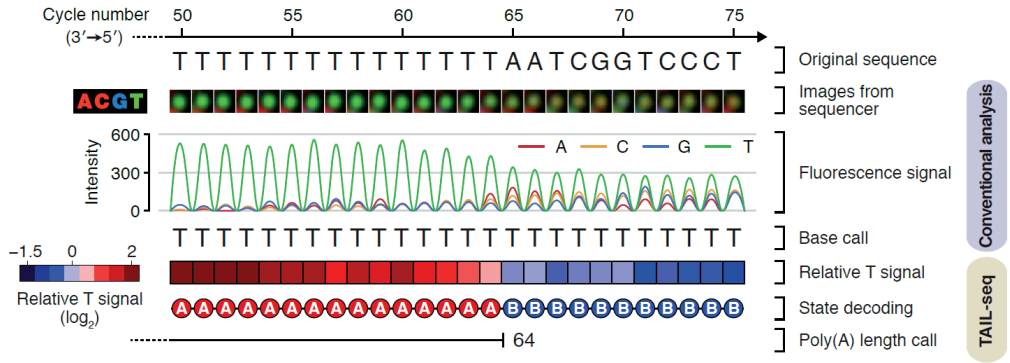

Figure 1.3 Analysis procedure for poly(A) tail length measurement.

terminome including uridylation, guanylation, and endonucleolytic cleavage sites. In future studies, current version of TAIL-seq can be modified further in order to focus on particular types of 3′ termini in greater depth with lower cost. In addition, it will be exciting to identify the enzymes involved in mRNA tailing and endonucleolytic cleavage event, and to understand underlying mechanisms and biological significance of them. To this end, TAIL-seq would be a valuable tool to tackle various questions regarding mRNA life cycle: the dynamics of mRNA deadenylation, cytoplasmic polyadenylation, translation, and decay. Especially, in specialized biological contexts, such as in neuronal synapse, late oogenesis, early embryogenesis, and circadian rhythm will be of great subjects to study where cytoplasmic polyadenylation is known to play a crucial role in translational activation (D'Ambrogio et al., 2013; Weill et al., 2012).

2. Uridylation marks mRNA for degradation

2.1 Background

RNA tailing (non-templated nucleotide addition to the 3′ end of RNA) is one of the most frequent types of RNA modification, with a deep evolutionary root and diverse molecular functions. In bacteria, adenylation of mRNA triggers RNA degradation whereas polyadenylation in eukaryotes increases the stability and translatability of mRNA (Dreyfus & Regnier, 2002). Tailing is catalyzed by a group of template-independent ribonucleotidyl transferases that contain DNA polymerase β-like nucleotidyl transferase domain (Aravind & Koonin, 1999). Apart from canonical poly(A) polymerases (PAPs) that generate poly(A) tail of mRNA, many noncanonical PAPs have been described from fission yeast to human (Martin & Keller, 2007; Norbury, 2013). Because some noncanonical PAPs catalyze uridylation instead of adenylation, noncanonical PAPs are also called terminal uridylyl transferases (TUTases or TUTs). Some PAPs/TUTs have more relaxed nucleotide specificity and carry out both uridylation and adenylation. Humans have seven noncanonical PAPs/TUTs with distinct substrate specificity and subcellular localization.

Uridylation of mRNA was initially noticed at the 3′ ends of miRNA-directed cleavage products in *Arabidopsis* and mammalian cells (Shen & Goodman, 2004). U tails were also detected on human replication-dependent histone mRNAs that lack a poly(A) tail (Mullen & Marzluff, 2008). Histone mRNAs are uridylated and degraded at the end of S phase or upon inhibition of DNA replication (Mullen & Marzluff, 2008). TUT4 (ZCCHC11) was reported to catalyze histone mRNA uridylation (Schmidt et al., 2011; Su et al., 2013), although two other TUTs (TUT1/MTPAP/PAPD1 and TUT3/PAPD5/TRF4-2) were proposed in an earlier study (Mullen & Marzluff, 2008). Uridylation induces rapid decay of histone mRNA through both the 5′–3′ degradation by XRN1, DCP2, and LSM1 and the 3′–5′ degradation by exosome and ERI1 (3′hExo) (Hoefig et al., 2013; Mullen & Marzluff, 2008; Slevin et al., 2014).

Interestingly, uridylation occurs not only on poly(A)-lacking mRNAs but also on poly(A)+ mRNAs, as shown first with the actin (*act1*) mRNA in fission yeast *S. pombe* (Rissland et al., 2007). When six mRNAs were examined by circularized rapid amplification of cDNA ends (cRACE) technique, all of them were found to bear short U-tails (usually one or two uridines) at the end of poly(A) tails albeit at varying frequencies, indicating that mRNA uridylation may be widespread in fission yeast (Rissland & Norbury, 2009). The stability of the *urg1* mRNA increased in a mutant lacking Cid1 which is one of the TUTs in fission yeast (Rissland et al., 2007; Rissland & Norbury, 2009). The uridylation frequency was enhanced in mutants defective of deadenylase and decapping enzyme (*ccr4*Δ and *dcp1-ts*). Based on these results, it was proposed that uridylation and deadenylation may act redundantly to induce decapping. A more recent study showed that *Arabidopsis* mRNAs are also subject to uridylation (Sement et al., 2013). Short uridyl residues (1–2 uridines) were detected on deadenylated, decapped mRNAs. The Cid1 homolog URT1 is required for uridylation. But, curiously, URT1 mutation did not have a major impact on mRNA turnover, and instead inhibited trimming of mRNA from the 3′ end (Sement et al., 2013), implying that uridylation may be necessary to establish the directionality (5′–3′) rather than to control the rate of mRNA decay. Therefore, although these observations are intriguing, it was unclear if uridylation has a conserved function across species and whether animal poly(A)$^+$ mRNAs are also uridylated. In addition, because previous studies examined a few individual mRNAs by RACE and small-scale cloning, it remained to be tested whether or not uridylation occurs globally and if the observed changes in uridylation and poly(A) length are statistically significant.

So as to investigate tail structures at the genomic scale, I recently developed a method called TAIL-seq which deep-sequences the 3′ most fragments of RNAs in collaboration with Dr. Hyeshik Chang (Chang et al., 2014b). The TAIL-seq protocol begins with removal of abundant noncoding RNAs such as rRNA, tRNA, snRNA, and snoRNA by affinity-based depletion and size fractionation. To avoid any bias against unconventional tails, TAIL-seq does not use splint ligation or oligo(dT) enrichment. The resulting RNA sample enriched with mRNA is subsequently ligated to the 3′ adaptor that contains biotin residues. Following partial fragmentation, the 3′ most fragments are purified using streptavidin beads, and ligated to the 5′ adaptor. Paired-end sequencing of the cDNA library yields 51

nt from the 5′ terminus of the fragment (to identify the transcript) and 231 nt from the 3′ terminus (to examine the tail sequences).

TAIL-seq provided us with a unique opportunity to investigate poly(A) tail length and additional 3′ modifications simultaneously at the genomic scale. Surprisingly, the vast majority of mRNAs are found to be subject to uridylation in mammals. Over 85 % of mRNAs are terminally uridylated at a frequency of higher than 1 % in both NIH 3T3 and HeLa cells(Chang et al., 2014b). Interestingly, U tails are found mainly on mRNAs with short A tails (<~25 nt), indicating that uridylation may occur following deadenylation. Furthermore, a negative correlation between uridylation frequency and mRNA half-life was detected, suggesting a role of uridylation in general mRNA decay.

Current model for eukaryotic mRNA decay pathway is mainly based on the pioneering genetic and biochemical studies in S. cerevisiae (Garneau et al., 2007; Houseley & Tollervey, 2009; Norbury, 2013; Parker & Song, 2004). Decay is generally initiated by deadenylation that is mediated by multiple deadenylases such as the Pan2-Pan3 complex and the Ccr4-Not complex. Subsequently, deadenylated mRNAs are subject to either of two major decay pathways. In the 5′–3′ decay pathway, the Lsm1–7 complex binds to the 3′ end of deadenylated mRNA and recruits the decapping complex (Dcp1/2) that removes 5′ cap structure. Subsequently, 5′ monophosphate-dependent exoribonuclease, Xrn1, digests mRNA processively. From the opposite orientation, a multi-subunit exosome complex degrades deadenylated mRNAs from the 3′ end. This model seems to apply generally to most, if not all, eukaryotic species. However, S. cerevisiae is unusual among eukaryotes in that it does not have any known TUT homolog with uridylation activity and that mRNAs in S. cerevisiae do not carry terminal U tails (Norbury, 2013). Thus, the current model for mRNA decay, particularly in mammals, may need to be revised to incorporate the recent findings of pervasive uridylation (Lee et al., 2014b).

In this study, I aimed to identify enzyme(s) that catalyze mRNA uridylation in mammals and understand the significance of uridylation in the mRNA decay pathway. I discover TUT4 and TUT7 as uridylyl transferases for poly(A)$^+$ mRNAs in humans and delineate in detail the action mechanism and molecular function of uridylation in the mRNA decay pathway. Based on these results, I propose a revised model for general mRNA decay in

mammals.

2.2 Results

2.2.1 TUT4 and TUT7 catalyze mRNA uridylation

In order to identify enzyme(s) responsible for mRNA uridylation, I took a candidate approach by depleting seven human TUTases (Figure 2.1). Because TUT2 (also known as GLD2 and PAPD4), TUT4 (ZCCHC11), and TUT7 (ZCCHC6) act redundantly in mono-uridylation of precursor of let-7 (pre-let-7) (Heo et al., 2012), I knocked down TUTases in two subgroups (TUT1/3/5/6 and TUT2/4/7) by transfecting siRNA mixtures into HeLa cells (Figure 2.2), and carried out TAIL-seq (Figure 2.3)[1]. Overall frequency of uridylation was quantified by dividing the read number of terminally uridylated mRNAs by that of total mRNAs. Because short A tails are preferentially uridylated (Chang et al., 2014b), uridylation frequency in short A tail range (5–25 nt) is shown. Interestingly, when TUT2/4/7 were depleted, terminal uridylation was significantly reduced while RNAi of TUT1/3/5/6 did not affect uridylation. To narrow down on individual TUTases, I generated knockout HeLa cell lines using TALENs (transcription activator-like effector nucleases) against the genes coding TUT2, TUT4, or TUT7 proteins (Figure 2.4). I observed a modest decrease of uridylation in both TUT4 and TUT7 knockout cells, but not in TUT2 knockout cells (Figure 2.5). Repeated attempts to generate double knockout of TUT4 and TUT7 by utilizing the TALEN and CRISPR/Cas9 (clustered regularly interspaced short palindromic repeats/CRISPR associated protein 9) systems have failed (Figure 2.6). Although genomic deletion was effectively introduced by the nucleases, mutant clones disappeared during clonal selection processes (Figure 2.6), which indicates that the combined activity of TUT4 and TUT7 is essential for cell viability. Of note, previous studies have shown that TUT4 and TUT7 are highly similar in their domain organization and activity in pre-miRNA uridylation (Heo et al., 2012; Liu et al., 2014; Thornton et al., 2012). Thus, TUT4 and TUT7 (TUT4/7) may act redundantly in mRNA uridylation as well as in pre-miRNA uridylation. To confirm this notion, I carried out simultaneous transient RNAi against TUT4/7 by

[1] In collaboration with Dr. Minju Ha and Dr. Hyeshik Chang

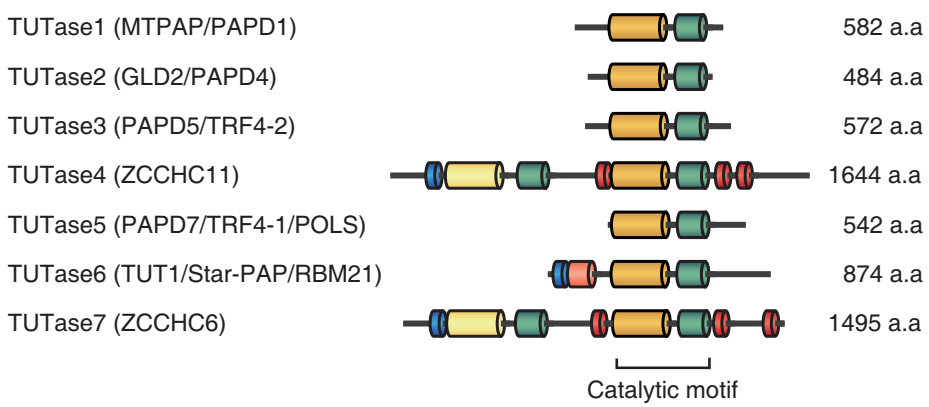

Figure 2.1 Domain organization of human TUTases. Yellow, nucleotidyl transferase domain; green, PAP-associated domain; light yellow, inactive nucleotidyl transferase domain due to sequence variations; blue, C2H2 zinc finger domain; red, CCHC zinc finger domain; pink, RNA recognition motif.

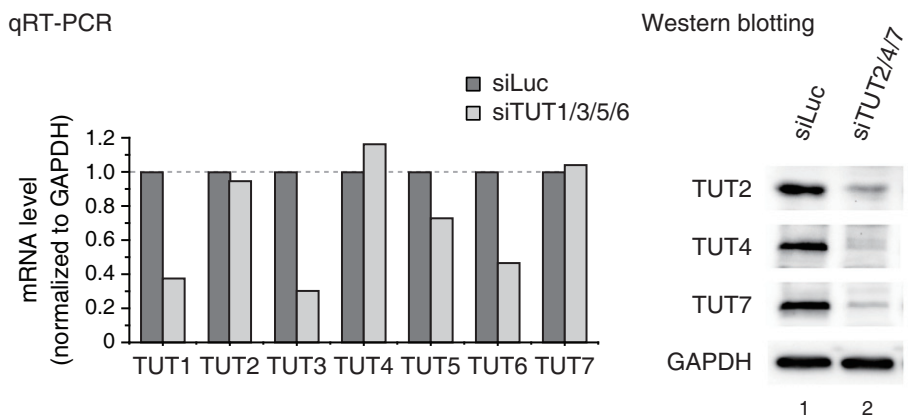

Figure 2.2 The level of seven TUTases after RNAi of TUT1/3/5/6 and TUT2/4/7, measured by qRT-PCR (left) and western blotting (right). *GAPDH* was used as a negative control in both qRT-PCR and western blotting.

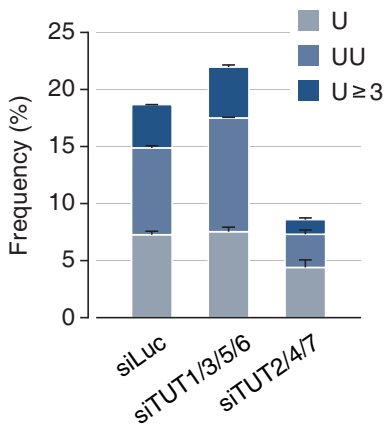

Figure 2.3 Uridylation frequency measured by small-scale TAIL-seq (with Illumina MiSeq) following RNAi of the indicated genes. Frequency (y-axis) is the fraction of uridylated reads among the total number of mRNA reads with short poly(A) tail (5–25 nt). Light blue refers to mono-uridylation (U), blue indicates di-uridylation (UU), and dark blue represents ≥ 3 uridines (U ≥ 3). Uridylation frequency significantly decreased in siTUT2/4/7 (P = 0.0378 for U; 0.0388 for UU; 0.0201 for U ≥ 3 by one-tailed t test). Error bar represents the standard error of the mean from two biologically independent replicates (n=2).

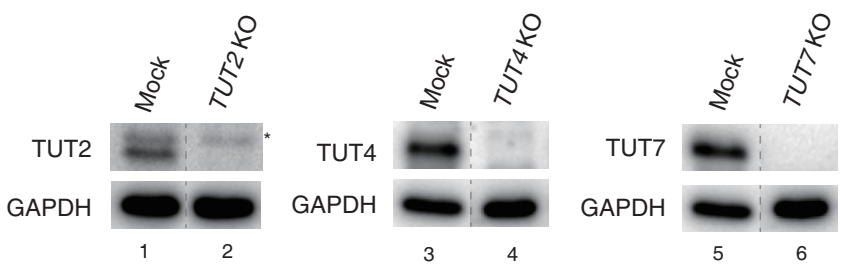

Figure 2.4 Validation of each knockout cell line by western blotting. An asterisk in TUT2 refers to a non-specific band. Dashed lines indicate discontinuous lanes from the same gel.

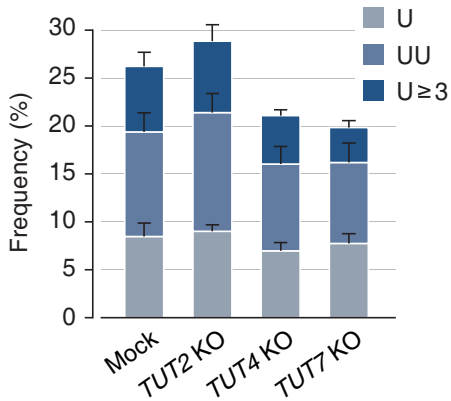

Figure 2.5 Uridylation frequency of mRNAs with short poly(A) tails (5–25 nt) measured by small-scale TAIL-seq in knockout HeLa cell lines. Uridylation frequency was reduced modestly in TUT4 and TUT7 knockout cells (P = 0.109 for U, 0.0273 for UU, 0.142 for U≥3 of TUT4 KO; P = 0.150 for U, 0.00685 for UU, 0.0713 for U ≥ 3 of TUT7 KO by one-tailed t test). Error bar indicates the standard error of the mean from two replicates.

transfecting siRNAs (Figures 2.10 and 2.7). The TUT4/7 knockdown cells looked largely normal and proliferated at a modestly reduced rate with a slight increase of apoptosis after 4 days of siRNA treatment (Figures 2.8 and 2.9)[2]. Under this condition, uridylation of mRNA was significantly reduced when both TUT4 and TUT7 are depleted (Figure 2.10). Oligo-uridylation (≥ 2 U) was more sensitive to TUT4/7 knockdown than mono-uridylation was (3.71 and 1.36 fold decrease, respectively), suggesting that a relatively high level of TUT4/7 may be required to generate oligo-U tails on mRNA.

Gene-level analyses revealed that the majority of mRNA species (638 out of 746 genes, 85.5 %) are decreased in uridylation following TUT4/7 knockdown ($P = 7.69 \times 10^{-100}$, one-tailed Mann-Whitney U test) (Figure 2.11 and Table 2.1)[3]. This result strongly indicates that TUT4/7 uridylate most, if not all, mRNAs. Figure 2.12 presents 21 most abundant mRNAs as examples, the majority of which are reduced in uridylation upon TUT4/7 knockdown. Two biological replicate experiments showed a comparable decrease of uridylation (Figure

[2] These experiments were carried out by Dr. Minju Ha.

[3] All analyses in this section are carried out by Dr. Hyeshik Chang.

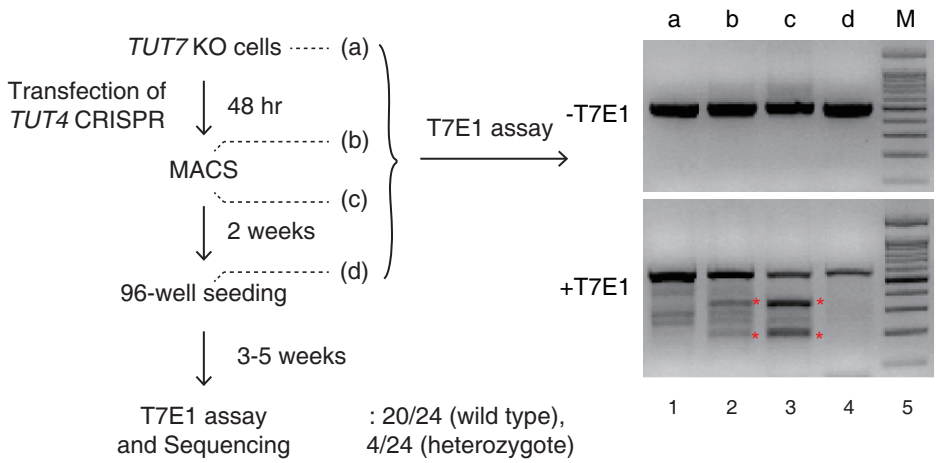

Figure 2.6 One of the unsuccessful attempts to generate TUT4/7 double knockout cell. TUT7 KO HeLa cell was used as a parental cell line, and transfected with TUT4 CRISPR-Cas9 to delete the TUT4 gene. To detect mutation in genomic DNA, target region was amplified by PCR and T7E1 (T7 Endonuclease I) assay was carried out. T7E1 recognizes and cleaves heteroduplex formed between wild type and mutated target sequence. "a to d" indicate the steps at which genomic DNA was extracted. (a) The parental TUT7 KO cells, (b) before MACS (magnetic-activated cell sorting for enrichment of mutated clones), (c) right after MACS, and (d) 2 weeks after MACS. Red asterisks denote cleaved DNA fragments detected by T7E1 assay, which indicate that genomic deletions had been effectively introduced. 3–5 weeks after 96-well seeding, ToolGen analyzed 24 individual colonies. T7E1 negative clones were thought to be 'wild type' clones. T7E1 positive clones were sequenced but all of them contained at least one wild type allele for TUT4 (heterozygote). Because none of the clones carried homozygous deletions for TUT4, our efforts to generate double knockout has failed despite the fact that the initial genomic deletion was successful. This indicates that double knockout of TUT4 and TUT7 may be lethal.

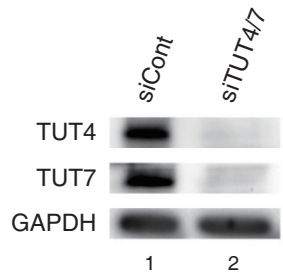

Figure 2.7 RNAi to deplete TUT4 and TUT7 simultaneously by transfecting siRNAs into HeLa cells. The TUT4 and TUT7 protein levels were monitored by western blotting.

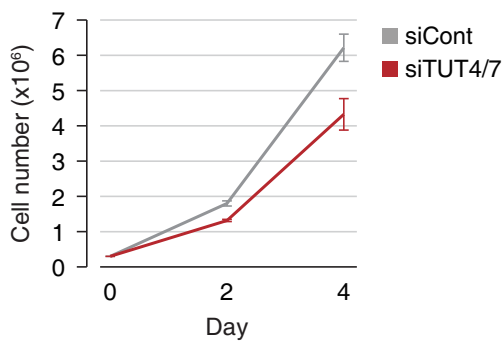

Figure 2.8 Cell proliferation rates shown by cell counting. Cell numbers are presented as mean ± standard error of the mean (SEM) (n=3).

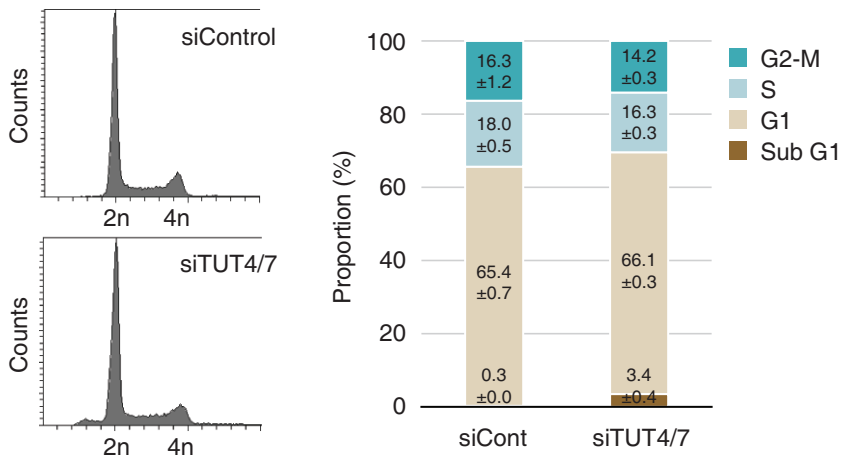

Figure 2.9 Cell cycle analysis. After 4 days of knockdown, cells were collected and profiled using BD FACSCanto and analyzed by BD FACSDiva software. (left) Cell cycle profiles. (right) The proportion of each cell cycle phase is displayed in stacked bar graph. The average percentages ± standard error of the mean (SEM) from three independent experiments are shown.

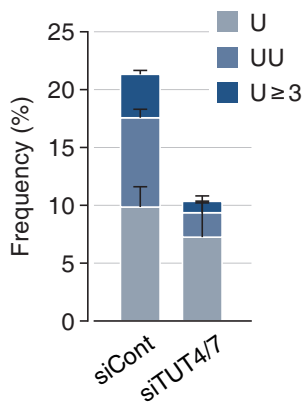

Figure 2.10 Uridylation frequency of mRNAs with short poly(A) tails (5–25 nt) measured by TAIL-seq following simultaneous TUT4 and TUT7 knockdown (siTUT4/7). Uridylation was reduced when both TUT4 and TUT7 were depleted (P = 0.0941 for U, 0.00922 for UU, 0.0105 for U≥3; one-tailed t test). Error bar represents the standard error of the mean from three biological replicates (n=3).

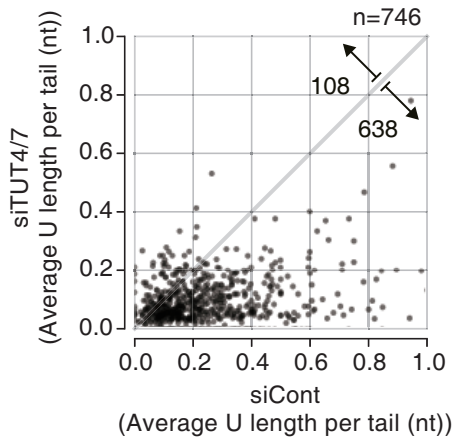

Figure 2.11 Changes in uridylation of individual mRNA species upon TUT4/7 knockdown. "Average U length per tail" (y-axis) is the sum of the number of all uridines on short A tails (5–25 nt) divided by the total number of reads with short A tails. Note that unlike "uridylation frequency", average U length per tail weighs every uridine in oligo-U tails. Each dot represents a transcript with ≥ 15 reads in both samples. Uridylation was significantly decreased following TUT4/7 knockdown ($P = 7.69 \times 10^{-100}$, one-tailed Mann-Whitney U test). The full list is shown in Table 2.1.

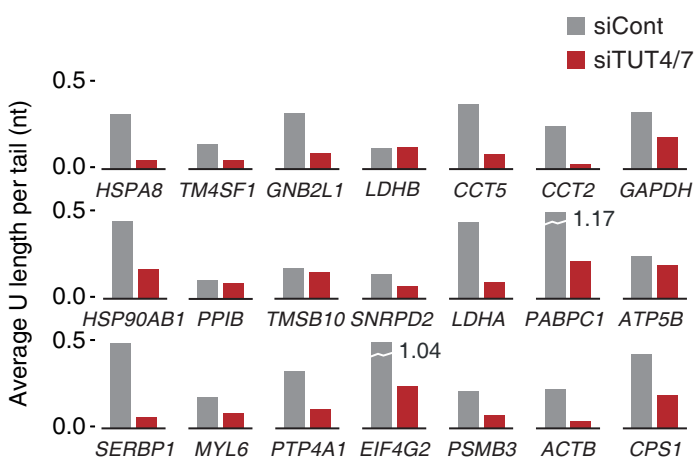

Figure 2.12 Examples of gene-level uridylation changes. Twenty-one most abundant mRNAs (not including ribosomal protein mRNAs and histone mRNAs) are shown in the order of mRNA abundance.

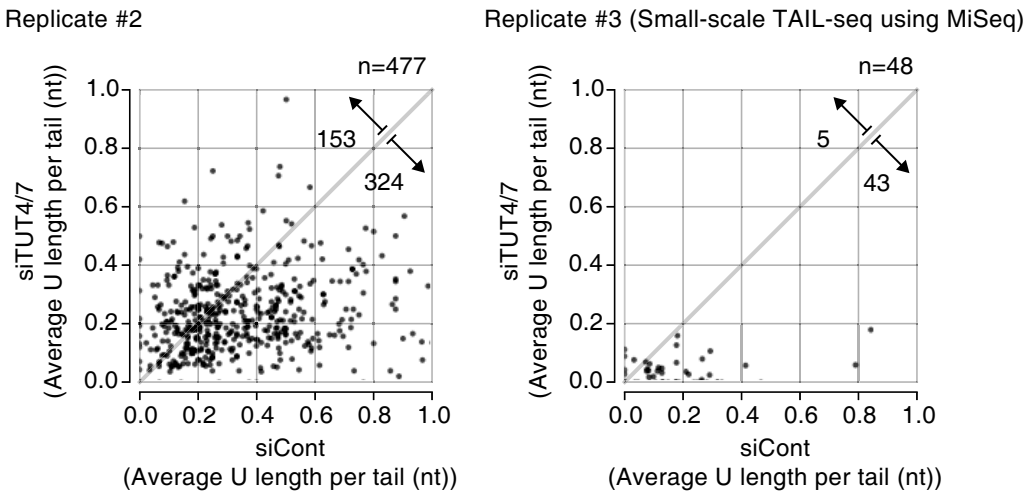

Figure 2.13 Changes in uridylation at transcript level upon TUT4/7 knockdown. Average U length per tail (y-axis) is the number of uridines on short A tails (5–25 nt) divided by the total number of reads with short A tails. Each dot represents a transcript with ≥ 15 reads in both samples. Replicate #3 was from "small-scale" TAIL-seq using Illumina MiSeq. Uridylation was significantly reduced when both TUT4 and TUT7 were knocked down ($P = 1.39 \times 10\text{-}15$ for replicate #2, and $P = 1.38 \times 10^{-9}$ for replicate #3 by one-tailed Mann-Whitney U test).

2.13).

Histone mRNAs that lack poly(A) tails are also uridylated and their uridylation is dependent modestly on TUT4/7, but not on TUT1/2/3/5/6 (data not shown). However, poly(A) histone mRNAs were excluded from my current data analyses because I used non-synchronous cell population for my experiments, and it is known that uridylation of histone mRNA occurs specifically at the end of S phase (Mullen & Marzluff, 2008; Schmidt et al., 2011; Su et al., 2013). It would be more appropriate to investigate histone mRNAs using synchronous cells in future studies.

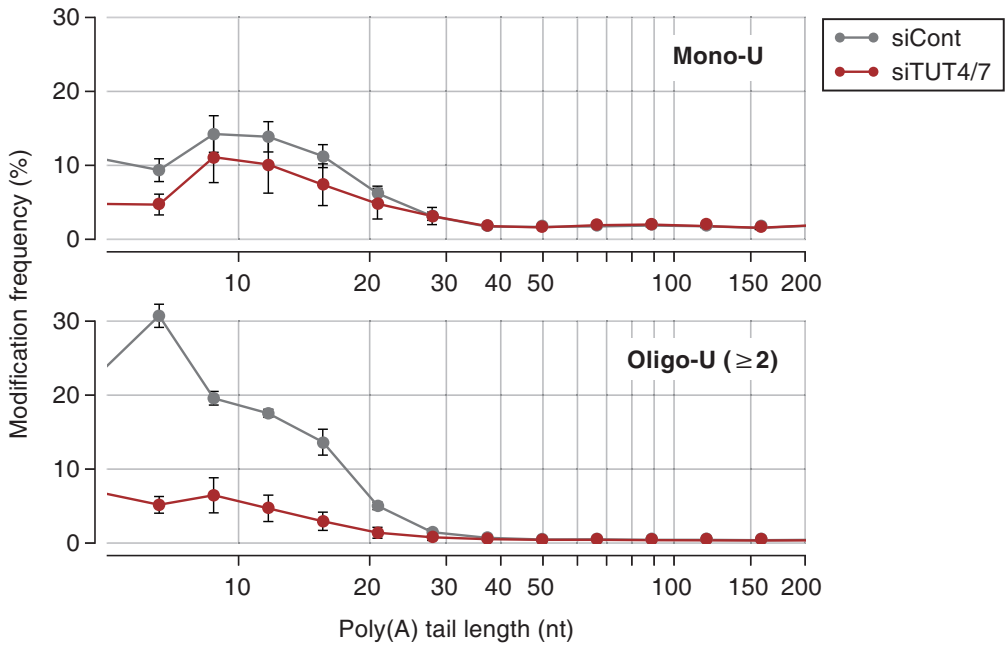

Figure 2.14 Distribution of mono-uridylation (top) and oligo-uridylation (bottom) according to the length of poly(A) tails. Poly(A) tail lengths from 5 nt to 231 nt are pooled into equal-width bins in the logarithmic scale (base 2) (x-axis). The left sides (inclusive) of bins are 5, 7, 9, 12, 15, 21, 28, 38, 50, 67, 89, 119, 159, and 212 nt. Uridylation frequency (y-axis) indicates the percentage of uridylated reads within each poly(A) tail size range. Error bar represents the standard error of the mean (n=3).

2.2.2 TUT4/7 selectively oligo-uridylate mRNAs with short A tails in vivo and in vitro

It is intriguing that uridylation occurs preferentially on shortened A tails in plants and animals (Chang et al., 2014b; Sement et al., 2013). Figure 2.14 shows the distribution of U tails over different lengths of A tails in HeLa cells. The frequency of uridylation on the transcripts with a short A tails (5–25 nt) is higher than that on the rest (A tails of >25 nt), especially when only oligo-U (≥ 2 U) is counted. Note that mRNAs with A tails of shorter than 5 nt were excluded from this analysis as it is sometimes difficult to distinguish them from genomic A-rich sequences in 3′ UTR. When TUT4/7 were depleted, uridylation on

short A tails was selectively reduced (especially for oligo-U), indicating that TUT4/7 are responsible for the specific uridylation of short A tails (Figure 2.14).

To understand the mechanism underlying such strong association with A tail length, I performed in vitro uridylation assays using immunopurified full-length TUTases (Figures 2.15, 2.16, 2.17, and 2.18)[4]. Substrate RNAs were chemically synthesized to contain heterogenous sequences (the last 20 nt from the *SHOC2* 3′ UTR) linked to A tails of various lengths (0, 10, 25, and 50 nt) at the 3′ end (Figure 2.15). I also used a "swapped" control (A25R) that has a 25 nt A segment at the 5′ side of the *SHOC2* 3′ UTR such that the RNA is identical to *SHOC2*-A25 (A25) in the overall length and base composition, but lacks an A tail at the 3′ end (Figure 2.15).

Interestingly, RNAs with no tail (A0) or a short A tail (A10) were oligo-uridylated efficiently by TUT4 under the condition where pre-let-7a-1 is mono-uridylated weakly (Figure 2.15). A25 and A50 were less efficiently uridylated than A0 and A10 were. The A25R RNA was a much better substrate than the A25 was, indicating that it is the 3′ A tail length (not the overall RNA length) that is measured by TUT4 (Figure 2.15). Comparable results were obtained with full-length TUT7 protein (Figures 2.16 and 2.17), again demonstrating that these two related enzymes are functional paralogs. The U-tail length in Figures S2A–B was overall shorter than those in Figure 2.15 because the amount of immunoprecipitated TUT7 was smaller than that of TUT4 in Figure 2.15 (data not shown).

I also prepared recombinant TUT7 protein (951–1,495 aa) from E. coli and used the fragment for in vitro uridylation assay (Figure 2.18). Apart from the *SHOC2* RNAs (Figure 2.19), I synthesized and tested another series of RNAs based on the *CALM1* 3′ UTR sequences (Figure 2.20)[5]. The purified protein fragment was fully capable of carrying out uridylation in an A tail length-dependent manner with both RNAs (Figures 2.20 and 2.19, see below). Thus, the C-terminal half of TUT7 is sufficient to recognize and uridylate single-stranded RNAs with a short A tails (<~25 nt), in a 3′ UTR sequence-independent manner. These results suggest that TUT4/7 possess an intrinsic ability to measure the 3′ terminal A length and avoid uridylation of long A tails.

[4] These experiments were carried out by Dr. Minju Ha.

[5] These experiments were carried out by Dr. Minju Ha.

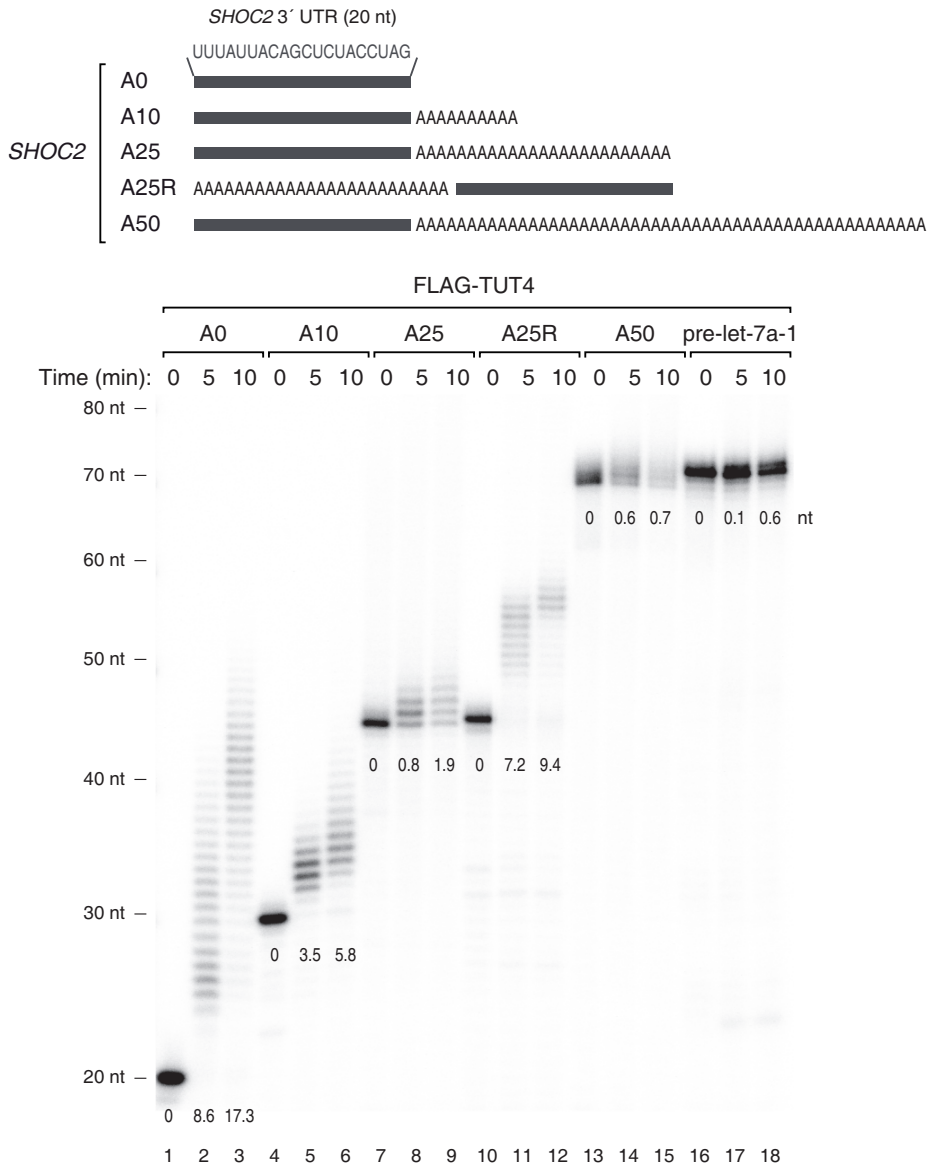

Figure 2.15 (top) Illustration of chemically synthesized RNA substrates. Grey bars represent the last 20 nt of *SHOC2* 3′ UTR and "A" indicates an adenosine. (bottom) In vitro uridylation assay using immunopurified FLAG-TUT4. 0.45 nM of RNA was used in each reaction. The products were resolved on 6 % polyacrylamide sequencing gel containing 7 M urea. The average length of uridylation is shown below each band. See 2.4 for quantification method.

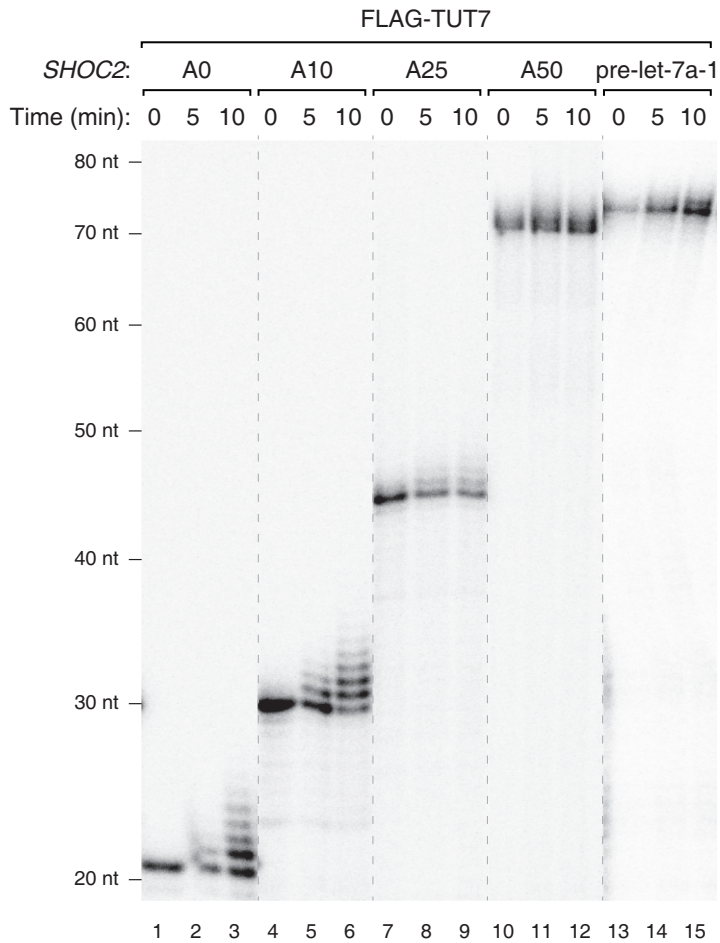

Figure 2.16 In vitro uridylation assay using immunopurified full-length TUT7 and *SHOC2* RNAs (the same RNA substrates and reaction conditions as shown in Figure 2.15). Dashed lines indicate discontinuous lanes from the same gel, which applies to all the dashed lines in the figure.

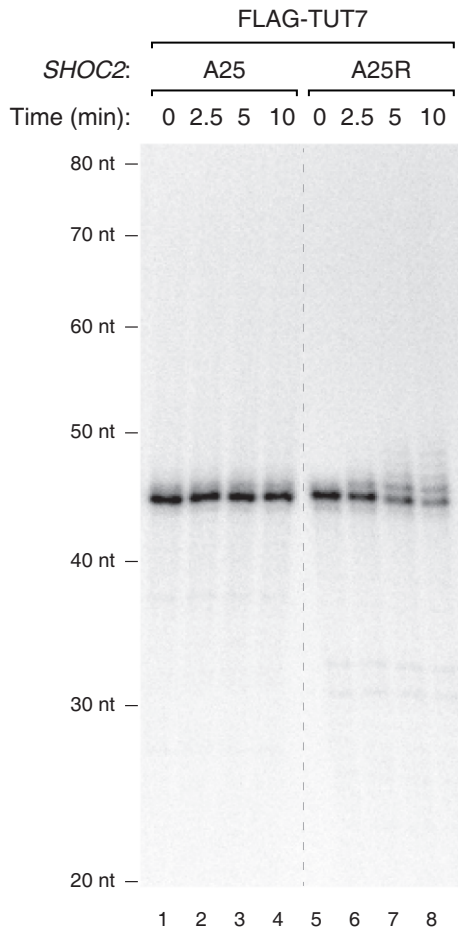

Figure 2.17 In vitro uridylation assay using immunopurified full-length TUT7 and *SHOC2* RNAs (A25 and A25R). Uridylation efficiency for A25R was higher than A25. Reaction conditions are the same as in Figure 2.16, except that the amount of TUT7 was smaller in Figure 2.17 than in Figure 2.16.

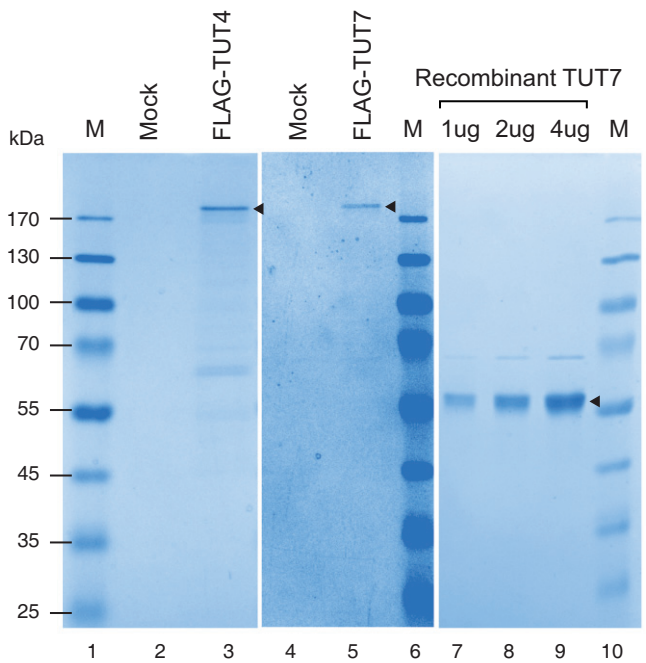

Figure 2.18 Coomassie staining of immunopurified FLAG-TUT4 (full length), FLAG-TUT7 (full length), and recombinant TUT7 (951–1,495 aa) resolved on 10 % SDS-PAGE gel. Each protein is indicated by arrowheads. M, size marker.

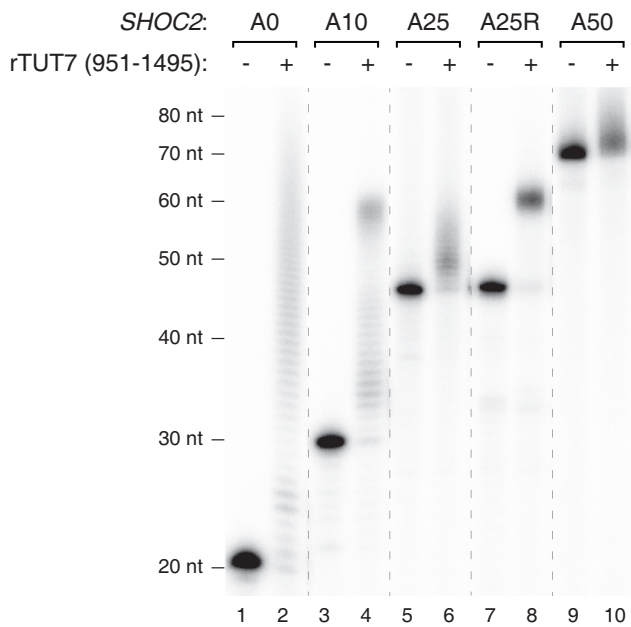

Figure 2.19 In vitro uridylation assay using recombinant TUT7 (951–1,495 aa) and *SHOC2* RNAs. 0.45 nM of RNA and 14 nM of recombinant TUT7 (rTUT7) were used in the reaction. Extension products were resolved on 12.5 % polyacrylamide gel with 7 M urea.

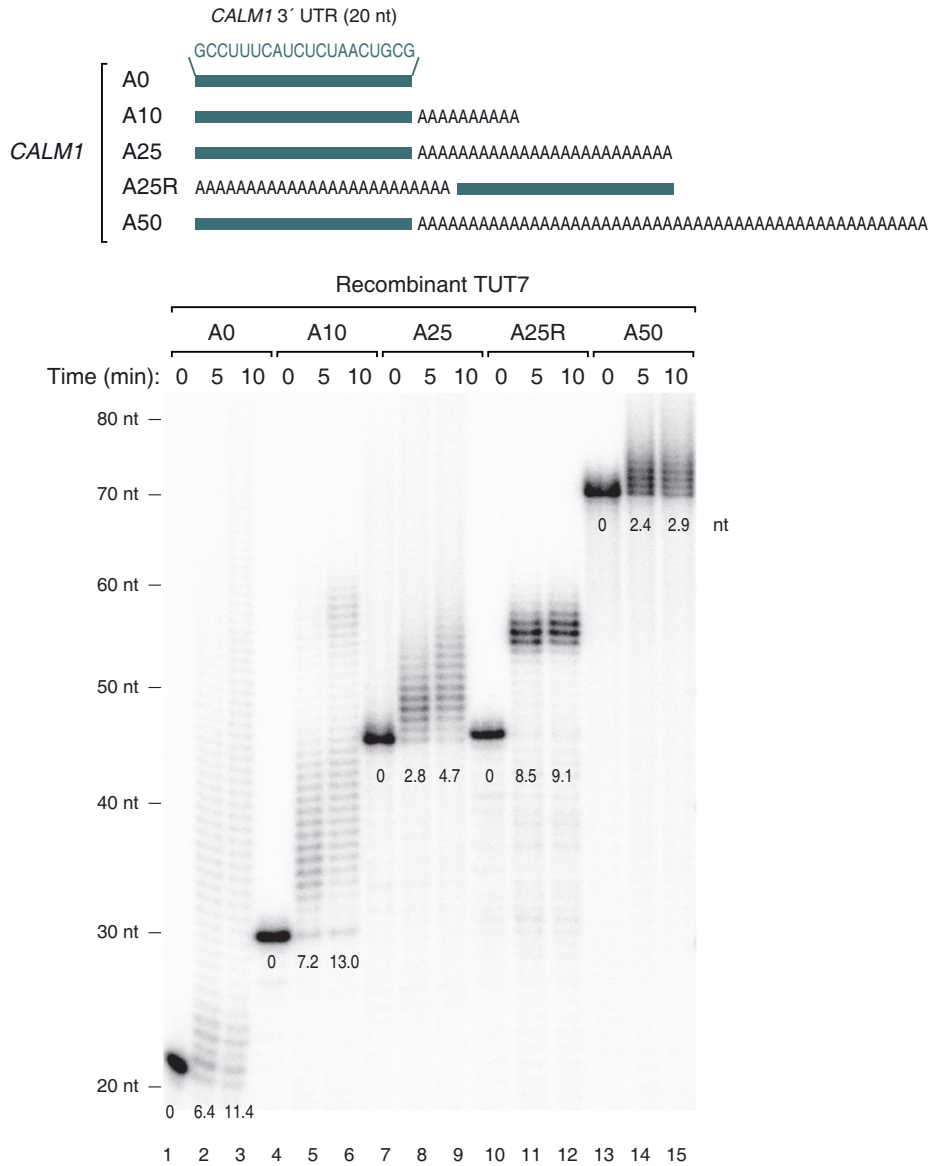

Figure 2.20 (top) Illustration of chemically synthesized RNA substrates. Green bars represent the last 20 nt of *CALM1* 3′ UTR and "A" indicates an adenosine. (bottom) In vitro uridylation assay using recombinant TUT7 C-terminal fragment (951-1,495 aa) purified from E. coli. 0.45 nM of RNA and 14 nM of recombinant TUT7 were used in each reaction. Extension products were resolved on 6 % polyacrylamide sequencing gel containing 7 M urea. The average length of uridylation was quantified as in Figure 2.15.

2.2.3 PABP suppresses uridylation of poly(A)$^+$ mRNA

As poly(A)$^+$ mRNAs are associated with poly(A) binding protein (PABP) in cells, I asked if PABP has an influence on mRNA uridylation. It was previously shown that PABP preferentially interacts with poly(A) or A-rich sequences (Eliseeva et al., 2013). The binding affinity increases as the A stretch gets longer (Eliseeva et al., 2013; Khanam et al., 2006; Kuhn & Pieler, 1996; Sachs et al., 1987). Full length PABP occupies a ~25 nt A tail as determined by nuclease digestion assay (Baer & Kornberg, 1983; Eliseeva et al., 2013). In order to test an effect of PABP on uridylation, in vitro uridylation assays was carried out in the presence of recombinant PABPC1 (Figure 2.21)[6]. When PABPC1 was added to RNA, uridylation of RNAs with long poly(A) tail (A25 and A50) was suppressed even at a low concentration of PABPC1 (10 nM) while those with no or short A-tail (A0, A10 and A25R) remained largely unaffected (Figure 2.21). This result suggests that PABPC1 binds preferentially to long poly(A) tails and protects them from TUT4/7, and thereby enhances the selectivity of uridylation according to poly(A) tail length.

Taken together, my results suggest that the strict dependence on the A tail length observed in vivo may be determined by the combination of two factors: (1) the intrinsic ability of TUT4/7 to measure poly(A) stretch (Figures 2.14, 2.15, and 2.20) and (2) the protective activity of PABP (Figure 2.21). As deadenylation is thought to occur mainly in the cytoplasm, I examined the localization of TUT4/7 by western blotting. The TUT4 and TUT7 proteins are mainly localized in the cytoplasm (Figure 2.22). Thus, TUT4/7 may function mainly in the metabolism of cytoplasmic, deadenylated mRNAs.

2.2.4 Uridylation facilitates global mRNA decay

To understand the functional consequences of uridylation, I measured mRNA half-life in HeLa cells with or without TUT4/7 knockdown (Figure 2.23)[7]. mRNA levels were determined by RNA-seq at 0, 1, 2, and 4 hr after actinomycin D treatment that blocks transcription. To avoid any bias from tail length variation, I omitted the oligo-dT enrichment step and instead used Ribo-Zero to remove abundant rRNAs prior to cDNA library

[6] These experiments were carried out by Dr. Minju Ha.

[7] All analyses in this section are carried out by Dr. Hyeshik Chang.

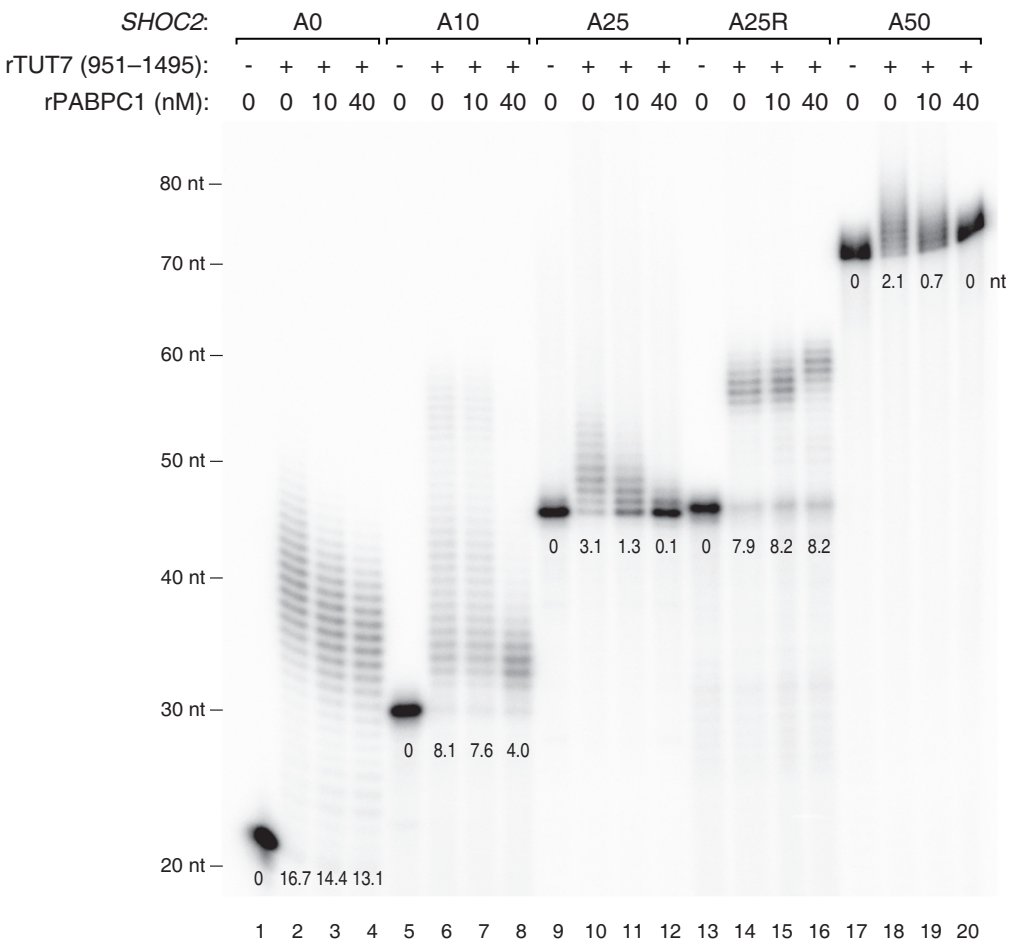

Figure 2.21 In vitro uridylation assay by using recombinant TUT7 (951–1,495 aa) with a varying concentration of recombinant PABPC1 (0, 10, or 40 nM). 0.45 nM of RNA and 160 nM of recombinant TUT7 (rTUT7) were used in the reaction. Extension products were resolved on 6 % polyacrylamide sequencing gel containing 7 M urea. The average length of uridylation was quantified as described in Methods and Materials and shown below each band.

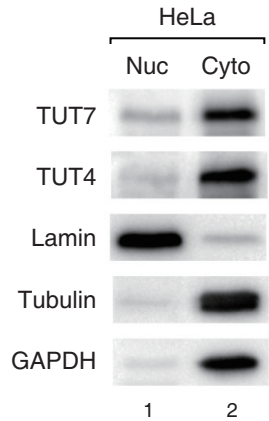

Figure 2.22 Relative amount of TUT4 and TUT7 proteins in the nucleus and cytoplasm was measured by western blotting. Lamin was used as a nuclear marker while Tubulin and GAPDH were used as cytoplasmic markers.

construction. I could measure turnover rates of 1,829 mRNAs. In TUT4/7-depleted cells, the majority of mRNAs (1,426 out of 1,829 [78.0 %]) showed increase stability (Figure 2.23, left panel, and Table 2.2). Half-lives were increased by ~30 % on average, and median half-life was extended from 9.45 hr to 11.2 hr (Figure 2.23, right panel).

Of note, although TUT4/7 contribute to let-7 biogenesis, double knockdown of TUT4/7 (without simultaneous knockdown of TUT2) did not substantially affect the let-7 level (Heo et al., 2012). In fact, the transcriptome analyses show that mRNAs are globally upregulated, indicating that the changes in mRNA half-life observed in this study cannot be attributed to specific regulation of let-7 biogenesis.

For validation of the impact of TUT4/7 deletion on mRNA stability, five mRNAs (*SHOC2*, *TRIM24*, *RB1CC1*, *MET*, and *XRN1*) were measured by quantitative RT-PCR after actinomycin D treatment (Figure 2.24)[8]. None of these mRNAs contains a let-7 binding site with seed match in their 3′ UTR, yet all of them showed increased stability when TUT4/7 were depleted. Therefore, my results demonstrate that TUT4/7 play an important role in bulk mRNA degradation in a let-7 independent manner.

[8] In collaboration with Dr. Minju Ha.

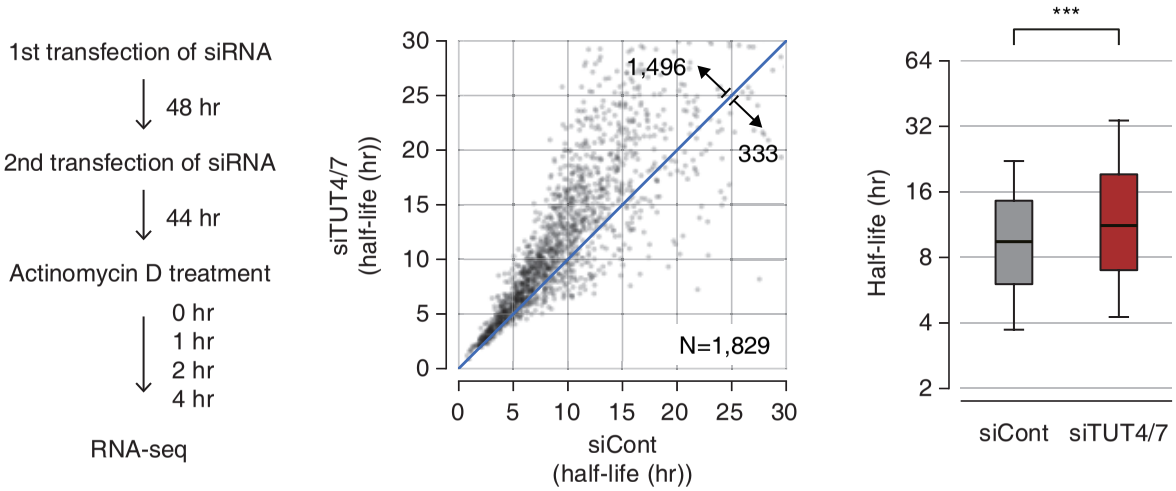

Figure 2.23 Transcriptome-wide change of mRNA half-life determined by RNA-seq. (left) Experimental scheme. HeLa cells were transfected twice and harvested at 0, 1, 2, and 4 hr following actinomycin D treatment. (center) Changes of average mRNA half-life upon TUT4/7 knockdown from two biological replicates. The range of display is limited to between 0 and 30 hr for the better visual recognition (232 out of 1,829 mRNAs are outside of the view). The full list is available in Table 2.2. (right) Distribution of mRNA half-lives in control or TUT4/7 knockdown cells. A box represents the first and third quartiles and an internal bar indicates median. Whiskers span between the 9th and the 91st percentiles. Half-lives of mRNAs are significantly extended by TUT4/7 knockdown (*** $P = 4.06 \times 10^{-155}$, one-tailed paired Mann-Whitney U test). See Methods and Materials for the detailed description of procedure.

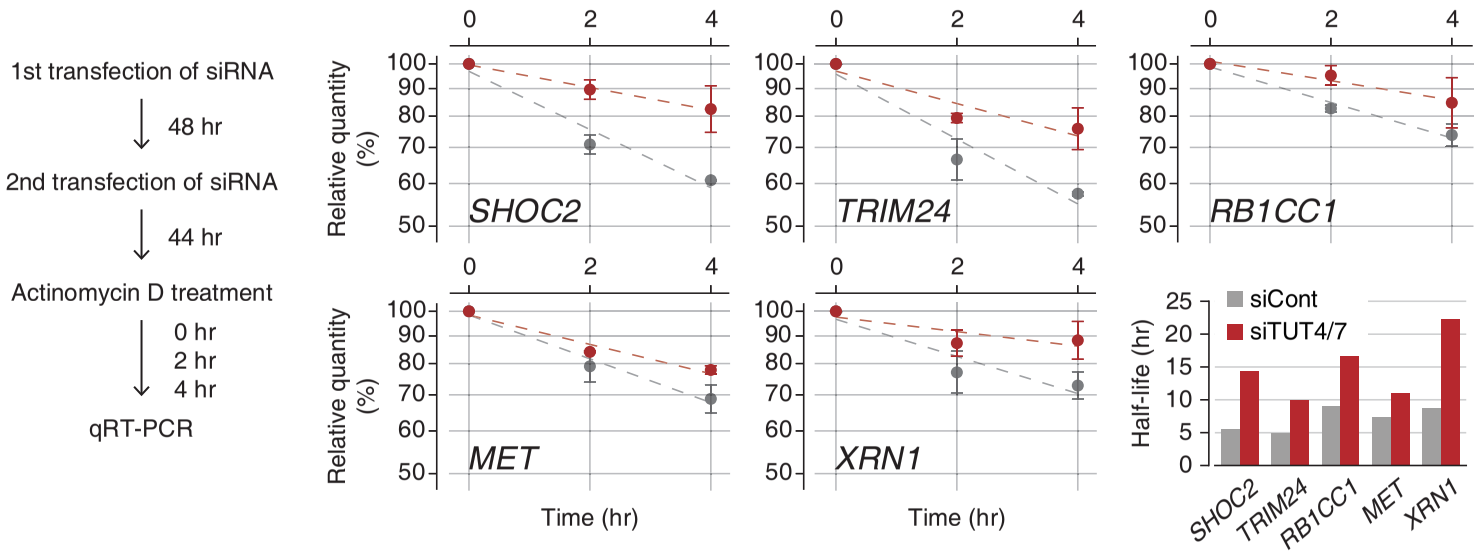

Figure 2.24 Measurement of mRNA half-life by qRT-PCR. (left) The experimental scheme. (right) Following 0, 2, and 4 hr of actinomycin D treatment, relative abundance (y-axis) of five selected genes were measured. For normalization, *GAPDH* mRNA was used because it was highly stable (half-life >24 hr, data not shown) and did not change noticeably by TUT4/7 depletion. Error bar represents the standard error of the mean (n=3). Half-lives are calculated by linear fitting of the log-transformed exponential decay function.

Next, to examine the effect of overexpressed TUTase on mRNA expression, I carried out tethering experiments in HeLa cells (Figure 2.25, left panel)[9]. A related experiment was reported recently in *Xenopus* oocytes: when Xenopus TUT7 homolog was tethered to the 3′ UTR of luciferase reporter mRNA, luciferase activity was reduced without significant changes in mRNA, implicating translational repression (Lapointe & Wickens, 2013). However, since mRNA decay activity is generally suppressed in oocytes (Barckmann & Simonelig, 2013), it was unclear if the observation from frog oocytes can be generalized. For tethering experiments, I generated constructs that express proteins tagged with the λN peptide that interacts with its specific binding sites (BoxB sites) in the 3′ UTR of luciferase mRNA (Figures 2.25 and 2.26)[10]. Expression of λN protein modestly increased luciferase expression non-specifically for an unknown reason (Figure 2.25, middle panel). Nevertheless, tethering of AGO2 repressed luciferase reporter expression (Figure 2.25), as previously shown (Pillai et al., 2004), indicating that this is a valid system to test the effect of RNA silencing factors. Neither the negative control TUT2 nor its mutant repressed luciferase reporter expression. But when wild type TUT4 was tethered to the reporter mRNA, luciferase activity was decreased to ~60 % while such reduction was not observed with the catalytically dead point mutant (D1011A) of TUT4 (Figure 2.25, middle panel), indicating that TUT4 suppressed gene expression via uridylation. Quantitative RT-PCR further showed that tethering of TUT4 induced a reduction of mRNA (Figure 2.25, right panel). Thus, these results collectively indicate that TUT4/7 function as suppressors of gene expression through mRNA destabilization.

2.2.5 Uridylation is involved in miRNA-induced gene silencing

My model predicts that if a gene-specific inducer of deadenylation is introduced into cells, uridylation of the given transcript will take place, which in turn will facilitate RNA decay. To test the model, I examined the effect of miRNA as an example, which is well established to induce specific deadenylation of its complementary targets (Ameres & Zamore, 2013; Djuranovic et al., 2011; Huntzinger & Izaurralde, 2011; Krol et al., 2010).

[9] These experiments were carried out by Dr. S.Chul Kwon.

[10] This experiment was carried out by Dr. S.Chul Kwon.

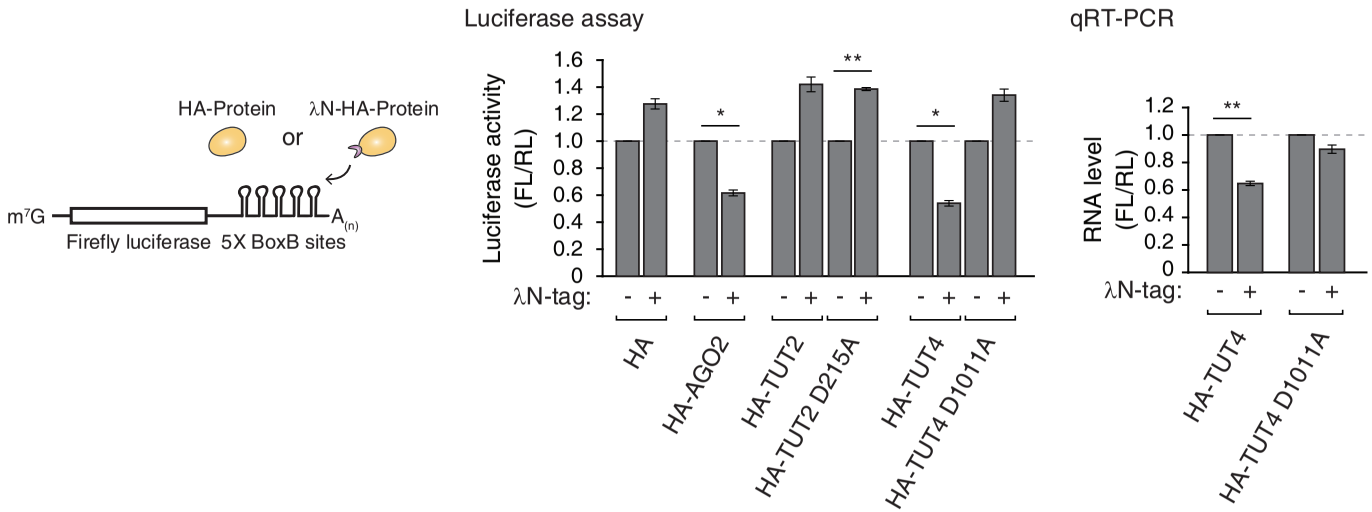

Figure 2.25 (left) Schematic representation of reporter assay system with the λN tethering. (center) Reporter (firefly) luciferase activity was measured and normalized to renilla luciferase activity (n=3). (right) Reporter mRNA levels were determined by qRT-PCR (n=4). Error bars represent the standard error of the mean. Luciferase activity or RNA level were significantly reduced when AGO2 or TUT4 were tethered (* P <0.01, ** P <0.001; two-tailed t test).

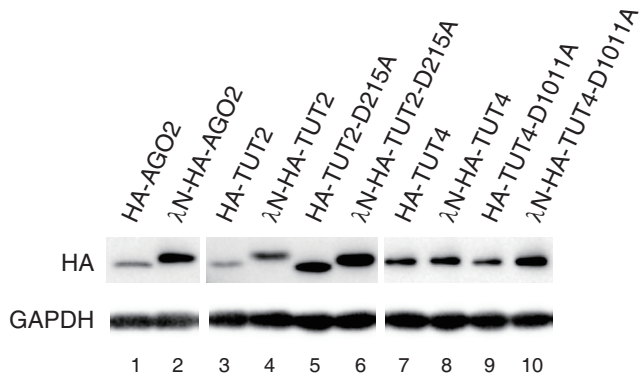

Figure 2.26 Western blotting showing the expression of transfected proteins in Figure 2.25. GAPDH was used as a loading control.

I first analyzed the TAIL-seq data from my previous experiment where miR-1 mimic was transfected into HeLa cells (Chang et al., 2014b). As expected, miR-1 targets undergo deadenylation and subsequent downregulation following miR-1 mimic transfection (Figure 2.27, middle and lower panels, respectively)[11]. Importantly, I detected a specific increase of uridylation on miR-1 targets whereas the rest of genes stayed largely unaffected (Figure 2.27, upper panel). This result is consistent with my model that deadenylation leads to uridylation.

I next measured turnover rates of miR-1 targets with or without TUT4/7 knockdown. The mRNAs tested (*PTMA*, *ADAR*, and *PGM2*) are normally stable (half-lives >24 hr) in cells that do not contain miR-1 (Figure 2.28, black line)[12]. When miR-1 was introduced, their half-lives were shortened to 6.5, 10.0, and 9.4 hr, respectively (Figure 2.28, blue line). Upon TUT4/7 depletion, the miR-1 target mRNAs were stabilized (with extended half-lives of 14.0, 36.1, and 18.1 hr, respectively) (Figure 2.28, red line). Therefore, TUT4/7 are necessary for the facilitated decay of miRNA targets. I propose that other factors that cause deadenylation may also induce uridylation and decay, as shown here with an example of miR-1.

[11] Analysis was done by Dr. Hyeshik Chang.

[12] In collaboration with Dr. Minju Ha.

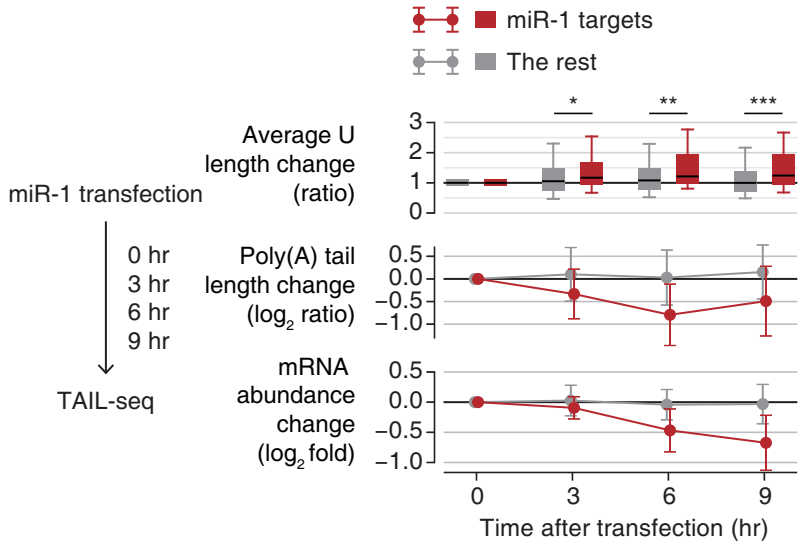

Figure 2.27 Changes in uridylation after miR-1 transfection. (left) Experimental scheme. miR-1 was transfected into HeLa cells and the cells were harvested after the indicated time for TAIL-seq. Targets are the transcripts with ≥1 miR-1 3′ UTR site and down-regulated by ≥30 % on 12 hr post-transfection of miR-1 (Guo et al., 2010). (right top) Average U length change relative to 0 hr is shown in each time point. Average U length per tail is the number of uridines on short A tails (5–25nt) divided by the total number of reads with short A tails. Box represents the interval between the first and third quartiles, and the internal bar indicates the median. Whiskers span between the 9th and 91st percentiles. Average U length of miR-1 target is significantly extended after miR-1 transfection (* P = 0.0152, ** P = 0.00318, *** P = 5.79×10^{-4}; one-tailed Mann-Whitney U test). (right middle) Poly(A) tail length change relative to 0 hr. The length change is represented by $\log_2$ odds ratio between long tails (>25 nt) and short tails (≤25 nt) in one among 3, 6, or 9 hr and 0 hr. A negative value (<0) indicates increase of the fraction of short tails compared to 0 hr. Error bars indicate standard deviation among mRNAs. The portion of short poly(A) tails expanded more for miR-1 targets than the others ($P=1.80\times10^{-6}$ for 3 hr, $P=8.47\times10^{-13}$ for 6 hr, $P=1.48\times10^{-11}$ for 9 hr; one-tailed Mann-Whitney U test). (right bottom) mRNA abundance ($poly(A)^+$ tag counts) change relative to 0 hr. Error bars indicate standard deviation among mRNAs. Expression levels of miR-1 targets were decreased more than the rest transcripts ($P=2.09\times10^{-4}$ for 3 hr, $P=2.65\times10^{-14}$ for 6 hr, $P=5.46\times10^{-18}$ for 9 hr; one-tailed Mann-Whitney U test).

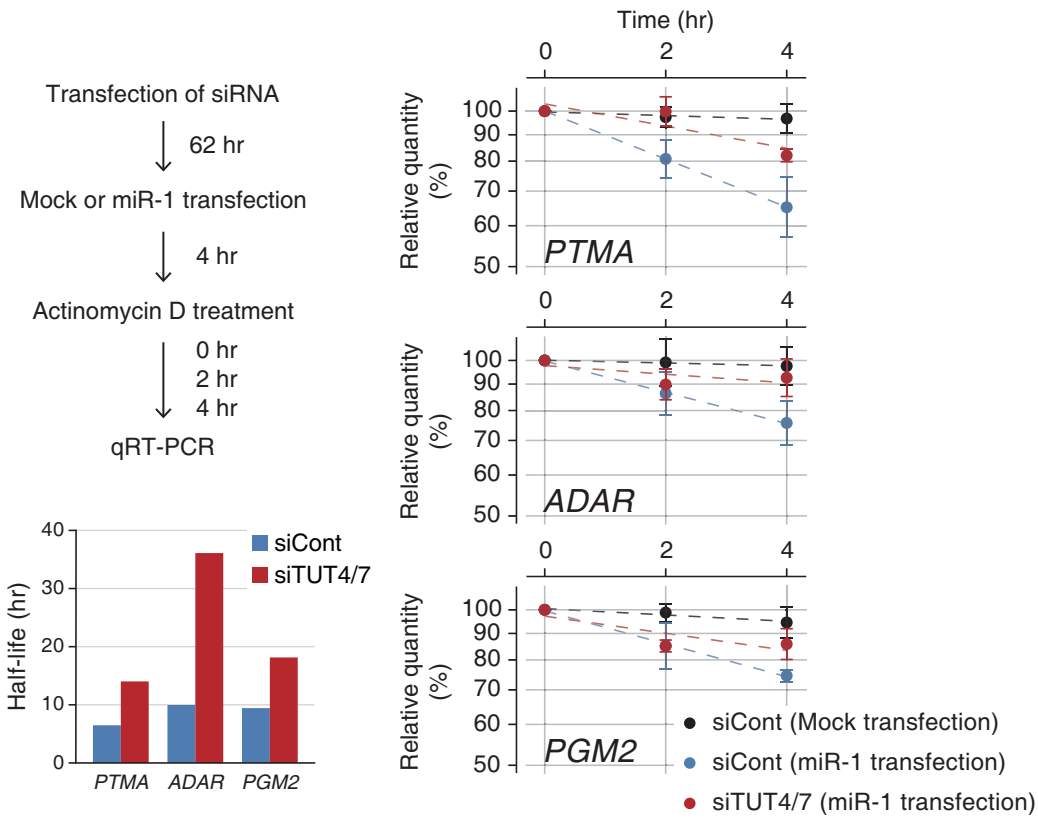

Figure 2.28 Measurement of half-life of miR-1 targets by qRT-PCR. (left) The experimental scheme. Following siRNA transfection for 62 hr, HeLa cells were transfected with miR-1 or mock transfected. After 4 hr, actinomycin D was treated and cells were harvested at 0, 1, 2, and 4 hr. (right) Relative abundance (y-axis) of miR-1 target mRNAs were measured. For the normalization, highly stable *GAPDH* mRNA was used because it did not change significantly by siTUT4/7 or miR-1 transfection. Error bar represents the standard error of the mean (n=3). Half-lives are determined by linear fitting of the log-transformed exponential decay function.

2.2.6 mRNA decay factors remove uridylated mRNAs

To understand downstream events of uridylation, I disrupted 5′–3′ or 3′–5′ exonucleolytic decay factors and examined the mRNA terminome (Figure 2.29)[13]. The popsicle-shaped bars in Figure 2.30 display the relative quantity of reads with a U tail (thick stem) or without a U tail (thin stem)[14]. As U-tail frequencies vary depending on poly(A) tail length, different A-tail ranges are shown separately along the horizontal axis. For more information, the overall uridylation frequency and poly(A) length distribution are presented in Figures 2.31 and 2.32, respectively.

In order to inhibit 5′–3′ decay, I initially depleted a major 5′–3′ exoribonuclease XRN1. Interestingly, interference of XRN1 resulted in a strong accumulation of uridylated mRNAs with short A tails (≤ 25 nt) (Figure 2.30A). Additionally, when I depleted LSM1 (a component of the LSM1-7 complex that is known to facilitate decapping) or overexpressed dominant-negative mutants of the decapping complex (DCP1 and DCP2) (Chang et al., 2014a), I detected an increase of uridylation among short A tailed mRNAs (≤ 25 nt) (Figure 2.30B). Short A tailed mRNAs increased in abundance (particularly, in the 5–15 nt range) when the 5′–3′ decay was suppressed. Note that the level of uridylated mRNA was upregulated substantially (U_1–U_{3+}), accounting for the overall increase of mRNA reads in this range, while mRNAs without a U tail did not change significantly (U_0). This result is consistent with a model that deadenylated, uridylated mRNAs are normally degraded rapidly by the 5′–3′ decay factors while poly(A)$^+$ mRNAs without U-tails are relatively stable. The LSM1–7 complex is known to preferentially bind to RNAs with 3′ terminal uridyl residues (Chowdhury et al., 2007; Sharif & Conti, 2013; Song & Kiledjian, 2007; Zhou et al., 2014), and facilitate decapping through PATL1 (Pat1 in yeast) (Marnef & Standart, 2010; Wilusz & Wilusz, 2013). Thus, a short U tail may first be recognized by the LSM1–7 complex which in turn facilitates decapping (by the DCP1/2 complex) and subsequent 5′–3′ degradation (by XRN1).

I also investigated the contribution of the 3′–5′ decay pathway by depleting 3′ exonucleolytic factors. When I knocked-down RRP41, a core subunit of human exosome, I

[13] In collaboration with Dr. Minju Ha.

[14] Analysis and data presentation were carried out by Dr. Hyeshik Chang.

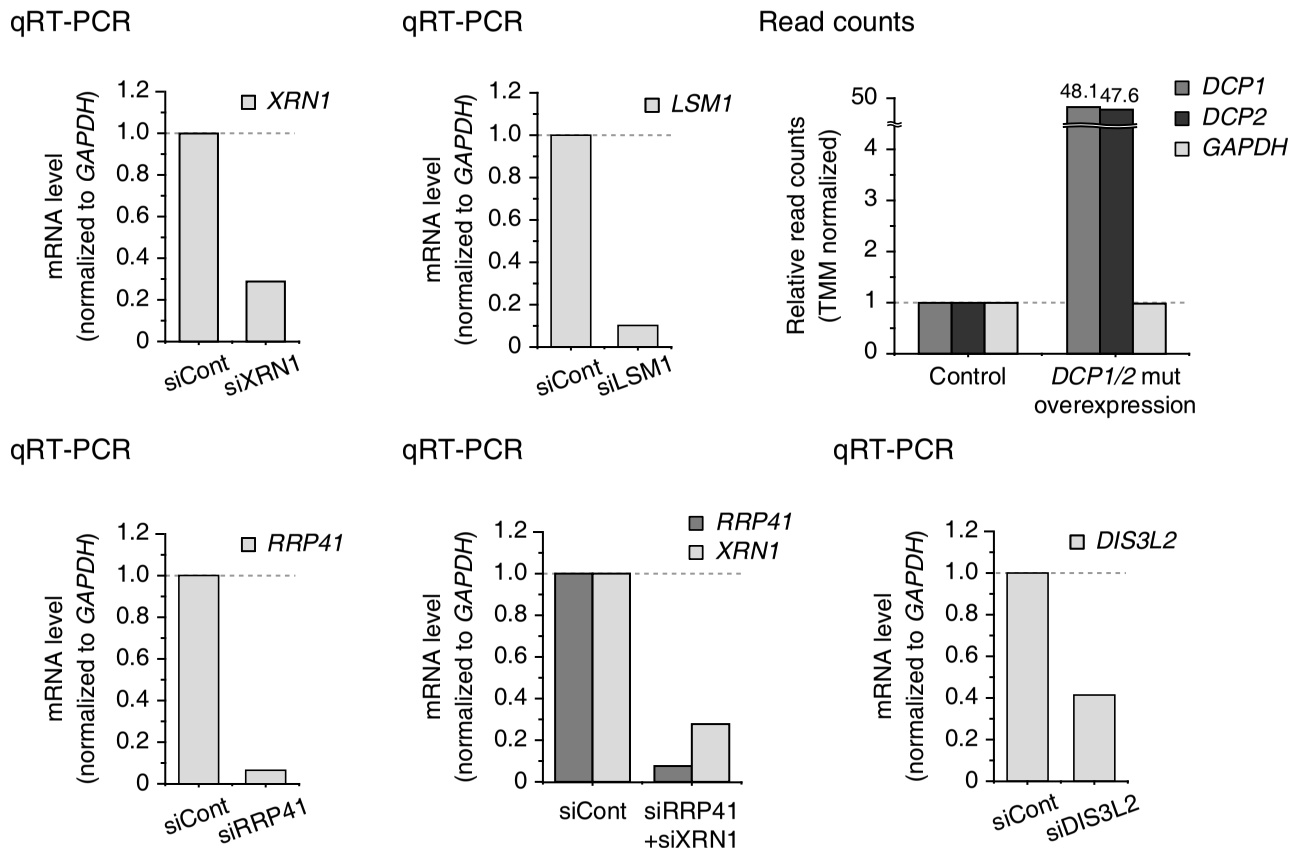

Figure 2.29 Validation of knockdown by qRT-PCR or sequencing. For the *DCP1/2* mutants overexpressed sample, the levels of *DCP1* and *DCP2* are shown in relative read counts (after trimmed mean of M values [TMM] normalized [Robinson & Oshlack, 2010]) from small-scale TAIL-seq experiments (with Illumina MiSeq). *GAPDH* was used as a negative control.

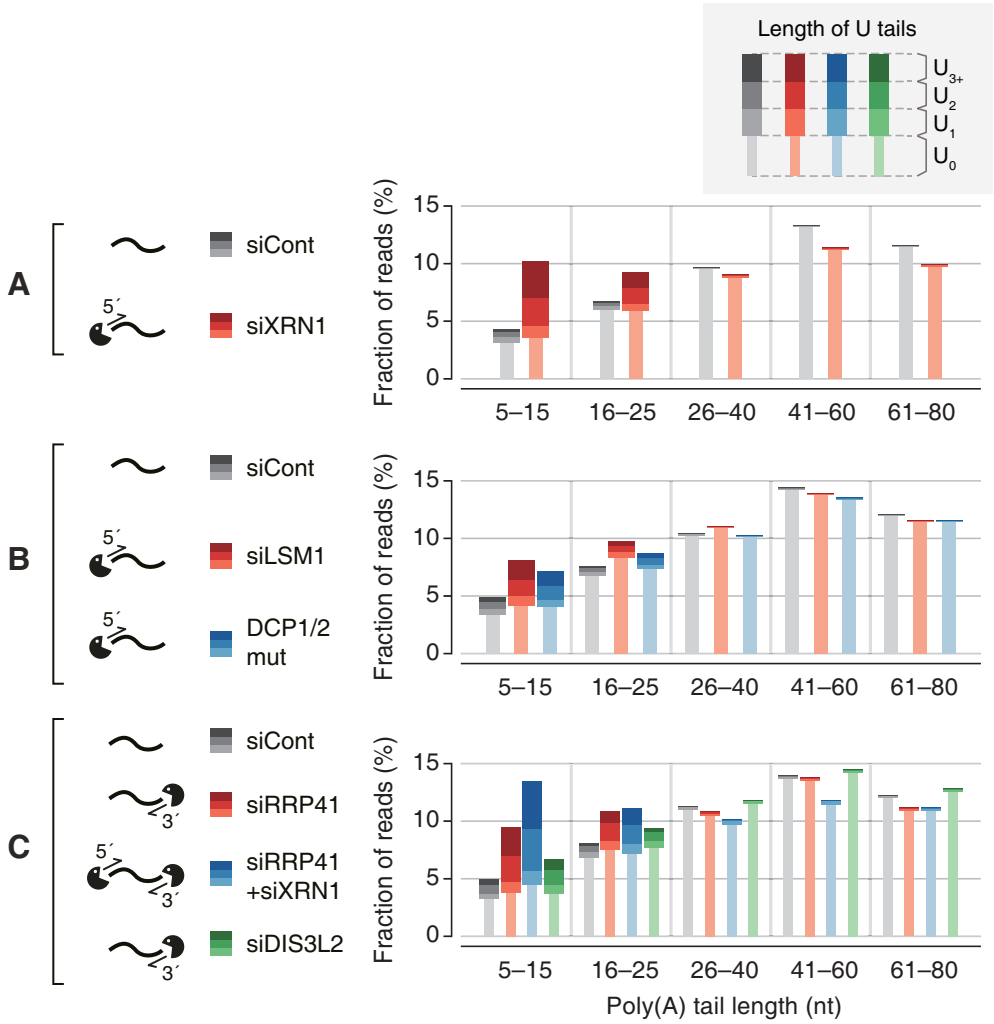

Figure 2.30 Changes of poly(A) tail and uridylation upon knockdown of decay factor(s) detected by small-scale TAIL-seq (with Illumina MiSeq). Fraction of mRNA reads out of the total poly(A)$^+$ mRNA reads is shown in each poly(A) tail size range. Narrow bars represent reads without U tails (U_0) and wider bars indicate uridylated reads (U_1–U_{3+}). The "DCP1/2 mut" sample derived from cells co-expressed of dominant-negative mutants of DCP1 and DCP2 (DCP1a-GSSG and DCP2-E148Q, respectively).

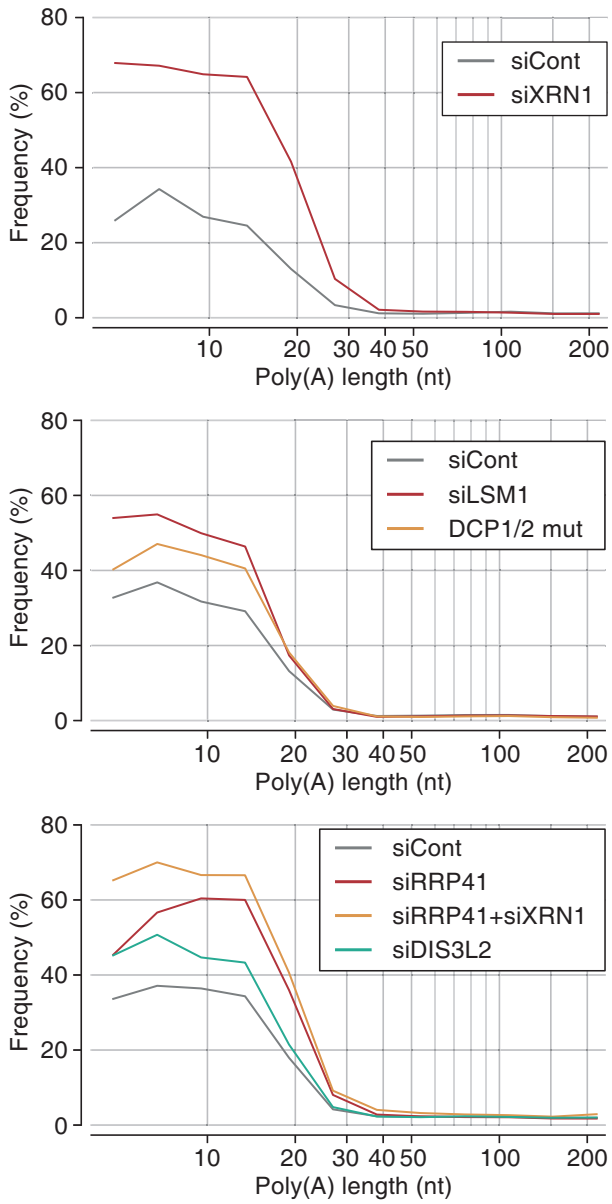

Figure 2.31 Changes in uridylation frequency upon knockdown of decay factor(s). Poly(A) tail lengths from 5 nt to 231 nt are pooled into equal-width bins in a logarithmic scale (base 2) (x-axis). The left sides (inclusive) of bins are 5, 7, 10, 14, 22, 33, 49, 74, 112, and 169 nt. Uridylation frequency (y-axis) indicates the fraction of uridylated reads within each poly(A) tail size range.

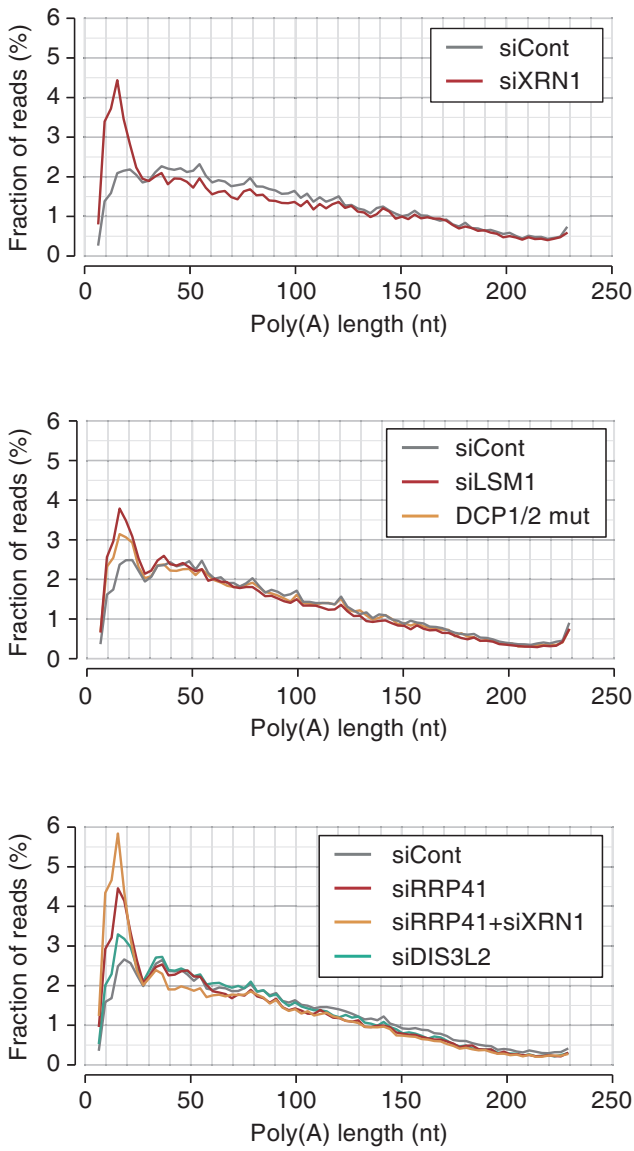

Figure 2.32 Global distribution of poly(A) tail length. Fraction of reads (y-axis) shows the density of poly(A)$^+$ reads in each 3 nt bin.

detected a substantial accumulation of uridylated mRNAs with short A tails (Figure 2.30C). Combinatorial knockdown of RRP41 and XRN1 resulted in a more pronounced increase of uridylation (Figure 2.30C). Therefore, both decay pathways (5′–3′ and 3′–5′) may act at the downstream of uridylation. I also tested a 3′–5′ exonuclease DIS3L2 which is related to DIS3 and DIS3L. While DIS3 and DIS3L function as components of exosome, DIS3L2 is known to work independently from exosome (Lubas et al., 2013; Malecki et al., 2013). It was recently shown that DIS3L2 preferentially binds to long U tails of pre-let-7 and is involved in turnover of pre-let-7 and some mRNAs in yeast and human (Chang et al., 2013; Faehnle et al., 2014; Lubas et al., 2013; Malecki et al., 2013; Ustianenko et al., 2013). My TAIL-seq experiment shows that DIS3L2 depletion results in a modest accumulation of uridylated reads (Figure 2.30C). Thus, although I cannot rule out the possibility of indirect effects, the results suggest that multiple decay pathways may participate in the removal of uridylated mRNAs. Due to the technical limitation of knockdown experiment, it is currently unclear which pathway plays a dominant role.

Interestingly, mRNAs with an oligo-U tail (U_2 and U_{3+}) responded more sensitively to the suppression of decay factors than those with a mono-U tail (U_1), suggesting that oligo-uridylated mRNAs are more rapidly degraded than mono-uridylated mRNAs (Figure 2.30). Taken together, I propose that uridylated mRNAs are subject to degradation by multiple factors, and that an oligo-U tail may serve as a decay mark for non-functional, deadenylated mRNAs.

2.3 Discussion

In conclusion, this study reveals an integral and general role of oligo-uridylation in mammalian mRNA decay (model shown in Figure 2.33). Upon deadenylation, mRNAs (with A tails shorter than ~25 nt) lose PABP and instead gain a U tail by the redundant action of TUT4 and TUT7. The oligo-U tail triggers decay by serving as a mark that is recognized by downstream decay factors. Thus, TUT4/7 function as the "writers" of the decay mark. It will be interesting in the future to identify the "readers" of the oligo-U tail and to ask if this modification can be reversed by "erasers". The LSM1–7 complex and DIS3L2 are likely candidates that recognize the oligo-U marks, but further investigations will be necessary

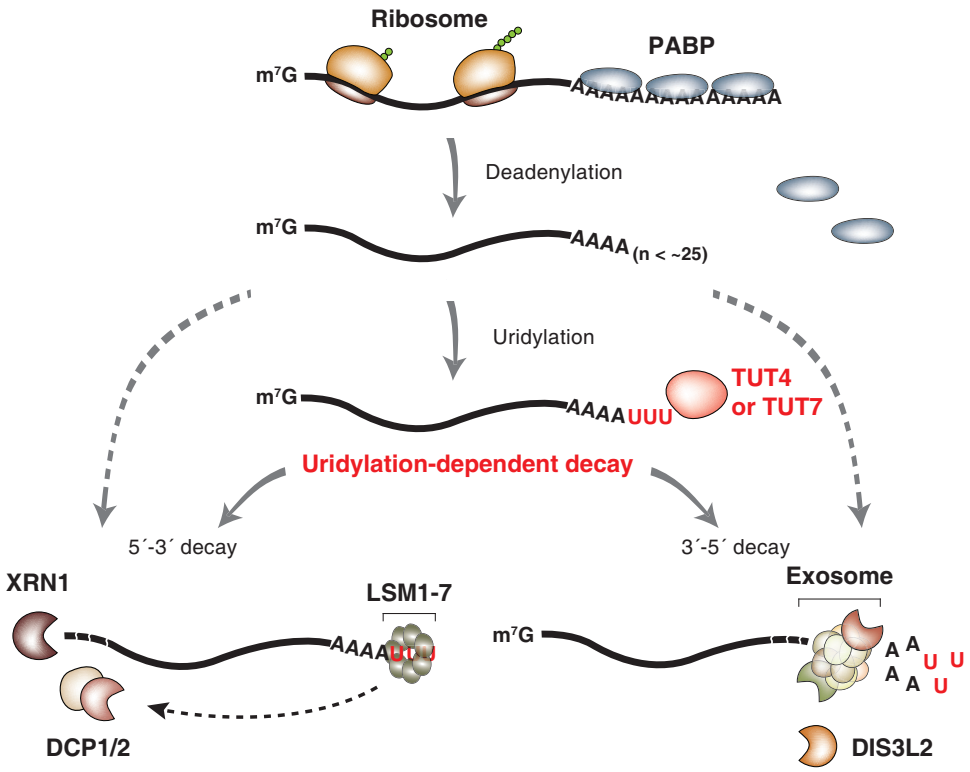

Figure 2.33 mRNA decay is generally initiated by deadenylation. PABP proteins are dissociated from mRNA as poly(A) tail becomes shorter (<~25 nt). TUT4 and TUT7 act redundantly to uridylate mRNAs with a short A tail. The U tail is in turn recognized by the downstream decay factors (uridylation-dependent mRNA decay pathway). The LSM1–7 complex binds to the U tail and facilitates decapping by the DCP1/2 complex. Decapped mRNAs are degraded by the 5′–3′ exonuclease XRN1. Alternatively, the U tail is recognized by exosome or DIS3L2 that degrade mRNA exonucleolytically from the 3′ end. It is currently unclear if and what fraction of deadenylated mRNAs are degraded through uridylation-independent alternative pathways (indicated with grey dashed lines).

to understand which factor(s) recognize the oligo-U tails mainly, whether there is any additional factor(s) that binds to the oligo-U-tails, and what is the molecular basis of the specific recognition (Lee et al., 2014b).

It is intriguing that TUT4/7 are capable of measuring poly(A) length (Figures 2.14, 2.15, and 2.20). Poly(A) tail is unlikely to form a certain structure through base-pairing, so I do not yet understand how RNA with a poly(A) tail is discriminated by TUT4/7. It would be interesting to carry out structural studies on TUT4/7 and RNA with an A tail of various length. Furthermore, I found that PABPC1 preferentially protects long poly(A) tails from uridylation (Figure 2.21). This specific inhibitory effect may come from the length dependent binding of PABPC1 (Kuhn & Pieler, 1996; Sachs et al., 1987). Thus, the combined action of TUT4/7 and PABP may selectively mark non-functional mRNAs while translationally active polyadenylated mRNAs are refractory to uridylation. Consequently, TUT4/7-mediated uridylation may provide the molecular basis for the tight control of mRNA stability according to poly(A) tail length.

I observed that oligo-uridylated mRNAs (with $\geq$2 uridines) are more sensitive than mono-uridylated mRNAs to the knockdown of TUT4/7 and decay factors. Moreover, oligo-U tails are found in a narrow range of short A tail length while mono-U tails are more loosely distributed and found in polyadenylated mRNAs as well to some extent (Chang et al., 2014b). Thus, mono-uridylation appears to be less specific than oligo-uridylation, and may be catalyzed in part by a TUT(s) other than TUT4/7. Furthermore, mono-U tails may be too short to recruit decay factors effectively. Oligo-uridylated mRNAs are detected more frequently after depletion of decay factors, indicating that they are less stable than mono-uridylated mRNAs in control cells. Therefore, oligo-U tails are likely to have a stronger effect in decay than mono-U tails do. In fission yeast and plants, it is currently unclear if there is such a distinction between oligo-U tails and mono-U tails because only a small number of reads from cloning has been analyzed thus far.

The transcriptome-wide analyses allowed us to propose a general model for the decay of poly(A)$^+$ mRNAs. In addition, given that poly(A) histone mRNA was also proposed to be uridylated by TUT4 (Schmidt et al., 2011; Su et al., 2013), it is possible that both poly(A)$^+$ mRNAs and poly(A) mRNAs are degraded by the same general principle

involving uridylation although there may be some differences in details such as the choice of downstream decay factors. In fact, I detected uridylation on histone mRNAs and on trimmed decay intermediates lacking poly(A) tail, and these U tails were also dependent on TUT4/7 (data not shown).

In addition, I found that miR-1 transfection results in an increased uridylation and facilitated decay of its targets (Figures 2.27 and 2.28). This results suggest that uridylation contributes to miRNA-mediated gene silencing by removing the body of deadenylated mRNAs. Uridylation may be involved in other decay and surveillance pathways in mammals, playing a general role. It is noted that I cannot currently assess if and to what extent uridylation-independent alternative pathway(s) contribute to bulk mRNA decay.

Tailing of mRNA is found in many eukaryotes, with some notable differences among the species. In filamentous fungus *Aspergillus nidulans*, mRNAs carry 3′ tails mixed with cytidine and uridine (Morozov et al., 2010). In a double deletion mutant of noncanonical PAPs, CutA and CutB, this "CUCU" modification was abrogated, and transcripts were stabilized, indicating that a CUCU tail also serves as a decay mark despite the difference in base composition (Morozov et al., 2012, 2010). In plants, although uridylation occurs similarly to mammals, mRNA half-life did not change in the *urt1* mutants, and the reason underlying the difference is currently unclear (Sement et al., 2013). Another variation among the species is that uridylation occurs selectively on deadenylated mRNAs in mammals and plants whereas uridylation appears to be independent of poly(A) tail length in *S. pombe* and *A. nidulans* (Morozov et al., 2010; Rissland & Norbury, 2009). Deadenylation may not be a prerequisite for uridylation in fungi as they possess shorter poly(A) tail (20–30 nt in median) than mammals (60–100 nt in median) and plants (50–60 nt in median) (Chang et al., 2014b; Morozov et al., 2010; Subtelny et al., 2014). Thus, further investigations are clearly necessary to delineate the commonalities and differences of uridylation in diverse systems.

Tailing-mediated decay is deeply conserved and found even in prokaryotes where mRNAs typically end with stem loop structure and are degraded in an adenylation-dependent manner (Belasco, 2010; Houseley et al., 2006). An oligo-A tail serves as a single-stranded toehold for 3′ exonucleases which are otherwise hindered by the terminal stem loop. A

related phenomenon was observed in budding yeast where non-canonical PAPs, Trf4 and Trf5, adenylate defective nuclear RNAs and facilitate their degradation by exosome (Houseley et al., 2006; Norbury, 2013). My current work shows that mammalian cytoplasmic mRNAs use uridylation, instead of adenylation, to promote mRNA decay. Together with previous findings (Morozov et al., 2010; Mullen & Marzluff, 2008; Rissland & Norbury, 2009), my study establishes a fundamental and conserved role for uridylation in the eukaryotic mRNA decay pathway.

2.4 Methods and Materials

Construction of TAIL-seq library

TAIL-seq was carried out as described previously (Chang et al., 2014b). Briefly, 25–50 μg of total RNA was extracted using TRIzol (Invitrogen), purified with RNeasy MinElute column (Qiagen), and rRNA-depleted by using Ribo-Zero kit (Epicentre). The RNAs were ligated to the biotinylated 3′ adaptor, and partially digested by RNase T1 (Ambion). The fragmented RNAs were precipitated with streptavidin beads, phosphorylated at the 5′ end, and gel purified (500–1,000 nt). The purified RNAs were ligated to the 5′ adaptor, reverse-transcribed, and amplified by PCR. The cDNA libraries were mixed with PhiX control library v3 (Illumina) and spike-in mixture and then sequenced by paired-end run (51 × 251 cycles) on Illumina MiSeq (small-scale TAIL-seq) or HiSeq 2500. Resulting data were processed as previously described (Chang et al., 2014b).

In vitro uridylation assay

For immunoprecipitation of FLAG-TUTases, HEK293T cells grown on 10 cm dishes were collected 48 hr after transfection with FLAG-TUTase expression plasmids (full-length human TUT4 (1–1,640 aa) and human TUT7 [1–1,495 aa]). The cells were incubated in ice-cold Buffer D (200 mM KCl, 10 mM Tris-HCl [pH 8.0], 0.2 mM EDTA) for 20 min followed by sonication on ice and centrifugation twice for 15 min at 4°C. The supernatant was incubated with 5 μL of anti-FLAG antibody-conjugated agarose beads (anti-FLAG M2

affinity gel, Sigma) with constant rotation for 1 hr at 4°C. The beads were washed six times with Buffer D. Uridylation reaction was done in a total volume of 30 μL in 3.2 mM $MgCl_2$, 1 mM DTT, 0.67 U/μl RNase inhibitor (Promega, N2515), 0.25 mM UTP, 0.45 nM of 5′ end labeled RNA, and 15 μL of immunopurified proteins on beads or 3X Flag-peptide (Sigma) eluted proteins in Buffer D. When uridylation assay was done with recombinant TUT7 (951–1,495 aa), 14 nM of protein was used. The reaction mixture was incubated at 37°C for upto 10 min. For uridylation assay in the presence of PABPC1, 10–40 nM of recombinant human PABPC1 (Origene, TP307354) was pre-incubated with RNA for 10 min and then uridylation was carried out by adding 160 nM of recombinant TUT7 (951–1,495 aa). Buffer D with final 300 mM KCl was used when uridylation assay was carried out in the presence of PABPC1. The RNA was purified from the reaction mixture by phenol extraction and run on 6 % polyacrylamide sequencing gel with 7M urea (20 x 40 cm, 0.4 mm thick) at constant 1500 V for 2 hr. The gel was exposed to phosphor imaging plate (Fujifilm) and read by Typhoon FLA 7000 (GE Healthcare). The signal intensity profile was quantified using MultiGauge v3.0 (Fujifilm). In Figure 2.19, 12.5 % polyacrylamide gel was used. The *SHOC2* 3′ UTR and *CALM1* 3′ UTR were selected as RNA substrates as they do not contain homopolymeric adenosines at the 3′ end. RNAs were synthesized by ST Pharm Inc. The list of RNA oligos is shown in Table 2.3.

Cell culture, transfection, and drug treatment

HeLa and HEK293T cells were maintained in DMEM (Welgene) supplemented with 10 % fetal bovine serum (Welgene). Knockout HeLa cell lines were generated by ToolGen Inc. by using TALENs targeting exons of *TUT2*, *TUT4*, and *TUT7*. For knockdown, HeLa cells were transfected twice with 40 nM of siRNAs using Lipofectamine 2000 (Invitrogen) for 4 days. A mixture of 2–4 different siRNAs was used to knockdown each gene. In combinatorial knockdown, I mixed siRNA pools to have a final concentration of 40 nM. I purchased siRNAs against LSM1 and DIS3L2 from ON-TARGETplus SMARTpool (Dharmacon). The sequence list of siRNAs is shown in Table 2.3. To block transcription, HeLa cells were treated with actinomycin D (Sigma, 4 μg/ml). To introduce miR-1, synthetic miR-1 mimic was transfected ~48 hours after siRNA transfection, and cells were collected every 2 hours. For plasmid transfection, HeLa cells were transfected by using Lipofectamine

2000 and HEK293T cells were transfected by the calcium-phosphate method for 2 days. Human DCP1a GSSG mutant (1–582 aa) and human DCP2 E148Q mutant (1–420 aa) plasmids are gifts from Dr. Elisa Izaurralde.

Determination of non-templated terminal nucleotidyl addition

After the primary measurement of poly(A) length from the TAIL-seq pipeline (Chang et al., 2014b), the poly(A) lengths are refined using a paired-end alignment of reads 1 and 2 to the UCSC hg19 genome using GSNAP 2013-03-31 (Wu & Nacu, 2010) to exclude genome-encoded A repeats from the measurement. First, the poly(A) length from the signal processing are considered valid when read 2 is not aligned. For those that aligned to the genome, the pairs of reads (1 and 2) are excluded from statistics when nearest alignments between them are farther away than 500,000 bp in genome coordinates so as to remove ligation artefacts. For the remaining ones, the 3′-most two nucleotides from 'matched or mismatched' ('M' in CIGAR string) are re-examined if they match to the genome. If there is any mismatch in the pairs, the first mismatched nucleotide and subsequent nucleotides including clipped ('S' in CIGAR string) are regarded as non-templated additions. Otherwise, the clipped sequences on the 3′-end of reads are considered as non-templated additions.

For the calculation of uridylation frequency or average U length, very short poly(A) tails between 1 and 4 nucleotides were excluded because a substantial fraction of them are ambiguous whether or not they come from genomic sequences or non-templated additions. Also, non-coding RNAs (mainly snoRNA precursors) and histone mRNAs were excluded due to their distinct nature of metabolism from the major portion of mRNAs. For shorter poly(A) tails ($\leq$10 nt), they were sorted again to remove artifacts from unwanted RNA ligations between the 3′ end of an mRNA and the 5′ end of abundant small RNAs (such as 5S rRNA, 5.8S rRNA, let-7, and miR-21). They are considered as poly(A) tails only if 80 % or more in the non-templated addition is composed of adenosines after trimming all consecutive uridines from the 3′ end. The length of U tails are measured by counting perfectly consecutive appearances of uridines from the 3′ end within the non-templated additions.

RNA-seq and calculation of RNA half-lives

Total RNA was extracted with TRIzol (Invitrogen), and the quality was checked by Agilent 2100 Bioanalyzer. rRNA was depleted from total RNA using Ribo-Zero (Epicentre). RNA-seq libraries were constructed by Macrogen Inc. using Illumina TruSeq RNA sample preparation kit v2. The reads were aligned to UCSC hg19 genome assembly using STAR (Dobin et al., 2013) with an option "–outFilterScoreMin 3" and splicing junction annotations generated from the NCBI RefSeq and the UCSC knownGene. The reduced RefSeq transcript set for non-overlapping representation was prepared as previously described (Chang et al., 2014b). Reads mapped to each transcript were counted using BEDTools multicov (Quinlan & Hall, 2010) with default options. Read counts of the 3, 6, and 9 hr samples were scale-normalized against those of the 0 hr sample. A scaling factor was calculated using all mRNAs with ≥5,000 raw reads from the 0 hr sample so that the 98th percentile of fold changes between 0 hr and other time points become 1 (unchanged). All mRNAs sequenced by ≥300 scaled reads at any time point were used for further processing. The scaled read counts were used for linear fitting to the log-transformed solution $logN(t) = -\lambda t + logN_0$ of the exponential decay function $dN = -\lambda N$, where N is the amount of a specific mRNA, λ is the decay rate constant, t is time elapsed after the initial time point. To ensure reliability, mRNAs with significant fitting error (residual ≥ 10 % of decay constant) were removed from the analysis. Dr. Hyeshik Chang discovered half-life values are often systematically biased by various scaling-related factors unlike the original decay constant (λ). To cancel out those errors, Dr. Hyeshik Chang shifted linearly the calculated decay constants to let the linear trend line (derived using least-squares regression) pass through the origin for decay constants from siControl and siTUT4/7 samples perpendicularly to the trend line. As this does not change the slope of trend lines for decay constants, this adjustment does not affect direct interpretations of the decay constants. Half-life of an mRNA was calculated using an equation $h = \frac{log2}{\lambda}$, where h is the half-life. The full list of calculated half-life and decay constant values are accompanied in Table 2.2.

Analysis for uridylation, poly(A) tail length and abundance of miR-1 targets

Among all transcripts having ≥1 "miR-1ab/206/613" target site in TargetScan human release 6.2 (http://www.targetscan.org/vert_61/ — "61" is not a typo), experimentally validated targets were chosen whose expression is represented by ≥100 raw reads in mock treatment and depressed by ≥30 % in RPM-normalized reads in miR-1 treated sample in the experiment by Guo and colleagues (Guo et al., 2010). "The rest" in Figure 2.27 are the remaining mRNAs after selecting the experimentally validated targets of miR-1 among the detectable mRNAs (for detection threshold, see below). For the average U length changes (top) in Figure 2.27, I selected all mRNAs whose short poly(A)$^+$ tags (5–25 nt) are ≥15 (raw reads) in the 0 hr samples of both siControl- and siTUT4/7-treated sets. For the poly(A) tail length changes (middle) and mRNA abundance changes (bottom), I selected all mRNAs whose poly(A)$^+$ tags (≥5 nt) are more than a hundred reads in the 0 hr samples of both siControl- and siTUT4/7-treated sets. Odds between short and long tails were calculated with a pseudocount of 1 to both.

Quantification of in vitro uridylation data

The signal intensity profiles (20 pixels/mm) were calculated from the whole blot phosphorimages using Fujifilm MultiGauge v3.0. For each lane, background signal is estimated using the arithmetic mean of the 25th and the 50th percentiles of the signal intensities. The signal intensities were subtracted by the estimated background level, then clipped to zero so that all intensities have zero or positive values. For the alignment of bands for size markers, the signals from a marker lane were transformed to the first and second derivatives using Savitzky-Golay filter (window=31 pixels, order=3). The marker positions were detected by searching points where the sign of first derivative turns from positive to negative, and the second derivative is smaller than 100. The detected positions of marker bands were verified by visual inspection. The function between physical position in the gel and RNA size was defined using cubic spline interpolation. The density of RNA amount in size space was calculated using the first order discrete differences of equal-width samples (0.1 nt) from cumulative density of the original intensity values. For the average length of extensions, the position having maximum signal intensity in the 0-min sample is used

as a reference position. The average length of extension was derived from an equation, $\overline{x} = \frac{\sum_p (s_p - r) I_p}{\sum_p I_p}$, where $\bar{x}$ is the average length of extension, p is a position in the gel (by 0.1 nt-wide intervals), s_p is the RNA size in nucleotides count for position p, r is the reference size of unextended RNA, and I_p is signal intensity for position p. I excluded signals from degraded products (shorter than the reference size by 3 nt) in the calculation of average extension. The average lengths of extension in Figures 2.15, 2.20, and 2.22 are shown as the difference between the average extension at 0-min and that at the other time points.

Plasmid construction

The λN sequence was amplified from pAc5.1B-λN-HA (Addgene #21302) using 'CTTGACACGAAGCTTATGGACGCACAAACACGAC' and 'GTTACTAGTGGATCCACCTTGAAAATACAAGTTTTCGGCATAGTCAGGCACGTCATAAGGATAAGCCATATGTGGAGGAGATCC' and subcloned into the pCK vector (a CMV promoter-driven vector) using EZ cloning kit (Enzynomics, EZ016S), to generate pCK-λN-HA-TEV. The coding sequences of AcGFP (from pLVX-EF1alpha-AcGFP-N1; Clontech, 631983), human AGO2 (1-859 aa), human TUT2 (1-484 aa), and human TUT4 (1-1,640 aa) were subcloned into pCK-λN-HA-TEV and pCK-HA-TEV (control). The 5XBoxB sequence was amplified from pAc5.1C-FLuc-Stop-5BoxB (Addgene, #21301) using 'CTCGCTAGCCTCGAGGCTAGCTTCCCTAAGTC' and 'GACTCTAGACTCGAGATAATATCCTCGATAGGGCCCTTC' and subcloned into the pmirGLO (Promega) using EZ cloning kit (Enzynomics, EZ016S), resulting in pmirGLO-5XBoxB.

Recombinant TUT7 purification

Human TUT7 cDNA region encoding amino acids 951-1,495 was cloned into a modified pRSF-Duet vector which has 6xHis and SUMO protein as an affinity tag at the N-terminus. The fusion protein was overexpressed in *E. coli* BL21(DE3) cells in LB medium. The cells were induced when OD600 reached a value of 0.6 by 1 mM IPTG overnight in a shaker at 20°C. Protein was purified from the soluble fraction by a nickel-chelating affinity column, followed by overnight treatment of SUMO protease Ulp1 at 4°C to cleave the

6xHis-SUMO tag, which was later removed via a second nickel-chelating column. Protein was further purified by heparin chromatography followed by gel filtration chromatography using HiLoad 16/60 Superdex-200 preparative grade column (GE Healthcare) in buffer containing 20 mM Tris-HCl, pH 8.0, 150 mM NaCl and 1mM DTT.

Luciferase assay and qRT-PCR

One day after seeding, HeLa cells grown in 24 well plates were transfected with 50 ng of pmirGLO-5XBoxB and 250 ng of HA-tagged or λN-HA-tagged protein expression plasmids using Metafectene (Biontex). Twenty four hours after transfection, cells were lysed and assayed by using Dual-Luciferase Reporter Assay (Promega) following manufacturer's instruction. Protein expression was confirmed by western blotting using anti-HA antibody (1:2,000, Santa Cruz, sc-7392) and anti-GAPDH antibody (1:2,000, Santa Cruz, sc-25778). Total RNA was prepared by using Maxwell 16 LEV simplyRNA Tissue kit (Promega, AS1280), treated with DNase I (Takara), and reverse transcribed by using RevertAid Reverse Transcriptase (Thermo Scientific, EP0442) and oligo(dT). Quantitative PCR was performed by using Power SYBR Green PCR master mix (Life Technologies, 4367659). The list of qRT-PCR primers is shown in Table 2.3.

Subcellular fractionation

To isolate the cytoplasmic and nuclear fractions, ~ 5×10^6 HeLa cells were harvested and washed with cold PBS at 1,000 xg for 2 min at 4°C. After washing, cells were resuspended in 200 µL of lysis buffer (50 mM Tris [pH 7.4], 140 mM NaCl, 1.5 mM $MgCl_2$, 0.1 % Igepal CA-630) and incubated on ice for 5 min. Centrifugation at 2,200 xg for 10 min at 4°C yielded the supernatant ("cytoplasmic" fraction). The remaining pellet was washed two times with wash buffer (50 mM Tris [pH 7.4], 140 mM NaCl, 1.5 mM $MgCl_2$) at 2,200 xg for 5 min at 4°C, followed by sonication and centrifugation at 16,000 xg for 15 min to collect the supernatant ("nuclear" fraction). The concentration of each fraction was measured by BCA assay (Pierce) and protein loading buffer was added to the lysate for western blotting.

Quantitative RT-PCR

Total RNA was extracted using TRIzol (Invitrogen), and 1–5 μg of total RNA was treated with DNase I (Takara), and reverse-transcribed by RevertAid Reverse Transcriptase (Thermo Scientific) and random hexamer. The mRNA levels were analyzed by SYBR green assays (Applied Biosystems) using ABI StepOne real-time PCR system. The list of primers used in qRT-PCR is shown in Table 2.3.

Western blotting

Cells were lysed in 0.1 % Triton X-100-Buffer D (200 mM KCl, 10 mM Tris-HCl [pH 8.0], 0.2 mM EDTA, 0.1 % Triton X-100). 50 μg of each protein sample were separated on 6-10 % SDS-PAGE gel and transferred to a methanol-activated PVDF membrane (GE Healthcare). The membrane was blocked for 1 hr in PBS-T containing 5 % milk and subsequently probed with primary antibody for ~16 hr at 4°C. After washing three times with PBS-T, the membrane was probed with anti-mouse or anti-rabbit HRP-conjugated secondary antibodies (Jackson ImmunoResearch Laboratories). The protein was detected with West Pico Luminol reagents (Thermo Scientific) by using ChemiDoc XRS+ System (BioRad). Anti-TUT7 (1:500, Sigma, HPA020620), anti-TUT2 (1:500, Abcam, ab103884), anti-GAPDH (1:2,000, Santa Cruz, sc-32233), anti-Tubulin (1:1,000, Abcam, ab52866), anti-Lamin A/C (1:500, Santa Cruz, sc-6215), and anti-PABPC1 (1:1,000, 10E10, from Dr. G.Dreyfuss) were used as primary antibodies. Anti-TUT4 (1:500) polyclonal antibody was generated from rabbit.

FACS analysis

HeLa cells were fixed in 70 % cold ethanol and incubated in 4°C for overnight. Fixed cells were treated with RNase A (5 μg/ml) and stained with propidium iodide (50 μg/ml). Stained cells were analyzed for DNA content in FACSCanto (Becton Dickinson) using FACSDiva software.

T7 endonuclease I assay

T7E1 (T7 Endonuclease I) assays were carried out by ToolGen Inc. to detect DNA mutation introduced by CRISPR-Cas9. Genomic DNA was extracted from CRISPR-Cas9 treated cell pools or single colonies. The DNA fragment encompassing the targeted region was amplified by PCR, treated with T7E1 and resolved by agarose gel electrophoresis. Primer sequences are listed in Table 2.3.

Accession	Gene name	Short poly(A) read count (siCont)	Uridylation frequency (siCont)	Number of Us on short tails (siCont)	Average U length (siCont)	Short poly(A) read count (siTUT4/7)	Uridylation frequency (siTUT4/7)	Number of Us on short tails (siTUT4/7)	Average U length (siTUT4/7)
NM_022130	GOLPH3	50	44.00%	41	0.820	28	3.57%	1	0.036
NM_004859	CLTC	83	43.37%	78	0.940	53	3.77%	2	0.038
NM_182972	IRF2BP2	46	41.30%	39	0.848	27	7.41%	2	0.074
NM_001134673	NFIA	25	40.00%	27	1.080	22	4.55%	1	0.045
NM_001127500	MET	20	40.00%	21	1.050	22	0.00%	0	0.000
NM_001001323	ATP2B1	20	40.00%	12	0.600	15	6.67%	6	0.400
NM_000179	MSH6	30	36.67%	24	0.800	15	6.67%	1	0.067
NM_003470	USP7	25	36.00%	17	0.680	18	5.56%	1	0.056
NM_002568	PABPC1	149	34.90%	146	0.980	117	10.26%	23	0.197
NM_006317	BASP1	69	34.78%	49	0.710	36	11.11%	8	0.222
NM_005559	LAMA1	23	34.78%	18	0.783	19	10.53%	3	0.158
NM_002105	H2AFX	26	34.62%	13	0.500	24	16.67%	4	0.167
NM_014014	SNRNP200	26	34.62%	26	1.000	23	13.04%	3	0.130
NM_005760	CEBPZ	26	34.62%	16	0.615	20	10.00%	4	0.200
NM_003292	TPR	26	34.62%	17	0.654	19	5.26%	7	0.368
NM_001172705	EIF4G2	128	34.38%	108	0.844	117	11.11%	23	0.197
NM_001067	TOP2A	44	34.09%	22	0.500	21	4.76%	1	0.048
NM_014445	SERP1	36	33.33%	25	0.694	17	11.76%	2	0.118
NM_006265	RAD21	18	33.33%	17	0.944	18	22.22%	14	0.778
NM_139276	STAT3	15	33.33%	6	0.400	15	6.67%	1	0.067
NM_001961	EEF2	31	32.26%	22	0.710	15	6.67%	3	0.200
NM_005968	HNRNPM	31	32.26%	23	0.742	15	6.67%	1	0.067
NM_133259	LRPPRC	41	31.71%	27	0.659	27	3.70%	1	0.037
NM_012179	FBXO7	19	31.58%	10	0.526	22	4.55%	1	0.045
NM_006644	HSPH1	19	31.58%	17	0.895	15	13.33%	3	0.200
NM_016355	DDX47	32	31.25%	24	0.750	20	15.00%	6	0.300
NM_007002	ADRM1	26	30.77%	22	0.846	16	0.00%	0	0.000
NM_005439	MLF2	23	30.43%	19	0.826	18	11.11%	3	0.167
NM_004741	NOLC1	33	30.30%	50	1.515	21	4.76%	1	0.048
NM_003927	MBD2	30	30.00%	18	0.600	18	0.00%	0	0.000
NM_001020658	PUM1	20	30.00%	9	0.450	16	6.25%	1	0.063
NM_003321	TUFM	27	29.63%	11	0.407	17	5.88%	1	0.059
NM_004924	ACTN4	17	29.41%	15	0.882	18	16.67%	10	0.556
NM_173496	MPP7	17	29.41%	7	0.412	18	0.00%	0	0.000
NM_001166417	SSX2IP	17	29.41%	7	0.412	16	6.25%	6	0.375
NM_012394	PFDN2	24	29.17%	13	0.542	21	9.52%	3	0.143
NM_018206	VPS35	24	29.17%	15	0.625	18	11.11%	6	0.333
NM_003347	UBE2L3	25	28.00%	13	0.520	19	5.26%	1	0.053
NM_005762	TRIM28	25	28.00%	15	0.600	19	15.79%	5	0.263
NM_032193	RNASEH2C	25	28.00%	15	0.600	16	12.50%	3	0.188
NM_005805	PSMD14	18	27.78%	11	0.611	16	6.25%	1	0.063
NM_183422	TSC22D1	55	27.27%	30	0.545	36	5.56%	2	0.056
NM_001256910	DDX21	48	27.08%	36	0.750	35	11.43%	8	0.229
NM_006839	IMMT	26	26.92%	16	0.615	15	6.67%	1	0.067
NM_001039590	USP9X	15	26.67%	11	0.733	16	18.75%	6	0.375
NM_014781	RB1CC1	34	26.47%	14	0.412	31	6.45%	2	0.065
NM_018890	RAC1	34	26.47%	19	0.559	22	4.55%	1	0.045
NM_003146	SSRP1	42	26.19%	27	0.643	20	10.00%	2	0.100
NM_004237	TRIP13	46	26.09%	23	0.500	24	8.33%	3	0.125
NM_002227	JAK1	54	25.93%	25	0.463	21	4.76%	3	0.143
NM_004415	DSP	27	25.93%	19	0.704	26	7.69%	2	0.077
NM_002522	NPTX1	43	25.58%	25	0.581	26	7.69%	2	0.077
NM_001206651	SH3GLB1	28	25.00%	10	0.357	28	3.57%	1	0.036
NM_014175	MRPL15	32	25.00%	26	0.813	21	9.52%	2	0.095
NM_001358	DHX15	32	25.00%	12	0.375	19	10.53%	3	0.158
NM_203413	ELP5	28	25.00%	20	0.714	21	4.76%	1	0.048
NM_001134422	CDV3	24	25.00%	11	0.458	19	5.26%	1	0.053
NM_006349	ZNHIT1	28	25.00%	22	0.786	15	20.00%	7	0.467
NM_001270482	PSMD11	24	25.00%	13	0.542	17	0.00%	0	0.000
NM_005570	LMAN1	24	25.00%	12	0.500	17	11.76%	4	0.235
NM_000108	DLD	16	25.00%	8	0.500	17	11.76%	2	0.118
NM_003365	UQCRC1	41	24.39%	30	0.732	16	0.00%	0	0.000

NM_014184	CNIH4	37	24.32%	22	0.595	26	7.69%	2	0.077
NM_001199534	C20orf24	37	24.32%	22	0.595	19	15.79%	4	0.211
NM_002858	ABCD3	33	24.24%	20	0.606	21	9.52%	2	0.095
NM_006601	PTGES3	29	24.14%	11	0.379	17	11.76%	2	0.118
NM_002037	FYN	25	24.00%	10	0.400	15	6.67%	1	0.067
NM_025065	RPF1	46	23.91%	18	0.391	22	13.64%	3	0.136
NM_003798	CTNNAL1	21	23.81%	12	0.571	17	0.00%	0	0.000
NM_001007245	IFRD1	17	23.53%	6	0.353	17	5.88%	2	0.118
NM_012433	SF3B1	30	23.33%	10	0.333	21	4.76%	1	0.048
NM_005898	CAPRIN1	56	23.21%	27	0.482	32	15.63%	12	0.375
NM_001748	CAPN2	52	23.08%	31	0.596	33	18.18%	8	0.242
NM_017934	PHIP	26	23.08%	13	0.500	25	8.00%	3	0.120
NM_030782	CLPTM1L	61	22.95%	22	0.361	37	2.70%	2	0.054
NM_000075	CDK4	35	22.86%	15	0.429	23	0.00%	0	0.000
NM_001271969	HSP90AB1	171	22.81%	68	0.398	93	11.83%	14	0.151
NM_006430	CCT4	57	22.81%	31	0.544	31	3.23%	1	0.032
NM_001201483	ENO1	110	22.73%	73	0.664	56	17.86%	17	0.304
NM_004698	PRPF3	22	22.73%	5	0.227	15	0.00%	0	0.000
NM_001037637	BTF3	53	22.64%	25	0.472	40	12.50%	6	0.150
NM_006761	YWHAE	31	22.58%	10	0.323	37	8.11%	4	0.108
NM_006452	PAICS	31	22.58%	12	0.387	25	16.00%	5	0.200
NM_031243	HNRNPA2B1	71	22.54%	33	0.465	49	12.24%	7	0.143
NM_006016	CD164	40	22.50%	11	0.275	39	2.56%	2	0.051
NM_002803	PSMC2	40	22.50%	13	0.325	18	5.56%	2	0.111
NM_022061	MRPL17	40	22.50%	22	0.550	17	0.00%	0	0.000
NM_001134484	TOMM5	27	22.22%	9	0.333	18	16.67%	3	0.167
NM_001184985	WNK1	18	22.22%	7	0.389	24	8.33%	2	0.083
NM_014933	SEC31A	18	22.22%	6	0.333	16	18.75%	3	0.188
NM_003379	EZR	59	22.03%	33	0.559	34	8.82%	4	0.118
NM_001001563	TIMM50	32	21.88%	12	0.375	16	12.50%	2	0.125
NM_001142298	SQSTM1	55	21.82%	30	0.545	32	3.13%	1	0.031
NM_016304	RSL24D1	23	21.74%	10	0.435	25	8.00%	6	0.240
NM_016237	ANAPC5	23	21.74%	9	0.391	19	5.26%	1	0.053
NM_003785	PAGE1	23	21.74%	6	0.261	15	0.00%	0	0.000
NM_080653	ATP6V1E2	37	21.62%	14	0.378	42	19.05%	8	0.190
NM_032359	CMSS1	37	21.62%	22	0.595	20	5.00%	1	0.050
NM_002810	PSMD4	37	21.62%	17	0.459	18	11.11%	2	0.111
NM_006622	PLK2	28	21.43%	12	0.429	25	4.00%	1	0.040
NM_003137	SRPK1	47	21.28%	21	0.447	29	20.69%	8	0.276
NM_145869	ANXA11	47	21.28%	18	0.383	26	7.69%	2	0.077
NM_002808	PSMD2	33	21.21%	20	0.606	27	14.81%	4	0.148
NM_178812	MTDH	33	21.21%	15	0.455	21	9.52%	2	0.095
NM_001823	CKB	33	21.21%	10	0.303	20	10.00%	2	0.100
NM_003486	SLC7A5	85	21.18%	34	0.400	51	3.92%	3	0.059
NM_001271014	KTN1	52	21.15%	26	0.500	22	4.55%	1	0.045
NM_001267809	ILF2	38	21.05%	13	0.342	23	0.00%	0	0.000
NM_006838	METAP2	43	20.93%	19	0.442	24	0.00%	0	0.000
NM_001098507	ZNF207	24	20.83%	11	0.458	22	9.09%	4	0.182
NM_006666	RUVBL2	24	20.83%	9	0.375	20	5.00%	4	0.200
NM_014394	GHITM	24	20.83%	9	0.375	16	0.00%	0	0.000
NM_030674	SLC38A1	53	20.75%	20	0.377	45	8.89%	5	0.111
NM_001539	DNAJA1	58	20.69%	24	0.414	42	4.76%	5	0.119
NM_001068	TOP2B	29	20.69%	14	0.483	22	9.09%	5	0.227
NM_001271918	SEC11A	29	20.69%	9	0.310	18	11.11%	2	0.111
NM_001033112	PAIP2	63	20.63%	33	0.524	34	11.76%	6	0.176
NM_032360	ACBD6	34	20.59%	20	0.588	29	0.00%	0	0.000
NM_016491	MRPL37	34	20.59%	18	0.529	25	4.00%	1	0.040
NM_002167	ID3	39	20.51%	9	0.231	34	5.88%	2	0.059
NM_004261	SEP15	39	20.51%	11	0.282	21	14.29%	5	0.238
NM_001316	CSE1L	114	20.18%	39	0.342	68	7.35%	8	0.118
NM_031844	HNRNPU	110	20.00%	37	0.336	52	1.92%	2	0.038
NM_003368	USP1	50	20.00%	20	0.400	37	5.41%	2	0.054
NM_014412	CACYBP	40	20.00%	16	0.400	38	13.16%	8	0.211
NM_001098576	TMBIM6	40	20.00%	14	0.350	22	22.73%	6	0.273
NM_006938	SNRPD1	35	20.00%	12	0.343	24	4.17%	1	0.042
NM_006513	SARS	40	20.00%	16	0.400	18	0.00%	0	0.000

NM_020532	RTN4	25	20.00%	8	0.320	21	4.76%	1	0.048
NM_001042749	STAG2	25	20.00%	12	0.480	19	0.00%	0	0.000
NM_001130007	GSPT1	20	20.00%	7	0.350	21	9.52%	4	0.190
NM_005839	SRRM1	25	20.00%	5	0.200	15	6.67%	1	0.067
NM_001134445	DDAH1	15	20.00%	7	0.467	15	26.67%	4	0.267
NM_003910	BUD31	56	19.64%	18	0.321	51	7.84%	7	0.137
NM_001404	EEF1G	41	19.51%	19	0.463	35	5.71%	2	0.057
NM_002266	KPNA2	108	19.44%	33	0.306	78	5.13%	6	0.077
NM_001253	CDC5L	36	19.44%	11	0.306	22	4.55%	1	0.045
NM_001904	CTNNB1	67	19.40%	20	0.299	34	5.88%	5	0.147
NM_006367	CAP1	31	19.35%	14	0.452	25	4.00%	1	0.040
NM_006232	POLR2H	31	19.35%	10	0.323	22	0.00%	0	0.000
NM_014765	TOMM20	31	19.35%	7	0.226	20	0.00%	0	0.000
NM_018955	UBB	119	19.33%	43	0.361	99	3.03%	4	0.040
NM_001762	CCT6A	78	19.23%	24	0.308	55	5.45%	5	0.091
NM_006585	CCT8	52	19.23%	15	0.288	42	4.76%	3	0.071
NM_006904	PRKDC	26	19.23%	9	0.346	17	11.76%	2	0.118
NM_007040	HNRNPUL1	26	19.23%	10	0.385	17	0.00%	0	0.000
NM_015462	NOL11	26	19.23%	10	0.385	16	0.00%	0	0.000
NM_004559	YBX1	120	19.17%	42	0.350	65	4.62%	4	0.062
NM_031966	CCNB1	63	19.05%	29	0.460	32	0.00%	0	0.000
NM_001271736	COPZ1	42	19.05%	14	0.333	15	0.00%	0	0.000
NM_080794	MRPL39	21	19.05%	7	0.333	16	0.00%	0	0.000
NM_001875	CPS1	142	19.01%	50	0.352	105	12.38%	17	0.162
NM_003753	EIF3D	37	18.92%	9	0.243	27	7.41%	6	0.222
NM_016451	COPB1	37	18.92%	10	0.270	22	9.09%	2	0.091
NM_006082	TUBA1B	53	18.87%	24	0.453	34	11.76%	6	0.176
NM_001165258	TMEM14C	48	18.75%	12	0.250	27	0.00%	0	0.000
NM_024297	PHF23	32	18.75%	9	0.281	15	0.00%	0	0.000
NM_001618	PARP1	16	18.75%	4	0.250	15	13.33%	2	0.133
NM_001191003	GSTO1	59	18.64%	16	0.271	38	2.63%	1	0.026
NM_080391	PTP4A2	59	18.64%	21	0.356	27	0.00%	0	0.000
NM_001018159	NAE1	43	18.60%	21	0.488	28	7.14%	4	0.143
NM_001126103	RACGAP1	27	18.52%	12	0.444	26	11.54%	4	0.154
NM_031157	HNRNPA1	65	18.46%	24	0.369	43	4.65%	2	0.047
NM_001160233	ATP1A1	38	18.42%	9	0.237	32	9.38%	6	0.188
NM_031420	MRPL9	38	18.42%	12	0.316	22	13.64%	6	0.273
NM_001197220	PDE4D	49	18.37%	23	0.469	31	9.68%	4	0.129
NM_001746	CANX	49	18.37%	13	0.265	29	10.34%	3	0.103
NM_177983	PPM1G	49	18.37%	15	0.306	28	10.71%	5	0.179
NM_004396	DDX5	49	18.37%	16	0.327	26	3.85%	2	0.077
NM_021129	PPA1	120	18.33%	44	0.367	86	2.33%	2	0.023
NM_002271	IPO5	55	18.18%	15	0.273	52	9.62%	6	0.115
NM_144772	APOA1BP	44	18.18%	14	0.318	19	5.26%	1	0.053
NM_018428	UTP6	33	18.18%	14	0.424	25	8.00%	2	0.080
NM_000224	KRT18	50	18.00%	18	0.360	40	5.00%	3	0.075
NM_003299	HSP90B1	50	18.00%	14	0.280	37	0.00%	0	0.000
NM_005336	HDLBP	117	17.95%	40	0.342	39	5.13%	2	0.051
NM_006191	PA2G4	28	17.86%	7	0.250	20	15.00%	3	0.150
NM_001159677	SYNCRIP	28	17.86%	10	0.357	19	0.00%	0	0.000
NM_003463	PTP4A1	129	17.83%	37	0.287	99	9.09%	12	0.121
NM_002792	PSMA7	45	17.78%	12	0.267	15	6.67%	2	0.133
NM_005051	QARS	34	17.65%	10	0.294	20	10.00%	2	0.100
NM_001039091	PRPS2	17	17.65%	5	0.294	22	0.00%	0	0.000
NM_006445	PRPF8	17	17.65%	5	0.294	18	5.56%	2	0.111
NM_181672	OGT	17	17.65%	5	0.294	16	0.00%	0	0.000
NM_012479	YWHAG	17	17.65%	5	0.294	15	6.67%	1	0.067
NM_006330	LYPLA1	40	17.50%	9	0.225	16	0.00%	0	0.000
NM_004494	HDGF	63	17.46%	14	0.222	45	4.44%	3	0.067
NM_001173454	PDHA1	23	17.39%	9	0.391	18	0.00%	0	0.000
NM_032378	EEF1D	58	17.24%	25	0.431	41	0.00%	0	0.000
NM_002951	RPN2	29	17.24%	7	0.241	17	11.76%	3	0.176
NM_001078166	SRSF1	29	17.24%	11	0.379	17	0.00%	0	0.000
NM_002495	NDUFS4	35	17.14%	10	0.286	27	7.41%	4	0.148
NM_001267818	OSTC	35	17.14%	7	0.200	25	8.00%	2	0.080
NM_003380	VIM	111	17.12%	52	0.468	60	6.67%	10	0.167

NM_004134	HSPA9	118	16.95%	35	0.297	81	9.88%	12	0.148
NM_001017963	HSP90AA1	132	16.67%	54	0.409	21	4.76%	1	0.048
NM_001416	EIF4A1	54	16.67%	28	0.519	46	2.17%	1	0.022
NM_152713	STT3A	42	16.67%	10	0.238	26	7.69%	3	0.115
NM_014390	SND1	36	16.67%	14	0.389	24	12.50%	6	0.250
NM_006335	TIMM17A	24	16.67%	7	0.292	34	0.00%	0	0.000
NM_033055	HIAT1	36	16.67%	7	0.194	21	9.52%	2	0.095
NM_001134493	TOMM6	36	16.67%	17	0.472	20	15.00%	4	0.200
NM_007006	NUDT21	30	16.67%	11	0.367	23	4.35%	1	0.043
NM_017840	MRPL16	30	16.67%	6	0.200	16	12.50%	2	0.125
NM_015878	AZIN1	18	16.67%	4	0.222	25	4.00%	1	0.040
NM_001258316	ECT2	24	16.67%	8	0.333	19	10.53%	3	0.158
NM_000317	PTS	18	16.67%	5	0.278	22	9.09%	2	0.091
NM_013411	AK2	24	16.67%	5	0.208	16	18.75%	5	0.313
NM_181892	UBE2D3	18	16.67%	6	0.333	20	15.00%	3	0.150
NM_005891	ACAT2	18	16.67%	3	0.167	16	6.25%	3	0.188
NM_012073	CCT5	223	16.59%	66	0.296	160	4.38%	14	0.088
NM_016589	TIMMDC1	67	16.42%	17	0.254	45	2.22%	1	0.022
NM_003016	SRSF2	49	16.33%	11	0.224	37	8.11%	6	0.162
NM_001159936	EBNA1BP2	43	16.28%	15	0.349	35	0.00%	0	0.000
NM_003144	SSR1	80	16.25%	35	0.438	44	4.55%	2	0.045
NM_001018067	SERBP1	142	16.20%	58	0.408	109	4.59%	6	0.055
NM_004766	COPB2	68	16.18%	32	0.471	23	8.70%	5	0.217
NM_001242891	CSDE1	62	16.13%	17	0.274	46	0.00%	0	0.000
NM_002195	INSL4	31	16.13%	9	0.290	27	3.70%	1	0.037
NM_013986	EWSR1	31	16.13%	7	0.226	24	16.67%	5	0.208
NM_003720	PSMG1	31	16.13%	6	0.194	23	0.00%	0	0.000
NM_003000	SDHB	31	16.13%	5	0.161	21	0.00%	0	0.000
NM_173647	RNF149	31	16.13%	8	0.258	17	0.00%	0	0.000
NM_001037494	DYNLL1	56	16.07%	14	0.250	30	3.33%	1	0.033
NM_001018136	NME1-NME2	106	16.04%	29	0.274	68	10.29%	9	0.132
NM_005917	MDH1	75	16.00%	19	0.253	41	4.88%	7	0.171
NM_006023	CDC123	50	16.00%	16	0.320	31	3.23%	2	0.065
NM_001013439	FXR1	25	16.00%	8	0.320	25	8.00%	5	0.200
NM_001145408	NONO	25	16.00%	6	0.240	20	0.00%	0	0.000
NM_000895	LTA4H	25	16.00%	5	0.200	19	0.00%	0	0.000
NM_004219	PTTG1	44	15.91%	21	0.477	36	8.33%	3	0.083
NM_001494	GDI2	38	15.79%	9	0.237	24	8.33%	3	0.125
NM_006496	GNAI3	38	15.79%	13	0.342	24	0.00%	0	0.000
NM_001261412	DCTN2	19	15.79%	5	0.263	17	23.53%	9	0.529
NM_004582	RABGGTB	64	15.63%	19	0.297	33	6.06%	4	0.121
NM_018060	IARS2	32	15.63%	8	0.250	26	0.00%	0	0.000
NM_002788	PSMA3	32	15.63%	6	0.188	24	0.00%	0	0.000
NM_001142418	MORF4L2	32	15.63%	7	0.219	21	4.76%	5	0.238
NM_004323	BAG1	32	15.63%	5	0.156	18	5.56%	1	0.056
NM_014267	C11orf58	32	15.63%	8	0.250	17	5.88%	1	0.059
NM_002787	PSMA2	77	15.58%	22	0.286	51	3.92%	2	0.039
NM_003870	IQGAP1	58	15.52%	13	0.224	43	4.65%	3	0.070
NM_001098616	C1orf43	78	15.38%	18	0.231	52	7.69%	5	0.096
NM_032408	BAZ1B	39	15.38%	9	0.231	27	7.41%	2	0.074
NM_001025248	DUT	26	15.38%	10	0.385	23	0.00%	0	0.000
NM_001193495	ADAR	26	15.38%	6	0.231	15	6.67%	2	0.133
NM_001267557	PDCD6	46	15.22%	15	0.326	46	6.52%	5	0.109
NM_182776	MCM7	46	15.22%	23	0.500	38	13.16%	8	0.211
NM_005918	MDH2	46	15.22%	8	0.174	25	16.00%	5	0.200
NM_002014	FKBP4	46	15.22%	17	0.370	25	12.00%	4	0.160
NM_002106	H2AFZ	99	15.15%	24	0.242	63	7.94%	6	0.095
NM_021074	NDUFV2	33	15.15%	7	0.212	28	7.14%	2	0.071
NM_002790	PSMA5	73	15.07%	16	0.219	54	7.41%	8	0.148
NM_003564	TAGLN2	73	15.07%	15	0.205	40	5.00%	3	0.075
NM_001099645	RPL22L1	80	15.00%	15	0.188	27	3.70%	1	0.037
NM_018841	GNG12	20	15.00%	8	0.400	21	9.52%	2	0.095
NM_152862	ARPC2	20	15.00%	11	0.550	15	0.00%	0	0.000
NM_003404	YWHAB	47	14.89%	26	0.553	25	0.00%	0	0.000
NM_014597	DNTTIP2	27	14.81%	5	0.185	26	3.85%	1	0.038
NM_000305	PON2	61	14.75%	17	0.279	32	6.25%	3	0.094

NM_004034	ANXA7	34	14.71%	10	0.294	30	0.00%	0	0.000
NM_004888	ATP6V1G1	34	14.71%	8	0.235	27	3.70%	1	0.037
NM_017758	ALKBH5	34	14.71%	7	0.206	25	0.00%	0	0.000
NM_006819	STIP1	34	14.71%	7	0.206	23	0.00%	0	0.000
NM_001142930	API5	34	14.71%	7	0.206	15	20.00%	3	0.200
NM_001113203	NACA	82	14.63%	30	0.366	54	3.70%	2	0.037
NM_016359	NUSAP1	41	14.63%	12	0.293	34	5.88%	3	0.088
NM_021732	AVPI1	41	14.63%	10	0.244	24	8.33%	2	0.083
NM_006196	PCBP1	41	14.63%	11	0.268	19	0.00%	0	0.000
NM_006597	HSPA8	424	14.62%	111	0.262	308	2.60%	14	0.045
NM_001664	RHOA	48	14.58%	11	0.229	40	2.50%	1	0.025
NM_002710	PPP1CC	55	14.55%	18	0.327	31	6.45%	2	0.065
NM_007178	STRAP	55	14.55%	12	0.218	30	3.33%	2	0.067
NM_001254752	UQCRB	76	14.47%	27	0.355	48	6.25%	3	0.063
NM_030969	TMEM14B	49	14.29%	10	0.204	34	5.88%	3	0.088
NM_001258438	TARS	49	14.29%	12	0.245	34	5.88%	2	0.059
NM_001916	CYC1	42	14.29%	10	0.238	29	0.00%	0	0.000
NM_016039	C14orf166	35	14.29%	8	0.229	28	7.14%	3	0.107
NM_014142	NUDT5	42	14.29%	7	0.167	18	5.56%	2	0.111
NM_001257293	HNRNPH1	35	14.29%	8	0.229	24	8.33%	4	0.167
NM_004593	TRA2B	35	14.29%	7	0.200	16	0.00%	0	0.000
NM_001537	HSBP1	28	14.29%	6	0.214	22	9.09%	2	0.091
NM_003902	FUBP1	28	14.29%	8	0.286	19	10.53%	4	0.211
NM_002629	PGAM1	28	14.29%	6	0.214	15	13.33%	3	0.200
NM_001202485	HSPE1-MOB4	21	14.29%	6	0.286	20	0.00%	0	0.000
NM_001747	CAPG	21	14.29%	3	0.143	20	5.00%	1	0.050
NM_000937	POLR2A	21	14.29%	6	0.286	19	5.26%	1	0.053
NM_003289	TPM2	21	14.29%	4	0.190	15	0.00%	0	0.000
NM_003011	SET	85	14.12%	23	0.271	79	7.59%	11	0.139
NM_001166285	CCT7	149	14.09%	41	0.275	83	6.02%	6	0.072
NM_003400	XPO1	71	14.08%	20	0.282	37	8.11%	4	0.108
NM_001033	RRM1	57	14.04%	12	0.211	31	6.45%	4	0.129
NM_001686	ATP5B	143	13.99%	31	0.217	110	10.00%	18	0.164
NM_000849	GSTM3	43	13.95%	9	0.209	31	3.23%	1	0.032
NM_005801	EIF1	43	13.95%	9	0.209	29	0.00%	0	0.000
NM_006636	MTHFD2	43	13.95%	17	0.395	15	0.00%	0	0.000
NM_004539	NARS	36	13.89%	16	0.444	27	3.70%	2	0.074
NM_013230	CD24	36	13.89%	10	0.278	20	15.00%	3	0.150
NM_001012662	SLC3A2	29	13.79%	4	0.138	35	2.86%	2	0.057
NM_005754	G3BP1	29	13.79%	7	0.241	21	4.76%	1	0.048
NM_001143674	MPC2	51	13.73%	10	0.196	18	5.56%	2	0.111
NM_005063	SCD	95	13.68%	21	0.221	56	5.36%	6	0.107
NM_002796	PSMB4	117	13.68%	37	0.316	73	5.48%	4	0.055
NM_001165414	LDHA	205	13.66%	54	0.263	150	5.33%	10	0.067
NM_004548	NDUFB10	44	13.64%	7	0.159	23	4.35%	1	0.043
NM_001198879	ATP5J2-PTCD1	22	13.64%	9	0.409	25	8.00%	2	0.080
NM_006164	NFE2L2	22	13.64%	3	0.136	21	0.00%	0	0.000
NM_003290	TPM4	22	13.64%	5	0.227	18	11.11%	2	0.111
NM_004939	DDX1	74	13.51%	19	0.257	39	7.69%	4	0.103
NM_006118	HAX1	37	13.51%	8	0.216	26	0.00%	0	0.000
NM_001178017	DBI	67	13.43%	11	0.164	25	4.00%	1	0.040
NM_000026	ADSL	45	13.33%	19	0.422	38	10.53%	4	0.105
NM_006304	SHFM1	45	13.33%	10	0.222	24	0.00%	0	0.000
NM_000100	CSTB	45	13.33%	10	0.222	19	5.26%	1	0.053
NM_003094	SNRPE	30	13.33%	6	0.200	18	5.56%	1	0.056
NM_002156	HSPD1	30	13.33%	9	0.300	18	11.11%	2	0.111
NM_002812	PSMD8	15	13.33%	3	0.200	21	4.76%	2	0.095
NM_024834	MCMBP	15	13.33%	4	0.267	16	6.25%	1	0.063
NM_004537	NAP1L1	53	13.21%	10	0.189	31	3.23%	1	0.032
NM_000884	IMPDH2	38	13.16%	17	0.447	24	8.33%	2	0.083
NM_004280	EEF1E1	38	13.16%	9	0.237	22	13.64%	5	0.227
NM_003128	SPTBN1	61	13.11%	13	0.213	39	5.13%	2	0.051
NM_001199954	ACTG1	115	13.04%	22	0.191	96	10.42%	11	0.115
NM_057175	NAA15	46	13.04%	15	0.326	29	13.79%	5	0.172
NM_005507	CFL1	23	13.04%	4	0.174	32	12.50%	7	0.219
NM_007173	PRSS23	23	13.04%	5	0.217	22	9.09%	2	0.091

NM_002497	NEK2	31	12.90%	5	0.161	25	8.00%	2	0.080
NM_003849	SUCLG1	31	12.90%	9	0.290	22	9.09%	3	0.136
NM_031370	HNRNPD	31	12.90%	7	0.226	20	5.00%	1	0.050
NM_001144944	MYL12B	70	12.86%	17	0.243	62	11.29%	9	0.145
NM_001356	DDX3X	47	12.77%	8	0.170	28	10.71%	7	0.250
NM_018648	NOP10	47	12.77%	17	0.362	27	0.00%	0	0.000
NM_004343	CALR	157	12.74%	33	0.210	76	10.53%	11	0.145
NM_002592	PCNA	55	12.73%	15	0.273	49	0.00%	0	0.000
NM_001002031	ATP5G2	63	12.70%	12	0.190	32	3.13%	1	0.031
NM_001003	RPLP1	284	12.68%	59	0.208	149	2.68%	4	0.027
NM_006098	GNB2L1	380	12.63%	95	0.250	232	6.90%	20	0.086
NM_006305	ANP32A	32	12.50%	6	0.188	30	6.67%	2	0.067
NM_001080415	U2SURP	40	12.50%	10	0.250	18	11.11%	4	0.222
NM_016126	HSPB11	32	12.50%	5	0.156	23	0.00%	0	0.000
NM_017838	NHP2	32	12.50%	11	0.344	18	0.00%	0	0.000
NM_015161	ARL6IP1	24	12.50%	5	0.208	21	9.52%	3	0.143
NM_014639	TTC37	24	12.50%	4	0.167	17	0.00%	0	0.000
NM_001256510	SSBP1	24	12.50%	3	0.125	16	0.00%	0	0.000
NM_020194	MFF	16	12.50%	2	0.125	15	0.00%	0	0.000
NM_030816	ANKRD13C	16	12.50%	4	0.250	15	0.00%	0	0.000
NM_000146	FTL	123	12.20%	38	0.309	71	1.41%	1	0.014
NM_005003	NDUFAB1	41	12.20%	6	0.146	21	0.00%	0	0.000
NM_003017	SRSF3	74	12.16%	10	0.135	47	4.26%	2	0.043
NM_000967	RPL3	99	12.12%	13	0.131	35	0.00%	0	0.000
NM_032704	TUBA1C	66	12.12%	11	0.167	39	7.69%	3	0.077
NM_001031684	SRSF7	33	12.12%	7	0.212	23	17.39%	8	0.348
NM_002493	NDUFB6	33	12.12%	6	0.182	22	9.09%	2	0.091
NM_001101	ACTB	157	12.10%	29	0.185	84	3.57%	3	0.036
NM_001256799	GAPDH	248	12.10%	66	0.266	164	12.20%	29	0.177
NM_001545	ICT1	58	12.07%	10	0.172	29	10.34%	4	0.138
NM_001417	EIF4B	108	12.04%	13	0.120	67	5.97%	8	0.119
NM_001827	CKS2	25	12.00%	4	0.160	30	3.33%	1	0.033
NM_016604	KDM3B	25	12.00%	5	0.200	20	10.00%	2	0.100
NM_001144831	PHB2	67	11.94%	14	0.209	50	2.00%	1	0.020
NM_016542	MST4	42	11.90%	12	0.286	21	4.76%	1	0.048
NM_002140	HNRNPK	42	11.90%	6	0.143	16	12.50%	2	0.125
NM_002789	PSMA4	59	11.86%	22	0.373	42	2.38%	2	0.048
NM_000975	RPL11	59	11.86%	10	0.169	38	10.53%	4	0.105
NM_015965	NDUFA13	85	11.76%	16	0.188	79	10.13%	9	0.114
NM_015895	GMNN	51	11.76%	15	0.294	29	3.45%	1	0.034
NM_004708	PDCD5	34	11.76%	6	0.176	28	10.71%	6	0.214
NM_203497	COMMD6	34	11.76%	7	0.206	27	11.11%	5	0.185
NM_005324	H3F3B	34	11.76%	6	0.176	23	13.04%	3	0.130
NM_006830	UQCR11	34	11.76%	7	0.206	17	0.00%	0	0.000
NM_007157	ZXDB	17	11.76%	2	0.118	20	10.00%	2	0.100
NM_002065	GLUL	17	11.76%	4	0.235	18	11.11%	3	0.167
NM_080425	GNAS	17	11.76%	3	0.176	17	0.00%	0	0.000
NM_212552	BOLA3	17	11.76%	3	0.176	16	0.00%	0	0.000
NM_178191	ATPIF1	17	11.76%	4	0.235	16	6.25%	1	0.063
NM_005066	SFPQ	43	11.63%	8	0.186	36	0.00%	0	0.000
NM_007276	CBX3	43	11.63%	8	0.186	32	9.38%	4	0.125
NM_001198842	CCT2	181	11.60%	36	0.199	173	2.31%	5	0.029
NM_016047	SF3B14	52	11.54%	13	0.250	37	10.81%	5	0.135
NM_021141	XRCC5	52	11.54%	9	0.173	36	5.56%	3	0.083
NM_000521	HEXB	26	11.54%	4	0.154	26	3.85%	1	0.038
NM_001862	COX5B	26	11.54%	3	0.115	24	8.33%	3	0.125
NM_002306	LGALS3	26	11.54%	8	0.308	22	9.09%	3	0.136
NM_006837	COPS5	26	11.54%	9	0.346	21	9.52%	4	0.190
NM_031206	LAS1L	26	11.54%	4	0.154	19	0.00%	0	0.000
NM_014236	GNPAT	26	11.54%	4	0.154	18	5.56%	1	0.056
NM_001206796	PKM	113	11.50%	19	0.168	64	9.38%	6	0.094
NM_005620	S100A11	61	11.48%	9	0.148	32	12.50%	4	0.125
NM_020189	ENY2	35	11.43%	5	0.143	21	14.29%	3	0.143
NM_001533	HNRNPL	79	11.39%	13	0.165	68	0.00%	0	0.000
NM_002709	PPP1CB	79	11.39%	14	0.177	54	1.85%	1	0.019
NM_002032	FTH1	53	11.32%	18	0.340	38	5.26%	2	0.053

NM_004553	NDUFS6	72	11.11%	11	0.153	49	12.24%	10	0.204
NM_003134	SRP14	54	11.11%	7	0.130	44	9.09%	5	0.114
NM_018685	ANLN	54	11.11%	14	0.259	36	0.00%	0	0.000
NM_002634	PHB	45	11.11%	15	0.333	34	8.82%	5	0.147
NM_016145	WDR83OS	36	11.11%	6	0.167	27	7.41%	2	0.074
NM_001099285	PTMA	36	11.11%	7	0.194	27	3.70%	1	0.037
NM_016131	RAB10	36	11.11%	11	0.306	22	0.00%	0	0.000
NM_001162429	PDCD6IP	36	11.11%	7	0.194	15	6.67%	3	0.200
NM_003348	UBE2N	27	11.11%	4	0.148	18	5.56%	1	0.056
NM_148976	PSMA1	27	11.11%	5	0.185	17	0.00%	0	0.000
NM_015343	CTDNEP1	27	11.11%	6	0.222	15	6.67%	1	0.067
NM_006827	TMED10	18	11.11%	6	0.333	15	6.67%	1	0.067
NM_000981	RPL19	191	10.99%	29	0.152	115	6.09%	8	0.070
NM_033251	RPL13	182	10.99%	28	0.154	103	3.88%	6	0.058
NM_001743	CALM2	82	10.98%	16	0.195	61	3.28%	5	0.082
NM_005016	PCBP2	55	10.91%	11	0.200	42	4.76%	2	0.048
NM_032731	TXNDC17	37	10.81%	6	0.162	25	16.00%	5	0.200
NM_004446	EPRS	65	10.77%	15	0.231	31	0.00%	0	0.000
NM_006815	TMED2	93	10.75%	14	0.151	51	7.84%	4	0.078
NM_031903	MRPL32	28	10.71%	8	0.286	27	0.00%	0	0.000
NM_012426	SF3B3	28	10.71%	7	0.250	20	5.00%	1	0.050
NM_000990	RPL27A	28	10.71%	4	0.143	17	11.76%	2	0.118
NM_001146110	MIER1	28	10.71%	4	0.143	15	13.33%	3	0.200
NM_001152	SLC25A5	103	10.68%	13	0.126	66	3.03%	2	0.030
NM_001003652	SMAD2	38	10.53%	6	0.158	18	5.56%	1	0.056
NM_001065	TNFRSF1A	38	10.53%	9	0.237	18	0.00%	0	0.000
NM_025238	BTBD1	19	10.53%	2	0.105	17	17.65%	3	0.176
NM_001436	FBL	19	10.53%	4	0.211	17	17.65%	7	0.412
NM_001199163	PSMC5	19	10.53%	2	0.105	15	0.00%	0	0.000
NM_001019	RPS15A	58	10.34%	7	0.121	51	1.96%	3	0.059
NM_004168	SDHA	29	10.34%	5	0.172	27	3.70%	1	0.037
NM_022746	MARC1	29	10.34%	6	0.207	22	4.55%	1	0.045
NM_001786	CDK1	39	10.26%	6	0.154	29	6.90%	3	0.103
NM_005742	PDIA6	39	10.26%	6	0.154	15	6.67%	2	0.133
NM_000972	RPL7A	196	10.20%	25	0.128	142	4.23%	6	0.042
NM_003472	DEK	49	10.20%	6	0.122	44	0.00%	0	0.000
NM_001688	ATP5F1	49	10.20%	8	0.163	30	0.00%	0	0.000
NM_005998	CCT3	118	10.17%	18	0.153	71	4.23%	5	0.070
NM_002799	PSMB7	59	10.17%	9	0.153	27	3.70%	1	0.037
NM_002795	PSMB3	160	10.00%	23	0.144	133	5.26%	7	0.053
NM_001001973	ATP5C1	40	10.00%	6	0.150	46	2.17%	1	0.022
NM_006694	JTB	50	10.00%	8	0.160	27	0.00%	0	0.000
NM_030939	C6orf62	60	10.00%	10	0.167	17	0.00%	0	0.000
NM_003334	UBA1	50	10.00%	6	0.120	22	4.55%	1	0.045
NM_001242597	TMEM147	30	10.00%	3	0.100	27	3.70%	1	0.037
NM_016497	MRPL51	30	10.00%	3	0.100	26	7.69%	2	0.077
NM_001204527	SSR4	40	10.00%	7	0.175	15	6.67%	1	0.067
NM_001127223	CD59	30	10.00%	4	0.133	21	14.29%	3	0.143
NM_000374	UROD	30	10.00%	6	0.200	21	4.76%	1	0.048
NM_004905	PRDX6	30	10.00%	6	0.200	15	0.00%	0	0.000
NM_004541	NDUFA1	30	10.00%	4	0.133	15	0.00%	0	0.000
NM_002496	NDUFS8	20	10.00%	5	0.250	22	4.55%	4	0.182
NM_001139499	LSM5	20	10.00%	4	0.200	19	10.53%	3	0.158
NM_006628	ARPP19	20	10.00%	3	0.150	19	5.26%	1	0.053
NM_032796	SYAP1	20	10.00%	4	0.200	16	12.50%	2	0.125
NM_016070	MRPS23	20	10.00%	6	0.300	15	6.67%	1	0.067
NM_006888	CALM1	131	9.92%	17	0.130	84	3.57%	3	0.036
NM_021130	PPIA	71	9.86%	10	0.141	54	5.56%	3	0.056
NM_021103	TMSB10	234	9.83%	32	0.137	104	9.62%	13	0.125
NM_001415	EIF2S3	143	9.79%	33	0.231	83	3.61%	7	0.084
NM_001009	RPS5	235	9.79%	33	0.140	132	6.82%	9	0.068
NM_004048	B2M	133	9.77%	21	0.158	89	6.74%	7	0.079
NM_001098504	DDX17	41	9.76%	8	0.195	30	6.67%	3	0.100
NM_213611	SLC25A3	134	9.70%	25	0.187	72	12.50%	19	0.264
NM_002882	RANBP1	62	9.68%	11	0.177	35	2.86%	1	0.029
NM_014294	TRAM1	31	9.68%	5	0.161	25	4.00%	4	0.160

NM_003234	TFRC	31	9.68%	4	0.129	20	20.00%	5	0.250
NM_003370	VASP	31	9.68%	7	0.226	18	0.00%	0	0.000
NM_001267864	SLIRP	42	9.52%	5	0.119	28	7.14%	2	0.071
NM_004892	SEC22B	42	9.52%	6	0.143	26	11.54%	5	0.192
NM_001256293	KRT8	21	9.52%	6	0.286	20	5.00%	2	0.100
NM_174909	TMEM167A	21	9.52%	2	0.095	16	18.75%	3	0.188
NM_002520	NPM1	95	9.47%	13	0.137	82	4.88%	4	0.049
NM_016045	SLMO2	117	9.40%	17	0.145	81	4.94%	7	0.086
NM_003171	SUPV3L1	32	9.38%	5	0.156	38	5.26%	3	0.079
NM_145341	PDCD4	32	9.38%	9	0.281	33	0.00%	0	0.000
NM_002533	NVL	32	9.38%	7	0.219	29	13.79%	4	0.138
NM_018838	NDUFA12	32	9.38%	4	0.125	28	0.00%	0	0.000
NM_032273	TMEM126A	32	9.38%	3	0.094	19	10.53%	2	0.105
NM_001605	AARS	32	9.38%	8	0.250	17	5.88%	2	0.118
NM_001098208	HNRNPF	43	9.30%	9	0.209	36	0.00%	0	0.000
NM_002901	RCN1	43	9.30%	5	0.116	28	3.57%	1	0.036
NM_000992	RPL29	43	9.30%	7	0.163	25	16.00%	4	0.160
NM_001000	RPL39	43	9.30%	5	0.116	19	15.79%	4	0.211
NM_001004	RPLP2	97	9.28%	12	0.124	51	5.88%	5	0.098
NM_000996	RPL35A	227	9.25%	32	0.141	153	6.54%	11	0.072
NM_000969	RPL5	315	9.21%	51	0.162	239	3.35%	13	0.054
NM_000988	RPL27	153	9.15%	26	0.170	107	11.21%	16	0.150
NM_014220	TM4SF1	341	9.09%	43	0.126	382	3.40%	17	0.045
NM_001190329	ATP5G3	110	9.09%	17	0.155	64	10.94%	8	0.125
NM_001861	COX4I1	77	9.09%	8	0.104	39	5.13%	5	0.128
NM_006476	ATP5L	33	9.09%	4	0.121	28	10.71%	3	0.107
NM_006701	TXNL4A	33	9.09%	5	0.152	24	4.17%	1	0.042
NM_004462	FDFT1	33	9.09%	7	0.212	21	9.52%	2	0.095
NM_006135	CAPZA1	33	9.09%	3	0.091	21	4.76%	2	0.095
NM_017633	FAM46A	33	9.09%	4	0.121	21	0.00%	0	0.000
NM_016308	CMPK1	22	9.09%	3	0.136	18	5.56%	1	0.056
NM_001919	ECI1	22	9.09%	6	0.273	18	5.56%	1	0.056
NM_001769	CD9	22	9.09%	2	0.091	16	12.50%	3	0.188
NM_021019	MYL6	177	9.04%	24	0.136	89	4.49%	6	0.067
NM_001260506	RPS3	280	8.93%	36	0.129	180	4.44%	10	0.056
NM_000968	RPL4	90	8.89%	13	0.144	80	3.75%	4	0.050
NM_019056	NDUFB11	79	8.86%	15	0.190	67	2.99%	3	0.045
NM_016640	MRPS30	34	8.82%	5	0.147	32	9.38%	5	0.156
NM_001012271	BIRC5	34	8.82%	3	0.088	21	4.76%	1	0.048
NM_002572	PAFAH1B2	34	8.82%	4	0.118	19	15.79%	5	0.263
NM_004800	TM9SF2	34	8.82%	5	0.147	19	10.53%	2	0.105
NM_001016	RPS12	91	8.79%	9	0.099	65	4.62%	4	0.062
NM_001863	COX6B1	114	8.77%	14	0.123	81	7.41%	7	0.086
NM_001865	COX7A2	114	8.77%	17	0.149	80	5.00%	6	0.075
NM_001136015	ANXA2	57	8.77%	7	0.123	42	2.38%	1	0.024
NM_006325	RAN	46	8.70%	7	0.152	35	11.43%	7	0.200
NM_002154	HSPA4	46	8.70%	6	0.130	27	14.81%	5	0.185
NM_032833	PPP1R15B	23	8.70%	2	0.087	30	0.00%	0	0.000
NM_002270	TNPO1	23	8.70%	4	0.174	30	3.33%	1	0.033
NM_020994	CTAG2	23	8.70%	2	0.087	20	20.00%	5	0.250
NM_020243	TOMM22	35	8.57%	12	0.343	27	14.81%	5	0.185
NM_014740	EIF4A3	35	8.57%	3	0.086	26	0.00%	0	0.000
NM_032025	EIF2A	35	8.57%	5	0.143	23	0.00%	0	0.000
NM_005175	ATP5G1	35	8.57%	3	0.086	22	0.00%	0	0.000
NM_016128	COPG1	35	8.57%	4	0.114	18	5.56%	1	0.056
NM_002295	RPSA	82	8.54%	9	0.110	42	7.14%	3	0.071
NM_013234	EIF3K	47	8.51%	7	0.149	27	3.70%	1	0.037
NM_006136	CAPZA2	59	8.47%	9	0.153	32	6.25%	3	0.094
NM_018976	SLC38A2	83	8.43%	10	0.120	68	5.88%	7	0.103
NM_001136134	RPL28	95	8.42%	10	0.105	65	6.15%	5	0.077
NM_001997	FAU	95	8.42%	9	0.095	44	11.36%	5	0.114
NM_032290	ANKRD32	48	8.33%	4	0.083	29	3.45%	1	0.034
NM_016292	TRAP1	48	8.33%	14	0.292	24	12.50%	5	0.208
NM_005032	PLS3	36	8.33%	3	0.083	23	0.00%	0	0.000
NM_030752	TCP1	36	8.33%	6	0.167	19	0.00%	0	0.000
NM_030920	ANP32E	24	8.33%	4	0.167	24	4.17%	1	0.042

NM_001527	HDAC2	24	8.33%	2	0.083	22	4.55%	1	0.045
NM_001032283	TMPO	24	8.33%	3	0.125	18	5.56%	1	0.056
NM_015920	RPS27L	24	8.33%	3	0.125	18	5.56%	1	0.056
NM_001419	ELAVL1	24	8.33%	3	0.125	15	0.00%	0	0.000
NM_002415	MIF	97	8.25%	12	0.124	56	5.36%	6	0.107
NM_001212	C1QBP	61	8.20%	8	0.131	39	12.82%	6	0.154
NM_005005	NDUFB9	61	8.20%	12	0.197	32	6.25%	2	0.063
NM_005001	NDUFA7	49	8.16%	4	0.082	19	5.26%	1	0.053
NM_002305	LGALS1	86	8.14%	11	0.128	30	0.00%	0	0.000
NM_000454	SOD1	111	8.11%	12	0.108	71	5.63%	6	0.085
NM_001034996	RPL14	198	8.08%	17	0.086	119	9.24%	11	0.092
NM_012423	RPL13A	112	8.04%	17	0.152	55	3.64%	2	0.036
NM_000858	GUK1	50	8.00%	4	0.080	35	5.71%	3	0.086
NM_001903	CTNNA1	25	8.00%	4	0.160	23	0.00%	0	0.000
NM_004074	COX8A	25	8.00%	3	0.120	22	0.00%	0	0.000
NM_021821	MRPS35	25	8.00%	3	0.120	19	5.26%	1	0.053
NM_016303	WBP5	25	8.00%	3	0.120	19	5.26%	3	0.158
NM_001130716	PLAC8	63	7.94%	6	0.095	46	2.17%	1	0.022
NM_001017	RPS13	129	7.75%	14	0.109	120	5.00%	6	0.050
NM_001206427	USMG5	52	7.69%	5	0.096	47	4.26%	2	0.043
NM_001257389	CD63	39	7.69%	6	0.154	45	8.89%	4	0.089
NM_001130089	KARS	39	7.69%	7	0.179	27	7.41%	3	0.111
NM_007096	CLTA	39	7.69%	8	0.205	25	8.00%	2	0.080
NM_001497	B4GALT1	26	7.69%	3	0.115	25	8.00%	2	0.080
NM_006717	SPIN1	26	7.69%	2	0.077	23	0.00%	0	0.000
NM_057180	VPS29	26	7.69%	4	0.154	20	0.00%	0	0.000
NM_004172	SLC1A3	26	7.69%	3	0.115	20	0.00%	0	0.000
NM_031314	HNRNPC	26	7.69%	4	0.154	18	22.22%	6	0.333
NM_004526	MCM2	26	7.69%	3	0.115	18	0.00%	0	0.000
NM_001271837	RCN2	26	7.69%	3	0.115	17	0.00%	0	0.000
NM_001174097	LDHB	353	7.65%	41	0.116	243	8.23%	25	0.103
NM_005782	ALYREF	66	7.58%	7	0.106	46	4.35%	2	0.043
NM_001024227	ARF1	53	7.55%	4	0.075	45	11.11%	6	0.133
NM_002489	NDUFA4	53	7.55%	7	0.132	43	0.00%	0	0.000
NM_001114752	CD55	40	7.50%	8	0.200	51	3.92%	2	0.039
NM_018164	ASUN	40	7.50%	6	0.150	25	0.00%	0	0.000
NM_006854	KDELR2	40	7.50%	4	0.100	20	10.00%	2	0.100
NM_007278	GABARAP	67	7.46%	14	0.209	43	6.98%	3	0.070
NM_000998	RPL37A	378	7.41%	34	0.090	188	7.45%	15	0.080
NM_001011	RPS7	81	7.41%	7	0.086	69	4.35%	3	0.043
NM_001256165	TMCO1	54	7.41%	5	0.093	35	0.00%	0	0.000
NM_004872	TMEM59	27	7.41%	2	0.074	24	4.17%	1	0.042
NM_001127328	ACADM	27	7.41%	5	0.185	23	8.70%	2	0.087
NM_032014	MRPS24	27	7.41%	3	0.111	21	0.00%	0	0.000
NM_002080	GOT2	27	7.41%	5	0.185	16	12.50%	2	0.125
NM_000986	RPL24	312	7.37%	31	0.099	211	4.74%	11	0.052
NM_001867	COX7C	109	7.34%	18	0.165	57	7.02%	4	0.070
NM_001679	ATP1B3	41	7.32%	3	0.073	34	2.94%	1	0.029
NM_001199356	RPL17-C18orf32	41	7.32%	4	0.098	20	5.00%	1	0.050
NM_003329	TXN	137	7.30%	11	0.080	78	0.00%	0	0.000
NM_001012	RPS8	55	7.27%	7	0.127	42	0.00%	0	0.000
NM_001253384	RPL15	83	7.23%	9	0.108	50	6.00%	3	0.060
NM_033301	RPL8	126	7.14%	11	0.087	93	4.30%	4	0.043
NM_007209	RPL35	112	7.14%	10	0.089	77	6.49%	5	0.065
NM_016403	CWC15	42	7.14%	4	0.095	39	7.69%	3	0.077
NM_006623	PHGDH	42	7.14%	9	0.214	20	10.00%	2	0.100
NM_002467	MYC	28	7.14%	3	0.107	17	11.76%	3	0.176
NM_000978	RPL23	323	7.12%	26	0.080	188	4.79%	9	0.048
NM_015414	RPL36	142	7.04%	21	0.148	81	3.70%	3	0.037
NM_002624	PFDN5	43	6.98%	4	0.093	40	12.50%	5	0.125
NM_001010	RPS6	561	6.95%	56	0.100	340	7.35%	28	0.082
NM_000976	RPL12	72	6.94%	8	0.111	54	5.56%	3	0.056
NM_005381	NCL	101	6.93%	17	0.168	61	4.92%	4	0.066
NM_018407	LAPTM4B	29	6.90%	2	0.069	36	11.11%	4	0.111
NM_173852	KRTCAP2	29	6.90%	4	0.138	25	0.00%	0	0.000
NM_005914	MCM4	29	6.90%	3	0.103	21	4.76%	1	0.048

NM_003756	EIF3H	29	6.90%	3	0.103	17	17.65%	4	0.235
NM_018321	BRIX1	29	6.90%	2	0.069	16	6.25%	1	0.063
NM_014624	S100A6	73	6.85%	6	0.082	54	7.41%	4	0.074
NM_000984	RPL23A	117	6.84%	9	0.077	53	11.32%	7	0.132
NM_004642	CDK2AP1	44	6.82%	4	0.091	32	0.00%	0	0.000
NM_001020	RPS16	370	6.76%	33	0.089	222	2.25%	5	0.023
NM_001166496	SLC16A1	74	6.76%	8	0.108	73	2.74%	2	0.027
NM_001024	RPS21	164	6.71%	14	0.085	110	7.27%	11	0.100
NM_177542	SNRPD2	209	6.70%	22	0.105	117	4.27%	6	0.051
NM_004040	RHOB	60	6.67%	6	0.100	65	0.00%	0	0.000
NM_001160354	LY6K	60	6.67%	14	0.233	41	2.44%	1	0.024
NM_004725	BUB3	45	6.67%	5	0.111	34	0.00%	0	0.000
NM_004965	HMGN1	45	6.67%	5	0.111	30	3.33%	1	0.033
NM_194259	UBE2I	30	6.67%	4	0.133	23	0.00%	0	0.000
NM_005034	POLR2K	30	6.67%	4	0.133	22	0.00%	0	0.000
NM_006808	SEC61B	30	6.67%	3	0.100	19	0.00%	0	0.000
NM_016058	TPRKB	30	6.67%	3	0.100	17	0.00%	0	0.000
NM_001168331	NDUFB4	30	6.67%	2	0.067	17	11.76%	3	0.176
NM_000291	PGK1	30	6.67%	4	0.133	16	0.00%	0	0.000
NM_003795	SNX3	30	6.67%	4	0.133	15	6.67%	1	0.067
NM_004925	AQP3	15	6.67%	2	0.133	23	4.35%	1	0.043
NM_032356	LSMD1	76	6.58%	7	0.092	44	4.55%	2	0.045
NM_007104	RPL10A	122	6.56%	10	0.082	81	3.70%	3	0.037
NM_022731	NUCKS1	46	6.52%	5	0.109	18	22.22%	5	0.278
NM_020412	CHMP1B	31	6.45%	3	0.097	37	0.00%	0	0.000
NM_004255	COX5A	31	6.45%	3	0.097	31	12.90%	6	0.194
NM_003243	TGFBR3	31	6.45%	4	0.129	28	3.57%	1	0.036
NM_002893	RBBP7	31	6.45%	3	0.097	26	0.00%	0	0.000
NM_001195291	SERPINB6	31	6.45%	3	0.097	24	12.50%	6	0.250
NM_001015	RPS11	233	6.44%	23	0.099	125	8.80%	28	0.224
NM_000979	RPL18	109	6.42%	9	0.083	77	11.69%	9	0.117
NM_003792	EDF1	47	6.38%	3	0.064	31	12.90%	7	0.226
NM_000716	C4BPB	63	6.35%	9	0.143	49	6.12%	3	0.061
NM_007108	TCEB2	79	6.33%	11	0.139	38	13.16%	7	0.184
NM_053275	RPLP0	127	6.30%	11	0.087	71	2.82%	3	0.042
NM_001025	RPS23	272	6.25%	21	0.077	154	6.49%	11	0.071
NM_001190452	MTRNR2L1	32	6.25%	2	0.063	29	3.45%	1	0.034
NM_001113546	LIMA1	32	6.25%	2	0.063	28	14.29%	6	0.214
NM_014161	MRPL18	32	6.25%	2	0.063	20	5.00%	1	0.050
NM_025146	NAA50	32	6.25%	3	0.094	17	0.00%	0	0.000
NM_001204858	TCEB1	32	6.25%	4	0.125	16	0.00%	0	0.000
NM_020216	RNPEP	16	6.25%	2	0.125	17	0.00%	0	0.000
NM_004637	RAB7A	16	6.25%	1	0.063	17	0.00%	0	0.000
NM_130398	EXO1	16	6.25%	2	0.125	16	6.25%	1	0.063
NM_002567	PEBP1	49	6.12%	6	0.122	30	6.67%	2	0.067
NM_006356	ATP5H	115	6.09%	9	0.078	72	1.39%	1	0.014
NM_000126	ETFA	33	6.06%	4	0.121	31	6.45%	4	0.129
NM_002492	NDUFB5	33	6.06%	3	0.091	29	6.90%	3	0.103
NM_007208	MRPL3	33	6.06%	3	0.091	26	0.00%	0	0.000
NM_014402	UQCRQ	83	6.02%	5	0.060	43	6.98%	3	0.070
NM_005340	HINT1	51	5.88%	5	0.098	28	0.00%	0	0.000
NM_206915	NGFRAP1	103	5.83%	10	0.097	72	4.17%	4	0.056
NM_001025071	RPS14	710	5.77%	54	0.076	489	6.95%	40	0.082
NM_000989	RPL30	572	5.77%	49	0.086	359	6.13%	22	0.061
NM_002950	RPN1	174	5.75%	14	0.080	91	2.20%	3	0.033
NM_000942	PPIB	227	5.73%	23	0.101	155	5.16%	13	0.084
NM_001028	RPS25	88	5.68%	7	0.080	77	3.90%	3	0.039
NM_001866	COX7B	53	5.66%	3	0.057	37	2.70%	1	0.027
NM_004814	SNRNP40	71	5.63%	5	0.070	44	0.00%	0	0.000
NM_001024662	RPL6	89	5.62%	10	0.112	71	5.63%	4	0.056
NM_173354	SIK1	90	5.56%	8	0.089	58	1.72%	1	0.017
NM_005008	NHP2L1	72	5.56%	6	0.083	45	4.44%	2	0.044
NM_014713	LAPTM4A	54	5.56%	8	0.148	31	3.23%	1	0.032
NM_021203	SRPRB	18	5.56%	1	0.056	23	0.00%	0	0.000
NM_001257335	ATP5A1	18	5.56%	2	0.111	19	5.26%	1	0.053
NM_001007074	RPL32	201	5.47%	19	0.095	161	3.11%	5	0.031

NM_003130	SRI	37	5.41%	3	0.081	40	7.50%	3	0.075
NM_006886	ATP5E	37	5.41%	2	0.054	28	10.71%	4	0.143
NM_005880	DNAJA2	131	5.34%	13	0.099	115	5.22%	7	0.061
NM_002793	PSMB1	76	5.26%	7	0.092	40	7.50%	4	0.100
NM_015934	NOP58	38	5.26%	3	0.079	26	7.69%	2	0.077
NM_018947	CYCS	38	5.26%	2	0.053	19	5.26%	1	0.053
NM_017994	TMEM248	38	5.26%	4	0.105	19	10.53%	2	0.105
NM_004068	AP2M1	19	5.26%	1	0.053	19	10.53%	2	0.105
NM_001206739	ITGB3BP	19	5.26%	1	0.053	18	0.00%	0	0.000
NM_002128	HMGB1	19	5.26%	2	0.105	18	16.67%	4	0.222
NM_006233	POLR2I	19	5.26%	1	0.053	18	5.56%	1	0.056
NM_016468	COX16	19	5.26%	2	0.105	16	6.25%	1	0.063
NM_181515	MRPL21	19	5.26%	4	0.211	16	0.00%	0	0.000
NM_006406	PRDX4	77	5.19%	7	0.091	46	8.70%	5	0.109
NM_002954	RPS27A	58	5.17%	4	0.069	40	5.00%	3	0.075
NM_024038	C19orf43	39	5.13%	8	0.205	25	4.00%	1	0.040
NM_001469	XRCC6	59	5.08%	4	0.068	35	5.71%	2	0.057
NM_001142285	RPS24	259	5.02%	19	0.073	208	4.81%	10	0.048
NM_001143676	SGK1	100	5.00%	13	0.130	82	2.44%	3	0.037
NM_014248	RBX1	40	5.00%	4	0.100	28	17.86%	6	0.214
NM_145729	MRPL24	20	5.00%	3	0.150	18	16.67%	3	0.167
NM_021639	GPBP1L1	20	5.00%	1	0.050	15	0.00%	0	0.000
NM_001022	RPS19	330	4.85%	24	0.073	191	5.24%	15	0.079
NM_004552	NDUFS5	83	4.82%	8	0.096	50	0.00%	0	0.000
NM_006793	PRDX3	42	4.76%	3	0.071	38	2.63%	1	0.026
NM_170739	MRPL11	21	4.76%	2	0.095	21	4.76%	1	0.048
NM_002574	PRDX1	150	4.67%	11	0.073	98	6.12%	7	0.071
NM_001127671	LIFR	43	4.65%	2	0.047	43	2.33%	3	0.070
NM_001193375	NDUFA11	43	4.65%	2	0.047	27	3.70%	2	0.074
NM_153477	UXT	43	4.65%	4	0.093	26	3.85%	1	0.038
NM_000997	RPL37	395	4.56%	21	0.053	293	5.12%	21	0.072
NM_181802	UBE2C	46	4.35%	2	0.043	35	2.86%	1	0.029
NM_001261445	TXNRD1	46	4.35%	3	0.065	23	8.70%	2	0.087
NM_023079	UBE2Z	23	4.35%	2	0.087	24	4.17%	1	0.042
NM_004152	OAZ1	23	4.35%	2	0.087	18	5.56%	1	0.056
NM_014736	KIAA0101	70	4.29%	5	0.071	46	4.35%	2	0.043
NM_001007794	CEPT1	24	4.17%	1	0.042	28	3.57%	1	0.036
NM_001967	EIF4A2	24	4.17%	1	0.042	26	3.85%	3	0.115
NM_000999	RPL38	193	4.15%	10	0.052	151	2.65%	6	0.040
NM_018997	MRPS21	49	4.08%	2	0.041	32	6.25%	2	0.063
NM_001146227	RPS20	173	4.05%	8	0.046	95	6.32%	8	0.084
NM_004546	NDUFB2	25	4.00%	1	0.040	29	0.00%	0	0.000
NM_004374	COX6C	25	4.00%	1	0.040	27	14.81%	4	0.148
NM_006347	PPIH	25	4.00%	1	0.040	15	0.00%	0	0.000
NM_025234	WDR61	25	4.00%	2	0.080	15	6.67%	1	0.067
NM_005022	PFN1	76	3.95%	3	0.039	57	7.02%	4	0.070
NM_001030001	RPS29	51	3.92%	2	0.039	52	1.92%	1	0.019
NM_024292	UBL5	51	3.92%	2	0.039	38	13.16%	6	0.158
NM_004549	NDUFC2	26	3.85%	3	0.115	15	6.67%	1	0.067
NM_002952	RPS2	161	3.73%	8	0.050	87	8.05%	10	0.115
NM_001199877	SERF2	55	3.64%	2	0.036	31	3.23%	2	0.065
NM_001007	RPS4X	139	3.60%	8	0.058	89	2.25%	2	0.022
NM_018492	PBK	29	3.45%	2	0.069	19	0.00%	0	0.000
NM_145690	YWHAZ	30	3.33%	2	0.067	16	0.00%	0	0.000
NM_014886	NSA2	31	3.23%	2	0.065	15	0.00%	0	0.000
NM_006713	SUB1	63	3.17%	2	0.032	42	2.38%	1	0.024
NM_001033930	UBA52	63	3.17%	4	0.063	35	8.57%	3	0.086
NM_007262	PARK7	32	3.13%	1	0.031	31	9.68%	3	0.097
NM_001102398	HNRNPR	32	3.13%	1	0.031	19	15.79%	3	0.158
NM_001199973	RPL36A-HNRNPH2	32	3.13%	2	0.063	18	5.56%	1	0.056
NM_006013	RPL10	33	3.03%	1	0.030	19	5.26%	1	0.053
NM_019554	S100A4	134	2.99%	5	0.037	61	1.64%	1	0.016
NM_003295	TPT1	135	2.96%	5	0.037	76	6.58%	5	0.066
NM_016104	RWDD1	34	2.94%	2	0.059	22	0.00%	0	0.000
NM_033625	RPL34	103	2.91%	4	0.039	92	5.43%	9	0.098
NM_006004	UQCRH	69	2.90%	6	0.087	47	6.38%	5	0.106

NM_031280	MRPS15	35	2.86%	2	0.057	22	9.09%	2	0.091
NM_080592	ATRAID	35	2.86%	2	0.057	21	9.52%	2	0.095
NM_015972	POLR1D	35	2.86%	2	0.057	19	0.00%	0	0.000
NM_002129	HMGB2	36	2.78%	1	0.028	32	0.00%	0	0.000
NM_001697	ATP5O	37	2.70%	5	0.135	43	11.63%	5	0.116
NM_017906	PAK1IP1	37	2.70%	1	0.027	22	4.55%	1	0.045
NM_004528	MGST3	37	2.70%	1	0.027	21	4.76%	1	0.048
NM_001154	ANXA5	37	2.70%	1	0.027	15	20.00%	4	0.267
NM_000019	ACAT1	40	2.50%	1	0.025	26	0.00%	0	0.000
NM_032574	DPY30	42	2.38%	2	0.048	22	4.55%	1	0.045
NM_001098577	RPL31	344	2.33%	18	0.052	232	3.45%	10	0.043
NM_006360	EIF3M	141	2.13%	3	0.021	103	5.83%	6	0.058
NM_004612	TGFBR1	53	1.89%	2	0.038	52	3.85%	2	0.038
NM_019059	TOMM7	56	1.79%	1	0.018	38	2.63%	1	0.026
NM_000987	RPL26	87	1.15%	1	0.011	41	2.44%	1	0.024
NM_004450	ERH	44	0.00%	0	0.000	43	11.63%	7	0.163
NM_014302	SEC61G	43	0.00%	0	0.000	29	6.90%	2	0.069
NM_001143842	TMEM106C	34	0.00%	0	0.000	22	4.55%	1	0.045
NM_015135	NUP205	30	0.00%	0	0.000	26	7.69%	2	0.077
NM_004417	DUSP1	17	0.00%	0	0.000	34	2.94%	1	0.029
NM_001004333	RNASEK	29	0.00%	0	0.000	19	15.79%	4	0.211
NM_004077	CS	32	0.00%	0	0.000	15	0.00%	0	0.000
NM_003374	VDAC1	27	0.00%	0	0.000	20	0.00%	0	0.000
NM_014325	CORO1C	28	0.00%	0	0.000	17	0.00%	0	0.000
NM_004175	SNRPD3	23	0.00%	0	0.000	21	0.00%	0	0.000
NM_020409	MRPL47	28	0.00%	0	0.000	16	18.75%	3	0.188
NM_016091	EIF3L	24	0.00%	0	0.000	19	5.26%	1	0.053
NM_005121	MED13	21	0.00%	0	0.000	21	4.76%	1	0.048
NM_006055	LANCL1	22	0.00%	0	0.000	19	5.26%	1	0.053
NM_004373	COX6A1	24	0.00%	0	0.000	16	12.50%	2	0.125
NM_019095	CRLS1	23	0.00%	0	0.000	17	5.88%	1	0.059
NM_023937	MRPL34	18	0.00%	0	0.000	20	5.00%	1	0.050
NM_005724	TSPAN3	18	0.00%	0	0.000	17	0.00%	0	0.000

Table 2.1 TAIL-seq data from TUT4/7-depleted cells. HeLa cells were transfected twice with siControl or a mixture of siRNAs against TUT4 and TUT7 (siTUT4/7) for 4 days. The short poly(A) read counts indicate the number of total reads with short A tail (5–25 nt). Uridylation frequency (%) on short poly(A) tail was calculated by dividing the number of uridylated reads by the number oftotal reads. The average U length was calculated by dividing the number of all terminal uridine residues by total number of read counts as in Figure 2.11.

Accession	Gene Name	Half-life (siCont_1)	Half-life (siTUT4/7_1)	Residual (siCont_1)	Residual (siTUT4/7_1)	Half-life (siCont_2)	Half-life (siTUT4/7_2)	Residual (siCont_2)	Residual (siTUT4/7_2)	Mean half-life (siCont)	Mean half-life (siTUT4/7)
NM_001402	EEF1A1	15.12	99.96	0.00	0.00	38.34	298.69	0.01	0.02	21.69	149.79
NM_198566	C5orf34	14.68	193.90	0.00	0.00	37.41	1489.02	0.01	0.02	21.09	343.11
NM_001961	EEF2	28.96	19.75	0.01	0.00	23.06	59.06	0.01	0.03	25.67	29.60
NM_006597	HSPA8	7.06	7.85	0.00	0.01	12.56	11.41	0.04	0.05	9.04	9.30
NM_006082	TUBA1B	10.18	15.43	0.00	0.00	19.64	17.82	0.01	0.05	13.41	16.54
NM_021009	UBC	1.23	1.87	0.08	0.03	1.30	1.71	0.04	0.01	1.26	1.79
NM_001271969	HSP90AB1	12.99	21.52	0.00	0.00	23.52	28.03	0.01	0.09	16.74	24.35
NM_001206796	PKM	24.23	29.40	0.00	0.00	29.35	80.62	0.01	0.07	26.54	43.09
NM_001018067	SERBP1	8.58	16.83	0.00	0.02	14.32	19.57	0.01	0.11	10.73	18.10
NM_001620	AHNAK	13.54	10.99	0.01	0.01	9.87	9.44	0.00	0.01	11.42	10.15
NM_017812	CHCHD3	13.22	24.39	0.01	0.00	20.70	27.10	0.02	0.05	16.14	25.68
NM_000968	RPL4	12.80	26.23	0.00	0.00	38.93	62.74	0.01	0.03	19.26	36.99
NM_032704	TUBA1C	8.13	10.61	0.00	0.01	14.14	12.37	0.01	0.05	10.32	11.42
NM_002520	NPM1	8.53	15.86	0.00	0.02	36.72	25.82	0.01	0.06	13.85	19.65
NM_001746	CANX	16.74	26.74	0.00	0.01	149.45	89.67	0.01	0.05	30.10	41.20
NM_001201483	ENO1	18.69	27.46	0.00	0.00	27.37	48.63	0.02	0.04	22.21	35.10
NM_001174097	LDHB	13.18	41.65	0.00	0.00	33.77	91.21	0.01	0.08	18.96	57.18
NM_032042	FAM172A	7.11	12.57	0.00	0.01	12.44	11.22	0.02	0.04	9.04	11.86
NM_001417	EIF4B	9.25	15.32	0.01	0.01	17.97	40.27	0.03	0.05	12.21	22.19
NM_001242891	CSDE1	10.14	18.55	0.00	0.01	30.99	35.10	0.01	0.05	15.28	24.27
NM_004343	CALR	18.56	20.47	0.00	0.01	128.41	43.24	0.02	0.07	32.43	27.79
NM_012073	CCT5	9.62	13.06	0.00	0.01	21.25	22.40	0.02	0.04	13.24	16.50
NM_018078	LARP1B	4.93	13.93	0.01	0.04	22.44	17.35	0.01	0.04	8.08	15.45
NM_000969	RPL5	10.30	24.62	0.00	0.00	43.75	43.68	0.01	0.06	16.67	31.49
NM_021130	PPIA	14.28	29.67	0.00	0.00	152.91	107.19	0.00	0.04	26.12	46.47
NM_016281	TAOK3	33.04	68.65	0.00	0.00	27.17	59.48	0.00	0.05	29.82	63.74
NM_001686	ATP5B	19.33	185.84	0.00	0.00	87.46	317.24	0.00	0.07	31.66	234.38
NM_002184	IL6ST	17.17	29.48	0.00	0.00	418.40	62.95	0.01	0.03	32.99	40.15
NM_006098	GNB2L1	17.10	22.74	0.00	0.00	27.89	36.49	0.02	0.02	21.20	28.02
NM_012423	RPL13A	9.53	23.08	0.00	0.00	11.94	78.86	0.02	0.03	10.60	35.71
NM_004721	MAP3K13	13.68	32.42	0.00	0.00	42.64	115.66	0.01	0.03	20.72	50.65
NM_153207	AEBP2	9.94	112.40	0.00	0.00	22.09	46.92	0.02	0.03	13.71	66.20
NM_001270399	TUBA1A	9.72	14.07	0.00	0.00	18.45	16.38	0.02	0.05	12.73	15.14
NM_001031695	RBFOX2	13.29	20.40	0.00	0.00	31.96	28.29	0.01	0.03	18.77	23.70
NM_001142285	RPS24	12.75	24.35	0.00	0.01	1457.97	57.51	0.01	0.04	25.28	34.21
NM_016343	CENPF	6.56	7.54	0.00	0.01	10.66	9.58	0.02	0.07	8.12	8.44
NM_002211	ITGB1	10.60	19.77	0.00	0.01	37.74	25.59	0.01	0.05	16.55	22.31
NM_005998	CCT3	11.08	18.05	0.00	0.01	22.43	27.97	0.01	0.04	14.83	21.94
NM_001416	EIF4A1	12.87	18.90	0.00	0.00	23.21	23.86	0.01	0.04	16.56	21.09
NM_002156	HSPD1	8.94	18.13	0.00	0.01	26.45	26.21	0.01	0.11	13.36	21.43
NM_004859	CLTC	8.45	10.49	0.01	0.01	8.98	11.69	0.01	0.01	8.71	11.06
NM_000291	PGK1	17.07	33.04	0.00	0.00	192.54	172.29	0.01	0.04	31.36	55.44
NM_031844	HNRNPU	8.65	17.78	0.00	0.01	13.94	15.81	0.00	0.10	10.67	16.73
NM_033251	RPL13	19.47	40.93	0.00	0.00	30.38	98.28	0.01	0.04	23.73	57.79
NM_018955	UBB	3.50	8.84	0.02	0.00	3.98	8.31	0.00	0.03	3.73	8.57
NM_003463	PTP4A1	18.12	8.89	0.08	0.06	9.53	6.79	0.01	0.02	12.49	7.70
NM_001017963	HSP90AA1	19.56	10.02	0.00	0.01	46.43	6.99	0.01	0.08	27.53	8.24
NM_032549	IMMP2L	1.83	2.31	0.04	0.02	1.88	2.03	0.02	0.01	1.86	2.16
NM_001904	CTNNB1	9.63	17.08	0.00	0.00	13.31	16.52	0.02	0.03	11.18	16.80
NM_004134	HSPA9	10.23	19.16	0.00	0.01	23.36	33.10	0.01	0.07	14.23	24.27
NM_003380	VIM	151.94	24.14	0.00	0.00	25.12	22.85	0.00	0.01	43.11	23.48
NM_003750	EIF3A	6.62	8.14	0.01	0.03	9.55	9.71	0.02	0.19	7.82	8.85
NM_001098504	DDX17	7.53	10.42	0.01	0.01	10.62	11.52	0.01	0.02	8.81	10.94
NM_001257293	HNRNPH1	11.14	20.67	0.00	0.01	22.99	22.55	0.01	0.11	15.01	21.57
NM_001260506	RPS3	16.54	79.52	0.00	0.00	58.13	215.89	0.00	0.15	25.75	116.23
NM_003299	HSP90B1	15.64	22.15	0.00	0.01	89.02	43.95	0.01	0.06	26.61	29.45
NM_005381	NCL	8.68	27.23	0.00	0.01	29.09	19.68	0.00	0.31	13.36	22.85
NM_139245	PPM1L	3.35	5.27	0.02	0.05	11.03	8.63	0.01	0.03	5.14	6.54
NM_003234	TFRC	8.05	7.99	0.00	0.02	15.42	10.22	0.02	0.05	10.58	8.97
NM_001376	DYNC1H1	31.03	19.57	0.02	0.00	17.35	19.76	0.01	0.01	22.25	19.66
NM_004768	SRSF11	4.38	7.50	0.00	0.02	4.43	5.65	0.00	0.00	4.40	6.44
NM_001267782	AMBRA1	12.54	16.47	0.01	0.00	13.44	29.28	0.03	0.04	12.97	21.08
NM_006267	RANBP2	5.12	6.11	0.01	0.01	6.89	7.03	0.02	0.04	5.87	6.54

NM_004446	EPRS	8.74	12.50	0.00	0.01	17.97	15.71	0.01	0.06	11.76	13.92
NM_000918	P4HB	35.87	21.55	0.01	0.00	35.03	33.88	0.01	0.03	35.45	26.34
NM_199000	LHFPL3	13.15	23.39	0.00	0.00	36.81	113.38	0.01	0.04	19.38	38.78
NM_001258438	TARS	7.36	11.07	0.00	0.02	14.42	18.36	0.02	0.08	9.75	13.82
NM_031243	HNRNPA2B1	7.11	32.82	0.00	0.03	14.08	9.12	0.01	0.29	9.45	14.27
NM_001167740	SMYD3	3.00	3.12	0.12	0.04	2.42	2.34	0.08	0.02	2.68	2.67
NM_001258026	TPI1	26.53	39.24	0.00	0.00	76.06	277.86	0.02	0.03	39.34	68.76
NM_000972	RPL7A	20.61	37.55	0.00	0.00	37.17	100.94	0.01	0.05	26.52	54.74
NM_018842	BAIAP2L1	11.84	46.46	0.00	0.00	54.93	77.52	0.02	0.03	19.48	58.10
NM_022731	NUCKS1	11.60	15.93	0.00	0.02	23.95	18.00	0.02	0.08	15.63	16.90
NM_013417	IARS	7.61	9.69	0.01	0.02	10.57	11.83	0.04	0.05	8.85	10.65
NM_003292	TPR	4.67	6.33	0.01	0.01	6.30	6.98	0.02	0.06	5.37	6.64
NM_000987	RPL26	12.71	25.32	0.00	0.00	#######	286.93	0.01	0.04	25.39	46.53
NM_002032	FTH1	120.16	103.90	0.00	0.01	140.06	59.34	0.02	0.02	129.35	75.54
NM_001356	DDX3X	7.70	15.37	0.00	0.02	15.92	19.70	0.01	0.09	10.38	17.27
NM_006013	RPL10	15.97	32.41	0.00	0.00	17.97	48.18	0.02	0.01	16.91	38.75
NM_001469	XRCC6	12.49	18.94	0.00	0.01	36.59	52.88	0.01	0.07	18.62	27.89
NM_005898	CAPRIN1	9.86	12.54	0.01	0.01	14.54	14.82	0.01	0.03	11.75	13.59
NM_000224	KRT18	21.84	42.91	0.00	0.00	170.11	82.58	0.01	0.04	38.71	56.48
NM_001142298	SQSTM1	8.66	13.26	0.01	0.01	11.72	19.40	0.03	0.07	9.96	15.75
NM_001923	DDB1	12.04	16.62	0.00	0.01	21.06	22.90	0.02	0.04	15.32	19.26
NM_024817	THSD4	12.85	18.52	0.00	0.00	57.82	35.64	0.01	0.04	21.03	24.37
NM_152653	UBE2E2	2.13	2.43	0.15	0.04	1.94	2.01	0.09	0.03	2.03	2.20
NM_025074	FRAS1	12.05	25.09	0.00	0.00	22.43	86.91	0.00	0.11	15.68	38.94
NM_005482	PIGK	10.23	14.54	0.00	0.00	17.75	20.31	0.02	0.04	12.98	16.95
NM_001271014	KTN1	7.70	10.27	0.01	0.02	16.56	10.93	0.04	0.09	10.52	10.59
NM_007126	VCP	12.56	13.51	0.00	0.01	14.63	20.21	0.02	0.05	13.51	16.20
NM_213611	SLC25A3	11.17	43.00	0.00	0.00	21.89	56.89	0.01	0.04	14.79	48.98
NM_001007074	RPL32	13.02	35.20	0.00	0.00	156.03	80.27	0.01	0.03	24.03	48.94
NM_001142864	PIEZO1	17.33	7.03	0.04	0.01	5.24	6.09	0.02	0.03	8.05	6.53
NM_004396	DDX5	7.77	13.32	0.00	0.01	12.40	13.43	0.00	0.05	9.56	13.38
NM_032968	PCDH11X	15.15	31.77	0.00	0.00	34.93	32.78	0.01	0.04	21.13	32.27
NM_002265	KPNB1	12.75	18.16	0.00	0.01	21.50	30.76	0.01	0.06	16.00	22.84
NM_001025071	RPS14	23.26	33.16	0.00	0.00	36.18	70.27	0.02	0.03	28.31	45.06
NM_001034996	RPL14	15.13	33.23	0.00	0.00	65.59	83.80	0.00	0.05	24.58	47.59
NM_000990	RPL27A	12.89	37.84	0.00	0.00	92.52	40.52	0.01	0.07	22.62	39.13
NM_014680	KIAA0100	20.56	15.27	0.00	0.00	31.22	18.80	0.02	0.02	24.80	16.85
NM_133509	RAD51B	7.32	9.96	0.01	0.01	7.02	7.01	0.01	0.01	7.17	8.23
NM_001145408	NONO	12.34	16.98	0.00	0.00	29.13	37.12	0.01	0.04	17.33	23.30
NM_001114132	NBEAL1	14.95	55.36	0.00	0.00	41.97	266.63	0.02	0.04	22.05	91.68
NM_001130438	SPTAN1	62.18	15.31	0.03	0.01	22.60	24.43	0.03	0.00	33.16	18.82
NM_018976	SLC38A2	1.92	2.74	0.04	0.04	2.08	2.74	0.04	0.07	2.00	2.74
NM_014220	TM4SF1	3.80	5.12	0.01	0.02	5.35	5.77	0.03	0.08	4.44	5.43
NM_001015	RPS11	30.64	36.72	0.00	0.00	73.48	456.23	0.01	0.03	43.25	67.97
NM_018136	ASPM	4.32	5.33	0.00	0.01	5.30	5.36	0.02	0.03	4.76	5.34
NM_001256910	DDX21	7.16	18.31	0.01	0.01	19.19	20.21	0.01	0.08	10.43	19.21
NM_001257335	ATP5A1	16.05	31.93	0.00	0.00	41.01	645.72	0.01	0.03	23.07	60.85
NM_001042465	PSAP	31.41	35.27	0.00	0.00	26.22	211.45	0.02	0.04	28.58	60.46
NM_006178	NSF	9.85	23.70	0.00	0.00	37.47	37.31	0.01	0.04	15.59	28.99
NM_006325	RAN	15.27	23.71	0.00	0.00	25.68	67.73	0.01	0.06	19.15	35.12
NM_001160233	ATP1A1	19.48	30.40	0.01	0.01	19.47	13.92	0.00	0.07	19.48	19.09
NM_000127	EXT1	2.67	2.59	0.17	0.06	2.22	2.13	0.10	0.03	2.43	2.34
NM_000992	RPL29	16.19	48.64	0.00	0.00	360.41	126.89	0.00	0.05	30.98	70.33
NM_001762	CCT6A	10.36	24.22	0.00	0.00	39.84	46.45	0.01	0.08	16.44	31.84
NM_001098576	TMBIM6	13.93	19.13	0.00	0.01	26.68	29.40	0.02	0.03	18.30	23.18
NM_024122	APOO	13.84	63.37	0.00	0.00	76.19	210.42	0.01	0.03	23.43	97.41
NM_001145418	TTC28	3.01	3.39	0.14	0.05	2.66	2.48	0.07	0.02	2.82	2.87
NM_001098398	COPA	10.30	17.88	0.00	0.01	14.13	17.62	0.01	0.04	11.92	17.75
NM_001199142	EIF3C	33.78	37.83	0.00	0.00	26.77	25.00	0.00	0.06	29.87	30.11
NM_031157	HNRNPA1	7.60	35.77	0.00	0.02	12.78	20.16	0.00	0.30	9.53	25.79
NM_002271	IPO5	10.66	17.33	0.00	0.01	17.06	25.68	0.02	0.03	13.12	20.69
NM_001098577	RPL31	17.09	160.17	0.00	0.01	101.38	61.31	0.01	0.05	29.25	88.67
NM_001273	CHD4	17.79	20.54	0.01	0.00	18.37	24.02	0.01	0.02	18.08	22.14
NM_001067	TOP2A	4.16	5.03	0.01	0.02	5.20	5.15	0.03	0.08	4.62	5.09
NM_032378	EEF1D	33.99	21.22	0.00	0.00	15.47	23.67	0.01	0.02	21.26	22.38
NM_001142550	WDR47	14.07	22.78	0.00	0.00	70.40	395.62	0.01	0.04	23.46	43.09

NM_001078166	SRSF1	10.89	16.52	0.01	0.01	22.07	23.06	0.01	0.06	14.58	19.25
NM_001316	CSE1L	7.23	13.41	0.00	0.01	15.12	18.35	0.01	0.05	9.79	15.49
NM_000976	RPL12	17.33	49.93	0.00	0.00	59.91	218.97	0.03	0.05	26.88	81.31
NM_001962	EFNA5	2.09	2.32	0.14	0.03	1.86	1.89	0.09	0.03	1.97	2.08
NM_001256877	KANK1	3.11	3.30	0.12	0.04	2.67	2.68	0.11	0.03	2.88	2.96
NM_001166285	CCT7	14.17	22.10	0.00	0.00	23.57	64.25	0.02	0.05	17.70	32.89
NM_005032	PLS3	8.63	12.33	0.00	0.01	16.10	14.60	0.02	0.06	11.23	13.37
NM_014865	NCAPD2	9.32	16.28	0.01	0.00	21.42	18.33	0.02	0.03	12.98	17.24
NM_006761	YWHAE	12.48	18.50	0.01	0.02	19.16	18.92	0.00	0.10	15.11	18.71
NM_001166496	SLC16A1	6.99	10.83	0.01	0.01	9.73	10.72	0.02	0.06	8.14	10.77
NM_002140	HNRNPK	8.92	15.77	0.01	0.01	14.25	12.05	0.01	0.07	10.97	13.66
NM_001242409	GAREM	9.25	45.95	0.00	0.01	18.49	39.69	0.00	0.23	12.33	42.59
NM_020750	XPO5	15.32	15.65	0.01	0.00	16.26	19.08	0.00	0.03	15.78	17.19
NM_080391	PTP4A2	8.63	11.75	0.01	0.02	14.39	14.03	0.02	0.06	10.79	12.79
NM_001003	RPLP1	29.72	370.68	0.00	0.00	47.75	206.77	0.00	0.19	36.64	265.46
NM_001131028	ATG10	10.38	23.53	0.00	0.00	31.81	21.75	0.00	0.04	15.65	22.60
NM_002154	HSPA4	7.61	11.21	0.00	0.01	14.65	14.54	0.02	0.06	10.02	12.66
NM_021103	TMSB10	28.59	30.02	0.01	0.00	167.83	83.84	0.01	0.01	48.85	44.21
NM_020731	AHRR	7.10	8.44	0.00	0.01	10.69	10.64	0.02	0.03	8.53	9.41
NM_014014	SNRNP200	28.38	19.29	0.01	0.00	16.63	15.81	0.00	0.01	20.97	17.38
NM_001139514	DACH2	12.66	90.87	0.00	0.00	85.63	227.14	0.01	0.01	22.06	129.80
NM_000984	RPL23A	16.12	23.51	0.00	0.00	195.39	160.54	0.01	0.04	29.78	41.02
NM_000942	PPIB	17.21	18.96	0.00	0.01	39.05	36.47	0.01	0.06	23.89	24.95
NM_207123	GAB1	26.82	41.24	0.00	0.00	21.02	41.13	0.00	0.05	23.57	41.19
NM_005095	ZMYM4	6.61	9.98	0.01	0.01	8.73	9.09	0.03	0.06	7.52	9.51
NM_018407	LAPTM4B	14.91	15.41	0.00	0.01	21.25	34.32	0.02	0.03	17.53	21.27
NM_012433	SF3B1	7.13	13.13	0.00	0.01	13.40	16.91	0.01	0.04	9.30	14.78
NM_032973	PCDH11Y	14.58	28.25	0.00	0.00	47.89	36.48	0.01	0.04	22.35	31.84
NM_002266	KPNA2	7.18	11.34	0.00	0.01	13.61	11.56	0.01	0.06	9.40	11.45
NM_001142418	MORF4L2	8.62	20.30	0.00	0.00	26.09	23.85	0.01	0.02	12.96	21.93
NM_015135	NUP205	6.00	9.17	0.01	0.01	8.00	10.16	0.03	0.04	6.86	9.64
NM_001743	CALM2	7.47	11.02	0.01	0.01	13.03	16.55	0.04	0.05	9.49	13.23
NM_005914	MCM4	11.64	19.03	0.00	0.01	22.81	37.26	0.01	0.03	15.41	25.19
NM_015635	GAPVD1	10.37	16.07	0.00	0.01	20.21	18.40	0.01	0.03	13.70	17.16
NM_018448	CAND1	6.97	11.34	0.01	0.01	11.17	10.83	0.02	0.03	8.58	11.08
NM_000979	RPL18	31.59	38.82	0.00	0.00	44.72	202.06	0.01	0.02	37.03	65.13
NM_005742	PDIA6	19.47	51.45	0.00	0.01	68.89	264.13	0.01	0.06	30.36	86.13
NM_007104	RPL10A	12.16	23.13	0.00	0.00	41.99	56.63	0.01	0.05	18.86	32.84
NM_020117	LARS	7.86	8.85	0.00	0.02	12.84	11.18	0.03	0.07	9.75	9.88
NM_015332	NUDCD3	7.73	11.88	0.00	0.00	14.26	12.76	0.02	0.03	10.03	12.30
NM_018685	ANLN	4.89	7.39	0.01	0.03	7.09	7.61	0.04	0.07	5.79	7.49
NM_014372	RNF11	29.83	65.28	0.00	0.00	30.90	35.89	0.00	0.05	30.35	46.31
NM_001136015	ANXA2	8.61	12.08	0.00	0.01	17.90	16.12	0.03	0.05	11.62	13.81
NM_001080415	U2SURP	5.02	7.47	0.01	0.02	6.95	8.30	0.04	0.08	5.83	7.86
NM_001198842	CCT2	10.03	18.41	0.00	0.00	28.40	35.21	0.02	0.04	14.83	24.18
NM_004061	CDH12	8.70	19.76	0.00	0.00	17.83	17.40	0.02	0.08	11.69	18.50
NM_021019	MYL6	21.45	44.51	0.00	0.00	482.87	102.37	0.02	0.03	41.07	62.04
NM_001267552	PEMT	12.59	37.04	0.00	0.00	28.64	35.98	0.01	0.01	17.50	36.51
NM_001037283	EIF3B	11.82	11.20	0.01	0.01	11.71	23.04	0.02	0.04	11.77	15.07
NM_005895	GOLGA3	28.90	36.44	0.00	0.00	32.83	183.57	0.01	0.02	30.74	60.80
NM_001207067	BZW1	9.06	16.62	0.00	0.02	39.82	26.53	0.01	0.03	14.77	20.43
NM_002950	RPN1	15.69	14.58	0.00	0.00	40.69	31.77	0.02	0.04	22.65	19.98
NM_004741	NOLC1	13.20	24.34	0.00	0.01	44.93	27.99	0.00	0.09	20.40	26.04
NM_138420	AHNAK2	17.85	13.32	0.01	0.00	13.86	12.67	0.01	0.00	15.60	12.98
NM_001144831	PHB2	16.11	23.03	0.00	0.00	44.12	59.27	0.01	0.04	23.60	33.18
NM_001494	GDI2	7.48	10.48	0.01	0.01	11.42	14.56	0.03	0.05	9.04	12.19
NM_032226	ZCCHC7	2.59	3.07	0.11	0.03	2.38	2.42	0.08	0.02	2.48	2.71
NM_013986	EWSR1	7.11	8.70	0.01	0.01	8.24	8.20	0.02	0.08	7.63	8.44
NM_177983	PPM1G	15.90	18.40	0.00	0.01	23.20	20.41	0.00	0.04	18.87	19.35
NM_006135	CAPZA1	5.81	7.60	0.01	0.03	9.84	7.18	0.03	0.09	7.31	7.39
NM_002893	RBBP7	13.19	21.79	0.00	0.00	43.41	51.56	0.01	0.07	20.23	30.63
NM_016045	SLMO2	7.09	19.33	0.01	0.02	23.47	21.91	0.02	0.08	10.89	20.54
NM_138927	SON	78.27	9.54	0.04	0.05	8.22	7.78	0.00	0.03	14.88	8.57
NM_001358	DHX15	5.89	7.15	0.01	0.02	7.59	7.47	0.04	0.08	6.63	7.30
NM_001568	EIF3E	4.88	9.30	0.01	0.01	8.83	10.94	0.03	0.05	6.29	10.05
NM_001270448	ACADVL	76.90	58.78	0.00	0.00	119.28	114.02	0.01	0.04	93.51	77.57

NM_001097615	POLR2J3	3.95	4.50	0.02	0.03	3.75	3.88	0.01	0.01	3.85	4.17
NM_022170	EIF4H	9.27	16.28	0.00	0.01	16.04	24.49	0.01	0.07	11.75	19.56
NM_003753	EIF3D	9.32	12.87	0.00	0.01	13.09	15.79	0.03	0.04	10.89	14.18
NM_181672	OGT	7.44	9.73	0.01	0.01	10.34	9.03	0.02	0.02	8.65	9.37
NM_018060	IARS2	14.80	25.11	0.00	0.00	51.64	37.18	0.01	0.03	23.00	29.98
NM_002901	RCN1	11.86	18.63	0.00	0.02	47.07	24.29	0.01	0.10	18.95	21.09
NM_001033	RRM1	7.66	14.16	0.00	0.01	15.07	27.27	0.02	0.06	10.16	18.64
NM_002790	PSMA5	6.08	7.73	0.01	0.02	7.82	8.85	0.04	0.08	6.84	8.25
NM_002709	PPP1CB	8.43	40.07	0.01	0.02	15.65	16.75	0.01	0.05	10.96	23.62
NM_006430	CCT4	10.19	24.42	0.00	0.00	19.05	24.60	0.02	0.05	13.28	24.51
NM_016091	EIF3L	7.67	9.36	0.01	0.01	12.37	13.83	0.02	0.06	9.47	11.16
NM_004905	PRDX6	11.85	19.88	0.01	0.01	22.56	22.70	0.02	0.04	15.54	21.20
NM_032959	POLR2J2	3.86	4.17	0.02	0.03	3.87	3.65	0.01	0.01	3.86	3.89
NM_001173454	PDHA1	19.76	25.11	0.00	0.00	83.56	44.55	0.01	0.04	31.96	32.12
NM_022445	TPK1	10.95	404.37	0.00	0.00	14.99	58.09	0.01	0.03	12.66	101.58
NM_001098208	HNRNPF	6.24	8.97	0.01	0.01	9.13	11.88	0.02	0.08	7.42	10.22
NM_006585	CCT8	7.60	16.49	0.00	0.01	21.73	41.34	0.01	0.04	11.26	23.58
NM_000884	IMPDH2	9.93	11.72	0.00	0.00	15.41	14.22	0.01	0.04	12.08	12.85
NM_006088	TUBB4B	7.21	6.30	0.00	0.00	5.94	6.27	0.00	0.04	6.51	6.29
NM_175866	UHMK1	11.21	12.98	0.00	0.02	42.42	17.41	0.02	0.07	17.74	14.87
NM_003017	SRSF3	5.74	9.58	0.01	0.03	7.23	10.02	0.04	0.11	6.40	9.79
NM_001605	AARS	10.74	13.67	0.00	0.01	10.24	9.99	0.01	0.08	10.48	11.55
NM_001256487	GOLGB1	6.61	8.57	0.00	0.02	9.70	9.66	0.01	0.05	7.86	9.09
NM_001199973	RPL36A-HNRNPH2	8.54	17.11	0.00	0.01	52.48	29.78	0.01	0.06	14.69	21.73
NM_003368	USP1	4.10	5.83	0.01	0.02	5.65	6.22	0.01	0.04	4.75	6.02
NM_001164317	FLNB	9.44	6.85	0.03	0.01	6.85	6.46	0.02	0.01	7.94	6.65
NM_032833	PPP1R15B	3.85	3.96	0.01	0.02	4.28	4.19	0.01	0.04	4.06	4.07
NM_002808	PSMD2	65.02	107.56	0.00	0.00	239.93	68.26	0.00	0.04	102.32	83.51
NM_020803	KLHL8	21.29	20.76	0.00	0.00	53.46	24.59	0.01	0.02	30.45	22.51
NM_004730	ETF1	8.20	18.45	0.00	0.01	15.18	14.72	0.02	0.05	10.65	16.38
NM_012062	DNM1L	7.80	14.23	0.01	0.01	12.82	15.13	0.02	0.04	9.70	14.67
NM_000716	C4BPB	4.89	9.90	0.00	0.00	7.84	11.40	0.01	0.02	6.02	10.60
NM_000249	MLH1	8.95	17.86	0.00	0.01	14.75	20.86	0.02	0.05	11.14	19.25
NM_003146	SSRP1	25.80	15.13	0.01	0.00	56.68	36.38	0.01	0.07	35.46	21.37
NM_001099432	BCAS3	7.66	8.16	0.01	0.01	12.25	8.07	0.03	0.02	9.43	8.12
NM_001015885	RAE1	3.26	5.98	0.02	0.04	28.57	17.06	0.00	0.06	5.85	8.86
NM_024766	CAMKMT	2.44	2.95	0.11	0.02	2.23	2.18	0.07	0.01	2.33	2.50
NM_004261	SEP15	6.90	12.92	0.01	0.02	11.26	9.48	0.04	0.06	8.55	10.94
NM_005455	ZRANB2	3.91	6.20	0.01	0.01	4.53	4.04	0.01	0.04	4.20	4.89
NM_003379	EZR	7.23	8.77	0.01	0.02	8.63	11.80	0.02	0.18	7.87	10.06
NM_182776	MCM7	11.13	15.22	0.00	0.01	11.75	19.71	0.02	0.04	11.43	17.18
NM_003329	TXN	10.39	31.12	0.00	0.01	37.42	672.32	0.02	0.07	16.26	59.49
NM_006191	PA2G4	12.20	12.38	0.01	0.01	23.48	18.67	0.02	0.03	16.06	14.89
NM_001688	ATP5F1	10.81	23.52	0.00	0.00	33.74	45.74	0.02	0.05	16.38	31.07
NM_005762	TRIM28	29.12	11.78	0.01	0.00	8.89	14.12	0.01	0.00	13.62	12.85
NM_001152	SLC25A5	31.84	23.31	0.00	0.00	44.28	77.45	0.00	0.06	37.05	35.84
NM_021629	GNB4	8.33	16.41	0.01	0.02	25.17	14.83	0.02	0.07	12.52	15.58
NM_001098616	C1orf43	11.85	19.87	0.00	0.01	25.99	28.41	0.02	0.06	16.28	23.39
NM_003681	PDXK	12.50	12.12	0.01	0.00	8.88	16.44	0.03	0.01	10.39	13.96
NM_005324	H3F3B	7.50	16.60	0.00	0.00	10.68	22.72	0.01	0.05	8.81	19.19
NM_004766	COPB2	9.24	15.28	0.00	0.01	16.03	15.80	0.01	0.07	11.72	15.54
NM_030752	TCP1	12.81	31.06	0.00	0.00	41.60	105.84	0.01	0.04	19.59	48.02
NM_013336	SEC61A1	10.65	11.82	0.01	0.00	11.82	13.43	0.02	0.02	11.20	12.57
NM_016451	COPB1	6.44	11.33	0.00	0.00	11.59	14.15	0.02	0.03	8.28	12.58
NM_001412	EIF1AX	12.28	24.99	0.00	0.01	65.61	27.03	0.01	0.06	20.69	25.97
NM_005911	MAT2A	4.52	4.72	0.01	0.02	5.31	4.41	0.01	0.09	4.88	4.56
NM_000986	RPL24	12.58	116.43	0.00	0.00	175.61	279.96	0.01	0.05	23.48	164.46
NM_006367	CAP1	10.42	18.70	0.00	0.00	33.95	44.17	0.01	0.05	15.95	26.28
NM_002389	CD46	5.95	7.64	0.00	0.01	8.27	8.66	0.03	0.06	6.92	8.12
NM_001204366	MGST2	15.80	353.59	0.00	0.00	45.21	42.99	0.00	0.06	23.41	76.66
NM_000182	HADHA	10.92	14.16	0.01	0.00	16.89	18.04	0.02	0.04	13.27	15.87
NM_002417	MKI67	49.19	8.79	0.06	0.03	10.01	8.60	0.00	0.04	16.64	8.70
NM_014691	AQR	7.32	13.98	0.00	0.02	36.54	13.97	0.02	0.05	12.19	13.97
NM_004826	ECEL1	5291.66	22.50	0.01	0.00	21.35	561.53	0.02	0.01	42.52	43.26
NM_006815	TMED2	16.94	31.98	0.00	0.01	270.04	100.66	0.01	0.05	31.87	48.54
NM_014639	TTC37	5.86	7.98	0.01	0.02	8.58	8.42	0.04	0.08	6.97	8.19

NM_015723	PNPLA8	13.79	43.83	0.00	0.00	40.91	70.02	0.02	0.02	20.62	53.91
NM_153618	SEMA6D	14.27	15.94	0.00	0.00	18.93	25.85	0.02	0.04	16.27	19.72
NM_006793	PRDX3	14.40	55.19	0.00	0.00	967.66	37.87	0.01	0.04	28.37	44.92
NM_206825	GNL3	3.19	4.02	0.00	0.01	4.29	4.42	0.01	0.06	3.66	4.21
NM_001040716	PC	9.29	9.05	0.03	0.01	6.17	8.40	0.05	0.02	7.42	8.71
NM_001024921	RPL9	14.15	88.11	0.00	0.00	62.64	183.11	0.01	0.04	23.09	118.97
NM_016237	ANAPC5	8.82	13.45	0.00	0.00	14.46	19.28	0.01	0.02	10.96	15.85
NM_183422	TSC22D1	1.75	2.29	0.04	0.01	1.72	2.27	0.03	0.04	1.73	2.28
NM_001008491	SEPT2	9.80	19.92	0.00	0.01	24.88	22.15	0.01	0.04	14.06	20.97
NM_001267809	ILF2	8.77	12.47	0.00	0.00	17.52	17.46	0.01	0.05	11.69	14.55
NM_000143	FH	9.34	14.96	0.00	0.00	18.92	24.13	0.02	0.03	12.50	18.47
NM_001136005	GART	6.89	11.21	0.00	0.01	9.54	11.61	0.02	0.05	8.00	11.40
NM_001134422	CDV3	5.34	7.23	0.00	0.02	7.79	9.73	0.02	0.06	6.33	8.30
NM_018206	VPS35	9.38	23.61	0.00	0.01	33.02	53.91	0.01	0.03	14.61	32.84
NM_002004	FDPS	10.39	13.79	0.00	0.00	15.76	21.91	0.01	0.05	12.52	16.93
NM_005124	NUP153	2.35	3.10	0.03	0.02	2.40	3.06	0.04	0.06	2.37	3.08
NM_003981	PRC1	6.31	8.34	0.01	0.01	8.47	11.65	0.03	0.06	7.24	9.72
NM_024798	SNX22	19.37	17.46	0.00	0.01	46.60	38.80	0.01	0.05	27.36	24.08
NM_001212	C1QBP	13.10	16.20	0.01	0.00	33.06	33.44	0.01	0.03	18.77	21.82
NM_002106	H2AFZ	11.24	27.60	0.00	0.00	46.38	31.02	0.01	0.05	18.09	29.21
NM_016578	RSF1	9.02	16.81	0.02	0.02	8.97	10.94	0.00	0.01	9.00	13.26
NM_015959	TMX2	11.21	16.08	0.00	0.01	15.90	16.70	0.02	0.03	13.15	16.39
NM_001127328	ACADM	8.51	18.44	0.00	0.02	18.23	15.12	0.02	0.06	11.60	16.62
NM_002819	PTBP1	8.07	8.09	0.02	0.01	6.21	7.64	0.01	0.02	7.02	7.86
NM_004892	SEC22B	6.37	9.92	0.00	0.02	9.01	10.23	0.02	0.07	7.47	10.07
NM_005340	HINT1	14.94	45.62	0.00	0.00	580.23	6041.31	0.01	0.06	29.13	90.56
NM_001539	DNAJA1	6.08	9.20	0.01	0.01	9.60	12.53	0.03	0.13	7.45	10.61
NM_025235	TNKS2	8.14	12.36	0.01	0.01	10.36	10.59	0.03	0.04	9.11	11.41
NM_001198879	ATP5J2-PTCD1	7.18	9.50	0.00	0.01	8.22	11.14	0.01	0.06	7.66	10.25
NM_152405	JMY	11.77	24.49	0.00	0.00	22.41	30.22	0.02	0.02	15.44	27.05
NM_014394	GHITM	14.67	83.81	0.00	0.00	47.07	159.50	0.01	0.05	22.37	109.88
NM_004939	DDX1	9.35	15.30	0.00	0.02	22.21	19.95	0.02	0.10	13.16	17.32
NM_017672	TRPM7	4.81	6.88	0.01	0.02	6.33	6.13	0.05	0.04	5.46	6.48
NM_006819	STIP1	10.76	13.88	0.00	0.01	17.08	20.40	0.02	0.05	13.20	16.52
NM_017664	ANKRD10	7.02	11.47	0.00	0.01	9.65	11.71	0.01	0.01	8.13	11.59
NM_014363	SACS	6.01	7.34	0.01	0.01	8.12	8.72	0.02	0.03	6.91	7.97
NM_001102398	HNRNPR	7.66	13.73	0.01	0.01	15.32	16.87	0.01	0.09	10.22	15.14
NM_018128	TSR1	9.72	10.96	0.01	0.02	12.19	16.85	0.02	0.06	10.82	13.28
NM_006601	PTGES3	8.36	7.12	0.01	0.03	13.92	6.07	0.00	0.12	10.44	6.55
NM_014966	DHX30	8.90	7.73	0.02	0.01	7.85	8.49	0.04	0.04	8.34	8.09
NM_005860	FSTL3	24.98	16.62	0.00	0.01	19.40	19.28	0.01	0.03	21.84	17.85
NM_001145260	NCOA4	6.89	14.16	0.00	0.01	17.68	18.64	0.02	0.04	9.91	16.10
NM_001154	ANXA5	8.85	13.22	0.00	0.01	39.54	54.74	0.03	0.07	14.46	21.29
NM_014322	OPN3	6.20	12.29	0.01	0.01	9.02	15.60	0.05	0.03	7.35	13.75
NM_001144944	MYL12B	12.59	20.95	0.00	0.01	818.33	52.19	0.01	0.03	24.79	29.90
NM_001204410	SEC14L1	8.13	10.43	0.05	0.04	6.03	5.17	0.07	0.01	6.92	6.92
NM_002525	NRD1	8.23	10.30	0.01	0.01	8.56	8.32	0.01	0.03	8.39	9.20
NM_007007	CPSF6	6.00	7.62	0.02	0.00	6.78	6.59	0.03	0.02	6.37	7.07
NM_015046	SETX	3.89	4.96	0.01	0.02	4.38	5.31	0.04	0.05	4.12	5.13
NM_004640	DDX39B	15.90	11.23	0.01	0.00	12.89	14.62	0.02	0.02	14.24	12.70
NM_001195291	SERPINB6	11.60	14.19	0.01	0.00	16.87	13.49	0.01	0.03	13.75	13.84
NM_007276	CBX3	9.32	21.76	0.00	0.01	19.44	22.24	0.01	0.06	12.60	22.00
NM_007192	SUPT16H	8.56	15.15	0.00	0.01	17.99	15.90	0.00	0.07	11.60	15.52
NM_014294	TRAM1	8.62	27.59	0.00	0.01	82.00	28.08	0.01	0.07	15.59	27.83
NM_175868	MAGEA6	13.79	26.56	0.00	0.00	29.44	37.83	0.02	0.04	18.78	31.20
NM_006513	SARS	7.28	11.32	0.00	0.01	12.03	11.09	0.01	0.06	9.07	11.21
NM_005721	ACTR3	6.46	13.15	0.01	0.02	10.33	12.79	0.04	0.08	7.95	12.97
NM_152635	OIT3	10.17	29.24	0.01	0.01	69.22	54.14	0.00	0.04	17.73	37.97
NM_001012267	CENPP	2.87	2.88	0.11	0.04	2.37	2.19	0.04	0.02	2.59	2.49
NM_203505	G3BP2	8.01	20.30	0.00	0.01	18.25	16.65	0.01	0.09	11.13	18.29
NM_006024	TAX1BP1	5.80	7.87	0.01	0.03	8.02	8.86	0.05	0.08	6.73	8.33
NM_002107	H3F3A	17.20	183.92	0.00	0.00	374.26	428.62	0.00	0.08	32.88	257.40
NM_152526	PARD3B	2.58	2.92	0.14	0.04	2.54	2.67	0.08	0.03	2.56	2.79
NM_002710	PPP1CC	6.83	14.94	0.01	0.02	12.11	14.57	0.02	0.06	8.74	14.75
NM_001142800	EYS	4.64	6.02	0.03	0.01	4.96	5.86	0.03	0.02	4.79	5.94
NM_000179	MSH6	6.22	7.77	0.01	0.01	8.10	9.42	0.01	0.04	7.04	8.52

NM_006496	GNAI3	8.25	20.01	0.01	0.00	15.85	17.19	0.02	0.07	10.85	18.49
NM_021129	PPA1	8.07	14.95	0.00	0.01	14.72	15.86	0.04	0.05	10.43	15.39
NM_001127223	CD59	10.29	22.33	0.00	0.01	44.12	34.36	0.01	0.05	16.68	27.07
NM_001634	AMD1	2.40	2.90	0.03	0.10	2.46	3.30	0.05	0.17	2.43	3.08
NM_002210	ITGAV	7.05	17.02	0.00	0.00	9.77	10.41	0.04	0.04	8.19	12.92
NM_006999	PAPD7	2.21	2.38	0.12	0.02	1.97	2.23	0.07	0.06	2.08	2.30
NM_005362	MAGEA3	14.30	27.70	0.00	0.00	31.83	35.16	0.02	0.04	19.74	30.98
NM_000028	AGL	10.18	15.78	0.00	0.01	11.10	10.58	0.02	0.01	10.62	12.67
NM_005570	LMAN1	9.33	16.43	0.00	0.01	26.10	20.73	0.02	0.05	13.75	18.33
NM_000454	SOD1	17.84	30.81	0.00	0.00	60.54	84.05	0.02	0.05	27.56	45.09
NM_015646	RAP1B	5.72	9.81	0.01	0.01	6.62	8.36	0.04	0.05	6.13	9.02
NM_001916	CYC1	37.55	21.59	0.00	0.00	18.00	29.97	0.02	0.03	24.34	25.10
NM_000052	ATP7A	20.24	33.12	0.00	0.00	55.00	87.42	0.01	0.04	29.59	48.04
NM_006360	EIF3M	7.73	12.12	0.00	0.01	15.62	18.45	0.03	0.04	10.35	14.63
NM_002634	PHB	21.71	27.34	0.00	0.00	35.63	79.01	0.02	0.04	26.98	40.62
NM_023924	BRD9	8.43	6.53	0.04	0.01	5.43	5.64	0.03	0.02	6.61	6.05
NM_001080396	FAM155A	1.95	2.33	0.05	0.01	2.05	1.93	0.02	0.02	2.00	2.11
NM_001002031	ATP5G2	10.02	17.36	0.00	0.01	25.23	19.90	0.01	0.05	14.34	18.55
NM_004725	BUB3	8.00	14.79	0.00	0.01	14.90	16.57	0.03	0.05	10.41	15.63
NM_004539	NARS	10.80	21.81	0.00	0.01	29.33	33.94	0.02	0.05	15.78	26.56
NM_001861	COX4I1	14.39	17.02	0.00	0.00	21.87	61.63	0.02	0.07	17.36	26.67
NM_006708	GLO1	8.90	19.72	0.00	0.02	56.77	24.73	0.01	0.06	15.39	21.94
NM_031966	CCNB1	5.30	7.51	0.00	0.00	7.37	7.97	0.01	0.07	6.17	7.73
NM_012341	GTPBP4	5.96	8.33	0.01	0.01	8.98	12.11	0.03	0.09	7.16	9.87
NM_006392	NOP56	4.72	5.45	0.00	0.01	5.07	5.71	0.01	0.07	4.89	5.57
NM_007178	STRAP	11.49	17.37	0.00	0.01	26.14	22.08	0.01	0.06	15.96	19.45
NM_005760	CEBPZ	4.33	6.35	0.00	0.01	6.13	6.71	0.02	0.04	5.07	6.53
NM_006612	KIF1C	29.30	21.55	0.02	0.00	23.35	30.60	0.01	0.03	25.99	25.29
NM_018638	ETNK1	4.10	5.84	0.02	0.01	3.96	4.01	0.03	0.00	4.03	4.76
NM_004965	HMGN1	9.14	13.57	0.01	0.01	15.23	13.87	0.02	0.06	11.43	13.71
NM_004818	DDX23	7.29	8.07	0.00	0.01	9.27	10.80	0.02	0.08	8.16	9.24
NM_001001973	ATP5C1	9.23	21.43	0.00	0.01	35.71	23.67	0.01	0.05	14.67	22.49
NM_000938	POLR2B	6.12	9.43	0.01	0.01	9.36	11.81	0.02	0.05	7.40	10.49
NM_145341	PDCD4	7.78	18.78	0.01	0.01	13.49	14.19	0.01	0.10	9.87	16.16
NM_002524	NRAS	10.02	22.91	0.00	0.01	162.61	21.85	0.01	0.05	18.88	22.37
NM_014117	C16orf72	6.61	7.66	0.01	0.01	8.10	7.73	0.02	0.02	7.28	7.69
NM_014720	SLK	6.03	9.15	0.01	0.02	9.99	10.31	0.03	0.09	7.52	9.69
NM_152788	ANKS1B	3.05	4.24	0.11	0.03	2.88	3.03	0.09	0.02	2.96	3.53
NM_006694	JTB	26.42	27.66	0.00	0.00	25.72	53.75	0.02	0.03	26.06	36.52
NM_001039348	EFEMP1	8.40	8.55	0.01	0.01	11.01	10.32	0.04	0.05	9.53	9.36
NM_006195	PBX3	2.04	2.32	0.12	0.04	2.06	1.99	0.09	0.03	2.05	2.14
NM_002841	PTPRG	13.44	16.92	0.00	0.00	80.22	26.23	0.01	0.03	23.03	20.57
NM_003071	HLTF	6.23	8.92	0.01	0.01	9.24	8.13	0.05	0.09	7.44	8.51
NM_006839	IMMT	7.36	11.00	0.01	0.01	10.65	13.41	0.03	0.06	8.70	12.09
NM_003365	UQCRC1	52.16	29.27	0.00	0.00	20.00	50.56	0.02	0.04	28.92	37.08
NM_212472	PRKAR1A	11.41	26.33	0.00	0.01	23.69	47.36	0.01	0.05	15.40	33.85
NM_001130440	SRP9	8.40	18.46	0.00	0.01	43.29	18.22	0.02	0.06	14.07	18.34
NM_001136033	PUF60	9.28	10.66	0.00	0.00	7.63	11.47	0.02	0.06	8.38	11.05
NM_198335	GANAB	315.24	26.46	0.01	0.01	34.85	17.58	0.00	0.02	62.75	21.12
NM_014278	HSPA4L	9.11	14.01	0.01	0.01	31.91	22.74	0.01	0.04	14.18	17.33
NM_001142648	SAR1A	7.77	18.93	0.00	0.01	13.22	22.61	0.02	0.05	9.79	20.61
NM_001145065	CCSER1	15.78	124.76	0.00	0.00	34.56	37.11	0.01	0.05	21.67	57.21
NM_021138	TRAF2	6.62	5.53	0.06	0.01	4.81	5.47	0.06	0.03	5.57	5.50
NM_015659	RSL1D1	6.64	11.63	0.01	0.02	13.89	25.45	0.02	0.04	8.98	15.96
NM_000305	PON2	6.74	10.42	0.01	0.03	10.57	8.24	0.02	0.02	8.23	9.20
NM_005499	UBA2	6.24	9.30	0.01	0.03	10.17	10.82	0.04	0.08	7.73	10.00
NM_001130089	KARS	11.08	16.95	0.00	0.00	26.06	29.77	0.03	0.04	15.55	21.60
NM_006004	UQCRH	13.72	39.79	0.00	0.01	113.60	35.28	0.01	0.04	24.49	37.40
NM_001126103	RACGAP1	5.22	9.93	0.01	0.02	7.24	8.48	0.03	0.07	6.06	9.15
NM_170711	DAZAP1	13.73	12.64	0.01	0.00	12.40	15.27	0.01	0.01	13.03	13.83
NM_001136232	SEC13	11.61	9.88	0.00	0.01	13.41	12.36	0.02	0.04	12.45	10.98
NM_019087	ARL15	2.64	2.94	0.13	0.06	2.37	2.34	0.05	0.01	2.50	2.61
NM_032773	LRCH3	8.55	11.05	0.01	0.00	11.05	15.66	0.02	0.03	9.64	12.95
NM_001258310	NOP2	4.84	5.79	0.00	0.00	4.63	5.56	0.01	0.03	4.73	5.67
NM_006275	SRSF6	8.65	13.15	0.00	0.01	11.03	12.69	0.00	0.07	9.70	12.92
NM_006713	SUB1	7.88	26.06	0.00	0.02	20.83	19.48	0.02	0.05	11.43	22.29

NM_006389	HYOU1	35.15	35.19	0.00	0.00	64.35	30.96	0.01	0.04	45.46	32.94
NM_017566	KLHDC4	8.05	7.39	0.02	0.00	5.13	5.19	0.01	0.01	6.27	6.10
NM_002796	PSMB4	14.42	23.42	0.00	0.00	25.81	58.85	0.01	0.04	18.50	33.51
NM_139168	SREK1	2.82	3.90	0.02	0.02	3.19	3.47	0.05	0.07	2.99	3.67
NM_024646	ZYG11B	9.34	19.00	0.00	0.00	17.48	29.00	0.02	0.02	12.18	22.96
NM_001113378	FANCI	4.63	5.75	0.01	0.01	5.38	5.75	0.04	0.04	4.98	5.75
NM_001080393	GXYLT2	12.66	14.89	0.01	0.02	16.01	15.17	0.00	0.01	14.14	15.03
NM_198082	CCDC57	10.03	7.36	0.02	0.00	5.62	5.01	0.02	0.01	7.21	5.97
NM_001166686	PFKM	15.44	21.75	0.00	0.00	16.45	23.57	0.02	0.04	15.93	22.62
NM_002539	ODC1	9.92	16.25	0.00	0.01	14.36	28.27	0.02	0.03	11.74	20.64
NM_006185	NUMA1	7.81	7.94	0.04	0.01	6.67	7.60	0.04	0.02	7.19	7.77
NM_001257389	CD63	17.86	45.88	0.00	0.00	248.08	424.04	0.00	0.06	33.32	82.81
NM_012243	SLC35A3	4.60	5.34	0.02	0.01	5.40	4.90	0.03	0.02	4.97	5.11
NM_001127192	CNBP	7.73	15.90	0.01	0.01	18.45	17.66	0.02	0.08	10.89	16.74
NM_001969	EIF5	2.86	7.47	0.03	0.00	3.46	5.75	0.02	0.03	3.13	6.50
NM_006838	METAP2	6.14	9.86	0.01	0.02	10.09	11.72	0.02	0.13	7.64	10.71
NM_003816	ADAM9	7.94	9.81	0.00	0.05	15.01	8.33	0.02	0.15	10.38	9.01
NM_003404	YWHAB	15.75	20.33	0.01	0.02	29.43	16.07	0.00	0.03	20.52	17.95
NM_002467	MYC	1.28	1.56	0.18	0.03	1.29	1.56	0.13	0.04	1.28	1.56
NM_001098507	ZNF207	4.77	6.76	0.01	0.03	7.87	6.14	0.03	0.07	5.94	6.44
NM_002305	LGALS1	40.15	36.04	0.00	0.01	75.88	192.81	0.02	0.05	52.52	60.73
NM_002940	ABCE1	6.50	11.99	0.01	0.01	13.47	19.49	0.04	0.05	8.77	14.84
NM_006231	POLE	13.02	8.45	0.02	0.00	8.03	8.52	0.02	0.01	9.93	8.48
NM_014597	DNTTIP2	4.93	5.71	0.00	0.01	7.07	6.83	0.01	0.07	5.81	6.22
NM_198868	TBC1D9B	16.10	8.97	0.01	0.01	10.16	11.52	0.03	0.03	12.46	10.09
NM_001114636	FANCL	3.50	4.71	0.02	0.03	3.48	3.78	0.03	0.01	3.49	4.20
NM_005231	CTTN	15.08	20.42	0.00	0.00	20.87	60.93	0.02	0.04	17.51	30.58
NM_181356	SUPT3H	2.10	2.65	0.08	0.01	2.07	2.07	0.07	0.02	2.09	2.32
NM_006784	WDR3	5.06	7.59	0.01	0.01	6.46	10.22	0.04	0.07	5.68	8.71
NM_004540	NCAM2	2.46	2.90	0.05	0.02	2.54	2.45	0.04	0.03	2.50	2.65
NM_005917	MDH1	10.49	22.86	0.00	0.00	41.45	35.60	0.01	0.04	16.74	27.84
NM_001011724	HNRNPA1L2	9.29	28.23	0.00	0.01	14.43	23.73	0.00	0.25	11.31	25.78
NM_006023	CDC123	5.59	7.78	0.01	0.02	7.43	8.62	0.05	0.09	6.38	8.17
NM_006888	CALM1	12.59	16.31	0.00	0.01	76.12	40.63	0.01	0.06	21.60	23.28
NM_001142966	GREB1L	3.33	3.51	0.14	0.06	3.10	2.97	0.10	0.02	3.21	3.22
NM_005646	TARBP1	4.07	4.09	0.03	0.01	3.89	4.15	0.06	0.02	3.98	4.12
NM_005271	GLUD1	11.87	13.62	0.01	0.01	11.77	18.72	0.03	0.06	11.82	15.77
NM_000903	NQO1	9.21	17.28	0.00	0.01	46.62	22.83	0.02	0.05	15.38	19.67
NM_080738	EDARADD	22.04	28.61	0.00	0.00	28.42	30.46	0.02	0.03	24.83	29.51
NM_014962	BTBD3	7.45	11.94	0.01	0.01	9.18	14.84	0.04	0.04	8.23	13.24
NM_033625	RPL34	10.68	31.33	0.00	0.01	42.06	63.11	0.02	0.04	17.03	41.88
NM_006933	SLC5A3	6.43	6.73	0.03	0.02	5.62	5.22	0.04	0.01	5.99	5.88
NM_013230	CD24	13.01	28.70	0.00	0.01	182.51	114.10	0.01	0.01	24.29	45.86
NM_001007022	ODF2L	2.75	4.14	0.02	0.02	3.13	3.58	0.03	0.01	2.93	3.84
NM_014820	TOMM70A	5.20	7.76	0.01	0.02	8.23	8.43	0.02	0.05	6.38	8.08
NM_002804	PSMC3	12.01	19.17	0.00	0.01	20.54	40.69	0.01	0.08	15.15	26.06
NM_000135	FANCA	9.33	7.97	0.04	0.00	6.69	6.16	0.01	0.02	7.80	6.95
NM_018063	HELLS	7.12	8.21	0.02	0.02	5.87	5.69	0.02	0.01	6.43	6.73
NM_007027	TOPBP1	3.97	4.95	0.01	0.02	5.09	5.12	0.04	0.05	4.46	5.03
NM_002715	PPP2CA	4.94	7.24	0.01	0.01	5.64	7.33	0.02	0.06	5.27	7.29
NM_003640	IKBKAP	6.70	9.78	0.00	0.01	7.84	11.57	0.02	0.05	7.22	10.60
NM_001143780	SLC25A39	30.60	23.06	0.00	0.00	20.79	55.85	0.02	0.02	24.76	32.65
NM_014781	RB1CC1	5.00	7.21	0.00	0.02	6.28	6.47	0.04	0.03	5.57	6.82
NM_173822	FAM126B	6.70	21.38	0.01	0.02	11.54	14.88	0.00	0.16	8.48	17.55
NM_001008528	MXRA7	15.72	29.66	0.00	0.00	33.43	106.67	0.02	0.03	21.39	46.42
NM_001363	DKC1	6.40	12.61	0.00	0.02	9.61	13.43	0.01	0.12	7.68	13.00
NM_001011546	DSTN	9.75	19.56	0.00	0.02	35.36	31.61	0.01	0.08	15.29	24.17
NM_014303	PES1	7.62	8.57	0.01	0.02	8.16	11.29	0.02	0.08	7.88	9.74
NM_182663	RASSF5	13.28	20.29	0.00	0.00	16.32	18.28	0.03	0.05	14.65	19.23
NM_001017	RPS13	15.84	41.82	0.00	0.00	112.93	115.95	0.00	0.04	27.78	61.47
NM_016308	CMPK1	9.80	26.19	0.00	0.01	21.54	26.89	0.02	0.04	13.48	26.53
NM_006845	KIF2C	3.98	6.47	0.01	0.02	4.52	7.33	0.04	0.09	4.23	6.87
NM_021960	MCL1	2.44	3.98	0.00	0.00	2.75	4.42	0.01	0.03	2.59	4.19
NM_001039802	CDC42	7.30	15.57	0.00	0.02	22.26	18.90	0.02	0.05	10.99	17.08
NM_002355	M6PR	9.21	11.91	0.00	0.01	17.54	18.85	0.01	0.03	12.08	14.60
NM_001098	ACO2	12.20	5.81	0.05	0.01	6.89	7.21	0.03	0.03	8.81	6.43

NM_020198	CCDC47	10.35	16.59	0.00	0.01	26.07	16.06	0.01	0.06	14.82	16.32
NM_002263	KIFC1	8.54	16.06	0.00	0.01	11.43	21.97	0.02	0.04	9.77	18.56
NM_012215	MGEA5	7.86	15.74	0.01	0.01	10.75	13.69	0.01	0.02	9.08	14.64
NM_001163315	FBXL17	2.41	2.65	0.11	0.03	2.36	2.36	0.07	0.02	2.38	2.49
NM_002810	PSMD4	12.42	15.88	0.00	0.01	17.89	22.15	0.01	0.06	14.66	18.50
NM_005918	MDH2	18.81	29.63	0.01	0.01	26.29	46.62	0.00	0.05	21.93	36.23
NM_018474	PLK1S1	9.35	16.54	0.00	0.00	31.45	19.85	0.01	0.02	14.41	18.05
NM_002945	RPA1	11.49	27.21	0.00	0.01	14.37	13.44	0.00	0.09	12.77	17.99
NM_001005291	SREBF1	20.00	7.14	0.04	0.01	6.39	6.31	0.01	0.00	9.69	6.70
NM_003088	FSCN1	107.01	14.41	0.02	0.00	13.52	18.59	0.01	0.01	24.01	16.23
NM_003792	EDF1	22.04	14.51	0.00	0.00	21.92	45.81	0.01	0.05	21.98	22.04
NM_001173988	RABL6	46.81	14.01	0.00	0.00	14.59	15.83	0.01	0.00	22.24	14.86
NM_002887	RARS	6.13	8.70	0.00	0.01	10.86	10.17	0.01	0.04	7.84	9.38
NM_006644	HSPH1	7.59	10.86	0.01	0.01	13.58	10.76	0.02	0.08	9.74	10.81
NM_006461	SPAG5	9.02	8.39	0.00	0.01	12.55	11.11	0.02	0.04	10.50	9.56
NM_002793	PSMB1	7.77	11.61	0.00	0.01	12.64	12.10	0.02	0.03	9.62	11.85
NM_006666	RUVBL2	22.79	18.56	0.00	0.01	20.43	35.94	0.02	0.04	21.54	24.48
NM_000051	ATM	5.41	6.20	0.02	0.01	6.11	6.59	0.06	0.04	5.74	6.39
NM_018321	BRIX1	3.80	5.07	0.00	0.03	5.20	5.55	0.02	0.08	4.39	5.30
NM_152636	METTL15	2.85	3.36	0.04	0.02	2.95	3.03	0.06	0.02	2.90	3.19
NM_002624	PFDN5	15.20	29.39	0.00	0.00	46.00	63.55	0.02	0.03	22.85	40.19
NM_017925	DENND4C	2.33	2.80	0.03	0.06	61.70	12.58	0.26	0.21	4.49	4.59
NM_003100	SNX2	5.34	10.30	0.01	0.02	8.68	10.87	0.05	0.08	6.61	10.58
NM_022768	RBM15	3.12	3.61	0.05	0.02	2.92	3.64	0.06	0.04	3.02	3.62
NM_003926	MBD3	7.18	6.37	0.02	0.01	6.17	8.18	0.01	0.02	6.64	7.16
NM_014342	MTCH2	9.04	13.30	0.00	0.00	16.53	19.62	0.01	0.06	11.69	15.85
NM_002792	PSMA7	17.09	35.01	0.00	0.01	22.64	60.55	0.01	0.05	19.48	44.36
NM_013234	EIF3K	15.39	16.42	0.00	0.00	22.30	18.01	0.03	0.03	18.21	17.18
NM_005008	NHP2L1	8.81	18.00	0.00	0.01	14.81	19.14	0.01	0.06	11.04	18.55
NM_001204083	MINOS1	9.76	22.91	0.00	0.01	24.91	17.41	0.03	0.06	14.03	19.78
NM_001242480	LOC389831	2.78	3.38	0.08	0.01	2.53	2.74	0.06	0.02	2.64	3.03
NM_002789	PSMA4	9.19	25.11	0.00	0.00	65.44	59.95	0.00	0.06	16.11	35.40
NM_206839	MORF4L1	11.30	43.37	0.01	0.01	13.62	12.40	0.00	0.04	12.36	19.29
NM_001122838	NAPEPLD	23.28	19.97	0.00	0.00	17.14	52.95	0.03	0.02	19.74	29.00
NM_001569	IRAK1	28.16	28.99	0.00	0.00	21.10	331.88	0.01	0.04	24.12	53.33
NM_080594	RNPS1	12.32	15.90	0.01	0.01	10.44	15.04	0.01	0.02	11.30	15.46
NM_002803	PSMC2	10.90	14.54	0.00	0.00	22.34	35.82	0.01	0.04	14.65	20.69
NM_001009944	PKD1	16.14	5.76	0.02	0.00	5.59	5.63	0.03	0.00	8.31	5.69
NM_001136195	TNPO2	13.53	9.25	0.03	0.00	9.16	10.72	0.03	0.03	10.92	9.93
NM_000108	DLD	9.71	32.37	0.00	0.01	19.63	26.69	0.01	0.11	12.99	29.26
NM_005724	TSPAN3	13.64	24.56	0.00	0.01	46.69	31.15	0.01	0.03	21.11	27.47
NM_006470	TRIM16	4.20	4.41	0.02	0.01	4.58	4.76	0.05	0.06	4.38	4.58
NM_006031	PCNT	13.57	9.12	0.03	0.00	8.22	8.81	0.03	0.01	10.23	8.96
NM_006332	IFI30	22.27	31.29	0.00	0.00	1182.79	96.14	0.00	0.03	43.72	47.22
NM_006406	PRDX4	14.33	41.63	0.00	0.01	45.53	91.96	0.02	0.03	21.80	57.32
NM_032121	MAGT1	10.27	19.88	0.00	0.01	16.85	17.08	0.02	0.04	12.76	18.37
NM_001567	INPPL1	79.32	16.67	0.01	0.00	18.14	23.12	0.01	0.00	29.53	19.37
NM_031266	HNRNPAB	9.47	9.05	0.01	0.01	8.71	16.42	0.01	0.12	9.08	11.67
NM_001080495	TNRC18	5.96	4.70	0.11	0.03	3.67	4.12	0.05	0.01	4.54	4.39
NM_003119	SPG7	97.48	13.95	0.01	0.01	13.75	16.20	0.00	0.00	24.11	14.99
NM_006587	CORIN	12.34	30.91	0.00	0.00	37.23	225.52	0.00	0.05	18.54	54.36
NM_194292	SASS6	2.87	3.64	0.06	0.01	2.83	3.29	0.06	0.03	2.85	3.45
NM_004336	BUB1	7.45	9.68	0.00	0.01	10.67	11.52	0.02	0.03	8.77	10.52
NM_006930	SKP1	8.90	27.15	0.00	0.01	30.76	26.02	0.01	0.05	13.80	26.57
NM_032358	CCDC77	3.53	3.70	0.06	0.01	3.18	3.54	0.06	0.06	3.35	3.62
NM_004175	SNRPD3	9.11	12.47	0.01	0.01	37.51	19.94	0.01	0.09	14.66	15.34
NM_001012271	BIRC5	10.37	12.74	0.01	0.01	16.37	39.51	0.02	0.08	12.70	19.26
NM_001288	CLIC1	8.37	15.31	0.00	0.01	14.19	21.80	0.02	0.02	10.53	17.99
NM_002592	PCNA	6.60	10.25	0.00	0.00	17.09	12.82	0.01	0.03	9.53	11.39
NM_022346	NCAPG	5.60	8.99	0.00	0.01	8.69	11.43	0.03	0.06	6.81	10.07
NM_001010854	TTC7B	14.67	27.06	0.00	0.00	21.15	19.47	0.03	0.03	17.32	22.65
NM_004040	RHOB	1.16	1.82	0.16	0.01	1.13	1.81	0.17	0.02	1.14	1.81
NM_001042550	SMC2	7.00	16.21	0.00	0.01	14.44	14.55	0.03	0.08	9.43	15.33
NM_014708	KNTC1	6.79	9.08	0.01	0.01	10.03	9.95	0.03	0.04	8.10	9.50
NM_003542	HIST1H4C	1.56	2.06	0.02	0.02	1.68	2.04	0.04	0.02	1.62	2.05
NM_001204199	SRP19	8.89	18.84	0.00	0.01	17.49	29.35	0.01	0.05	11.79	22.95

NM_005866	SIGMAR1	174.09	31.50	0.01	0.00	78.42	57.44	0.00	0.03	108.13	40.68
NM_018328	MBD5	2.40	2.81	0.11	0.01	2.26	2.41	0.08	0.05	2.33	2.59
NM_003909	CPNE3	7.64	17.49	0.00	0.01	15.78	16.44	0.01	0.04	10.30	16.95
NM_014412	CACYBP	10.09	17.95	0.00	0.01	24.68	42.59	0.02	0.05	14.33	25.26
NM_004553	NDUFS6	6.68	9.22	0.00	0.01	11.33	12.41	0.01	0.15	8.40	10.58
NM_000982	RPL21	8.50	13.72	0.01	0.02	63.16	21.76	0.02	0.03	14.99	16.83
NM_021931	DHX35	5.04	7.58	0.01	0.05	8.59	7.59	0.06	0.09	6.35	7.58
NM_001002033	HN1	10.07	10.61	0.02	0.00	12.40	15.54	0.06	0.04	11.11	12.61
NM_018117	WDR11	6.85	8.54	0.01	0.01	8.15	9.37	0.04	0.02	7.44	8.94
NM_004827	ABCG2	6.51	9.93	0.01	0.02	9.00	9.49	0.04	0.04	7.56	9.70
NM_007145	ZNF146	3.49	3.26	0.01	0.02	4.02	3.35	0.01	0.03	3.73	3.30
NM_016122	CCDC41	2.72	2.92	0.14	0.02	2.58	2.82	0.14	0.06	2.65	2.87
NM_001008566	TPST2	12.91	34.96	0.00	0.01	59.31	147.06	0.01	0.12	21.21	56.48
NM_006141	DYNC1LI2	10.50	18.98	0.00	0.02	24.03	17.42	0.02	0.04	14.61	18.17
NM_001165258	TMEM14C	13.54	33.34	0.00	0.00	40.51	50.13	0.01	0.07	20.30	40.04
NM_018890	RAC1	8.15	9.55	0.01	0.02	10.16	11.85	0.02	0.12	9.05	10.57
NM_001253	CDC5L	4.95	8.07	0.00	0.01	8.10	8.10	0.04	0.07	6.14	8.08
NM_005339	UBE2K	5.90	6.18	0.03	0.02	5.55	4.11	0.01	0.01	5.72	4.94
NM_002907	RECQL	7.38	11.64	0.00	0.01	19.27	16.32	0.01	0.05	10.68	13.59
NM_015114	ANKLE2	5.98	5.60	0.02	0.01	7.38	6.20	0.03	0.01	6.61	5.89
NM_019014	POLR1B	3.35	3.93	0.03	0.02	3.30	3.77	0.04	0.05	3.32	3.85
NM_033296	MRFAP1	21.33	55.44	0.00	0.00	35.92	31.24	0.00	0.13	26.77	39.96
NM_152261	C12orf23	6.10	9.65	0.01	0.01	9.88	11.09	0.01	0.05	7.54	10.32
NM_005051	QARS	21.18	19.47	0.00	0.00	27.02	24.47	0.00	0.07	23.75	21.68
NM_005006	NDUFS1	9.30	18.89	0.01	0.01	15.42	22.74	0.02	0.04	11.61	20.64
NM_003545	HIST1H4E	0.92	0.73	0.12	0.25	0.91	0.74	0.13	0.09	0.91	0.73
NM_000026	ADSL	8.68	11.87	0.00	0.00	11.73	12.58	0.03	0.05	9.98	12.21
NM_018368	LMBRD1	6.15	12.89	0.00	0.02	14.71	13.62	0.03	0.07	8.68	13.25
NM_015904	EIF5B	5.71	9.58	0.00	0.03	9.15	5.49	0.01	0.17	7.03	6.98
NM_024844	NUP85	5.77	6.04	0.01	0.02	6.21	5.72	0.02	0.03	5.98	5.88
NM_005778	RBM5	1.93	2.57	0.03	0.05	1.98	2.48	0.02	0.09	1.95	2.53
NM_181806	AASDH	10.77	15.96	0.00	0.01	23.99	23.30	0.03	0.05	14.86	18.95
NM_003550	MAD1L1	4.14	3.82	0.13	0.05	3.23	3.72	0.12	0.01	3.63	3.77
NM_003715	USO1	6.45	14.65	0.01	0.01	12.19	13.50	0.04	0.08	8.44	14.05
NM_020401	NUP107	5.35	8.07	0.01	0.02	7.34	9.22	0.04	0.08	6.19	8.60
NM_003754	EIF3F	16.35	11.76	0.01	0.00	17.06	18.83	0.02	0.02	16.70	14.48
NM_017647	FTSJ3	6.63	9.16	0.00	0.01	9.28	13.32	0.01	0.09	7.74	10.85
NM_018227	UBA6	5.12	7.87	0.01	0.02	6.83	7.67	0.05	0.04	5.85	7.77
NM_177542	SNRPD2	24.40	34.37	0.00	0.00	29.98	89.28	0.01	0.04	26.90	49.64
NM_006907	PYCR1	19.50	14.36	0.00	0.01	14.20	28.91	0.02	0.04	16.43	19.19
NM_012401	PLXNB2	24.08	11.70	0.02	0.00	7.91	8.44	0.01	0.00	11.91	9.81
NM_002687	PNN	6.60	18.60	0.00	0.02	17.60	27.95	0.00	0.35	9.60	22.34
NM_014142	NUDT5	7.76	10.08	0.01	0.01	13.14	9.31	0.03	0.05	9.75	9.68
NM_004034	ANXA7	7.76	22.16	0.00	0.01	16.01	15.97	0.04	0.06	10.45	18.56
NM_005653	TFCP2	3.62	3.72	0.06	0.03	3.35	3.23	0.02	0.02	3.48	3.46
NM_004111	FEN1	6.35	8.06	0.00	0.00	7.30	9.85	0.01	0.04	6.79	8.86
NM_003091	SNRPB	13.13	21.47	0.00	0.01	14.53	26.27	0.02	0.06	13.80	23.63
NM_001821	CHML	6.67	15.20	0.00	0.01	15.72	23.13	0.03	0.02	9.37	18.35
NM_016238	ANAPC7	6.90	10.31	0.01	0.00	9.97	9.56	0.01	0.01	8.16	9.92
NM_002092	GRSF1	8.30	11.84	0.00	0.01	10.42	23.86	0.01	0.04	9.24	15.83
NM_000251	MSH2	6.92	13.66	0.02	0.01	11.08	14.03	0.04	0.04	8.52	13.85
NM_001199291	HSD17B4	5.44	10.43	0.01	0.01	8.21	9.39	0.04	0.10	6.55	9.88
NM_016359	NUSAP1	4.99	7.99	0.01	0.01	11.30	10.95	0.04	0.05	6.93	9.24
NM_006305	ANP32A	5.80	10.48	0.01	0.02	7.67	9.69	0.02	0.11	6.60	10.07
NM_015641	TES	3.95	5.56	0.02	0.04	4.29	5.62	0.10	0.06	4.12	5.59
NM_001031618	SPDYE2	3.10	3.42	0.02	0.03	3.20	3.31	0.01	0.00	3.15	3.36
NM_031858	NBR1	8.76	20.27	0.00	0.00	18.69	20.33	0.01	0.05	11.93	20.30
NM_005729	PPIF	6.58	6.70	0.03	0.01	5.39	9.55	0.02	0.04	5.92	7.88
NM_014972	TCF25	21.14	15.82	0.01	0.00	15.96	15.69	0.01	0.01	18.19	15.76
NM_003366	UQCRC2	8.90	13.87	0.00	0.01	12.88	17.81	0.01	0.04	10.53	15.59
NM_018981	DNAJC10	8.76	14.05	0.00	0.02	12.88	11.75	0.03	0.06	10.43	12.80
NM_001037494	DYNLL1	8.37	13.46	0.00	0.01	16.67	14.85	0.00	0.08	11.15	14.12
NM_000786	CYP51A1	10.63	27.55	0.00	0.01	55.38	41.80	0.02	0.04	17.83	33.21
NM_002794	PSMB2	8.26	11.50	0.02	0.01	9.17	9.19	0.01	0.02	8.69	10.22
NM_198433	AURKA	2.94	4.10	0.00	0.02	3.51	4.51	0.04	0.09	3.20	4.30
NM_032025	EIF2A	6.29	9.20	0.01	0.01	11.43	9.38	0.03	0.06	8.11	9.29

NM_182969	XRRA1	3.52	4.43	0.05	0.01	3.68	4.37	0.07	0.01	3.60	4.40
NM_138391	TMEM183A	10.40	12.32	0.00	0.00	12.78	23.74	0.04	0.03	11.46	16.22
NM_001271918	SEC11A	6.04	7.67	0.01	0.01	7.56	10.73	0.05	0.09	6.72	8.94
NM_001001	RPL36AL	22.02	183.09	0.00	0.00	26.28	677.51	0.03	0.04	23.96	288.28
NM_001254	CDC6	5.92	6.06	0.01	0.01	8.38	8.80	0.02	0.07	6.94	7.18
NM_001184796	ESYT1	54.84	22.75	0.02	0.00	30.68	42.25	0.02	0.01	39.35	29.57
NM_202002	FOXM1	27.45	12.48	0.04	0.01	12.30	12.57	0.00	0.00	16.98	12.52
NM_002795	PSMB3	11.31	18.98	0.00	0.00	14.07	31.74	0.03	0.05	12.54	23.76
NM_004552	NDUFS5	26.34	26.57	0.00	0.00	88.41	502.29	0.01	0.04	40.59	50.47
NM_005632	SOLH	19.67	8.43	0.01	0.00	5.44	6.71	0.01	0.01	8.53	7.47
NM_005915	MCM6	10.79	14.57	0.00	0.01	12.11	9.86	0.00	0.05	11.41	11.76
NM_138555	KIF23	3.60	4.54	0.03	0.02	4.09	5.26	0.04	0.09	3.83	4.87
NM_004252	SLC9A3R1	11.30	6.99	0.02	0.00	8.66	8.27	0.02	0.04	9.80	7.58
NM_007263	COPE	12.26	18.68	0.00	0.01	10.87	22.13	0.03	0.02	11.53	20.26
NM_022757	CCDC14	3.23	4.71	0.01	0.00	3.98	4.57	0.01	0.03	3.56	4.64
NM_017542	POGK	3.41	3.92	0.04	0.01	3.71	4.49	0.06	0.04	3.55	4.19
NM_022497	MRPS25	7.47	9.12	0.02	0.01	7.62	10.24	0.04	0.03	7.55	9.65
NM_001165931	RRM2	12.19	20.96	0.01	0.01	21.55	24.98	0.00	0.06	15.57	22.79
NM_006756	TCEA1	7.20	11.92	0.01	0.02	10.51	10.00	0.04	0.07	8.54	10.87
NM_006764	IFRD2	11.09	11.19	0.01	0.00	9.92	13.39	0.03	0.06	10.47	12.19
NM_022087	GALNT11	5.43	6.01	0.04	0.01	5.01	4.65	0.07	0.01	5.21	5.25
NM_006622	PLK2	1.04	1.62	0.07	0.03	1.06	1.65	0.08	0.07	1.05	1.63
NM_002882	RANBP1	14.84	21.70	0.01	0.00	30.27	95.68	0.02	0.04	19.92	35.38
NM_005567	LGALS3BP	53.34	21.46	0.00	0.00	17.65	29.31	0.01	0.02	26.52	24.78
NM_012343	NNT	10.68	32.67	0.00	0.00	358.74	50.66	0.00	0.06	20.75	39.72
NM_199360	TPD52L2	7.76	9.16	0.01	0.01	6.60	8.36	0.02	0.02	7.13	8.74
NM_170589	CASC5	5.79	7.68	0.01	0.02	9.08	10.05	0.03	0.05	7.07	8.71
NM_015338	ASXL1	3.20	3.23	0.06	0.03	3.09	2.67	0.05	0.02	3.15	2.92
NM_001326	CSTF3	3.62	4.96	0.03	0.02	4.00	3.72	0.05	0.02	3.80	4.25
NM_006047	RBM12	5.73	7.66	0.01	0.01	7.18	8.81	0.03	0.05	6.37	8.19
NM_054016	SRSF10	5.66	5.01	0.01	0.03	9.45	5.77	0.03	0.08	7.08	5.36
NM_001080825	TMEM120B	5.45	5.31	0.02	0.01	5.05	5.67	0.01	0.01	5.24	5.48
NM_016299	HSPA14	4.06	5.28	0.01	0.02	5.28	5.52	0.07	0.06	4.59	5.39
NM_001527	HDAC2	7.71	11.51	0.00	0.02	12.18	13.54	0.01	0.09	9.44	12.44
NM_001256879	POLD2	20.56	19.06	0.00	0.01	39.43	25.54	0.01	0.05	27.03	21.83
NM_001145437	LSS	171.21	15.43	0.01	0.00	9.23	9.04	0.01	0.01	17.51	11.40
NM_016129	COPS4	6.81	12.23	0.00	0.01	14.51	19.10	0.02	0.06	9.27	14.91
NM_032271	TRAF7	26.47	12.98	0.03	0.00	11.39	14.90	0.03	0.01	15.92	13.88
NM_024102	WDR77	11.91	18.97	0.00	0.01	10.90	17.74	0.03	0.05	11.39	18.33
NM_001171508	MCFD2	7.91	8.35	0.00	0.04	19.46	8.36	0.02	0.07	11.24	8.35
NM_001242400	GHR	9.91	16.71	0.00	0.01	139.06	31.66	0.00	0.11	18.50	21.87
NM_152713	STT3A	9.56	10.85	0.01	0.01	18.77	16.27	0.01	0.09	12.67	13.02
NM_004300	ACP1	8.63	18.84	0.00	0.01	16.80	22.65	0.03	0.07	11.40	20.57
NM_005804	DDX39A	8.60	8.03	0.00	0.01	7.93	7.82	0.03	0.11	8.25	7.93
NM_021821	MRPS35	6.16	12.20	0.01	0.01	7.61	11.71	0.05	0.06	6.81	11.95
NM_022735	ACBD3	3.58	5.51	0.01	0.02	4.26	5.96	0.03	0.11	3.89	5.73
NM_001166159	NDUFS2	13.79	19.86	0.00	0.00	20.77	34.01	0.00	0.09	16.57	25.08
NM_006500	MCAM	21.06	15.95	0.01	0.00	15.58	27.23	0.03	0.03	17.91	20.12
NM_001144932	PSMB5	11.91	17.01	0.00	0.01	16.04	17.80	0.01	0.07	13.67	17.39
NM_001018159	NAE1	6.02	9.36	0.00	0.01	11.20	11.12	0.02	0.06	7.83	10.16
NM_013446	MKRN1	8.66	10.41	0.00	0.03	14.14	13.32	0.02	0.07	10.74	11.69
NM_001130040	SHC1	10.67	13.16	0.01	0.01	10.56	14.50	0.02	0.03	10.61	13.80
NM_004060	CCNG1	9.25	26.23	0.00	0.00	48.68	89.59	0.02	0.02	15.54	40.58
NM_016258	YTHDF2	2.88	3.42	0.01	0.00	2.88	3.77	0.01	0.05	2.88	3.58
NM_000183	HADHB	10.06	26.16	0.00	0.00	32.96	28.06	0.01	0.03	15.41	27.08
NM_004094	EIF2S1	7.59	17.71	0.01	0.01	24.20	35.39	0.02	0.07	11.55	23.61
NM_006773	DDX18	6.83	15.84	0.00	0.01	15.53	14.21	0.01	0.07	9.49	14.98
NM_006510	TRIM27	2.48	2.75	0.02	0.01	2.35	2.80	0.05	0.07	2.41	2.78
NM_018131	CEP55	4.83	7.57	0.00	0.02	7.83	7.22	0.04	0.05	5.97	7.39
NM_003506	FZD6	5.20	8.22	0.01	0.01	7.51	7.44	0.04	0.04	6.14	7.81
NM_004922	SEC24C	24.16	11.43	0.01	0.00	11.67	14.25	0.01	0.03	15.74	12.69
NM_025219	DNAJC5	6.98	7.08	0.03	0.01	5.93	7.32	0.01	0.01	6.41	7.20
NM_006979	SLC39A7	11.97	50.36	0.00	0.00	10.95	28.50	0.00	0.07	11.44	36.40
NM_020680	SCYL1	8.56	9.91	0.01	0.01	8.57	9.33	0.03	0.05	8.57	9.61
NM_001267550	TTN	2.66	3.17	0.03	0.01	2.52	2.86	0.03	0.02	2.59	3.01
NM_003653	COPS3	5.93	8.55	0.01	0.02	8.89	10.51	0.04	0.06	7.11	9.43

NM_001031806	ALDH3A2	10.12	17.01	0.00	0.01	19.73	37.32	0.02	0.04	13.38	23.37
NM_002292	LAMB2	132.84	57.33	0.01	0.00	18.90	41.37	0.01	0.01	33.09	48.06
NM_005880	DNAJA2	6.68	9.95	0.00	0.01	8.73	12.20	0.03	0.06	7.57	10.96
NM_003115	UAP1	4.89	6.43	0.01	0.03	6.81	7.80	0.03	0.05	5.69	7.05
NM_015720	PODXL2	12.12	11.96	0.01	0.00	11.93	24.97	0.03	0.04	12.02	16.18
NM_015264	KIAA0930	11.52	8.39	0.00	0.01	8.51	9.62	0.02	0.04	9.79	8.96
NM_005896	IDH1	8.39	15.33	0.00	0.00	16.15	22.36	0.02	0.06	11.04	18.19
NM_174909	TMEM167A	5.07	9.20	0.01	0.02	12.15	9.44	0.05	0.09	7.16	9.32
NM_004528	MGST3	7.40	15.56	0.01	0.02	11.30	10.87	0.04	0.06	8.94	12.80
NM_033018	CDK16	20.42	11.76	0.02	0.00	13.00	13.96	0.01	0.02	15.88	12.76
NM_015496	KIAA1429	4.50	6.54	0.01	0.02	6.12	6.13	0.02	0.05	5.19	6.33
NM_001098272	HMGCS1	7.86	14.25	0.01	0.01	10.80	19.42	0.02	0.05	9.10	16.44
NM_019020	TBC1D16	10.14	7.94	0.05	0.02	7.46	8.07	0.03	0.00	8.60	8.01
NM_007189	ABCF2	12.32	11.81	0.01	0.00	17.51	31.51	0.02	0.05	14.46	17.18
NM_007375	TARDBP	5.42	12.38	0.00	0.01	9.90	11.63	0.01	0.23	7.00	11.99
NM_198488	FAM83H	17.98	10.77	0.02	0.00	6.10	10.74	0.01	0.00	9.11	10.76
NM_018225	SMU1	8.84	13.04	0.01	0.00	16.53	18.50	0.03	0.04	11.52	15.30
NM_178001	PPP2R4	9.20	13.66	0.03	0.01	8.61	11.12	0.04	0.05	8.89	12.26
NM_003849	SUCLG1	5.45	10.06	0.01	0.01	7.44	12.65	0.04	0.08	6.29	11.21
NM_007262	PARK7	13.13	16.64	0.00	0.00	21.28	72.75	0.01	0.11	16.24	27.09
NM_021145	DMTF1	3.60	4.60	0.02	0.03	3.75	4.73	0.07	0.04	3.67	4.67
NM_175744	RHOC	14.76	24.21	0.00	0.01	20.24	40.95	0.01	0.03	17.07	30.43
NM_001536	PRMT1	12.92	13.39	0.00	0.01	10.87	17.07	0.02	0.07	11.81	15.01
NM_022173	TIA1	5.31	9.36	0.01	0.02	8.17	8.47	0.03	0.03	6.44	8.90
NM_001769	CD9	8.66	31.35	0.00	0.01	17.43	24.87	0.01	0.15	11.57	27.73
NM_001697	ATP5O	11.52	17.93	0.00	0.00	35.38	28.57	0.01	0.06	17.38	22.03
NM_014846	KIAA0196	5.45	7.14	0.01	0.01	6.60	7.46	0.03	0.04	5.97	7.29
NM_005993	TBCD	12.77	10.27	0.04	0.02	10.72	6.80	0.01	0.01	11.66	8.18
NM_006471	MYL12A	11.36	14.39	0.00	0.01	31.82	23.00	0.02	0.06	16.74	17.70
NM_001202485	HSPE1-MOB4	6.68	9.47	0.00	0.01	14.91	13.07	0.00	0.13	9.23	10.99
NM_003139	SRPR	50.86	10.75	0.02	0.00	14.09	19.39	0.03	0.02	22.06	13.83
NM_002787	PSMA2	9.36	26.49	0.00	0.00	19.07	29.46	0.02	0.05	12.56	27.90
NM_005163	AKT1	23.91	10.32	0.01	0.01	12.73	21.08	0.02	0.03	16.61	13.86
NM_025222	WDR82	3.23	5.93	0.02	0.02	3.50	5.63	0.01	0.05	3.36	5.78
NM_021080	DAB1	10.18	54.72	0.00	0.00	136.34	242.15	0.01	0.06	18.94	89.27
NM_002613	PDPK1	8.24	10.57	0.05	0.02	7.47	11.34	0.01	0.00	7.84	10.94
NM_005207	CRKL	3.70	5.04	0.04	0.01	4.04	5.67	0.02	0.03	3.86	5.34
NM_000019	ACAT1	10.62	23.76	0.00	0.01	45.47	73.76	0.01	0.05	17.21	35.95
NM_001146210	SPDYE6	2.75	2.84	0.03	0.02	2.73	2.77	0.01	0.01	2.74	2.80
NM_022061	MRPL17	6.23	7.00	0.00	0.01	6.99	15.12	0.02	0.03	6.59	9.57
NM_001786	CDK1	4.06	6.75	0.02	0.02	5.80	6.92	0.07	0.11	4.78	6.84
NM_002811	PSMD7	5.64	6.27	0.01	0.02	8.58	8.07	0.02	0.09	6.80	7.05
NM_005857	ZMPSTE24	7.85	13.78	0.01	0.01	24.92	15.93	0.02	0.06	11.94	14.77
NM_001938	DR1	6.59	10.61	0.01	0.01	10.48	13.56	0.04	0.06	8.09	11.91
NM_014501	UBE2S	9.04	7.35	0.02	0.01	7.98	9.41	0.04	0.08	8.48	8.25
NM_006328	RBM14	10.26	11.85	0.02	0.01	8.15	10.01	0.00	0.00	9.08	10.86
NM_016018	PHF20L1	3.47	4.93	0.01	0.01	4.32	4.88	0.05	0.05	3.85	4.91
NM_001170543	PGAM5	11.47	8.99	0.01	0.01	8.36	19.83	0.02	0.05	9.67	12.37
NM_005733	KIF20A	7.53	7.50	0.00	0.01	10.82	9.37	0.03	0.06	8.88	8.33
NM_144598	LRRC28	11.89	14.43	0.00	0.01	18.50	19.72	0.01	0.08	14.47	16.66
NM_001521	GTF3C2	7.09	6.44	0.00	0.00	7.51	6.36	0.01	0.01	7.30	6.40
NM_014949	KIAA0907	4.82	4.21	0.03	0.00	5.70	4.04	0.05	0.03	5.22	4.12
NM_012235	SCAP	15.35	8.74	0.02	0.01	9.98	8.59	0.03	0.01	12.10	8.67
NM_000310	PPT1	12.31	17.47	0.00	0.01	374.59	32.09	0.00	0.05	23.84	22.62
NM_003908	EIF2S2	5.86	8.44	0.01	0.03	7.98	10.88	0.05	0.08	6.76	9.51
NM_001270439	ARPC5	10.32	28.73	0.00	0.01	24.11	58.55	0.02	0.06	14.46	38.55
NM_003255	TIMP2	20.95	10.11	0.02	0.03	14.91	10.37	0.00	0.00	17.42	10.24
NM_005483	CHAF1A	6.64	7.72	0.02	0.01	5.72	9.03	0.03	0.07	6.15	8.33
NM_174952	STPG2	16.72	36.64	0.00	0.00	16.89	84.16	0.01	0.04	16.81	51.06
NM_001166386	MAGEA12	8.83	13.76	0.00	0.01	17.09	20.85	0.04	0.04	11.65	16.57
NM_001211	BUB1B	4.34	6.73	0.01	0.02	5.25	6.30	0.05	0.07	4.75	6.51
NM_144981	IMMP1L	2.60	3.83	0.05	0.01	2.76	2.96	0.03	0.01	2.68	3.34
NM_000633	BCL2	3.00	3.23	0.11	0.05	2.49	2.61	0.07	0.03	2.72	2.89
NM_003945	ATP6V0E1	5.63	7.09	0.01	0.03	7.31	8.02	0.09	0.09	6.36	7.53
NM_032272	MAF1	12.57	8.64	0.00	0.01	15.46	11.04	0.02	0.04	13.87	9.70
NM_001205281	PPP5D1	16.54	41.20	0.00	0.00	394.93	32.27	0.00	0.01	31.75	36.19

NM_052937	PCMTD1	3.75	3.95	0.04	0.02	4.17	3.47	0.05	0.02	3.95	3.69
NM_005080	XBP1	2.22	3.35	0.01	0.02	2.85	3.44	0.03	0.06	2.50	3.39
NM_013237	PRELID1	30.48	30.45	0.01	0.00	314.47	85.81	0.01	0.05	55.58	44.95
NM_031444	GUCD1	6.01	6.62	0.01	0.02	7.91	9.00	0.05	0.06	6.83	7.63
NM_015938	NMD3	5.13	10.48	0.01	0.04	7.51	7.62	0.04	0.08	6.09	8.82
NM_178229	IQGAP3	5.99	4.64	0.05	0.01	5.05	4.82	0.06	0.04	5.48	4.73
NM_018247	TMEM30A	11.60	27.85	0.00	0.01	41.27	12.56	0.02	0.09	18.11	17.32
NM_014819	PJA2	6.34	11.94	0.01	0.03	9.55	7.51	0.03	0.09	7.62	9.22
NM_017843	BCAS4	15.98	530.42	0.00	0.00	57.73	44.58	0.01	0.06	25.03	82.24
NM_002788	PSMA3	8.02	12.19	0.00	0.02	11.45	11.07	0.02	0.06	9.44	11.60
NM_003795	SNX3	7.58	12.43	0.01	0.01	11.28	10.42	0.02	0.07	9.06	11.34
NM_015462	NOL11	4.55	5.69	0.00	0.01	6.89	8.05	0.02	0.06	5.48	6.67
NM_001242898	PPP6R2	7.16	7.19	0.02	0.01	5.70	7.06	0.03	0.01	6.35	7.12
NM_007157	ZXDB	4.94	5.13	0.03	0.01	5.73	5.62	0.04	0.02	5.31	5.36
NM_181361	KCNMB2	2.33	2.60	0.06	0.01	2.28	2.23	0.05	0.03	2.30	2.40
NM_001145297	EXOC7	13.29	14.90	0.00	0.00	12.41	16.56	0.01	0.01	12.84	15.69
NM_181836	TMED7	10.22	24.49	0.01	0.01	27.02	23.58	0.02	0.05	14.83	24.03
NM_182552	WDR27	4.27	5.41	0.08	0.01	3.04	3.69	0.05	0.02	3.55	4.39
NM_005005	NDUFB9	13.17	22.74	0.00	0.00	22.14	29.94	0.01	0.07	16.51	25.85
NM_002690	POLB	12.25	14.75	0.00	0.00	68.86	81.64	0.00	0.05	20.81	24.98
NM_006505	PVR	6.66	7.14	0.02	0.01	6.08	9.29	0.02	0.02	6.36	8.08
NM_016823	CRK	4.90	8.19	0.01	0.01	6.80	9.59	0.02	0.04	5.70	8.83
NM_001237	CCNA2	5.18	13.97	0.00	0.01	10.53	16.53	0.03	0.05	6.95	15.14
NM_006816	LMAN2	34.47	18.79	0.00	0.01	41.63	24.56	0.01	0.05	37.71	21.29
NM_032870	PNISR	4.08	6.61	0.01	0.03	6.09	7.26	0.02	0.14	4.89	6.92
NM_016352	CPA4	9.48	12.63	0.01	0.01	12.25	11.17	0.03	0.06	10.69	11.85
NM_018140	CEP72	6.05	5.19	0.09	0.04	5.01	4.57	0.06	0.01	5.48	4.86
NM_014049	ACAD9	6.06	6.44	0.01	0.01	6.35	6.68	0.01	0.04	6.20	6.56
NM_001130067	TRIM2	5.26	9.35	0.01	0.02	7.67	8.23	0.02	0.04	6.24	8.75
NM_005782	ALYREF	13.41	12.53	0.01	0.00	12.64	23.84	0.03	0.05	13.01	16.42
NM_024038	C19orf43	11.21	11.13	0.00	0.00	12.23	14.88	0.01	0.08	11.70	12.74
NM_014779	TSC22D2	2.95	2.98	0.17	0.04	2.80	2.63	0.12	0.02	2.87	2.80
NM_001145268	FAM185A	6.83	13.36	0.02	0.00	6.78	8.99	0.04	0.03	6.81	10.75
NM_000696	ALDH9A1	8.73	13.16	0.00	0.01	13.70	15.54	0.03	0.06	10.66	14.25
NM_016065	MRPS16	8.63	12.51	0.00	0.00	14.70	17.05	0.01	0.03	10.88	14.43
NM_020738	KIDINS220	6.43	9.55	0.01	0.02	8.48	11.01	0.01	0.05	7.31	10.23
NM_003087	SNCG	19.06	19.47	0.00	0.02	21.51	36.69	0.03	0.05	20.21	25.44
NM_003920	TIMELESS	15.08	39.63	0.01	0.01	19.51	14.56	0.00	0.08	17.01	21.30
NM_001001998	EXOSC10	7.32	7.11	0.00	0.01	8.09	9.62	0.02	0.02	7.69	8.18
NM_001039465	SRSF5	4.46	10.47	0.00	0.01	5.98	10.18	0.00	0.10	5.11	10.32
NM_001160354	LY6K	10.80	14.69	0.00	0.01	18.78	19.57	0.01	0.05	13.72	16.78
NM_207012	AP3M1	8.24	12.16	0.01	0.02	14.34	15.80	0.02	0.04	10.46	13.74
NM_032380	GFM2	5.60	8.10	0.01	0.04	7.61	8.45	0.05	0.09	6.45	8.27
NM_000895	LTA4H	7.67	12.20	0.00	0.01	16.23	19.66	0.01	0.04	10.42	15.06
NM_019082	DDX56	6.30	7.25	0.00	0.01	7.58	8.92	0.02	0.02	6.88	8.00
NM_014953	DIS3	4.60	9.28	0.01	0.01	6.93	9.56	0.06	0.07	5.53	9.42
NM_014713	LAPTM4A	9.58	85.91	0.00	0.02	72.17	16.17	0.00	0.13	16.92	27.22
NM_001256165	TMCO1	7.77	13.59	0.00	0.02	20.25	23.78	0.03	0.07	11.23	17.29
NM_000075	CDK4	9.94	9.42	0.02	0.00	10.52	12.10	0.02	0.03	10.22	10.59
NM_001003722	GLE1	10.58	13.78	0.00	0.01	32.40	18.37	0.01	0.06	15.95	15.74
NM_016640	MRPS30	4.64	6.82	0.02	0.01	5.41	8.04	0.04	0.04	4.99	7.38
NM_012405	ICMT	10.23	12.51	0.01	0.00	12.97	32.30	0.02	0.05	11.44	18.03
NM_004508	IDI1	7.05	22.38	0.00	0.01	24.60	23.09	0.01	0.04	10.96	22.73
NM_019613	WDR45B	8.35	8.16	0.02	0.01	8.34	16.09	0.03	0.05	8.35	10.83
NM_000374	UROD	8.77	11.87	0.00	0.01	14.36	26.84	0.01	0.05	10.89	16.46
NM_001166010	ECI2	9.67	13.11	0.00	0.01	19.58	23.48	0.02	0.06	12.95	16.82
NM_145212	MRPL30	6.48	11.60	0.00	0.01	15.32	18.51	0.02	0.03	9.11	14.27
NM_032350	C7orf50	4.47	5.24	0.05	0.01	3.92	4.04	0.03	0.00	4.18	4.56
NM_014267	C11orf58	7.38	12.62	0.01	0.02	14.80	13.38	0.02	0.12	9.85	12.99
NM_006565	CTCF	2.60	2.81	0.02	0.01	2.51	2.70	0.02	0.03	2.55	2.75
NM_015087	SPG20	5.65	8.89	0.01	0.02	7.93	7.59	0.04	0.07	6.60	8.19
NM_181783	TMTC3	7.35	8.30	0.00	0.02	12.03	7.68	0.02	0.04	9.12	7.98
NM_001130847	AIFM1	11.59	21.54	0.00	0.01	27.18	21.19	0.00	0.09	16.25	21.36
NM_016589	TIMMDC1	7.00	11.12	0.00	0.01	10.50	9.71	0.03	0.07	8.40	10.37
NM_001174129	SLC11A2	5.25	4.94	0.01	0.01	6.58	4.99	0.02	0.04	5.84	4.96
NM_015971	MRPS7	11.35	26.57	0.00	0.00	20.50	44.88	0.01	0.06	14.61	33.38

NM_020216	RNPEP	10.20	8.73	0.05	0.01	7.83	10.85	0.06	0.04	8.86	9.68
NM_002335	LRP5	21.72	6.97	0.08	0.03	6.20	6.13	0.07	0.01	9.65	6.52
NM_005736	ACTR1A	6.81	11.80	0.00	0.01	10.18	11.07	0.02	0.04	8.16	11.43
NM_014235	UBL4A	3.33	7.16	0.01	0.01	3.91	6.12	0.02	0.04	3.60	6.60
NM_001270976	IST1	2.99	4.57	0.02	0.01	3.27	4.55	0.03	0.07	3.12	4.56
NM_001037330	TRIM16L	4.80	5.17	0.01	0.01	5.52	6.67	0.04	0.06	5.13	5.83
NM_002294	LAMP2	11.89	75.68	0.00	0.01	45.18	15.33	0.01	0.04	18.83	25.50
NM_001146699	RBM19	4.95	4.56	0.06	0.01	5.06	4.54	0.07	0.02	5.01	4.55
NM_018428	UTP6	6.01	10.42	0.01	0.01	9.50	12.05	0.03	0.05	7.36	11.17
NM_015216	PPIP5K2	5.17	8.30	0.01	0.01	6.63	7.28	0.03	0.03	5.81	7.76
NM_006303	AIMP2	5.11	5.55	0.00	0.02	6.08	5.69	0.03	0.04	5.55	5.62
NM_004696	SLC16A4	4.14	4.75	0.04	0.01	4.68	4.04	0.06	0.02	4.40	4.37
NM_014306	C22orf28	8.20	14.13	0.00	0.01	9.61	18.45	0.02	0.06	8.85	16.00
NM_007173	PRSS23	10.58	9.63	0.00	0.01	17.50	13.36	0.01	0.04	13.19	11.19
NM_031921	ATAD3B	16.65	21.08	0.01	0.00	9.63	24.59	0.02	0.02	12.20	22.70
NM_014445	SERP1	12.55	41.98	0.00	0.00	27.33	46.16	0.02	0.05	17.20	43.98
NM_021731	MFSD12	21.05	12.59	0.01	0.00	11.28	9.72	0.02	0.01	14.68	10.97
NM_001163280	HTATSF1	15.08	24.88	0.00	0.01	200.07	53.89	0.01	0.11	28.05	34.05
NM_005625	SDCBP	9.21	21.02	0.00	0.02	20.97	23.58	0.01	0.07	12.80	22.23
NM_019030	DHX29	6.45	6.16	0.00	0.03	11.02	7.93	0.03	0.07	8.13	6.93
NM_199054	MKNK2	6.43	6.30	0.02	0.00	4.70	5.76	0.03	0.01	5.43	6.02
NM_018475	TMEM165	5.96	6.52	0.00	0.01	5.98	6.27	0.03	0.01	5.97	6.39
NM_006812	OS9	16.54	27.04	0.00	0.00	33.62	172.50	0.01	0.04	22.17	46.75
NM_014602	PIK3R4	4.23	4.75	0.03	0.01	4.47	5.00	0.05	0.06	4.34	4.87
NM_001007094	ZNF37A	7.41	9.73	0.01	0.01	9.22	8.83	0.01	0.02	8.22	9.26
NM_001144823	DENND4A	4.46	4.60	0.03	0.03	4.48	4.51	0.02	0.01	4.47	4.56
NM_006003	UQCRFS1	6.83	8.78	0.00	0.00	8.08	10.20	0.02	0.04	7.41	9.43
NM_016038	SBDS	9.13	14.40	0.00	0.01	18.35	22.99	0.02	0.06	12.19	17.71
NM_001080952	PLAGL1	2.93	2.54	0.09	0.05	2.60	2.13	0.03	0.03	2.75	2.32
NM_145243	OMA1	5.55	7.44	0.01	0.01	6.61	7.53	0.03	0.03	6.04	7.49
NM_003755	EIF3G	16.09	12.33	0.01	0.00	15.97	23.85	0.01	0.02	16.03	16.25
NM_018997	MRPS21	10.98	13.30	0.00	0.01	17.37	13.15	0.01	0.05	13.45	13.23
NM_001199534	C20orf24	8.72	12.23	0.00	0.00	11.70	10.22	0.01	0.06	9.99	11.14
NM_003145	SSR2	7.98	8.01	0.00	0.00	12.89	12.71	0.03	0.06	9.86	9.83
NM_012415	RAD54B	2.63	3.73	0.09	0.01	2.81	3.30	0.06	0.03	2.72	3.50
NM_014607	UBXN4	5.87	9.19	0.01	0.02	8.89	9.17	0.02	0.04	7.07	9.18
NM_024946	FAM192A	5.00	5.99	0.01	0.02	6.69	6.77	0.02	0.05	5.72	6.36
NM_006600	NUDC	8.37	11.67	0.02	0.01	9.08	13.52	0.01	0.19	8.71	12.53
NM_003769	SRSF9	16.31	16.35	0.00	0.00	14.00	33.62	0.02	0.06	15.07	22.00
NM_018112	TMEM38B	6.15	9.08	0.01	0.05	7.92	6.07	0.07	0.05	6.92	7.28
NM_014963	SBNO2	8.24	7.21	0.04	0.00	5.13	6.12	0.04	0.01	6.32	6.62
NM_023936	MRPS34	10.26	15.17	0.01	0.02	12.83	21.27	0.01	0.07	11.40	17.71
NM_006503	PSMC4	15.76	12.70	0.00	0.01	15.62	19.84	0.02	0.04	15.69	15.49
NM_018198	DNAJC11	5.79	5.31	0.03	0.01	5.61	5.38	0.02	0.03	5.70	5.35
NM_001037540	SCML1	4.87	5.25	0.01	0.01	5.78	4.95	0.01	0.04	5.29	5.10
NM_001135865	LOC100132247	2.50	2.69	0.03	0.03	2.43	2.30	0.02	0.04	2.46	2.48
NM_001271837	RCN2	8.96	23.60	0.00	0.01	23.81	36.06	0.01	0.03	13.02	28.53
NM_002853	RAD1	6.10	11.18	0.01	0.01	8.34	17.18	0.02	0.03	7.05	13.54
NM_005765	ATP6AP2	13.67	42.85	0.00	0.00	49.93	54.89	0.01	0.03	21.47	48.13
NM_175732	PTPMT1	8.70	8.57	0.00	0.01	10.37	14.27	0.02	0.03	9.46	10.71
NM_001010858	RNF187	16.39	11.79	0.00	0.01	10.01	18.56	0.01	0.04	12.43	14.42
NM_001007027	ALG8	5.17	5.80	0.01	0.02	5.60	5.44	0.03	0.04	5.38	5.62
NM_017975	ZWILCH	7.23	17.22	0.00	0.01	17.14	23.66	0.02	0.07	10.17	19.93
NM_001204468	RBM10	8.41	6.58	0.02	0.01	5.81	8.41	0.03	0.03	6.87	7.38
NM_003931	WASF1	3.20	3.24	0.05	0.00	3.53	3.59	0.05	0.02	3.36	3.41
NM_018188	ATAD3A	75.02	19.74	0.00	0.00	12.36	101.19	0.07	0.02	21.22	33.03
NM_000849	GSTM3	14.70	33.47	0.00	0.00	27.99	41.34	0.02	0.02	19.27	36.99
NM_001256534	SLC25A1	52.02	26.66	0.01	0.00	14.88	33.62	0.02	0.02	23.15	29.74
NM_005105	RBM8A	10.90	24.88	0.00	0.00	26.38	722.05	0.01	0.03	15.43	48.11
NM_005657	TP53BP1	6.59	7.06	0.03	0.01	6.97	7.88	0.02	0.03	6.78	7.44
NM_030786	SYNC	12.26	13.24	0.00	0.01	13.84	12.74	0.01	0.01	13.00	12.98
NM_000700	ANXA1	10.38	10.05	0.00	0.03	25.69	15.53	0.03	0.08	14.79	12.20
NM_033540	MFN1	6.27	10.80	0.00	0.01	9.43	10.36	0.02	0.05	7.53	10.58
NM_012111	AHSA1	9.94	13.96	0.00	0.01	13.64	15.08	0.01	0.06	11.50	14.50
NM_003142	SSB	11.13	32.92	0.00	0.01	63.59	133.79	0.00	0.13	18.95	52.84
NM_006083	IK	9.55	13.54	0.00	0.00	16.60	26.89	0.01	0.14	12.12	18.01

NM_016167	NOL7	8.50	12.27	0.01	0.01	15.55	16.39	0.02	0.05	11.00	14.04
NM_000883	IMPDH1	17.43	7.30	0.02	0.00	10.79	10.95	0.03	0.02	13.33	8.76
NM_130464	NPIPL3	2.44	2.71	0.03	0.03	2.40	2.31	0.02	0.05	2.42	2.49
NM_001242829	IP6K1	4.33	5.35	0.05	0.02	3.64	4.91	0.02	0.03	3.95	5.12
NM_001626	AKT2	12.41	16.77	0.01	0.00	9.06	10.78	0.02	0.02	10.47	13.12
NM_006649	UTP14A	4.89	6.08	0.01	0.02	7.28	8.63	0.06	0.08	5.85	7.13
NM_019556	MOSPD1	5.44	7.16	0.01	0.02	8.34	8.81	0.03	0.04	6.58	7.90
NM_005877	SF3A1	67.89	11.00	0.07	0.05	8.48	8.39	0.00	0.01	15.08	9.52
NM_004317	ASNA1	19.23	52.51	0.00	0.00	26.53	174.58	0.00	0.06	22.30	80.73
NM_021203	SRPRB	9.39	17.02	0.00	0.01	15.55	34.82	0.03	0.07	11.71	22.86
NM_001018050	POLR3H	9.92	5.57	0.03	0.00	6.70	7.02	0.02	0.01	8.00	6.21
NM_031902	MRPS5	4.87	6.09	0.01	0.03	6.25	6.81	0.07	0.16	5.47	6.43
NM_014285	EXOSC2	4.96	5.95	0.01	0.01	6.21	8.17	0.03	0.07	5.51	6.88
NM_020170	NCLN	21.45	10.50	0.01	0.00	10.38	17.27	0.01	0.01	13.99	13.06
NM_001919	ECI1	9.93	12.16	0.00	0.00	8.24	19.20	0.01	0.03	9.00	14.89
NM_005530	IDH3A	9.81	10.25	0.00	0.01	12.85	15.96	0.03	0.03	11.13	12.48
NM_006817	ERP29	9.20	15.72	0.00	0.01	38.22	53.98	0.02	0.12	14.83	24.34
NM_006476	ATP5L	13.18	24.19	0.00	0.01	82.69	101.72	0.01	0.08	22.73	39.08
NM_031206	LAS1L	8.64	16.36	0.00	0.01	10.18	12.04	0.01	0.10	9.35	13.87
NM_004815	ARHGAP29	3.57	4.15	0.06	0.01	3.33	3.70	0.09	0.06	3.45	3.91
NM_007062	PWP1	5.48	7.68	0.01	0.03	7.51	10.90	0.04	0.10	6.34	9.01
NM_001083538	POTEE	190.98	23.09	0.02	0.01	16.89	11.58	0.00	0.00	31.03	15.43
NM_020746	MAVS	7.64	7.50	0.02	0.00	7.30	9.52	0.02	0.02	7.46	8.39
NM_015475	FAM98A	7.40	14.14	0.00	0.01	9.96	9.84	0.00	0.09	8.49	11.60
NM_002497	NEK2	9.73	13.60	0.00	0.00	13.69	24.02	0.02	0.03	11.37	17.36
NM_004748	CCPG1	6.63	9.60	0.00	0.01	13.98	11.44	0.03	0.07	9.00	10.44
NM_001166691	TTK	3.67	5.10	0.01	0.03	5.12	4.94	0.05	0.08	4.28	5.02
NM_001696	ATP6V1E1	7.44	13.00	0.00	0.02	16.88	16.59	0.03	0.08	10.33	14.58
NM_004280	EEF1E1	5.73	9.94	0.01	0.02	11.80	7.65	0.02	0.04	7.71	8.64
NM_015721	GEMIN4	2.92	3.70	0.01	0.01	2.70	3.60	0.01	0.05	2.80	3.65
NM_004804	CIAO1	11.23	30.06	0.00	0.00	15.20	46.80	0.01	0.03	12.91	36.61
NM_006337	MCRS1	9.35	7.93	0.01	0.00	8.82	10.94	0.03	0.03	9.08	9.19
NM_001143842	TMEM106C	14.32	18.93	0.00	0.00	32.45	19.02	0.01	0.05	19.88	18.98
NM_001042371	PGP	12.93	7.72	0.00	0.00	8.11	13.27	0.01	0.06	9.97	9.76
NM_007204	DDX20	2.23	2.71	0.01	0.01	2.49	2.69	0.03	0.04	2.35	2.70
NM_001164496	WDR52	2.98	3.09	0.09	0.02	2.99	2.85	0.11	0.08	2.99	2.97
NM_001198690	PPAN-P2RY11	4.51	6.18	0.01	0.01	4.09	6.37	0.01	0.04	4.29	6.27
NM_017443	POLE3	8.97	18.60	0.01	0.02	21.29	32.34	0.02	0.09	12.62	23.62
NM_018457	PRR13	12.05	12.87	0.00	0.00	18.21	22.47	0.00	0.04	14.50	16.36
NM_032892	FRMD5	13.92	10.14	0.03	0.02	8.82	9.69	0.01	0.00	10.79	9.91
NM_001185011	NCAPH2	5.75	6.03	0.00	0.01	5.53	6.72	0.02	0.02	5.64	6.36
NM_003309	TSPYL1	10.10	19.93	0.00	0.00	15.39	18.91	0.01	0.06	12.20	19.41
NM_017895	DDX27	10.42	13.20	0.01	0.02	15.01	19.56	0.01	0.10	12.30	15.76
NM_018471	ZC3H15	5.49	8.45	0.01	0.03	8.97	10.31	0.06	0.09	6.81	9.28
NM_022111	CLSPN	8.65	14.90	0.01	0.02	15.65	18.98	0.01	0.10	11.15	16.70
NM_018269	ADI1	11.63	23.31	0.00	0.01	30.10	44.70	0.01	0.03	16.77	30.64
NM_031934	RAB34	16.46	15.10	0.00	0.01	15.32	12.06	0.01	0.02	15.87	13.41
NM_032450	MROH1	28.69	13.57	0.01	0.00	9.58	10.99	0.01	0.01	14.37	12.15
NM_013392	NRBP1	9.30	16.49	0.00	0.00	20.57	19.69	0.01	0.05	12.80	17.95
NM_015251	ATMIN	5.38	5.63	0.01	0.01	9.09	6.63	0.03	0.06	6.76	6.09
NM_004047	ATP6V0B	21.11	43.28	0.00	0.01	52.03	29.15	0.01	0.03	30.03	34.84
NM_004879	EI24	13.09	21.85	0.00	0.01	31.73	34.97	0.01	0.09	18.53	26.90
NM_021732	AVPI1	2.48	2.98	0.01	0.01	2.42	3.04	0.02	0.05	2.45	3.01
NM_001005862	ERBB2	12.17	6.50	0.01	0.01	8.73	7.05	0.04	0.03	10.17	6.77
NM_006938	SNRPD1	4.66	8.73	0.00	0.02	9.92	12.57	0.01	0.14	6.34	10.31
NM_032985	SEC23B	6.35	9.58	0.01	0.02	9.15	11.18	0.06	0.08	7.50	10.32
NM_017864	INTS8	4.69	6.97	0.01	0.02	6.07	6.25	0.05	0.04	5.29	6.59
NM_032458	PHF6	7.16	15.23	0.01	0.01	10.49	9.52	0.00	0.02	8.51	11.72
NM_001863	COX6B1	20.94	19.85	0.01	0.00	41.46	23.80	0.01	0.02	27.83	21.65
NM_017951	SMPD4	6.42	4.84	0.03	0.00	4.49	5.29	0.02	0.02	5.28	5.05
NM_001461	FMO5	14.39	21.02	0.00	0.00	56.54	89.25	0.01	0.03	22.94	34.03
NM_012121	CDC42EP4	2.41	3.15	0.02	0.01	2.11	3.22	0.04	0.06	2.25	3.18
NM_001080392	KIAA1147	7.27	10.47	0.03	0.00	7.83	9.67	0.05	0.03	7.54	10.05
NM_003000	SDHB	8.56	12.04	0.01	0.01	13.07	20.28	0.03	0.05	10.34	15.11
NM_182679	GPATCH4	6.41	10.14	0.00	0.04	10.16	11.34	0.02	0.33	7.86	10.70
NM_014067	MACROD1	4.35	4.80	0.10	0.01	3.04	3.65	0.08	0.04	3.58	4.15

NM_016127	TMEM66	15.72	30.38	0.00	0.01	135.59	44.23	0.01	0.07	28.18	36.02
NM_001085401	C6orf201	10.15	13.80	0.00	0.02	19.01	23.51	0.02	0.06	13.23	17.39
NM_201397	GPX1	14.94	30.18	0.00	0.00	43.43	107.37	0.00	0.04	22.23	47.12
NM_024612	DHX40	9.99	18.65	0.00	0.00	28.07	27.51	0.01	0.03	14.74	22.23
NM_002197	ACO1	7.94	9.80	0.01	0.02	12.89	13.22	0.03	0.07	9.83	11.25
NM_018122	DARS2	8.21	14.00	0.01	0.00	13.03	17.12	0.01	0.04	10.07	15.40
NM_002768	CHMP1A	8.63	8.92	0.01	0.00	7.92	15.82	0.02	0.03	8.26	11.41
NM_057161	KLHDC3	18.31	25.95	0.00	0.00	26.50	51.67	0.01	0.03	21.66	34.55
NM_001099668	HIGD1A	9.37	21.94	0.00	0.01	40.07	18.83	0.01	0.05	15.19	20.26
NM_001039619	PRMT5	14.06	16.60	0.01	0.00	15.01	20.05	0.01	0.04	14.52	18.16
NM_001261403	NFKB2	21.80	10.30	0.01	0.00	11.64	12.73	0.00	0.01	15.18	11.39
NM_017673	SWT1	11.30	16.17	0.01	0.01	25.94	17.20	0.02	0.07	15.74	16.67
NM_175932	PSMD13	8.49	11.38	0.00	0.00	13.67	13.98	0.02	0.05	10.47	12.55
NM_007002	ADRM1	9.45	8.09	0.02	0.00	7.80	13.90	0.04	0.02	8.55	10.23
NM_003502	AXIN1	2.77	2.87	0.03	0.04	2.37	2.95	0.06	0.02	2.56	2.91
NM_005638	VAMP7	6.36	12.62	0.00	0.02	12.01	13.64	0.03	0.11	8.31	13.11
NM_178042	ACTL6A	6.98	11.10	0.00	0.02	13.16	13.08	0.01	0.11	9.12	12.01
NM_016022	APH1A	9.13	13.99	0.00	0.01	10.55	19.63	0.01	0.06	9.79	16.33
NM_004279	PMPCB	7.43	12.65	0.01	0.01	18.13	18.27	0.03	0.03	10.54	14.95
NM_007184	NISCH	13.42	8.77	0.02	0.00	7.08	8.64	0.04	0.01	9.27	8.71
NM_000270	PNP	9.09	8.53	0.00	0.01	12.27	12.94	0.02	0.07	10.44	10.28
NM_001827	CKS2	3.35	5.77	0.01	0.01	4.89	5.99	0.03	0.07	3.98	5.88
NM_032828	ZNF587	3.71	4.18	0.05	0.02	4.28	4.38	0.03	0.01	3.97	4.28
NM_014236	GNPAT	7.17	9.13	0.01	0.01	12.26	12.62	0.02	0.04	9.05	10.60
NM_144772	APOA1BP	19.73	20.72	0.00	0.00	47.93	22.20	0.01	0.04	27.95	21.43
NM_017802	HEATR2	14.35	7.76	0.06	0.02	6.89	7.04	0.03	0.01	9.31	7.38
NM_005999	TSNAX	8.29	13.44	0.01	0.03	18.28	13.15	0.04	0.07	11.41	13.29
NM_014931	PPP6R1	515.92	12.08	0.02	0.00	11.69	9.13	0.01	0.01	22.86	10.40
NM_002631	PGD	9.41	15.29	0.01	0.01	10.85	17.68	0.00	0.08	10.08	16.40
NM_004888	ATP6V1G1	11.07	26.36	0.00	0.01	80.87	38.55	0.02	0.04	19.48	31.31
NM_001037171	ACOT9	5.62	8.06	0.01	0.01	6.55	7.73	0.03	0.04	6.05	7.89
NM_001559	IL12RB2	1.87	2.31	0.13	0.04	1.85	2.02	0.09	0.03	1.86	2.16
NM_006893	EIF2D	10.51	8.68	0.01	0.01	16.69	9.47	0.02	0.05	12.90	9.06
NM_032288	FYTTD1	8.47	31.62	0.00	0.01	22.61	31.96	0.04	0.07	12.32	31.79
NM_001261412	DCTN2	10.17	22.82	0.01	0.00	12.95	12.92	0.02	0.03	11.39	16.50
NM_002695	POLR2E	26.30	15.62	0.00	0.00	10.90	17.21	0.01	0.05	15.42	16.38
NM_002668	PLP2	18.53	15.80	0.01	0.00	577.46	61.06	0.00	0.02	35.92	25.10
NM_003720	PSMG1	6.51	10.32	0.00	0.00	12.04	16.96	0.02	0.04	8.45	12.83
NM_007034	DNAJB4	4.36	8.15	0.00	0.02	6.21	8.67	0.03	0.10	5.12	8.40
NM_004925	AQP3	10.97	26.28	0.01	0.01	18.42	37.13	0.00	0.07	13.75	30.78
NM_001310	CREBL2	7.81	11.31	0.00	0.01	15.66	11.67	0.02	0.05	10.42	11.49
NM_032223	PCNXL3	15.37	8.08	0.06	0.01	5.18	5.42	0.01	0.03	7.75	6.48
NM_001032410	USP16	5.63	8.37	0.00	0.01	8.26	10.86	0.03	0.05	6.70	9.46
NM_001005369	MTIF2	6.57	11.19	0.00	0.01	15.28	13.86	0.02	0.05	9.19	12.38
NM_031271	TEX15	7.65	12.33	0.00	0.02	13.57	17.73	0.01	0.02	9.78	14.55
NM_004656	BAP1	25.88	27.63	0.01	0.00	16.51	32.75	0.02	0.04	20.16	29.97
NM_013442	STOML2	15.08	14.69	0.00	0.01	18.92	16.66	0.01	0.09	16.79	15.62
NM_014329	EDC4	11.39	8.97	0.01	0.00	7.92	10.97	0.01	0.00	9.34	9.87
NM_001098525	CKAP2	4.85	6.95	0.01	0.02	7.55	8.72	0.02	0.09	5.91	7.74
NM_007010	DDX52	5.72	11.68	0.02	0.01	11.09	12.14	0.03	0.04	7.55	11.90
NM_152385	CLHC1	3.87	5.19	0.04	0.01	4.43	4.08	0.03	0.00	4.13	4.57
NM_001264573	KIF18B	6.90	6.75	0.02	0.01	5.55	5.16	0.01	0.02	6.15	5.85
NM_006946	SPTBN2	65.33	17.69	0.03	0.00	29.42	43.39	0.04	0.00	40.58	25.13
NM_020313	CIAPIN1	4.63	7.39	0.01	0.01	5.99	7.58	0.05	0.06	5.22	7.48
NM_001242854	ARFIP2	7.50	9.06	0.01	0.00	8.41	8.26	0.02	0.02	7.93	8.64
NM_004872	TMEM59	13.21	34.36	0.00	0.00	67.65	241.61	0.02	0.05	22.10	60.16
NM_173547	TRIM65	4.74	6.78	0.01	0.01	4.05	9.77	0.03	0.03	4.37	8.00
NM_001014795	ILK	14.51	14.66	0.00	0.00	16.46	14.85	0.01	0.03	15.42	14.75
NM_005719	ARPC3	8.79	16.64	0.01	0.01	104.44	27.03	0.01	0.07	16.22	20.60
NM_022736	MFSD1	7.95	15.02	0.00	0.02	21.71	17.53	0.03	0.06	11.64	16.18
NM_001320	CSNK2B	22.16	27.59	0.00	0.00	65.34	94.91	0.01	0.03	33.09	42.75
NM_018114	DALRD3	18.28	10.59	0.01	0.00	11.73	10.25	0.02	0.02	14.29	10.41
NM_001079839	OCIAD1	6.45	11.85	0.00	0.02	10.12	8.81	0.02	0.06	7.88	10.11
NM_018385	LSG1	5.48	7.79	0.00	0.01	6.86	9.40	0.03	0.03	6.10	8.52
NM_005746	NAMPT	4.95	8.28	0.01	0.03	8.69	7.86	0.05	0.09	6.31	8.06
NM_133474	ZNF721	4.42	4.55	0.03	0.03	4.73	4.02	0.02	0.02	4.57	4.27

NM_001191003	GSTO1	7.78	14.23	0.00	0.00	10.16	17.13	0.04	0.06	8.81	15.55
NM_024772	ZMYM1	3.55	4.76	0.02	0.02	4.08	4.11	0.04	0.02	3.80	4.41
NM_005189	CBX2	2.81	4.26	0.02	0.01	2.79	4.32	0.04	0.02	2.80	4.29
NM_005439	MLF2	23.59	20.43	0.01	0.00	20.24	26.57	0.02	0.01	21.79	23.10
NM_002863	PYGL	14.88	17.05	0.00	0.01	17.43	27.48	0.02	0.04	16.05	21.04
NM_007043	KRR1	7.84	13.68	0.01	0.01	18.55	19.77	0.02	0.07	11.02	16.17
NM_004282	BAG2	3.94	4.79	0.02	0.03	4.98	4.10	0.04	0.06	4.40	4.41
NM_014886	NSA2	9.66	16.32	0.00	0.01	116.73	21.39	0.01	0.09	17.85	18.52
NM_001184889	NIPA2	6.71	9.56	0.01	0.02	9.37	9.81	0.02	0.04	7.82	9.68
NM_001798	CDK2	12.15	24.35	0.00	0.01	18.78	40.21	0.01	0.04	14.76	30.33
NM_178448	SAPCD2	7.11	7.06	0.00	0.02	5.38	6.08	0.02	0.05	6.12	6.53
NM_001198961	ECHDC2	7.06	10.30	0.01	0.00	6.61	8.53	0.01	0.01	6.83	9.33
NM_001641	APEX1	7.47	21.35	0.00	0.00	12.47	12.73	0.00	0.13	9.34	15.95
NM_001166373	MARCH1	9.94	11.24	0.00	0.01	10.71	6.85	0.00	0.04	10.31	8.51
NM_004424	E4F1	4.15	3.54	0.01	0.00	3.28	3.82	0.03	0.01	3.66	3.68
NM_005934	MLLT1	6.77	7.19	0.04	0.01	5.19	5.44	0.03	0.01	5.88	6.19
NM_015710	GLTSCR2	9.89	55.16	0.01	0.01	11.63	35.35	0.00	0.12	10.69	43.08
NM_001145860	POP1	3.96	5.94	0.02	0.03	4.73	5.94	0.07	0.12	4.31	5.94
NM_004622	TSN	11.95	16.10	0.01	0.00	18.65	25.07	0.02	0.06	14.57	19.61
NM_004689	MTA1	16.92	8.88	0.03	0.01	6.97	8.80	0.02	0.01	9.87	8.84
NM_014887	N4BP2L2	3.82	5.52	0.01	0.00	4.90	5.11	0.03	0.01	4.30	5.31
NM_001199917	PGM3	5.78	7.60	0.01	0.01	9.09	7.49	0.02	0.04	7.06	7.55
NM_147188	FBXO22	3.94	4.75	0.06	0.01	3.94	4.66	0.08	0.06	3.94	4.71
NM_001757	CBR1	8.22	8.56	0.00	0.01	8.34	10.00	0.02	0.03	8.28	9.22
NM_014956	CEP164	5.51	5.74	0.05	0.01	5.53	6.47	0.07	0.06	5.52	6.09
NM_001130965	SUN1	17.75	16.00	0.01	0.00	21.41	20.11	0.01	0.02	19.41	17.82
NM_004339	PTTG1IP	10.17	10.19	0.00	0.01	9.97	11.96	0.04	0.02	10.07	11.00
NM_006805	HNRNPA0	5.67	10.75	0.00	0.03	7.62	11.64	0.02	0.13	6.50	11.18
NM_014786	ARHGEF17	5.47	4.36	0.06	0.01	3.81	4.01	0.05	0.04	4.49	4.18
NM_001134420	CDC7	5.57	6.56	0.01	0.02	6.31	7.59	0.02	0.03	5.92	7.04
NM_018362	LIN7C	8.01	14.67	0.01	0.04	20.34	11.62	0.01	0.04	11.49	12.97
NM_001034841	ITPRIPL2	9.51	8.41	0.02	0.01	7.82	9.22	0.03	0.02	8.58	8.80
NM_013354	CNOT7	7.57	12.64	0.01	0.01	19.31	19.56	0.03	0.06	10.88	15.36
NM_001761	CCNF	2.39	2.81	0.01	0.01	2.17	3.07	0.02	0.01	2.27	2.94
NM_016630	SPG21	10.04	17.03	0.01	0.01	13.94	27.09	0.01	0.03	11.67	20.91
NM_001257231	ALG13	4.00	4.82	0.04	0.01	4.18	3.68	0.03	0.04	4.09	4.17
NM_178454	DRAM2	4.69	6.54	0.02	0.01	6.81	6.12	0.04	0.04	5.55	6.32
NM_182515	ZNF714	3.76	4.73	0.01	0.01	4.29	3.88	0.03	0.01	4.01	4.26
NM_138363	CEP95	3.08	3.43	0.03	0.02	3.49	3.27	0.03	0.02	3.27	3.35
NM_001258289	SELENBP1	12.82	12.64	0.00	0.01	20.43	62.68	0.01	0.04	15.76	21.04
NM_002079	GOT1	8.95	9.74	0.01	0.02	7.58	9.24	0.04	0.09	8.21	9.48
NM_006000	TUBA4A	6.35	6.62	0.00	0.01	6.09	6.24	0.00	0.05	6.22	6.42
NM_018492	PBK	6.10	15.80	0.01	0.01	12.80	12.30	0.02	0.07	8.26	13.83
NM_017785	SPDL1	5.08	7.64	0.01	0.00	6.87	10.54	0.03	0.07	5.84	8.86
NM_002109	HARS	8.09	16.12	0.00	0.01	10.56	15.32	0.01	0.03	9.16	15.71
NM_005234	NR2F6	5.47	5.14	0.03	0.01	3.62	5.93	0.04	0.05	4.36	5.51
NM_020773	TBC1D14	3.62	3.85	0.05	0.01	3.58	4.20	0.05	0.05	3.60	4.02
NM_001257360	AMPD2	18.98	10.79	0.02	0.00	7.63	10.39	0.04	0.03	10.89	10.59
NM_004757	AIMP1	8.25	17.06	0.01	0.01	17.15	33.39	0.02	0.10	11.14	22.58
NM_014935	PLEKHA6	12.65	12.23	0.00	0.01	76.61	35.47	0.02	0.02	21.71	18.18
NM_030969	TMEM14B	8.04	17.88	0.00	0.01	25.88	43.40	0.01	0.07	12.27	25.33
NM_018116	MSTO1	6.01	6.05	0.00	0.01	6.40	7.21	0.03	0.05	6.20	6.58
NM_001242875	ELP2	4.65	6.58	0.01	0.01	4.95	6.82	0.05	0.06	4.80	6.70
NM_020444	KIAA1191	8.88	18.06	0.00	0.01	15.51	16.94	0.01	0.05	11.29	17.48
NM_030919	FAM83D	2.12	2.75	0.03	0.00	2.05	2.47	0.02	0.02	2.08	2.60
NM_001243689	LETMD1	4.37	4.52	0.01	0.01	4.49	4.87	0.02	0.03	4.43	4.69
NM_032997	ZWINT	7.43	10.68	0.00	0.01	13.02	16.54	0.02	0.04	9.46	12.98
NM_001540	HSPB1	31.86	18.14	0.01	0.00	11.76	34.09	0.00	0.09	17.17	23.68
NM_018392	C4orf21	5.82	13.21	0.01	0.01	8.87	11.86	0.01	0.04	7.03	12.50
NM_014573	TMEM97	7.06	7.54	0.00	0.01	7.71	10.74	0.03	0.03	7.37	8.86
NM_001015892	TAF9	8.83	18.06	0.00	0.00	42.99	22.50	0.01	0.03	14.65	20.04
NM_004548	NDUFB10	25.81	37.77	0.00	0.00	41.94	89.16	0.00	0.03	31.95	53.07
NM_003262	SEC62	5.53	7.96	0.01	0.06	7.79	7.42	0.03	0.20	6.47	7.68
NM_015014	RBM34	3.86	5.73	0.00	0.03	4.22	5.74	0.03	0.07	4.03	5.74
NM_005480	TROAP	5.66	6.39	0.01	0.00	5.48	7.59	0.01	0.02	5.57	6.94
NM_001113525	ZNF276	24.09	9.56	0.03	0.00	9.15	9.22	0.02	0.01	13.26	9.39

NM_002791	PSMA6	7.57	10.36	0.00	0.01	14.66	16.19	0.02	0.05	9.99	12.63
NM_053055	THEM4	6.88	8.20	0.01	0.01	9.66	9.18	0.02	0.03	8.04	8.67
NM_006837	COPS5	9.67	10.66	0.00	0.01	12.33	13.95	0.03	0.05	10.84	12.09
NM_015411	SUMF2	13.93	15.50	0.00	0.01	12.15	14.13	0.01	0.03	12.98	14.78
NM_007114	TMF1	6.57	8.70	0.01	0.02	10.56	10.67	0.02	0.05	8.10	9.59
NM_033112	RRP36	6.36	7.06	0.00	0.01	11.03	22.57	0.02	0.02	8.07	10.75
NM_001164746	RASSF8	6.27	10.32	0.01	0.02	13.08	12.03	0.04	0.11	8.48	11.11
NM_017750	RETSAT	9.55	11.28	0.00	0.02	17.76	16.59	0.02	0.10	12.43	13.43
NM_001206427	USMG5	10.82	22.94	0.00	0.01	38.44	64.56	0.00	0.04	16.89	33.86
NM_019056	NDUFB11	37.66	33.25	0.00	0.00	72.13	119.77	0.02	0.03	49.49	52.05
NM_005716	GIPC1	10.57	10.54	0.00	0.00	8.12	9.51	0.01	0.04	9.19	10.00
NM_006811	SERINC3	12.84	21.34	0.01	0.01	15.80	51.87	0.02	0.03	14.17	30.24
NM_032299	DCUN1D5	3.99	6.15	0.01	0.02	4.68	5.08	0.05	0.11	4.31	5.56
NM_001256849	POLD1	40.49	20.55	0.01	0.00	9.45	21.32	0.03	0.01	15.32	20.93
NM_152519	KANSL1L	4.08	5.19	0.02	0.02	4.56	4.31	0.03	0.01	4.30	4.71
NM_001242546	ANAPC16	6.86	13.82	0.01	0.02	11.05	12.10	0.02	0.04	8.47	12.90
NM_001071	TYMS	18.31	11.36	0.01	0.02	9.10	8.06	0.00	0.01	12.16	9.43
NM_033338	CASP7	5.19	7.88	0.01	0.02	8.27	7.25	0.07	0.11	6.38	7.55
NM_006212	PFKFB2	8.09	10.88	0.01	0.02	13.77	14.30	0.03	0.04	10.19	12.36
NM_052850	GADD45GIP1	10.15	12.08	0.01	0.00	12.51	18.19	0.01	0.08	11.21	14.52
NM_015453	THUMPD3	4.70	5.34	0.00	0.02	5.02	6.84	0.01	0.05	4.86	5.99
NM_001439	EXTL2	4.69	7.16	0.00	0.01	5.92	6.79	0.01	0.02	5.24	6.97
NM_007271	STK38	4.11	3.89	0.03	0.02	4.50	4.23	0.04	0.05	4.30	4.05
NM_004255	COX5A	11.43	20.13	0.01	0.01	22.60	20.78	0.00	0.11	15.18	20.45
NM_001070	TUBG1	76.53	11.74	0.02	0.00	19.39	16.12	0.02	0.00	30.94	13.58
NM_005526	HSF1	19.57	11.45	0.02	0.00	8.59	9.49	0.00	0.00	11.94	10.38
NM_000373	UMPS	5.00	7.33	0.01	0.02	6.22	7.79	0.02	0.03	5.54	7.55
NM_025181	SLC35F5	5.27	8.32	0.01	0.01	5.30	7.31	0.06	0.03	5.29	7.78
NM_015161	ARL6IP1	8.23	29.14	0.01	0.00	21.69	29.27	0.02	0.06	11.94	29.20
NM_001378	DYNC1I2	4.92	9.72	0.01	0.03	7.57	7.64	0.05	0.07	5.97	8.55
NM_015702	MMADHC	7.33	19.83	0.00	0.01	10.19	16.05	0.05	0.03	8.53	17.74
NM_001912	CTSL1	14.29	18.77	0.00	0.00	19.59	50.57	0.01	0.08	16.53	27.37
NM_147780	CTSB	11.86	12.31	0.01	0.00	23.87	23.98	0.05	0.04	15.84	16.27
NM_001002878	THOC5	6.24	8.56	0.02	0.01	9.68	10.06	0.05	0.05	7.59	9.25
NM_004147	DRG1	7.18	11.36	0.00	0.01	9.54	13.05	0.02	0.08	8.19	12.14
NM_020973	GBA3	13.76	43.59	0.00	0.00	172.28	117.65	0.00	0.04	25.48	63.61
NM_022064	RNF123	10.12	10.13	0.02	0.00	7.78	8.71	0.04	0.02	8.80	9.37
NM_003677	DENR	8.29	19.65	0.01	0.01	20.56	17.07	0.01	0.07	11.81	18.27
NM_018396	METTL2B	4.47	5.19	0.01	0.01	5.67	5.27	0.03	0.04	5.00	5.23
NM_014748	SNX17	12.42	16.25	0.00	0.00	12.39	25.13	0.03	0.08	12.40	19.74
NM_001098426	SMARCD2	6.36	10.28	0.03	0.01	6.40	10.09	0.05	0.04	6.38	10.18
NM_004295	TRAF4	6.05	4.47	0.01	0.01	5.34	5.30	0.04	0.04	5.67	4.85
NM_004649	C21orf33	10.65	19.27	0.00	0.01	11.88	13.61	0.01	0.02	11.23	15.96
NM_014188	SSU72	8.67	7.10	0.01	0.02	8.15	7.92	0.01	0.05	8.40	7.49
NM_032595	PPP1R9B	5.47	6.23	0.02	0.01	4.77	6.83	0.06	0.09	5.10	6.52
NM_003758	EIF3J	7.25	11.07	0.02	0.02	14.15	9.06	0.00	0.11	9.59	9.96
NM_004546	NDUFB2	23.36	32.20	0.00	0.01	17.78	32.15	0.02	0.05	20.19	32.17
NM_015284	SZT2	8.63	6.66	0.03	0.01	5.78	5.57	0.04	0.02	6.92	6.06
NM_198398	ERGIC3	16.04	16.80	0.00	0.00	34.49	39.70	0.01	0.04	21.89	23.61
NM_003302	TRIP6	6.91	5.79	0.01	0.00	7.30	7.25	0.01	0.03	7.10	6.44
NM_001142935	MXD3	16.54	16.31	0.01	0.00	50.03	41.30	0.01	0.05	24.86	23.38
NM_018120	ARMC1	6.73	13.81	0.01	0.01	15.08	18.61	0.02	0.04	9.31	15.85
NM_004699	FAM50A	35.25	14.32	0.00	0.00	25.36	3868.13	0.01	0.12	29.50	28.52
NM_014047	C19orf53	16.27	9.67	0.01	0.00	38.15	22.27	0.01	0.05	22.81	13.48
NM_001018004	TPM1	10.06	10.42	0.00	0.03	14.93	18.84	0.03	0.03	12.02	13.42
NM_002802	PSMC1	9.10	18.37	0.00	0.01	12.13	17.44	0.01	0.08	10.40	17.89
NM_181501	ITGA1	2.91	3.80	0.05	0.01	3.23	4.09	0.04	0.06	3.06	3.94
NM_175609	ARFGAP1	6.29	7.88	0.00	0.00	5.31	7.91	0.02	0.01	5.76	7.90
NM_001077664	URGCP	2.14	2.14	0.09	0.02	1.89	2.36	0.10	0.06	2.01	2.25
NM_001038618	NARF	8.06	10.62	0.01	0.00	8.95	10.92	0.03	0.05	8.48	10.77
NM_016219	MAN1B1	10.56	13.65	0.00	0.01	8.30	13.22	0.02	0.01	9.30	13.43
NM_004642	CDK2AP1	18.23	243.47	0.00	0.02	81.58	45.62	0.02	0.04	29.79	76.84
NM_003093	SNRPC	9.26	14.41	0.01	0.02	14.68	19.69	0.00	0.09	11.36	16.64
NM_006950	SYN1	15.25	29.40	0.00	0.00	101.26	53.33	0.00	0.04	26.50	37.90
NM_003634	NIPSNAP1	9.53	14.29	0.01	0.00	18.11	37.52	0.03	0.04	12.48	20.69
NM_018294	CWF19L1	5.93	10.47	0.01	0.01	7.74	11.08	0.03	0.06	6.72	10.77

NM_023008	KRI1	5.32	7.62	0.01	0.00	5.43	7.04	0.01	0.10	5.37	7.32
NM_001135694	VDAC3	8.88	16.69	0.00	0.00	14.84	31.67	0.01	0.04	11.12	21.86
NM_001170714	BCAR1	3.43	3.80	0.09	0.02	2.72	3.25	0.04	0.01	3.03	3.51
NM_016047	SF3B14	10.01	16.88	0.00	0.01	55.23	112.73	0.01	0.03	16.95	29.36
NM_006635	ZNF460	6.84	7.37	0.06	0.03	5.17	5.33	0.04	0.01	5.89	6.19
NM_002812	PSMD8	10.76	24.27	0.00	0.00	25.10	253.83	0.01	0.03	15.06	44.30
NM_016497	MRPL51	14.36	33.91	0.00	0.00	33.10	42.49	0.00	0.05	20.03	37.72
NM_001319	CSNK1G2	10.06	8.53	0.03	0.00	7.79	7.62	0.03	0.02	8.78	8.05
NM_016030	TRAPPC12	3.56	3.38	0.03	0.01	2.98	3.29	0.08	0.01	3.24	3.34
NM_014046	MRPS18B	7.92	17.33	0.00	0.01	10.00	20.94	0.01	0.07	8.84	18.97
NM_004636	SEMA3B	36.20	11.74	0.00	0.00	14.35	12.66	0.02	0.03	20.55	12.18
NM_032389	ARFGAP2	5.89	6.12	0.00	0.00	5.24	8.45	0.02	0.01	5.54	7.10
NM_005255	GAK	17.22	7.77	0.04	0.01	8.77	6.85	0.05	0.01	11.62	7.28
NM_004219	PTTG1	8.73	14.39	0.00	0.01	26.33	28.78	0.03	0.05	13.12	19.18
NM_004630	SF1	7.66	6.99	0.07	0.05	4.14	5.78	0.00	0.02	5.38	6.33
NM_003799	RNMT	5.63	7.11	0.01	0.02	5.59	9.43	0.04	0.03	5.61	8.11
NM_001859	SLC31A1	17.58	45.46	0.00	0.00	38.11	23.81	0.01	0.05	24.06	31.25
NM_033133	CNP	7.70	12.46	0.01	0.00	11.68	16.04	0.01	0.06	9.28	14.03
NM_001127204	HMOX2	5.53	5.33	0.01	0.01	4.75	6.23	0.06	0.05	5.11	5.75
NM_001172895	CAV1	9.93	9.10	0.01	0.02	9.96	10.50	0.03	0.04	9.94	9.75
NM_006331	EMG1	6.41	9.14	0.01	0.01	8.90	12.04	0.01	0.04	7.45	10.39
NM_014700	RAB11FIP3	7.40	8.08	0.04	0.01	4.27	5.00	0.03	0.00	5.42	6.18
NM_001199868	GLRX3	5.17	8.14	0.01	0.03	6.78	9.35	0.05	0.07	5.87	8.70
NM_021003	PPM1A	3.86	4.87	0.03	0.00	4.10	4.01	0.02	0.02	3.98	4.40
NM_004705	PRKRIR	3.00	3.66	0.01	0.02	3.51	3.38	0.05	0.06	3.24	3.52
NM_001271675	LOC441155	6.24	7.73	0.02	0.00	8.17	8.52	0.01	0.01	7.08	8.10
NM_017577	GRAMD1C	23.36	24.64	0.00	0.00	11.87	44.79	0.02	0.01	15.74	31.79
NM_152707	SLC25A16	7.67	6.97	0.01	0.02	8.19	7.25	0.01	0.00	7.92	7.11
NM_001146015	DLGAP5	5.78	13.15	0.00	0.01	9.24	15.81	0.05	0.06	7.11	14.36
NM_012245	SNW1	3.87	6.92	0.02	0.03	5.46	6.39	0.04	0.07	4.53	6.64
NM_022753	S100PBP	3.57	6.16	0.04	0.00	4.39	5.48	0.04	0.03	3.94	5.80
NM_003254	TIMP1	15.11	33.48	0.00	0.00	140.12	69.63	0.00	0.04	27.28	45.22
NM_014138	FAM156A	11.68	11.09	0.01	0.00	8.04	9.69	0.02	0.02	9.53	10.34
NM_178314	RILPL1	5.21	6.32	0.03	0.03	4.94	4.71	0.03	0.01	5.07	5.40
NM_001065	TNFRSF1A	3.94	4.16	0.02	0.01	3.63	4.15	0.01	0.02	3.78	4.16
NM_173808	NEGR1	5.45	6.65	0.01	0.01	5.49	6.95	0.04	0.02	5.47	6.80
NM_001009566	CLSTN1	47.76	7.57	0.09	0.03	6.88	10.16	0.04	0.01	12.03	8.67
NM_001033112	PAIP2	9.80	14.33	0.00	0.03	19.33	17.34	0.01	0.12	13.01	15.69
NM_152902	TIPRL	7.42	15.15	0.01	0.01	17.74	21.61	0.01	0.05	10.47	17.81
NM_177439	FTSJ1	14.49	10.51	0.00	0.01	15.35	37.62	0.03	0.03	14.91	16.43
NM_001127695	CTSA	39.23	23.30	0.01	0.00	22.18	18.99	0.00	0.02	28.34	20.92
NM_001168331	NDUFB4	7.08	12.71	0.00	0.00	18.82	23.50	0.00	0.03	10.29	16.50
NM_207043	ENSA	7.36	9.67	0.01	0.04	22.48	12.78	0.05	0.08	11.09	11.01
NM_021137	TNFAIP1	7.31	8.39	0.01	0.01	7.28	9.76	0.01	0.02	7.29	9.03
NM_003372	VBP1	7.72	13.73	0.01	0.03	14.97	17.41	0.04	0.07	10.18	15.35
NM_001122823	GTF3C5	4.73	5.25	0.01	0.02	3.98	5.30	0.03	0.05	4.32	5.27
NM_003352	SUMO1	7.43	15.68	0.00	0.01	13.51	25.57	0.03	0.06	9.58	19.44
NM_030981	RAB1B	15.63	24.98	0.02	0.00	19.21	21.76	0.02	0.04	17.24	23.26
NM_004551	NDUFS3	12.37	11.68	0.00	0.00	12.45	18.48	0.01	0.07	12.41	14.31
NM_015989	CSAD	33.35	19.38	0.01	0.02	19.17	13.07	0.00	0.00	24.35	15.61
NM_006402	LAMTOR5	11.76	24.62	0.00	0.00	84.19	22.76	0.00	0.09	20.64	23.65
NM_212554	METTL10	5.15	5.44	0.01	0.01	6.49	5.95	0.03	0.03	5.75	5.68
NM_000801	FKBP1A	14.15	20.47	0.01	0.01	12.18	10.97	0.00	0.01	13.09	14.28
NM_007362	NCBP2	11.49	44.96	0.00	0.00	31.94	56.00	0.01	0.07	16.90	49.87
NM_001142651	NEURL1B	10.80	14.69	0.02	0.00	62.26	17.04	0.01	0.04	18.41	15.78
NM_032830	CIRH1A	7.30	9.08	0.04	0.04	4.99	5.57	0.01	0.06	5.93	6.91
NM_006965	ZNF24	4.53	7.92	0.01	0.02	6.64	7.91	0.02	0.05	5.38	7.92
NM_004274	AKAP6	2.11	2.15	0.04	0.02	2.22	1.91	0.05	0.03	2.16	2.02
NM_021174	KIAA1967	6.58	10.03	0.01	0.01	7.46	7.74	0.02	0.07	7.00	8.74
NM_001083535	CEP57L1	2.70	3.29	0.06	0.01	3.46	2.82	0.08	0.02	3.03	3.03
NM_019606	MEPCE	2.45	2.90	0.02	0.03	2.81	3.08	0.03	0.10	2.62	2.99
NM_001025579	NDEL1	3.41	5.27	0.05	0.01	3.65	4.82	0.04	0.05	3.53	5.03
NM_005180	BMI1	7.17	11.34	0.01	0.01	17.14	12.58	0.02	0.05	10.11	11.93
NM_015012	TMEM41B	10.60	13.06	0.01	0.00	17.68	13.34	0.01	0.02	13.25	13.20
NM_014345	ZNF318	11.70	6.35	0.00	0.01	7.27	8.47	0.02	0.02	8.97	7.26
NM_032231	FAM96A	9.22	9.95	0.00	0.03	11.78	11.24	0.03	0.10	10.34	10.56

NM_002129	HMGB2	4.34	8.07	0.00	0.01	5.88	10.56	0.01	0.12	4.99	9.15
NM_000688	ALAS1	7.62	10.10	0.01	0.00	8.92	11.41	0.02	0.03	8.22	10.71
NM_014641	MDC1	63.13	15.18	0.06	0.03	11.79	9.17	0.00	0.00	19.87	11.43
NM_015483	KBTBD2	2.90	3.29	0.02	0.02	3.37	3.40	0.02	0.03	3.12	3.35
NM_002167	ID3	0.85	1.25	0.19	0.04	0.84	1.24	0.24	0.03	0.84	1.25
NM_001142353	PPP3CB	5.37	4.91	0.05	0.02	4.21	4.96	0.05	0.01	4.72	4.93
NM_144584	HENMT1	8.48	8.15	0.00	0.03	18.82	12.22	0.01	0.05	11.69	9.78
NM_001034194	EXOSC9	4.65	7.54	0.01	0.01	9.64	7.88	0.02	0.04	6.27	7.71
NM_018358	ABCF3	6.76	6.91	0.00	0.00	6.72	7.72	0.01	0.06	6.74	7.29
NM_021034	IFITM3	39.83	20.64	0.01	0.00	42.32	29.20	0.00	0.04	41.04	24.18
NM_001256270	KIF22	5.52	6.27	0.00	0.01	6.48	6.27	0.01	0.03	5.96	6.27
NM_013291	CPSF1	25.67	26.65	0.01	0.00	11.71	15.67	0.01	0.00	16.08	19.74
NM_001102396	SIKE1	9.11	21.63	0.01	0.02	35.46	27.28	0.02	0.03	14.50	24.13
NM_002103	GYS1	12.19	7.15	0.03	0.02	8.60	7.24	0.01	0.00	10.08	7.20
NM_001143688	DIS3L	6.01	8.29	0.01	0.01	7.09	9.28	0.04	0.04	6.51	8.76
NM_031488	L3MBTL2	6.48	5.84	0.01	0.02	6.91	6.90	0.03	0.04	6.69	6.33
NM_182972	IRF2BP2	2.32	2.86	0.05	0.01	1.92	2.95	0.04	0.01	2.10	2.91
NM_020127	TUFT1	4.67	4.69	0.01	0.02	4.03	6.10	0.10	0.08	4.33	5.30
NM_006861	RAB35	4.01	4.42	0.02	0.01	3.80	5.05	0.02	0.09	3.90	4.72
NM_001080522	CC2D2A	6.82	7.29	0.05	0.01	6.20	7.25	0.08	0.07	6.49	7.27
NM_006101	NDC80	3.14	4.15	0.01	0.02	4.19	4.09	0.07	0.12	3.59	4.12
NM_021075	NDUFV3	4.59	5.18	0.02	0.01	5.32	5.89	0.03	0.02	4.93	5.51
NM_019592	RNF20	5.51	8.33	0.01	0.01	9.03	12.60	0.04	0.13	6.84	10.03
NM_022145	CENPK	3.37	5.78	0.06	0.01	3.63	4.29	0.04	0.02	3.49	4.92
NM_019088	PAF1	10.11	10.62	0.01	0.01	11.66	11.86	0.01	0.07	10.83	11.20
NM_032125	TMEM222	13.35	11.87	0.01	0.00	11.77	13.65	0.00	0.06	12.51	12.70
NM_194259	UBE2I	5.75	7.19	0.01	0.01	7.64	10.93	0.01	0.13	6.56	8.67
NM_001436	FBL	14.28	13.50	0.00	0.00	14.06	11.92	0.01	0.06	14.17	12.66
NM_005370	RAB8A	6.66	7.68	0.01	0.02	7.84	9.45	0.01	0.04	7.20	8.47
NM_018032	LUC7L	2.83	4.05	0.09	0.03	2.79	3.67	0.08	0.02	2.81	3.85
NM_144567	ANGEL2	5.84	8.48	0.02	0.01	9.36	10.35	0.02	0.03	7.19	9.32
NM_181573	RFC4	3.66	5.16	0.01	0.01	5.08	5.44	0.04	0.08	4.26	5.30
NM_005027	PIK3R2	143.91	9.69	0.05	0.03	10.58	14.88	0.00	0.00	19.72	11.74
NM_032287	LDOC1L	2.44	4.09	0.01	0.01	2.48	4.20	0.01	0.01	2.46	4.15
NM_198887	NUP43	7.59	13.14	0.00	0.00	14.58	15.63	0.01	0.01	9.98	14.28
NM_001001563	TIMM50	9.34	9.68	0.01	0.00	13.45	16.18	0.01	0.05	11.02	12.11
NM_001243756	PXN	8.52	8.59	0.04	0.05	5.77	5.99	0.02	0.00	6.88	7.06
NM_017722	TRMT1	12.38	9.45	0.01	0.00	8.95	9.91	0.06	0.01	10.39	9.67
NM_032656	DHX37	9.97	7.60	0.04	0.01	6.72	9.17	0.04	0.04	8.03	8.31
NM_139355	MATK	34.06	17.89	0.01	0.00	15.83	18.89	0.02	0.02	21.61	18.37
NM_013432	TONSL	76.66	10.79	0.03	0.00	8.24	9.50	0.02	0.00	14.88	10.11
NM_015610	WIPI2	11.29	9.67	0.01	0.01	9.41	10.85	0.02	0.03	10.26	10.22
NM_014389	PELP1	21.02	8.66	0.09	0.03	7.13	7.79	0.02	0.00	10.65	8.20
NM_003036	SKI	5.46	4.96	0.09	0.06	3.05	3.87	0.00	0.13	3.92	4.35
NM_001033549	BABAM1	9.81	12.21	0.00	0.00	15.17	26.93	0.01	0.03	11.91	16.80
NM_006351	TIMM44	5.38	6.37	0.01	0.01	4.83	7.46	0.03	0.05	5.09	6.87
NM_000671	ADH5	8.06	16.83	0.00	0.01	12.73	31.84	0.02	0.08	9.87	22.02
NM_005057	RBBP5	3.71	5.88	0.02	0.03	5.35	7.89	0.04	0.11	4.38	6.74
NM_007346	OGFR	4.56	4.63	0.00	0.04	3.85	6.03	0.02	0.07	4.18	5.24
NM_000906	NPR1	25.72	11.14	0.01	0.00	14.07	38.01	0.02	0.00	18.19	17.23
NM_001013699	H3F3C	8.46	17.47	0.00	0.00	10.45	18.21	0.01	0.05	9.35	17.83
NM_004708	PDCD5	10.89	16.91	0.00	0.01	50.70	48.52	0.01	0.05	17.93	25.08
NM_001024210	S100A13	10.96	21.32	0.00	0.00	16.25	74.06	0.04	0.03	13.09	33.10
NM_001177	ARL1	8.39	24.15	0.00	0.01	117.15	45.32	0.01	0.04	15.67	31.51
NM_002096	GTF2F1	9.88	10.42	0.00	0.00	8.42	17.65	0.01	0.04	9.09	13.10
NM_004368	CNN2	26.11	30.39	0.01	0.01	12.66	24.82	0.00	0.01	17.05	27.32
NM_033414	ZNF622	2.51	3.50	0.00	0.00	2.79	3.66	0.04	0.08	2.64	3.58
NM_016404	TRMT112	12.26	77.68	0.00	0.01	27.57	111.74	0.03	0.04	16.97	91.65
NM_175064	SPDYE1	2.54	2.86	0.01	0.02	2.71	2.97	0.01	0.01	2.62	2.91
NM_007033	RER1	19.19	20.96	0.00	0.00	28.82	25.14	0.01	0.02	23.04	22.86
NM_152329	LRR1	14.08	19.69	0.00	0.02	7.81	13.99	0.09	0.10	10.05	16.36
NM_001242841	ZNF195	4.92	6.76	0.02	0.00	5.80	7.31	0.02	0.01	5.33	7.02
NM_004290	RNF14	5.30	10.33	0.01	0.03	8.10	10.96	0.04	0.07	6.41	10.64
NM_021128	POLR2L	63.45	17.54	0.00	0.01	18.59	61.70	0.00	0.05	28.76	27.31
NM_006851	GLIPR1	9.28	21.87	0.01	0.00	21.29	31.80	0.01	0.07	12.92	25.92
NM_016039	C14orf166	9.36	20.11	0.00	0.01	57.83	23.68	0.01	0.04	16.12	21.75

NM_014633	CTR9	6.86	11.15	0.00	0.00	12.27	16.39	0.00	0.09	8.80	13.27
NM_078469	BCCIP	5.15	8.74	0.01	0.02	8.93	9.15	0.02	0.10	6.53	8.94
NM_001039690	CHTF8	5.73	5.23	0.01	0.01	5.41	6.11	0.01	0.02	5.57	5.64
NM_031280	MRPS15	8.55	12.99	0.00	0.00	34.11	20.95	0.01	0.04	13.67	16.04
NM_014399	TSPAN13	12.20	2240.78	0.01	0.00	51.25	68.02	0.00	0.08	19.70	132.03
NM_030755	TMX1	7.68	23.92	0.01	0.01	13.41	17.16	0.03	0.07	9.76	19.98
NM_178831	GATS	7.07	4.64	0.03	0.00	5.64	4.56	0.03	0.01	6.28	4.60
NM_003021	SGTA	5.66	7.05	0.02	0.01	4.28	10.02	0.03	0.04	4.88	8.28
NM_001134484	TOMM5	7.50	9.34	0.00	0.01	43.04	24.56	0.01	0.04	12.77	13.54
NM_002337	LRPAP1	10.28	11.88	0.01	0.01	10.84	14.84	0.04	0.03	10.55	13.20
NM_000544	TAP2	19.07	20.24	0.01	0.00	16.93	22.60	0.01	0.01	17.93	21.35
NM_004426	PHC1	12.43	13.61	0.00	0.01	18.80	22.63	0.01	0.01	14.96	17.00
NM_003129	SQLE	5.10	6.96	0.02	0.00	8.57	8.18	0.02	0.06	6.39	7.52
NM_020990	CKMT1B	20.13	13.60	0.01	0.00	11.86	21.24	0.01	0.07	14.92	16.59
NM_032364	DNAJC14	6.26	7.35	0.01	0.02	6.49	7.09	0.04	0.07	6.37	7.22
NM_001810	CENPB	4.55	6.30	0.00	0.00	3.22	6.19	0.02	0.02	3.77	6.24
NM_025234	WDR61	7.40	7.83	0.01	0.04	10.58	12.88	0.05	0.05	8.71	9.74
NM_030933	SHCBP1L	10.93	39.63	0.00	0.00	350.96	47.70	0.01	0.03	21.19	43.29
NM_004663	RAB11A	7.93	14.67	0.00	0.01	16.77	29.32	0.01	0.06	10.77	19.56
NM_020194	MFF	3.33	6.67	0.01	0.02	5.46	5.80	0.06	0.02	4.14	6.21
NM_181725	METTL2A	5.05	5.65	0.01	0.01	5.29	5.77	0.04	0.05	5.17	5.71
NM_006118	HAX1	11.83	18.96	0.00	0.01	37.31	18.69	0.01	0.03	17.97	18.83
NM_002598	PDCD2	6.44	7.39	0.01	0.01	7.58	10.21	0.02	0.02	6.96	8.58
NM_003171	SUPV3L1	4.94	7.10	0.01	0.01	6.26	6.65	0.02	0.06	5.52	6.87
NM_001005920	JMJD8	20.38	14.22	0.00	0.01	17.64	26.24	0.02	0.02	18.92	18.44
NM_001033088	NGRN	7.44	13.59	0.01	0.00	14.39	18.64	0.03	0.05	9.81	15.72
NM_006693	CPSF4	5.94	6.14	0.01	0.01	5.78	7.07	0.03	0.05	5.86	6.57
NM_174912	FAAH2	5.59	7.46	0.03	0.01	4.83	5.26	0.04	0.03	5.18	6.17
NM_001039707	SDCCAG3	17.12	14.44	0.00	0.00	17.11	16.89	0.01	0.01	17.11	15.57
NM_001271779	PSMD6	8.68	16.84	0.00	0.01	14.15	10.72	0.01	0.04	10.76	13.10
NM_005802	TOPORS	2.76	2.88	0.01	0.03	3.12	3.01	0.02	0.06	2.93	2.94
NM_005858	AKAP8	4.44	5.36	0.01	0.03	4.71	5.39	0.04	0.06	4.57	5.38
NM_030791	SGPP1	4.74	4.63	0.04	0.01	5.03	3.66	0.05	0.04	4.88	4.09
NM_016072	GOLT1B	6.04	9.20	0.00	0.01	14.86	10.95	0.03	0.02	8.59	10.00
NM_030940	ISCA1	5.74	5.59	0.01	0.03	17.37	9.15	0.03	0.04	8.63	6.94
NM_001014283	DCUN1D2	5.26	8.31	0.05	0.02	5.44	5.74	0.02	0.01	5.35	6.79
NM_001127370	CDCA7L	5.34	7.64	0.01	0.03	6.88	10.71	0.04	0.08	6.01	8.92
NM_006754	SYPL1	9.98	18.32	0.03	0.01	16.32	11.61	0.00	0.06	12.38	14.21
NM_015380	SAMM50	8.65	14.86	0.00	0.01	11.84	14.93	0.01	0.08	10.00	14.90
NM_016410	CHMP5	10.38	20.52	0.00	0.01	17.08	45.12	0.03	0.05	12.91	28.21
NM_020131	UBQLN4	19.59	13.18	0.03	0.00	9.05	16.48	0.04	0.02	12.39	14.65
NM_000713	BLVRB	13.89	9.47	0.00	0.01	16.02	12.81	0.02	0.09	14.88	10.89
NM_002024	FMR1	12.16	16.28	0.03	0.02	8.76	12.56	0.02	0.00	10.19	14.18
NM_005611	RBL2	7.91	6.63	0.02	0.01	7.93	5.75	0.02	0.03	7.92	6.16
NM_021254	C21orf59	8.65	12.43	0.01	0.00	11.12	28.88	0.01	0.07	9.73	17.37
NM_001199815	GGCT	9.13	34.58	0.00	0.01	39.01	1015.43	0.02	0.09	14.79	66.88
NM_003136	SRP54	4.78	10.69	0.00	0.01	10.39	12.13	0.03	0.04	6.55	11.36
NM_020474	GALNT1	8.44	18.13	0.01	0.02	13.12	22.21	0.05	0.06	10.27	19.97
NM_024611	NARG2	4.62	7.00	0.01	0.02	6.29	5.58	0.04	0.04	5.32	6.21
NM_145729	MRPL24	13.25	22.03	0.00	0.01	20.31	23.29	0.01	0.04	16.04	22.64
NM_020191	MRPS22	6.17	13.29	0.00	0.01	13.31	11.54	0.02	0.05	8.44	12.35
NM_030666	SERPINB1	9.86	9.23	0.01	0.01	13.51	20.60	0.02	0.07	11.40	12.75
NM_005094	SLC27A4	14.63	2435.73	0.00	0.00	18.12	21.21	0.01	0.05	16.19	42.06
NM_052985	IFT122	5.21	4.46	0.02	0.01	4.85	5.20	0.08	0.05	5.02	4.80
NM_001983	ERCC1	7.36	7.54	0.01	0.01	8.42	9.74	0.01	0.04	7.86	8.50
NM_001136194	FASTKD2	5.74	7.59	0.01	0.01	7.51	8.77	0.02	0.06	6.51	8.14
NM_031485	GRWD1	3.91	4.44	0.01	0.00	3.18	5.55	0.02	0.02	3.50	4.93
NM_001193653	C17orf62	15.07	8.20	0.01	0.01	8.89	6.86	0.02	0.00	11.18	7.47
NM_004490	GRB14	10.17	30.54	0.00	0.00	67.36	111.30	0.02	0.03	17.67	47.92
NM_007097	CLTB	12.44	13.03	0.00	0.01	11.68	21.44	0.05	0.05	12.05	16.21
NM_015932	POMP	7.60	20.41	0.00	0.01	44.48	18.30	0.01	0.05	12.98	19.29
NM_032451	SPIRE2	16.21	7.74	0.03	0.00	7.79	7.29	0.01	0.01	10.52	7.51
NM_178238	PILRB	8.62	5.71	0.01	0.00	6.92	6.02	0.01	0.01	7.68	5.86
NM_016026	RDH11	8.44	12.46	0.00	0.02	13.03	21.04	0.02	0.07	10.25	15.65
NM_004718	COX7A2L	7.77	16.84	0.01	0.01	19.96	25.69	0.02	0.04	11.19	20.35
NM_001142761	KNSTRN	4.10	6.12	0.01	0.01	4.87	5.99	0.04	0.05	4.45	6.05

NM_000821	GGCX	6.39	7.95	0.01	0.01	8.87	7.73	0.01	0.09	7.43	7.84
NM_001202519	CFLAR	6.22	6.03	0.03	0.01	7.03	8.31	0.04	0.03	6.60	6.99
NM_015921	CUTA	25.03	75.98	0.01	0.00	55.02	415.69	0.01	0.03	34.41	128.47
NM_198055	MZF1	23.52	6.53	0.01	0.00	11.85	9.19	0.00	0.00	15.76	7.64
NM_001018113	FANCB	3.79	4.27	0.01	0.01	4.03	4.33	0.02	0.03	3.91	4.30
NM_020243	TOMM22	10.64	15.42	0.00	0.00	62.70	13.42	0.00	0.05	18.19	14.35
NM_144609	CCDC43	5.43	9.04	0.01	0.01	8.50	9.41	0.02	0.07	6.62	9.22
NM_004059	CCBL1	4.55	4.68	0.04	0.01	4.77	4.93	0.04	0.02	4.66	4.80
NM_006555	YKT6	12.17	26.97	0.00	0.02	15.13	34.81	0.01	0.08	13.49	30.39
NM_025233	COASY	7.36	7.41	0.00	0.00	6.98	5.95	0.01	0.02	7.17	6.60
NM_021932	RIC8A	7.37	8.19	0.01	0.01	7.23	14.82	0.01	0.02	7.30	10.55
NM_133639	RHOV	1.35	2.17	0.04	0.01	1.39	2.15	0.05	0.10	1.37	2.16
NM_003683	RRP1	5.41	5.17	0.03	0.01	4.55	6.00	0.02	0.06	4.94	5.55
NM_004451	ESRRA	6.37	8.50	0.01	0.02	5.78	10.09	0.01	0.07	6.06	9.23
NM_005642	TAF7	5.14	5.85	0.00	0.00	8.02	6.75	0.00	0.05	6.27	6.27
NM_006709	EHMT2	94.21	56.09	0.01	0.00	16.60	57.67	0.01	0.02	28.22	56.87
NM_016304	RSL24D1	6.70	16.63	0.00	0.01	14.58	16.74	0.03	0.06	9.18	16.69
NM_014176	UBE2T	5.90	9.39	0.01	0.03	10.46	10.66	0.03	0.08	7.54	9.99
NM_014853	SGSM2	12.42	10.09	0.00	0.00	8.45	9.74	0.01	0.00	10.06	9.91
NM_005452	WDR46	9.67	17.14	0.00	0.01	12.94	18.31	0.03	0.06	11.07	17.71
NM_181578	RFC5	7.48	14.32	0.00	0.01	12.53	13.94	0.03	0.06	9.37	14.13
NM_001069	TUBB2A	8.53	6.64	0.01	0.01	7.18	10.90	0.02	0.03	7.80	8.25
NM_025204	TRABD	17.30	8.42	0.01	0.00	8.41	11.03	0.02	0.03	11.32	9.55
NM_013355	PKN3	9.05	10.85	0.01	0.01	8.29	9.01	0.02	0.05	8.66	9.84
NM_005003	NDUFAB1	7.52	10.16	0.01	0.02	13.53	17.22	0.03	0.05	9.67	12.78
NM_003025	SH3GL1	7.14	9.40	0.05	0.01	5.35	8.20	0.03	0.04	6.12	8.76
NM_032864	PRPF38A	7.16	16.47	0.01	0.01	17.12	15.77	0.00	0.12	10.09	16.11
NM_001099435	SPDYE5	2.95	2.59	0.06	0.02	2.79	2.49	0.01	0.02	2.86	2.54
NM_006927	ST3GAL2	6.08	6.04	0.06	0.04	4.78	4.55	0.05	0.01	5.35	5.19
NM_016458	FAM203A	6.79	5.29	0.03	0.00	4.88	8.48	0.07	0.02	5.68	6.52
NM_001025780	FAM108B1	2.04	2.46	0.05	0.02	2.15	2.35	0.07	0.05	2.10	2.40
NM_014803	ZNF518A	3.14	3.48	0.03	0.02	3.30	3.41	0.05	0.02	3.22	3.45
NM_001242491	FAM156A	17.60	14.62	0.00	0.00	9.90	12.49	0.02	0.03	12.67	13.47
NM_006767	LZTR1	8.67	6.05	0.02	0.01	6.33	7.46	0.03	0.02	7.32	6.68
NM_004260	RECQL4	22.62	11.73	0.01	0.00	8.12	9.72	0.01	0.03	11.95	10.63
NM_018006	TRMU	3.28	4.32	0.03	0.01	3.45	4.00	0.07	0.05	3.36	4.16
NM_022072	NSUN3	5.10	7.57	0.01	0.01	6.85	6.18	0.04	0.04	5.85	6.81
NM_007215	POLG2	4.49	6.12	0.01	0.00	5.64	5.66	0.00	0.02	5.00	5.88
NM_001127244	LRRC8A	5.85	7.81	0.04	0.01	4.79	7.31	0.02	0.03	5.27	7.55
NM_006066	AKR1A1	6.57	9.67	0.01	0.02	8.03	10.41	0.04	0.07	7.23	10.03
NM_016390	C9orf114	6.14	6.43	0.01	0.02	5.62	7.38	0.03	0.05	5.87	6.87
NM_017906	PAK1IP1	4.76	4.70	0.00	0.02	6.17	5.27	0.04	0.10	5.37	4.97
NM_080872	UNC5D	12.49	9.75	0.02	0.01	13.31	16.02	0.01	0.04	12.88	12.12
NM_001114118	C17orf85	5.33	7.73	0.01	0.01	6.72	8.02	0.02	0.04	5.95	7.87
NM_019107	C19orf10	17.35	18.96	0.00	0.01	26.96	69.71	0.01	0.08	21.11	29.82
NM_024955	FOXRED2	65.48	11.39	0.04	0.02	11.27	7.96	0.00	0.02	19.22	9.37
NM_006397	RNASEH2A	13.43	12.84	0.00	0.00	17.05	21.46	0.00	0.04	15.02	16.07
NM_014060	MCTS1	9.65	18.29	0.00	0.00	20.75	34.80	0.01	0.01	13.17	23.98
NM_003491	NAA10	25.11	38.56	0.00	0.00	59.72	43.08	0.00	0.07	35.36	40.69
NM_001143679	GSTK1	14.95	12.66	0.00	0.00	17.74	31.66	0.02	0.01	16.23	18.09
NM_002919	RFX3	2.34	2.54	0.06	0.01	2.59	2.65	0.04	0.03	2.46	2.60
NM_000107	DDB2	4.73	6.67	0.00	0.01	5.88	5.95	0.01	0.01	5.24	6.29
NM_138439	FLYWCH2	8.74	6.78	0.01	0.01	9.08	10.08	0.04	0.05	8.91	8.11
NM_004710	SYNGR2	20.06	15.09	0.01	0.00	30.27	26.60	0.00	0.06	24.13	19.26
NM_023934	FUNDC2	8.94	12.16	0.00	0.02	15.80	15.46	0.04	0.05	11.42	13.61
NM_024036	LRFN4	8.72	10.21	0.01	0.00	7.43	12.08	0.00	0.04	8.02	11.07
NM_174869	IDH3G	20.53	15.11	0.01	0.00	21.89	37.13	0.01	0.02	21.19	21.47
NM_025215	PUS1	4.18	3.92	0.03	0.01	3.45	3.81	0.02	0.02	3.78	3.86
NM_001324	CSTF1	2.17	2.75	0.02	0.02	2.06	3.23	0.03	0.05	2.11	2.97
NM_001001852	PIM3	2.08	1.98	0.04	0.04	1.83	2.36	0.03	0.10	1.94	2.15
NM_019100	DMAP1	6.44	9.16	0.00	0.00	4.92	4.99	0.01	0.05	5.58	6.46
NM_017797	BTBD2	13.21	10.12	0.05	0.01	5.68	6.63	0.03	0.01	7.94	8.01
NM_001130969	NSMF	10.93	12.43	0.01	0.00	9.15	14.32	0.01	0.01	9.96	13.31
NM_006342	TACC3	8.19	6.43	0.04	0.01	4.58	5.19	0.01	0.03	5.88	5.74
NM_005791	MPHOSPH10	1.86	2.59	0.00	0.00	2.26	2.75	0.00	0.18	2.04	2.67
NM_014815	MED24	22.17	15.78	0.02	0.00	10.04	12.85	0.00	0.00	13.83	14.16

NM_024836	ZNF672	2.79	2.30	0.03	0.01	2.53	2.40	0.06	0.03	2.66	2.35
NM_032860	LTV1	3.16	4.85	0.02	0.04	4.63	4.94	0.04	0.15	3.76	4.89
NM_032177	PHAX	4.86	7.63	0.01	0.03	5.59	7.97	0.02	0.08	5.20	7.80
NM_002408	MGAT2	16.85	266.85	0.00	0.00	7.09	23.90	0.11	0.08	9.98	43.87
NM_138368	AP5B1	3.46	5.91	0.03	0.02	3.33	5.11	0.02	0.02	3.39	5.48
NM_000033	ABCD1	13.13	7.85	0.02	0.01	5.75	6.86	0.02	0.01	8.00	7.32
NM_005175	ATP5G1	13.35	30.81	0.00	0.00	29.55	43.21	0.00	0.05	18.39	35.97
NM_012207	HNRNPH3	4.15	9.12	0.01	0.03	5.23	3.97	0.02	0.22	4.63	5.53
NM_016547	SDF4	91.42	20.11	0.01	0.00	12.37	22.19	0.01	0.03	21.78	21.10
NM_001271006	STRA13	13.75	18.06	0.00	0.00	7.83	16.68	0.01	0.03	9.98	17.34
NM_001006941	ALG3	18.13	10.71	0.03	0.01	13.80	11.38	0.02	0.01	15.67	11.03
NM_032494	ZC3H8	4.14	4.98	0.02	0.03	4.56	5.22	0.05	0.03	4.34	5.09
NM_001143888	BSDC1	8.02	10.95	0.00	0.00	11.15	12.40	0.06	0.03	9.33	11.63
NM_004251	RAB9A	2.32	2.89	0.02	0.07	2.73	3.04	0.03	0.16	2.51	2.96
NM_019034	RHOF	8.36	8.11	0.01	0.01	7.48	7.81	0.01	0.04	7.90	7.96
NM_032940	POLR2C	8.98	16.16	0.01	0.01	12.85	14.67	0.02	0.08	10.57	15.38
NM_006502	POLH	4.15	6.73	0.04	0.01	4.48	5.34	0.02	0.02	4.31	5.96
NM_023011	UPF3A	5.59	8.60	0.00	0.02	8.97	8.30	0.03	0.07	6.89	8.45
NM_006339	HMG20B	40.08	14.53	0.00	0.00	17.23	44.45	0.00	0.04	24.10	21.90
NM_015884	MBTPS2	36.96	11.62	0.06	0.03	5.57	4.96	0.01	0.06	9.67	6.95
NM_003851	CREG1	39.56	23.37	0.00	0.00	37.14	55.52	0.01	0.02	38.31	32.90
NM_017819	TRMT10C	4.97	9.73	0.01	0.02	9.81	8.88	0.01	0.07	6.60	9.28
NM_001164093	COPS7A	15.21	19.34	0.00	0.02	18.59	62.31	0.02	0.04	16.73	29.52
NM_020755	SERINC1	7.81	41.88	0.00	0.01	29.11	20.08	0.01	0.04	12.32	27.15
NM_024293	FAM134A	15.11	17.18	0.00	0.01	11.59	15.88	0.01	0.03	13.12	16.50
NM_023077	SELRC1	3.75	6.12	0.02	0.01	4.10	6.43	0.02	0.05	3.92	6.27
NM_032390	MKI67IP	3.19	6.14	0.00	0.01	4.96	5.59	0.01	0.04	3.89	5.85
NM_001003694	BRPF1	2.04	2.36	0.05	0.01	1.96	2.86	0.06	0.02	2.00	2.59
NM_001077351	RBM23	4.20	4.86	0.00	0.00	5.22	5.42	0.03	0.03	4.65	5.12
NM_017426	NUP54	3.50	3.90	0.02	0.06	4.17	3.68	0.04	0.04	3.80	3.79
NM_025054	VCPIP1	4.81	7.02	0.07	0.03	5.09	5.16	0.01	0.02	4.94	5.95
NM_015190	DNAJC9	6.59	9.17	0.00	0.00	10.13	16.73	0.01	0.05	7.99	11.85
NM_015953	NOSIP	7.95	9.71	0.00	0.00	6.99	10.16	0.02	0.05	7.44	9.93
NM_001163560	MEIOB	3.94	6.12	0.01	0.01	5.32	6.12	0.01	0.03	4.53	6.12
NM_013286	RBM15B	3.86	4.35	0.03	0.01	3.81	5.35	0.01	0.01	3.83	4.80
NM_006899	IDH3B	20.78	21.03	0.00	0.00	17.02	263.21	0.01	0.04	18.71	38.94
NM_007030	TPPP	24.01	9.45	0.02	0.01	7.56	6.47	0.00	0.01	11.50	7.68
NM_054013	MGAT4B	55.91	12.84	0.02	0.00	8.93	17.79	0.00	0.00	15.40	14.92
NM_005275	GNL1	11.64	14.74	0.01	0.00	11.03	15.55	0.02	0.05	11.33	15.13
NM_133373	PLCD3	12.17	7.72	0.01	0.00	8.79	12.10	0.02	0.01	10.21	9.43
NM_194271	RNF34	3.11	3.79	0.05	0.02	3.30	3.63	0.04	0.03	3.21	3.71
NM_001172696	TSFM	8.19	11.49	0.01	0.01	14.21	15.23	0.02	0.05	10.40	13.10
NM_001184975	PACSIN3	11.06	14.24	0.01	0.01	6.70	10.30	0.03	0.06	8.34	11.95
NM_001272036	LRRC14	9.28	6.03	0.01	0.01	5.29	8.39	0.03	0.03	6.74	7.02
NM_017798	YTHDF1	3.12	3.35	0.04	0.01	2.80	3.27	0.02	0.01	2.96	3.31
NM_001145309	LRTOMT	12.87	19.58	0.01	0.00	15.09	26.27	0.01	0.04	13.89	22.44
NM_015665	AAAS	11.25	9.88	0.01	0.00	10.41	17.73	0.02	0.02	10.81	12.69
NM_020944	GBA2	6.68	5.94	0.02	0.01	6.12	6.03	0.06	0.04	6.39	5.98
NM_016617	UFM1	6.94	11.34	0.00	0.01	11.53	8.77	0.03	0.04	8.66	9.89
NM_006145	DNAJB1	1.58	2.22	0.02	0.05	1.78	2.29	0.01	0.04	1.67	2.25
NM_001171162	ZMYM3	11.34	11.39	0.04	0.00	11.68	15.42	0.04	0.02	11.51	13.10
NM_022574	GIGYF1	9.82	8.30	0.02	0.00	6.62	8.76	0.03	0.02	7.91	8.53
NM_001242336	MFAP3	6.76	7.78	0.01	0.01	9.64	12.22	0.03	0.06	7.94	9.51
NM_015260	SIN3B	6.83	6.36	0.03	0.01	5.84	5.14	0.01	0.01	6.29	5.69
NM_019096	GTPBP2	4.92	5.83	0.00	0.00	4.60	5.33	0.02	0.02	4.76	5.57
NM_005872	BCAS2	7.14	10.99	0.00	0.01	14.80	18.75	0.02	0.02	9.63	13.86
NM_016207	CPSF3	6.17	7.58	0.01	0.01	9.29	10.05	0.01	0.07	7.41	8.64
NM_001199629	MYL6B	18.33	69.05	0.00	0.01	124.77	1984.50	0.02	0.03	31.96	133.46
NM_025150	TARS2	8.92	11.33	0.01	0.01	8.78	20.55	0.02	0.08	8.85	14.61
NM_002065	GLUL	12.51	13.52	0.00	0.02	17.45	28.50	0.04	0.04	14.58	18.34
NM_006111	ACAA2	8.80	25.81	0.00	0.00	49.31	24.60	0.01	0.06	14.94	25.19
NM_016183	MRTO4	7.41	9.14	0.01	0.01	8.26	14.39	0.02	0.06	7.81	11.18
NM_016403	CWC15	4.99	7.15	0.00	0.03	7.15	12.18	0.05	0.04	5.88	9.01
NM_001204818	ZNF587B	3.72	3.63	0.05	0.02	4.00	3.75	0.02	0.02	3.86	3.69
NM_181507	HPS5	5.24	8.23	0.00	0.01	7.23	10.82	0.05	0.05	6.08	9.35
NM_178167	ZNF598	13.88	8.22	0.02	0.00	6.26	8.51	0.02	0.01	8.63	8.36

NM_000426	LAMA2	4.58	9.13	0.01	0.03	4.63	7.06	0.04	0.02	4.60	7.96
NM_198489	CCDC84	10.64	7.07	0.00	0.01	14.12	9.93	0.00	0.00	12.13	8.26
NM_005977	RNF6	6.53	19.53	0.00	0.02	19.71	20.49	0.03	0.07	9.81	20.00
NM_016222	DDX41	14.19	14.10	0.00	0.01	11.05	13.20	0.02	0.04	12.42	13.63
NM_152512	ENTHD1	10.14	9.78	0.00	0.00	8.29	10.53	0.01	0.04	9.12	10.14
NM_181468	EIF6	9.14	9.92	0.00	0.00	11.92	18.75	0.01	0.07	10.34	12.98
NM_004330	BNIP2	5.46	7.49	0.01	0.03	6.54	10.51	0.04	0.07	5.96	8.75
NM_014106	ZNF770	6.23	9.98	0.00	0.02	7.86	8.54	0.01	0.04	6.95	9.20
NM_032111	MRPL14	5.81	5.76	0.01	0.01	6.27	6.49	0.03	0.07	6.03	6.11
NM_014160	MKRN2	4.53	7.55	0.01	0.01	5.61	8.39	0.04	0.04	5.01	7.95
NM_017916	PIH1D1	12.12	11.17	0.00	0.00	13.27	17.31	0.02	0.03	12.67	13.58
NM_182915	STEAP3	23.61	12.37	0.05	0.00	9.49	9.96	0.05	0.02	13.54	11.03
NM_032124	HDHD2	4.68	4.88	0.03	0.02	4.22	3.91	0.05	0.01	4.44	4.34
NM_005891	ACAT2	11.72	18.57	0.00	0.00	22.70	82.07	0.01	0.05	15.46	30.28
NM_004589	SCO1	5.27	10.41	0.01	0.02	7.58	9.62	0.04	0.06	6.22	10.00
NM_032479	MRPL36	4.36	5.91	0.00	0.00	6.24	7.18	0.00	0.04	5.13	6.48
NM_005781	TNK2	14.66	16.40	0.05	0.01	6.72	8.50	0.02	0.00	9.22	11.20
NM_014604	TAX1BP3	13.44	32.54	0.00	0.00	44.67	92.96	0.01	0.01	20.66	48.21
NM_015247	CYLD	6.39	11.37	0.00	0.02	9.49	10.97	0.06	0.06	7.64	11.16
NM_052988	CDK10	24.92	9.34	0.00	0.00	8.10	7.57	0.02	0.00	12.23	8.36
NM_138689	PPP1R14B	20.97	15.37	0.00	0.00	14.87	22.00	0.02	0.03	17.40	18.09
NM_005342	HMGB3	10.79	29.92	0.00	0.01	27.30	50.29	0.00	0.09	15.47	37.52
NM_006302	MOGS	10.92	9.71	0.00	0.00	8.52	12.49	0.00	0.04	9.57	10.93
NM_015154	MESDC2	6.82	8.11	0.01	0.01	11.78	8.80	0.04	0.06	8.64	8.44
NM_016565	COA4	7.46	8.20	0.00	0.01	10.21	10.58	0.01	0.04	8.62	9.24
NM_024006	VKORC1	17.78	20.42	0.00	0.02	54.53	33.11	0.00	0.07	26.82	25.26
NM_001008697	TFIP11	2.85	3.84	0.01	0.00	3.11	3.79	0.01	0.02	2.98	3.82
NM_180989	GPR180	8.41	8.20	0.01	0.01	13.30	8.48	0.03	0.02	10.31	8.34
NM_001287	CLCN7	19.18	7.44	0.01	0.00	6.67	8.26	0.02	0.01	9.90	7.82
NM_002441	MSH5	12.66	6.61	0.01	0.00	8.88	6.85	0.00	0.02	10.44	6.72
NM_172165	MSH5	12.66	6.61	0.01	0.00	8.88	6.85	0.00	0.02	10.44	6.72
NM_001193388	UNKL	20.75	8.64	0.00	0.00	8.74	8.31	0.02	0.02	12.30	8.48
NM_004264	MED21	8.23	11.76	0.00	0.02	14.77	10.18	0.02	0.04	10.57	10.91
NM_016552	ANKMY1	4.63	3.40	0.10	0.02	3.41	3.44	0.05	0.05	3.93	3.42
NM_020531	APMAP	12.09	14.80	0.00	0.00	18.02	28.02	0.01	0.05	14.47	19.37
NM_016094	COMMD2	9.78	13.86	0.00	0.02	19.64	18.61	0.03	0.06	13.06	15.89
NM_015549	PLEKHG3	3.11	2.96	0.05	0.02	2.62	2.92	0.06	0.11	2.85	2.94
NM_016070	MRPS23	7.27	12.28	0.00	0.02	10.41	15.62	0.02	0.08	8.56	13.75
NM_001271848	ZNF700	3.43	3.03	0.02	0.03	3.14	3.03	0.02	0.02	3.28	3.03
NM_001142290	MGRN1	12.93	5.07	0.20	0.04	4.55	5.05	0.03	0.01	6.73	5.06
NM_003096	SNRPG	6.28	11.04	0.01	0.01	8.26	8.76	0.02	0.08	7.14	9.77
NM_144723	ZMAT2	8.23	13.73	0.01	0.00	22.34	12.66	0.00	0.13	12.03	13.17
NM_001270896	TRAPPC3	5.63	6.60	0.00	0.01	6.69	8.52	0.03	0.08	6.11	7.44
NM_001135647	FAM53C	2.63	3.39	0.02	0.02	2.75	3.26	0.02	0.04	2.69	3.32
NM_001025237	TSPAN4	76.41	17.52	0.01	0.01	8.61	10.73	0.02	0.00	15.48	13.31
NM_006830	UQCR11	11.05	9.69	0.02	0.00	9.36	14.92	0.03	0.05	10.13	11.75
NM_014838	ZBED4	4.25	5.22	0.08	0.03	4.18	5.26	0.03	0.01	4.21	5.24
NM_020145	SH3GLB2	20.72	13.47	0.00	0.00	13.11	12.19	0.02	0.04	16.06	12.80
NM_001134456	NXPE3	5.44	8.67	0.01	0.02	7.90	5.83	0.01	0.09	6.44	6.97
NM_001173517	MAP7D3	7.02	7.76	0.00	0.01	10.14	11.20	0.02	0.08	8.30	9.17
NM_018374	TMEM106B	9.62	40.88	0.01	0.00	18.73	16.08	0.04	0.02	12.71	23.09
NM_021831	AGBL5	11.26	16.80	0.00	0.00	26.30	24.40	0.00	0.03	15.77	19.90
NM_001112726	CEP170B	15.67	11.56	0.01	0.00	7.46	7.56	0.01	0.00	10.10	9.14
NM_022494	ZDHHC6	4.61	5.58	0.01	0.02	6.24	7.04	0.04	0.08	5.30	6.23
NM_177968	PPM1B	4.45	5.01	0.02	0.02	4.57	4.63	0.04	0.01	4.51	4.81
NM_001130858	PPIP5K1	9.01	9.52	0.02	0.00	7.35	7.81	0.02	0.00	8.09	8.58
NM_016647	THEM6	3.44	3.57	0.02	0.00	2.82	3.84	0.05	0.01	3.10	3.70
NM_014280	DNAJC8	5.69	10.02	0.00	0.02	9.72	13.15	0.04	0.13	7.18	11.37
NM_152524	SGOL2	5.49	6.41	0.01	0.03	6.09	5.31	0.04	0.06	5.77	5.81
NM_001136042	PTGES3L-AARSD1	5.76	6.02	0.00	0.04	5.38	5.98	0.04	0.09	5.56	6.00
NM_017613	DONSON	6.03	9.23	0.02	0.01	10.59	10.28	0.03	0.02	7.69	9.73
NM_021633	KLHL12	3.90	5.47	0.03	0.01	3.79	5.85	0.05	0.06	3.84	5.66
NM_080725	SRXN1	5.11	9.33	0.01	0.01	6.05	13.30	0.01	0.03	5.54	10.97
NM_001042476	CARHSP1	9.53	13.29	0.00	0.02	9.19	13.75	0.03	0.04	9.35	13.52
NM_003969	UBE2M	42.30	8.83	0.01	0.00	32.06	11.09	0.00	0.09	36.47	9.83
NM_005761	PLXNC1	2.94	3.64	0.01	0.01	2.89	2.86	0.04	0.01	2.92	3.20

NM_019005	MIOS	2.78	3.66	0.02	0.02	3.17	3.82	0.04	0.07	2.96	3.74
NM_020899	ZBTB4	8.00	6.79	0.02	0.00	4.53	7.07	0.01	0.00	5.78	6.93
NM_001174150	ARL13B	3.01	3.66	0.01	0.03	3.14	2.99	0.05	0.01	3.08	3.29
NM_001950	E2F4	5.68	5.48	0.02	0.01	6.00	7.08	0.06	0.03	5.84	6.18
NM_005333	HCCS	6.96	7.30	0.01	0.02	9.23	8.39	0.01	0.09	7.94	7.81
NM_012463	ATP6V0A2	6.35	9.76	0.01	0.03	7.13	10.45	0.03	0.02	6.72	10.09
NM_024735	FBXO31	4.34	4.27	0.03	0.03	3.65	4.36	0.05	0.01	3.96	4.31
NM_032361	THOC3	8.88	12.12	0.00	0.00	8.44	13.96	0.03	0.04	8.65	12.97
NM_002957	RXRA	4.44	4.35	0.09	0.01	3.18	4.34	0.03	0.02	3.71	4.35
NM_001122956	DBNL	11.11	12.61	0.00	0.01	10.17	12.82	0.03	0.04	10.62	12.71
NM_002492	NDUFB5	10.26	22.23	0.01	0.02	33.32	95.05	0.04	0.05	15.68	36.04
NM_007183	PKP3	62.67	18.19	0.00	0.01	15.81	26.75	0.01	0.06	25.25	21.66
NM_025072	PTGES2	17.57	13.42	0.01	0.00	15.06	15.31	0.01	0.04	16.22	14.30
NM_032296	FLYWCH1	6.11	5.30	0.01	0.01	4.58	6.56	0.05	0.03	5.23	5.86
NM_057180	VPS29	6.46	12.09	0.00	0.01	15.78	12.72	0.00	0.06	9.17	12.40
NM_001010983	GLT8D1	5.83	8.54	0.01	0.02	7.27	8.42	0.02	0.04	6.47	8.48
NM_001261390	CALCOCO2	11.12	12.25	0.01	0.02	16.64	18.49	0.01	0.08	13.33	14.74
NM_138462	ZMYND19	2.82	3.20	0.00	0.00	2.61	3.60	0.01	0.03	2.71	3.39
NM_001008540	CXCR4	1.37	2.05	0.00	0.00	1.39	2.01	0.00	0.02	1.38	2.03
NM_001628	AKR1B1	37.56	18.95	0.00	0.00	26.85	43.84	0.01	0.02	31.32	26.47
NM_001031725	DDX59	3.81	5.06	0.01	0.02	5.16	4.72	0.04	0.05	4.38	4.88
NM_012257	HBP1	4.36	6.37	0.01	0.03	6.93	7.73	0.04	0.05	5.35	6.98
NM_139159	DPP9	12.43	9.16	0.06	0.02	7.24	10.24	0.03	0.01	9.15	9.67
NM_000925	PDHB	10.00	17.77	0.00	0.01	28.54	47.14	0.00	0.04	14.81	25.82
NM_001127605	LIPA	9.28	31.23	0.00	0.01	54.84	27.39	0.00	0.04	15.87	29.18
NM_003958	RNF8	3.06	4.24	0.02	0.03	3.11	4.11	0.07	0.14	3.09	4.17
NM_019852	METTL3	7.35	10.93	0.00	0.00	7.99	12.47	0.02	0.04	7.66	11.65
NM_181716	CENPV	7.28	8.54	0.01	0.01	9.00	11.18	0.03	0.04	8.05	9.68
NM_032478	MRPL38	8.15	8.47	0.01	0.01	7.12	10.43	0.01	0.02	7.60	9.35
NM_203500	KEAP1	4.45	4.14	0.01	0.01	4.08	5.00	0.01	0.04	4.26	4.53
NM_018288	PHF10	12.00	8.15	0.02	0.04	8.01	8.81	0.03	0.01	9.61	8.47
NM_144582	TEX261	8.81	9.93	0.04	0.00	6.81	10.68	0.02	0.06	7.68	10.29
NM_006234	POLR2J	10.18	9.76	0.00	0.03	15.60	16.73	0.01	0.07	12.32	12.33
NM_001170747	PIN4	5.64	5.82	0.02	0.01	6.29	6.41	0.02	0.09	5.95	6.10
NM_001806	CEBPG	3.69	5.23	0.00	0.02	4.46	5.20	0.03	0.09	4.04	5.22
NM_019095	CRLS1	3.57	5.01	0.03	0.01	4.07	5.18	0.05	0.05	3.80	5.09
NM_001193538	TMEM126B	6.15	8.26	0.00	0.01	8.86	9.77	0.02	0.04	7.26	8.95
NM_005783	TXNDC9	5.73	10.78	0.01	0.01	10.70	9.73	0.05	0.07	7.46	10.23
NM_199133	FAM173B	6.23	7.08	0.02	0.01	5.78	7.23	0.03	0.02	6.00	7.15
NM_001256435	PCYT2	10.44	10.03	0.00	0.01	7.74	12.94	0.01	0.05	8.89	11.30
NM_006712	FASTK	12.74	16.27	0.01	0.00	8.61	10.02	0.01	0.02	10.28	12.40
NM_005870	SAP18	11.56	20.34	0.00	0.01	34.24	26.08	0.01	0.06	17.28	22.86
NM_018285	IMP3	2.09	3.70	0.01	0.01	2.12	3.82	0.01	0.05	2.11	3.76
NM_020199	C5orf15	11.02	16.27	0.00	0.00	22.87	15.91	0.01	0.01	14.87	16.09
NM_015935	METTL13	4.44	5.97	0.01	0.01	4.00	5.42	0.01	0.07	4.21	5.68
NM_019015	CHPF2	9.23	11.71	0.03	0.00	8.20	8.98	0.01	0.00	8.68	10.17
NM_001242820	DEF8	10.03	15.58	0.00	0.00	7.83	13.94	0.02	0.02	8.80	14.72
NM_016579	CD320	17.35	9.16	0.00	0.01	10.90	27.23	0.03	0.04	13.39	13.71
NM_001042762	FIGNL1	5.67	8.98	0.00	0.00	7.31	8.53	0.01	0.06	6.39	8.75
NM_001085454	GIT1	13.62	8.51	0.03	0.00	5.92	9.66	0.02	0.01	8.26	9.05
NM_001199514	TGIF2	3.09	3.40	0.02	0.01	2.91	4.05	0.02	0.03	2.99	3.70
NM_002455	MTX1	13.03	9.86	0.00	0.01	9.46	11.29	0.01	0.02	10.96	10.53
NM_144627	TSACC	9.20	14.58	0.01	0.01	23.78	36.60	0.02	0.09	13.27	20.85
NM_012458	TIMM13	18.21	12.12	0.00	0.01	7.50	14.67	0.00	0.09	10.63	13.28
NM_145637	APOL2	5.83	11.47	0.00	0.01	7.64	7.56	0.01	0.05	6.61	9.11
NM_001113756	TYMP	14.66	14.58	0.00	0.02	12.85	16.72	0.02	0.09	13.69	15.57
NM_138501	TECR	15.55	16.91	0.01	0.01	11.00	11.80	0.01	0.10	12.89	13.90
NM_003090	SNRPA1	4.20	5.41	0.01	0.03	5.19	4.99	0.01	0.17	4.65	5.19
NM_006085	BPNT1	6.86	10.59	0.00	0.01	9.83	13.22	0.02	0.03	8.08	11.76
NM_138995	MYO3B	8.27	18.74	0.00	0.01	61.19	79.80	0.01	0.10	14.58	30.35
NM_001127181	CENPL	2.41	3.30	0.03	0.02	2.73	3.62	0.08	0.10	2.56	3.45
NM_001256409	LRRC42	3.99	5.61	0.01	0.03	4.39	5.47	0.05	0.07	4.18	5.54
NM_198046	ZDHHC16	7.56	4.62	0.01	0.01	9.83	6.88	0.02	0.05	8.54	5.53
NM_001003703	ATP5J	8.83	18.11	0.01	0.01	73.16	34.76	0.00	0.14	15.76	23.81
NM_018390	PLCXD1	11.49	10.03	0.02	0.00	8.11	7.45	0.01	0.01	9.51	8.55
NM_024297	PHF23	1.48	2.07	0.03	0.01	1.50	2.13	0.03	0.06	1.49	2.10

NM_152731	BEND6	44.65	24.10	0.00	0.04	327.11	25.25	0.02	0.01	78.57	24.66
NM_032758	PHF5A	3.36	4.26	0.01	0.01	4.42	4.91	0.07	0.12	3.82	4.56
NM_021930	RINT1	5.29	7.65	0.01	0.01	6.14	6.29	0.01	0.05	5.68	6.90
NM_017438	SETD4	4.93	6.68	0.04	0.01	5.37	6.26	0.06	0.06	5.14	6.47
NM_017828	COMMD4	16.29	15.03	0.00	0.01	29.10	54.65	0.01	0.05	20.89	23.58
NM_001243766	POMGNT1	15.90	6.15	0.00	0.02	35.15	8.95	0.02	0.03	21.89	7.29
NM_003811	TNFSF9	2.92	3.53	0.01	0.01	2.65	3.61	0.01	0.04	2.78	3.57
NM_001172663	RAB40C	4.41	3.99	0.04	0.01	3.41	3.81	0.03	0.01	3.85	3.90
NM_001421	ELF4	3.69	3.08	0.10	0.02	3.06	2.90	0.04	0.01	3.35	2.99
NM_024627	C22orf29	4.08	5.10	0.06	0.01	4.01	4.69	0.08	0.02	4.04	4.89
NM_001128608	MAPKBP1	5.77	4.76	0.11	0.02	4.49	4.78	0.05	0.01	5.05	4.77
NM_016077	PTRH2	4.62	4.68	0.01	0.07	5.34	4.33	0.01	0.14	4.95	4.50
NM_001344	DAD1	10.57	14.22	0.00	0.01	68.98	25.77	0.01	0.03	18.33	18.32
NM_144999	LRRC45	12.88	6.85	0.00	0.00	9.41	9.95	0.03	0.05	10.87	8.12
NM_173074	PIGF	7.99	9.92	0.02	0.03	8.67	8.76	0.01	0.00	8.31	9.30
NM_015701	ERLEC1	9.57	17.23	0.00	0.03	12.18	9.05	0.03	0.13	10.72	11.87
NM_014175	MRPL15	5.67	10.18	0.00	0.02	7.27	12.53	0.00	0.08	6.37	11.23
NM_020695	REXO1	9.45	6.14	0.06	0.01	4.73	4.64	0.03	0.01	6.30	5.28
NM_004701	CCNB2	5.51	8.88	0.00	0.01	10.89	8.79	0.03	0.05	7.32	8.83
NM_080592	ATRAID	10.94	10.99	0.00	0.00	33.03	24.78	0.01	0.03	16.43	15.23
NM_001031827	BOLA2	24.53	11.37	0.00	0.01	9.59	20.73	0.00	0.03	13.79	14.68
NM_017891	C1orf159	15.81	8.85	0.02	0.01	8.02	8.06	0.00	0.02	10.64	8.44
NM_004661	CDC23	6.60	14.05	0.00	0.00	8.70	14.40	0.03	0.03	7.51	14.22
NM_004281	BAG3	6.17	5.11	0.07	0.02	4.25	4.09	0.03	0.01	5.03	4.54
NM_001047160	NET1	2.97	3.93	0.02	0.04	3.16	3.91	0.06	0.13	3.06	3.92
NM_015037	ZSWIM8	13.53	8.79	0.02	0.00	8.21	7.29	0.01	0.01	10.22	7.97
NM_014337	PPIL2	8.19	7.68	0.02	0.01	7.48	10.81	0.01	0.03	7.82	8.98
NM_176096	CDK5RAP3	32.66	18.31	0.00	0.00	170.64	19.37	0.01	0.03	54.82	18.82
NM_001170402	CDC20B	7.99	14.48	0.00	0.00	55.00	30.16	0.02	0.01	13.96	19.56
NM_001249	ENTPD5	9.59	11.21	0.01	0.01	13.94	17.30	0.02	0.03	11.37	13.61
NM_020901	PHRF1	3.68	4.49	0.04	0.01	3.05	4.58	0.06	0.01	3.34	4.54
NM_020428	SLC44A2	21.04	33.05	0.01	0.00	13.01	19.96	0.00	0.04	16.08	24.89
NM_002490	NDUFA6	10.74	15.32	0.00	0.00	50.16	22.54	0.01	0.03	17.69	18.24
NM_138558	PPP1R8	2.95	4.11	0.01	0.01	4.04	3.98	0.02	0.05	3.41	4.04
NM_004645	COIL	1.91	2.91	0.01	0.02	2.44	2.76	0.03	0.18	2.14	2.84
NM_005225	E2F1	10.76	6.98	0.01	0.01	8.76	9.07	0.02	0.04	9.66	7.89
NM_004146	NDUFB7	13.00	13.81	0.00	0.01	13.10	30.98	0.04	0.03	13.05	19.10
NM_001197181	TUBB3	10.52	5.98	0.01	0.00	7.50	7.90	0.01	0.01	8.76	6.81
NM_006948	HSPA13	8.66	16.02	0.01	0.01	19.82	61.09	0.03	0.05	12.05	25.38
NM_006455	LEPREL4	15.39	6.18	0.02	0.00	10.44	7.85	0.02	0.05	12.44	6.92
NM_175605	IFT88	4.44	4.70	0.03	0.01	5.49	5.96	0.04	0.05	4.91	5.26
NM_016200	NAA38	4.20	7.25	0.00	0.00	7.40	7.04	0.02	0.01	5.36	7.14
NM_018462	BRK1	11.33	15.92	0.01	0.02	203.91	23.88	0.01	0.06	21.48	19.10
NM_173659	RPUSD3	9.32	12.15	0.00	0.01	9.55	9.57	0.02	0.07	9.44	10.70
NM_024407	NDUFS7	46.71	24.22	0.00	0.02	18.96	37.51	0.00	0.03	26.97	29.44
NM_014062	NOB1	3.50	3.68	0.02	0.03	3.87	3.84	0.00	0.16	3.68	3.76
NM_004805	POLR2D	4.76	6.04	0.01	0.03	6.19	6.49	0.03	0.12	5.38	6.25
NM_004444	EPHB4	7.91	6.80	0.03	0.01	6.32	5.80	0.04	0.03	7.03	6.26
NM_001267818	OSTC	5.70	17.20	0.01	0.01	16.08	26.80	0.02	0.07	8.41	20.96
NM_002561	P2RX5	10.85	8.70	0.01	0.01	7.98	8.74	0.02	0.02	9.19	8.72
NM_170607	MLX	5.97	7.79	0.01	0.01	9.79	7.92	0.01	0.12	7.42	7.85
NM_182796	MAT2B	8.44	16.88	0.00	0.01	17.18	18.47	0.04	0.05	11.32	17.64
NM_001024660	KALRN	11.68	112.57	0.00	0.01	188.58	54.79	0.03	0.05	22.00	73.70
NM_001256185	SNX12	13.34	23.47	0.01	0.01	22.32	24.77	0.00	0.09	16.70	24.10
NM_053046	EGLN2	3.38	3.61	0.01	0.00	3.17	3.08	0.03	0.02	3.27	3.33
NM_000629	IFNAR1	8.48	6.87	0.00	0.03	16.22	6.97	0.01	0.05	11.14	6.92
NM_002226	JAG2	13.08	6.73	0.05	0.00	4.24	5.90	0.02	0.01	6.40	6.29
NM_018256	WDR12	5.88	9.12	0.03	0.01	7.99	9.38	0.03	0.10	6.77	9.25
NM_001002926	TWISTNB	6.34	8.53	0.00	0.02	10.57	8.85	0.02	0.06	7.93	8.69
NM_001099784	FBXL19	7.07	7.96	0.03	0.03	4.34	4.86	0.01	0.03	5.38	6.03
NM_022366	TFB2M	4.08	5.84	0.01	0.02	4.62	5.96	0.09	0.04	4.34	5.90
NM_032492	JAGN1	4.09	6.22	0.00	0.00	4.67	6.44	0.01	0.08	4.36	6.33
NM_178012	TUBB2B	9.40	5.86	0.01	0.01	7.15	10.42	0.01	0.04	8.13	7.51
NM_017607	PPP1R12C	7.24	9.59	0.01	0.01	5.78	8.39	0.05	0.00	6.42	8.95
NM_017615	NSMCE4A	4.25	4.88	0.01	0.01	5.20	5.32	0.04	0.03	4.68	5.09
NM_020412	CHMP1B	7.01	11.03	0.00	0.01	11.55	10.67	0.02	0.05	8.73	10.85

NM_173555	TYSND1	4.92	4.52	0.06	0.01	3.58	4.62	0.08	0.03	4.15	4.57
NM_022745	ATPAF1	6.64	12.03	0.01	0.01	12.37	23.83	0.04	0.07	8.64	15.99
NM_001825	CKMT2	5.86	9.06	0.01	0.01	15.15	5.80	0.02	0.00	8.45	7.07
NM_002904	RDBP	12.72	14.82	0.00	0.01	12.52	18.16	0.01	0.05	12.62	16.32
NM_032014	MRPS24	36.89	52.99	0.00	0.00	16.05	27.61	0.03	0.01	22.36	36.30
NM_021008	DEAF1	7.85	4.93	0.04	0.00	5.27	5.61	0.04	0.01	6.31	5.25
NM_001008397	GPX8	7.96	14.42	0.00	0.00	65.73	28.22	0.02	0.01	14.20	19.08
NM_001197247	BTN3A2	8.27	12.60	0.01	0.02	10.95	13.70	0.02	0.07	9.43	13.13
NM_001004333	RNASEK	38.77	70.29	0.00	0.00	24.39	17.19	0.00	0.04	29.94	27.62
NM_015963	THAP4	5.40	4.58	0.03	0.01	4.33	4.77	0.05	0.03	4.81	4.67
NM_001031703	ELP6	4.81	6.16	0.01	0.01	5.64	5.46	0.02	0.07	5.19	5.79
NM_015528	RNF167	17.17	12.52	0.03	0.02	24.72	9.08	0.00	0.07	20.27	10.52
NM_001100117	RIMS2	19.20	27.72	0.00	0.00	11.74	76.97	0.04	0.02	14.57	40.76
NM_025082	CENPT	3.74	4.38	0.01	0.00	3.34	5.20	0.04	0.03	3.53	4.76
NM_002493	NDUFB6	8.34	13.97	0.01	0.01	13.93	18.03	0.02	0.04	10.44	15.74
NM_001098512	PRKG1	4.85	5.97	0.01	0.02	5.77	7.58	0.02	0.07	5.27	6.68
NM_001127393	C14orf2	11.77	12.90	0.00	0.01	88.21	33.31	0.01	0.12	20.77	18.59
NM_004733	SLC33A1	6.25	8.03	0.02	0.00	13.24	9.17	0.05	0.02	8.49	8.56
NM_001167741	MTX3	7.17	9.66	0.01	0.00	12.16	10.06	0.01	0.03	9.02	9.86
NM_006059	LAMC3	16.16	10.12	0.03	0.00	6.80	6.92	0.01	0.00	9.57	8.22
NM_006833	COPS6	49.85	943.74	0.00	0.00	27.38	16.47	0.00	0.01	35.35	32.38
NM_016080	GLOD4	5.62	8.23	0.00	0.01	7.52	9.88	0.02	0.06	6.43	8.98
NM_145201	NAPRT1	302.67	31.02	0.00	0.00	12.52	29.95	0.01	0.01	24.05	30.48
NM_001114618	MGAT1	5.40	4.64	0.01	0.01	4.44	7.01	0.02	0.05	4.88	5.58
NM_032847	C8orf76	6.39	5.87	0.01	0.01	6.53	5.97	0.01	0.03	6.46	5.92
NM_001141969	DAXX	5.98	6.29	0.02	0.00	5.67	6.42	0.01	0.02	5.82	6.35
NM_014028	OSTM1	7.51	15.27	0.00	0.02	24.23	12.71	0.02	0.06	11.46	13.87
NM_173481	C19orf21	6.45	6.91	0.00	0.01	5.09	7.29	0.03	0.04	5.69	7.10
NM_003907	EIF2B5	5.03	6.81	0.01	0.01	5.19	8.61	0.02	0.08	5.11	7.60
NM_001098522	HTATIP2	8.04	12.35	0.00	0.01	26.18	19.36	0.01	0.12	12.30	15.08
NM_130443	DPP3	20.98	16.75	0.00	0.00	20.46	24.32	0.04	0.06	20.71	19.84
NM_004435	ENDOG	7.99	6.89	0.00	0.02	5.37	9.04	0.02	0.04	6.42	7.82
NM_016391	NOP16	2.54	3.28	0.00	0.01	2.92	3.40	0.01	0.19	2.72	3.34
NM_025113	KIAA0226L	10.80	46.39	0.02	0.00	4.61	23.82	0.13	0.03	6.47	31.48
NM_002208	ITGAE	2.82	3.65	0.04	0.02	3.22	4.20	0.04	0.04	3.01	3.91
NM_052965	TSEN15	4.07	5.48	0.06	0.01	4.26	5.19	0.06	0.06	4.16	5.33
NM_007188	ABCB8	19.35	10.08	0.02	0.00	9.25	7.50	0.00	0.01	12.51	8.60
NM_004870	MPDU1	11.72	17.92	0.00	0.00	34.77	13.43	0.01	0.04	17.53	15.35
NM_031420	MRPL9	7.18	6.49	0.00	0.00	8.61	5.96	0.02	0.02	7.83	6.21
NM_138794	LYPLAL1	3.02	4.42	0.01	0.02	3.62	3.76	0.02	0.03	3.29	4.06
NM_001127460	PAN2	13.97	17.36	0.00	0.01	13.02	12.77	0.02	0.04	13.48	14.71
NM_005833	RABEPK	6.30	6.49	0.01	0.01	6.88	6.76	0.02	0.04	6.58	6.63
NM_001025300	RAB12	3.15	3.04	0.02	0.04	3.13	2.47	0.07	0.05	3.14	2.73
NM_001144878	IMPA1	4.73	8.27	0.01	0.04	5.99	9.23	0.05	0.15	5.29	8.72
NM_001220484	HEATR4	3.95	4.69	0.04	0.01	3.66	4.52	0.03	0.04	3.80	4.60
NM_001142733	ASB14	11.30	24.53	0.00	0.00	54.37	48.73	0.01	0.02	18.71	32.63
NM_025241	UBXN6	33.55	38.43	0.00	0.00	20.15	28.94	0.02	0.01	25.18	33.01
NM_032574	DPY30	8.76	13.28	0.01	0.01	14.19	12.03	0.01	0.04	10.83	12.63
NM_002653	PITX1	6.62	4.98	0.01	0.02	3.91	8.16	0.01	0.07	4.91	6.18
NM_015214	DDHD2	10.80	12.87	0.01	0.00	11.88	8.40	0.02	0.03	11.31	10.17
NM_024104	SMIM7	5.53	6.37	0.00	0.06	6.49	8.23	0.06	0.13	5.97	7.18
NM_003850	SUCLA2	6.47	11.25	0.01	0.01	10.29	11.78	0.05	0.04	7.94	11.51
NM_003724	JRK	4.39	3.91	0.13	0.01	3.75	4.53	0.07	0.04	4.05	4.20
NM_032822	FAM136A	17.14	15.22	0.01	0.00	30.08	68.31	0.02	0.05	21.84	24.89
NM_001080437	SNED1	5.81	4.68	0.08	0.03	5.61	4.58	0.01	0.01	5.71	4.63
NM_015666	GTPBP5	4.31	4.16	0.02	0.01	4.18	6.13	0.02	0.02	4.25	4.96
NM_175063	EMC10	60.69	22.84	0.00	0.01	18.06	44.66	0.02	0.05	27.83	30.22
NM_001135752	ECD	6.97	9.44	0.02	0.01	7.16	9.87	0.03	0.04	7.06	9.65
NM_018158	SLC4A1AP	5.89	6.74	0.00	0.01	12.14	8.14	0.03	0.04	7.93	7.37
NM_001040436	YARS2	4.39	6.99	0.00	0.01	4.40	6.62	0.02	0.04	4.39	6.80
NM_152285	ARRDC1	14.61	14.89	0.00	0.00	14.84	16.35	0.00	0.00	14.72	15.58
NM_001008391	CCDC73	7.88	27.03	0.00	0.00	22.54	29.10	0.03	0.03	11.68	28.03
NM_001171876	MCF2	5.71	9.38	0.01	0.02	7.19	9.56	0.05	0.05	6.36	9.47
NM_017570	OPLAH	21.30	12.05	0.00	0.00	7.20	9.14	0.02	0.00	10.77	10.39
NM_017902	HIF1AN	7.37	15.80	0.01	0.01	8.71	9.90	0.00	0.01	7.99	12.18
NM_002306	LGALS3	11.97	25.37	0.00	0.01	20.94	22.66	0.00	0.09	15.24	23.94

NM_032345	WIBG	2.32	3.22	0.02	0.04	2.26	2.88	0.02	0.06	2.29	3.04
NM_138446	MALSU1	3.05	3.39	0.02	0.02	3.12	3.76	0.04	0.10	3.08	3.57
NM_175876	EXOC8	3.62	5.90	0.01	0.00	4.72	6.26	0.02	0.02	4.10	6.07
NM_177924	ASAH1	10.51	21.64	0.01	0.01	23.53	36.69	0.02	0.04	14.53	27.22
NM_001007467	SFI1	9.42	5.67	0.05	0.03	6.50	4.64	0.03	0.01	7.69	5.10
NM_152743	BRAT1	11.70	7.70	0.05	0.01	5.99	7.03	0.06	0.03	7.92	7.35
NM_001481	GAS8	5.08	5.52	0.01	0.02	5.56	5.00	0.01	0.04	5.31	5.25
NM_024075	TSEN34	10.64	27.73	0.01	0.01	21.96	19.93	0.01	0.04	14.34	23.19
NM_213720	CHCHD10	34.94	13.06	0.01	0.00	14.06	29.64	0.00	0.13	20.05	18.13
NM_022839	MRPS11	4.97	7.24	0.03	0.01	5.68	8.69	0.02	0.03	5.30	7.90
NM_001160305	SETD6	8.18	9.48	0.01	0.01	9.69	12.49	0.00	0.05	8.88	10.78
NM_014648	DZIP3	3.65	4.39	0.03	0.02	4.48	4.98	0.08	0.08	4.02	4.67
NM_006460	HEXIM1	5.86	16.98	0.01	0.00	6.36	8.94	0.01	0.05	6.10	11.71
NM_002105	H2AFX	2.03	2.41	0.03	0.01	2.37	2.26	0.06	0.06	2.19	2.33
NM_001145316	DSN1	6.33	8.38	0.00	0.00	9.10	10.62	0.01	0.03	7.47	9.37
NM_003968	UBA3	4.92	9.70	0.01	0.01	9.62	9.94	0.03	0.06	6.51	9.82
NM_004623	TTC4	3.32	4.63	0.01	0.05	3.80	4.47	0.05	0.15	3.54	4.55
NM_017736	THUMPD1	5.62	7.60	0.01	0.01	6.56	9.39	0.02	0.09	6.05	8.40
NM_005710	PQBP1	11.68	12.01	0.00	0.01	12.12	10.48	0.01	0.07	11.90	11.19
NM_021934	C12orf44	2.20	2.73	0.00	0.02	2.36	2.73	0.00	0.09	2.28	2.73
NM_014184	CNIH4	6.35	12.29	0.01	0.00	12.36	10.02	0.03	0.06	8.39	11.04
NM_015679	TRUB2	10.95	14.78	0.00	0.01	16.50	15.25	0.02	0.04	13.16	15.01
NM_012208	HARS2	4.14	8.12	0.01	0.01	5.43	9.51	0.05	0.12	4.70	8.76
NM_001167820	BLCAP	5.45	8.48	0.02	0.00	5.70	6.11	0.01	0.05	5.57	7.10
NM_003538	HIST1H4A	1.01	0.91	0.05	0.19	1.00	0.90	0.37	0.04	1.00	0.91
NM_019112	ABCA7	36.91	18.32	0.03	0.00	8.44	17.09	0.01	0.00	13.73	17.68
NM_015626	WSB1	4.74	6.15	0.01	0.03	4.61	6.86	0.03	0.07	4.67	6.49
NM_032819	ZNF341	7.91	37.47	0.00	0.00	20.97	18.10	0.01	0.06	11.49	24.41
NM_001110781	SLC35E2B	6.91	7.33	0.03	0.00	6.56	7.14	0.00	0.01	6.73	7.23
NM_031213	FAM108A1	10.40	8.10	0.01	0.01	6.44	6.78	0.01	0.03	7.95	7.38
NM_032175	UTP15	4.36	6.60	0.01	0.00	7.01	8.68	0.00	0.07	5.38	7.50
NM_016622	MRPL35	6.05	14.18	0.01	0.02	11.96	13.59	0.02	0.05	8.04	13.88
NM_138346	KIAA2013	7.86	6.90	0.00	0.01	8.23	13.03	0.03	0.04	8.04	9.02
NM_003878	GGH	11.18	161.16	0.00	0.01	20.72	24.12	0.01	0.07	14.52	41.96
NM_080388	S100A16	23.42	22.94	0.00	0.00	23.98	47.35	0.01	0.04	23.69	30.90
NM_014948	UBOX5	3.28	3.32	0.01	0.01	3.64	4.39	0.02	0.03	3.45	3.78
NM_012416	RANBP6	5.83	5.04	0.00	0.03	8.26	9.10	0.01	0.05	6.83	6.48
NM_001256163	BIRC2	5.14	6.40	0.01	0.01	6.93	6.36	0.03	0.05	5.90	6.38
NM_016034	MRPS2	6.31	7.02	0.01	0.01	5.37	8.98	0.00	0.04	5.80	7.88
NM_005827	SLC35B1	8.36	14.22	0.00	0.01	13.58	50.64	0.01	0.04	10.35	22.21
NM_003860	BANF1	10.78	26.19	0.00	0.01	19.38	56.31	0.01	0.26	13.86	35.75
NM_001173488	NKRF	4.22	5.63	0.01	0.03	3.90	5.09	0.01	0.00	4.05	5.35
NM_175748	UBR7	11.63	29.59	0.00	0.00	28.29	22.56	0.01	0.04	16.48	25.60
NM_005926	MFAP1	4.57	9.09	0.01	0.02	6.06	10.21	0.03	0.26	5.21	9.61
NM_014077	FAM32A	7.89	13.05	0.00	0.01	9.63	12.02	0.01	0.03	8.68	12.52
NM_020218	ATXN7L3	10.83	8.73	0.02	0.01	8.01	8.70	0.03	0.05	9.21	8.71
NM_004217	AURKB	4.23	4.86	0.02	0.01	4.27	5.90	0.03	0.05	4.25	5.33
NM_201222	MAGED2	12.38	44.44	0.00	0.00	33.96	41.77	0.00	0.01	18.15	43.06
NM_001002000	GMPR2	11.15	13.22	0.01	0.00	12.58	18.92	0.02	0.06	11.82	15.57
NM_003130	SRI	6.66	12.88	0.00	0.01	9.60	14.12	0.02	0.04	7.86	13.47
NM_018048	MAGOHB	5.73	9.20	0.00	0.03	8.57	10.79	0.02	0.08	6.87	9.93
NM_024622	FASTKD1	5.40	6.74	0.01	0.02	7.75	6.36	0.01	0.02	6.37	6.54
NM_032731	TXNDC17	14.31	28.44	0.01	0.00	73.31	23.59	0.01	0.08	23.95	25.79
NM_052969	RPL39L	12.73	51.65	0.01	0.00	12.97	26.01	0.06	0.08	12.85	34.60
NM_001256617	TUBGCP2	14.17	14.29	0.00	0.00	15.03	29.95	0.01	0.03	14.59	19.35
NM_001258217	MIS12	3.27	4.37	0.02	0.02	4.23	6.43	0.05	0.07	3.69	5.21
NM_015392	NPDC1	14.04	9.36	0.00	0.01	5.79	7.68	0.01	0.00	8.20	8.44
NM_018447	EMC3	8.90	11.78	0.01	0.01	13.14	14.58	0.03	0.03	10.61	13.03
NM_025115	TTI2	6.27	9.95	0.01	0.03	8.75	12.10	0.03	0.04	7.31	10.92
NM_006353	HMGN4	7.67	10.57	0.01	0.01	14.89	12.25	0.03	0.06	10.12	11.35
NM_004629	FANCG	7.55	7.18	0.00	0.00	10.04	7.37	0.01	0.03	8.62	7.27
NM_014241	PTPLA	4.98	7.80	0.01	0.00	7.06	5.78	0.01	0.02	5.84	6.64
NM_016331	ZNF639	1.97	2.55	0.03	0.03	2.19	3.07	0.08	0.07	2.07	2.79
NM_003910	BUD31	5.67	9.73	0.00	0.02	8.42	15.87	0.04	0.04	6.78	12.07
NM_006602	TCFL5	5.27	8.94	0.01	0.01	5.82	10.12	0.02	0.04	5.53	9.49
NM_013247	HTRA2	9.33	14.65	0.00	0.01	7.54	18.88	0.02	0.02	8.34	16.50

NM_024884	L2HGDH	4.13	4.42	0.06	0.00	4.38	3.63	0.05	0.06	4.25	3.99
NM_016286	DCXR	18.63	23.55	0.00	0.02	20.29	20.59	0.02	0.04	19.43	21.97
NM_000692	ALDH1B1	7.52	12.35	0.02	0.01	7.56	10.90	0.01	0.03	7.54	11.58
NM_003260	TLE2	26.18	11.30	0.01	0.00	8.00	11.85	0.01	0.01	12.25	11.57
NM_018044	NSUN5	7.42	7.22	0.00	0.00	6.45	7.77	0.01	0.02	6.90	7.48
NM_006232	POLR2H	8.12	10.70	0.00	0.01	9.57	14.57	0.01	0.04	8.79	12.34
NM_020409	MRPL47	6.16	11.83	0.01	0.01	19.26	16.48	0.02	0.06	9.33	13.78
NM_001033030	FAIM	5.38	8.75	0.00	0.01	10.91	9.56	0.01	0.04	7.21	9.14
NM_020189	ENY2	10.38	38.25	0.00	0.01	26.08	28.32	0.01	0.05	14.85	32.55
NM_006808	SEC61B	10.86	29.00	0.00	0.00	61.71	22.15	0.01	0.07	18.46	25.12
NM_001025248	DUT	7.91	19.38	0.01	0.01	12.60	14.41	0.02	0.08	9.72	16.53
NM_001662	ARF5	21.83	27.47	0.00	0.00	24.39	87.52	0.01	0.05	23.04	41.82
NM_002669	PLRG1	6.32	12.88	0.00	0.01	12.74	17.66	0.02	0.04	8.45	14.90
NM_004763	ITGB1BP1	9.24	14.80	0.00	0.02	11.89	8.98	0.02	0.07	10.40	11.18
NM_001171948	KXD1	9.30	8.56	0.03	0.03	11.12	18.77	0.01	0.09	10.13	11.76
NM_004375	COX11	11.35	45.20	0.01	0.00	56.82	75.48	0.01	0.04	18.92	56.55
NM_017971	MRPL20	8.19	9.32	0.01	0.01	14.51	15.64	0.01	0.04	10.47	11.68
NM_005837	POP7	3.19	3.79	0.00	0.00	3.02	4.35	0.00	0.02	3.10	4.05
NM_152392	AHSA2	8.14	10.86	0.01	0.01	13.52	16.31	0.04	0.08	10.16	13.04
NM_001037277	GGPS1	7.55	10.84	0.00	0.03	12.05	12.34	0.01	0.06	9.28	11.54
NM_001267039	LARP7	4.74	11.14	0.00	0.02	14.70	9.60	0.04	0.10	7.16	10.31
NM_001663	ARF6	3.67	6.32	0.01	0.02	3.73	7.08	0.01	0.09	3.70	6.68
NM_004527	MEOX1	2.71	3.45	0.05	0.02	3.06	3.39	0.03	0.10	2.88	3.42
NM_018848	MKKS	5.09	13.59	0.00	0.03	9.40	8.76	0.03	0.07	6.60	10.65
NM_021107	MRPS12	5.28	6.06	0.01	0.02	5.29	7.05	0.01	0.04	5.28	6.52
NM_002225	IVD	6.08	9.52	0.01	0.03	5.94	5.61	0.01	0.06	6.01	7.06
NM_001384	DPH2	9.28	13.74	0.02	0.00	11.17	16.54	0.01	0.02	10.14	15.01
NM_001015049	BAG5	3.41	4.17	0.01	0.02	4.53	5.86	0.01	0.03	3.89	4.87
NM_006428	MRPL28	8.82	14.69	0.00	0.01	13.27	19.01	0.01	0.07	10.59	16.57
NM_014161	MRPL18	7.46	8.82	0.00	0.00	11.12	11.11	0.01	0.04	8.93	9.83
NM_014222	NDUFA8	7.66	12.02	0.01	0.01	15.06	9.42	0.00	0.12	10.16	10.56
NM_024068	NABP2	24.11	29.71	0.00	0.00	23.37	22.48	0.02	0.03	23.73	25.59
NM_014828	TOX4	7.87	16.81	0.01	0.00	14.27	16.26	0.00	0.06	10.14	16.53
NM_001271610	STX10	11.63	23.81	0.01	0.00	13.80	90.55	0.02	0.03	12.62	37.70
NM_018195	C11orf57	3.67	8.16	0.01	0.00	5.12	9.38	0.02	0.08	4.28	8.73
NM_178539	FAM19A2	13.61	26.96	0.00	0.00	28.07	130.86	0.00	0.11	18.33	44.70
NM_001003684	UQCR10	11.45	30.64	0.01	0.01	15.55	38.56	0.00	0.03	13.19	34.15
NM_000466	PEX1	5.22	8.38	0.00	0.00	7.58	9.53	0.03	0.02	6.19	8.92
NM_018847	KLHL9	4.28	7.61	0.01	0.05	5.44	5.53	0.03	0.04	4.79	6.40
NM_018838	NDUFA12	8.22	8.41	0.01	0.02	13.17	10.93	0.02	0.06	10.12	9.51
NM_000194	HPRT1	6.87	8.37	0.04	0.02	6.49	6.32	0.01	0.01	6.67	7.20
NM_022916	VPS33A	6.13	9.04	0.01	0.01	8.52	10.34	0.01	0.04	7.13	9.64
NM_002013	FKBP3	6.72	15.23	0.00	0.01	19.87	11.84	0.00	0.06	10.04	13.33
NM_001136262	ATXN7L3B	5.75	4.90	0.01	0.01	6.03	5.71	0.01	0.08	5.89	5.27
NM_032356	LSMD1	43.50	20.72	0.00	0.00	53.42	24.23	0.00	0.01	47.95	22.34
NM_001976	ENO3	6.56	10.14	0.00	0.01	12.40	8.23	0.01	0.13	8.58	9.08
NM_001739	CA5A	5.75	8.30	0.01	0.00	6.15	10.62	0.03	0.08	5.95	9.32
NM_138442	CCDC124	31.31	32.85	0.00	0.02	16.62	18.69	0.00	0.22	21.71	23.83
NM_001425	EMP3	18.93	23.65	0.00	0.01	44.18	28.26	0.00	0.05	26.50	25.75
NM_003095	SNRPF	9.19	10.71	0.02	0.00	14.89	18.38	0.01	0.20	11.37	13.54

Table 2.2 List of mRNA half-life following TUT4/7 knockdown. The list shows the half-lives of genes in siCont and siTUT4/7 treated samples detected by RNA-seq. HeLa cells were harvested at 0, 1, 2, and 4 hr after actinomycin D treatment. See Methods and Materials for the description ofthe procedure ofhalf-life calculations.

Oligonucleotide name	Sequence (5′ to 3′)
siLuc	CUUACGCUGAGUACUUCGA
siCont	CCUACGCCACCAAUUUCGU
siTUT1_1	CGAGCACAUUCACUAACAA
siTUT1_2	CCCUUACAAUGAUGGUCAU
siTUT1_3	GCACAUUUGUUCGUGACUU
siTUT1_4	GCUGGUAUCCCUAUUGCUA
siTUT2_1	CGUUAGUGCUGGUGAUUAA
siTUT2_2	ACAUCAAGCUCCAUGUAAU
siTUT2_3	GAGCAGUGAUGGUGAUUUA
siTUT2_4	CAACAGAAACTGAGATCAA
siTUT3_1	GGACGACACUUCAAUUAUU
siTUT3_2	GGCCUUUGAUUAUGCCUAC
siTUT3_3	GCGCUGACGUCCAGAUAUU
siTUT3_4	CCUAUUGCAGAGGGACCUU
siTUT4_1	GGUUGCUUCAGACUUUAUA
siTUT4_2	GGAAUGAAGAAGAGAAAGA
siTUT4_3	GGAGAAACGACAUAAGAAA
siTUT4_4	GGUUAGAGCUGCUUAAAUU
siTUT5_1	CUACGGUACCAAUAAUAAA
siTUT5_2	GGAAGAAUCAUCAAAGUAA
siTUT5_3	CCAAACAGAGACGCCGAAA
siTUT5_4	GCGAAUAGCCACAUGCAAU
siTUT6_1	AACUACGAGCUGCGAGAAA
siTUT6_2	GUGUGUUUGUCAGUGGCUU
siTUT6_3	GCCACGUUACUACAGCCAA
siTUT6_4	GCUCUUCCAUAAAUAGCUU
siTUT7_1	GAAAAGAGGCACAAGAAAA
siTUT7_2	GCAAAGAGGACAAAGAAAU
siTUT7_3	GAUAAGUAUUCGUGUCAAA
siTUT7_4	GAACAUGAGUACCUAUUUA
siXRN1-1	GGUGUUGUUUCGCAUUAUU
siXRN1-2	GCACCUUUCCUGUCUGAUA
siXRN1-3	GCUGGGAACUCCCUAUUAU
siXRN1-4	GCUAAUGAAAUCCCUGUUU
siRRP41-1	CUAUGCAGCUUGUGUGAAU
siRRP41-2	CGGACAGGGCCCUAGUGAA
GAPDH_F(q-PCR)	CTCTCTGCTCCTCCTGTTCGAC
GAPDH_R(q-PCR)	TGAGCGATGTGGCTCGGCT
TUT1_F(q-PCR)	AATGGGACTCATACTCCAAGCA
TUT1_R(q-PCR)	CCGTTCAGAAGTCTGGTTTTTCA
TUT3_F(q-PCR)	TGCCCCTAGAGACGACCAA
TUT3_R(q-PCR)	GTAGTTGAGTCCATACGTGCTG
TUT5_F(q-PCR)	CCCACCACTTCCAGAACACT
TUT5_R(q-PCR)	GCTTTCAAAGACGCAGTTCC
TUT6_F(q-PCR)	TGTGTTTTTGTCGGTACAGGAG
TUT6_R(q-PCR)	AGCTCGTAGTTCTACCAGGTG
DIS3L2_F(q-PCR)	TCCCCGGATGGTGATCGAG
DIS3L2_R(q-PCR)	GGAAGCAGTTTCACGACCAC
LSM1_F(q-PCR)	GCACTTGGTTCTGCTTCGAGATG
LSM1_R(q-PCR)	GGAAAGACCTCGGTCCTTCAGG
RRP41_F(q-PCR)	GCTCGGCCTACATTGAGCAG
RRP41_R(q-PCR)	GGACTTACGGTCCCCATGTG
XRN1_F(q-PCR)	TCCAACTGTATCACACCAGGA
XRN1_R(q-PCR)	GCTTTGCTTTCTCGGATCTGA
MET_F(q-PCR)	TTCTGACCGAGGGAATCATCA
MET_R(q-PCR)	CCTTCACTTCGCAGGCAGAT
SHOC2_F(q-PCR)	GTTGACAATACGATCAAACGGC
SHOC2_R(q-PCR)	CTCTTCCCGGCATTTGTTGAG
TRIM24_F(q-PCR)	TGTGAAGGACACTACTGAGGTT
TRIM24_R(q-PCR)	GCTCTGATACACGTCTTGCAG
RB1CC1_F(q-PCR)	ATCGAAGAGTGTGTACCTACAGT
RB1CC1_R(q-PCR)	GCAGGTGGACGATCACATAAGAT
Firefly_F(q-PCR)	CCCATCTTCGGCAACCAGAT
Firefly_R(q-PCR)	GTACATGAGCACGACCCGAA
Renilla_F(q-PCR)	CTGGACGAAGAGCATCAGG

Renilla_R(q-PCR)	TGATATTCGGCAAGCAGGCA
PTMA_F(q-PCR)	ATGTCAGACGCAGCCGTAGA
PTMA_R(q-PCR)	CTAGTCATCCTCGTCGGTCTTCTGC
ADAR_F(q-PCR)	ATCAGCGGGCTGTTAGAATATG
ADAR_R(q-PCR)	AAACTCTCGGCCATTGATGAC
PGM2_F(q-PCR)	GAGCTGCTATGGGACCTGGA
PGM2_R(q-PCR)	GCTCGGGCGTCAAAACTGA
SHOC2-A0	UUUAUUACAGCUCUACCUAG
SHOC2-A10	UUUAUUACAGCUCUACCUAGAAAAAAAAAA
SHOC2-A25	UUUAUUACAGCUCUACCUAGAAAAAAAAAAAAAAAAAAAAAAAAA
SHOC2-A25R	AAAAAAAAAAAAAAAAAAAAAAAAAAUUUAUUACAGCUCUACCUAG
SHOC2-A50	UUUAUUACAGCUCUACCUAGAAAAAAAAAAAAAAAAAAAAAAAAAAAAAAAAAAAAAAAAAAAAAAAAAAAAAAA
CALM1-A0	GCCUUUCAUCUCUAACUGCG
CALM1-A10	GCCUUUCAUCUCUAACUGCGAAAAAAAAAA
CALM1-A25	GCCUUUCAUCUCUAACUGCGAAAAAAAAAAAAAAAAAAAAAAAAA
CALM1-A25R	AAAAAAAAAAAAAAAAAAAAAAAAAAGCCUUUCAUCUCUAACUGCG
CALM1-A50	GCCUUUCAUCUCUAACUGCGAAAAAAAAAAAAAAAAAAAAAAAAAAAAAAAAAAAAAAAAAAAAAAAAAAAAAAA
miR-1_guide	UGGAAUGUAAAGAAGUAUGUA
miR-1_passenger	CAUACUUCUUUACAUUCCAUU
Primer for T7E1 assay_F	TGGCTGGAAATTGTAAATGC
Primer for T7E1 assay_R	TGAGTCAAACAAAAACTGACCTTC

Table 2.3 Lists of oligonucleotides used in this study. For siRNA, only passenger (sense) strand is shown.

3. In-depth profiling of poly(A) tail length by mTAIL-seq

3.1 Background

Eukaryotic mRNA experiences multiple types of modifications at its 3′ end throughout its life cycle. Newly synthesized mRNA is known to acquire a long poly(A) tail (up to ~250 nt) through canonical polyadenylation coupled to transcription, which facilitates mRNA export from the nucleus (Wahle & Keller, 1996). In the cytoplasm, poly(A) tail is associated with cytoplasmic poly(A) binding proteins (PABPCs) that stabilize mRNA by acting as a safeguard against multiple decay machineries and promotes protein synthesis (Eliseeva et al., 2013; Norbury, 2013). Once mRNA is deadenylated to a certain threshold (~25 nt), PABPC is released and mRNA becomes translationally inactive and prone to degradation. Poly(A) tails can be elongated post-transcriptionally by noncanonical poly(A) polymerases which can play a particularly important role in cells with limited transcriptional activity (D'Ambrogio et al., 2013; Weill et al., 2012). For instance, in neuronal synapses and oocytes, deadenylated mRNAs are not degraded, but stored in a dormant state until protein production is required (D'Ambrogio et al., 2013; Weill et al., 2012). In response to cellular signals during meiotic maturation or synaptic stimulation, some deadenylated mRNAs are known to undergo cytoplasmic polyadenylation, which enhances translation, promoting rapid accumulation of protein independently of transcription. In such conditions, poly(A) tail length serves as a determining factor in translational re-activation.

Cytoplasmic polyadenylation has been mainly studied with maternal mRNAs stored in oocytes and early embryos of *Drosophila*, *Xenopus*, and mouse (Mendez & Richter, 2001; Richter, 2007; Salles et al., 1994). Previous analyses showed that cell cycle genes and embryo patterning factors are regulated via polyadenylation, which is critical for normal development. In vertebrates, the cytoplasmic polyadenylation element (CPE)

is enriched in the 3′ UTRs of target mRNAs (Pique et al., 2008). GLD-2 (also known as TUTase2 or PAPD4 in mammals) is a noncanonical poly(A) polymerase and acts on mRNAs containing CPE through the interaction with CPE binding protein (CPEB) (Kwak et al., 2004; Norbury, 2013). In *Drosophila*, a GLD-2 homolog, Wispy, is known to be required for poly(A) tail elongation (Benoit et al., 2008; Cui et al., 2008, 2013).

Our current knowledge on cytoplasmic polyadenylation is mainly from analyses on individual genes using Northern blotting- or RT-PCR-based methods. This is largely due to the technical difficulties in the sequencing of homopolymers (Salles et al., 1999; Zheng & Tian, 2014). Microarray analyses following differential elution from oligo(dT) column has been applied to estimate the ratio between long and short A-tails (Cui et al., 2013; Du & Richter, 2005; Meijer et al., 2007; Novoa et al., 2010). Although this approach allowed genome-wide estimation of poly(A) tail length, the resolution and accuracy of the measurement were highly limited, precluding deeper investigation of mRNA tailing. Thus, many questions remain unanswered: 1) at which developmental stage does cytoplasmic polyadenylation occur, 2) which mRNAs are affected by cytoplasmic polyadenylation, and 3) is GLD-2 a main enzyme for cytoplasmic polyadenylation and, if so, is its specificity restricted to a subset of mRNAs?

Overcoming this technical hurdle for determining poly(A) tail length, I recently developed a method called "TAIL-seq" which enabled us to explore the 3′ extremity of mRNA using Illumina sequencing platform (Chang et al., 2014b). In brief, total RNA is depleted of rRNAs by using affinity beads and ligated to the 3′ adaptor that contains biotin residues (Figure 3.1, left). Following fragmentation by RNase T1, the 3′ most fragments are purified by using streptavidin beads, and ligated to the 5′ adaptor. After reverse transcription and PCR amplification, the library is sequenced following a paired-end sequencing protocol; 51 cycles for read 1 (forward direction) to identify the transcript and 231 cycles for read 2 (reverse direction) to examine the 3′ tail sequences. As the sequence quality of the homopolymeric T (corresponding to poly(A) tail) is very low, TAIL-seq analyzes the raw fluorescence signals from read 2, from which a machine learning algorithm detects the transition from poly(T) to non-T sequences. Because the transition occurs at the boundary between poly(A) tail and 3′ UTR, one can use this information to precisely measure poly(A) tail length.

Apart from allowing high-resolution, genome-wide measurement of poly(A) tail length, TAIL-seq has some unique strengths. Firstly, it uses the regular sequencing protocol so one can run the library in any Illumina sequencer. Another method based on high throughput sequencing, called "PAL-seq", also offers a genome-wide measurement of poly(A) tail length with high resolution (Subtelny et al., 2014), but widespread accessibility of PAL-seq is precluded by its requirement for special manipulation of the sequencing machine and an additional imaging step. Secondly, TAIL-seq preserves the sequence information of the 3′ end so as to reveal 3′ end modifications such as uridylation and guanylation. TAIL-seq also detects numerous other types of 3′ ends such as endonucleolytic cleavage sites and decay intermediates.

The ability to cover the complex terminome is a strength of TAIL-seq, but at the same time, the wide coverage of TAIL-seq library inevitably reduces sensitivity for mRNA, limiting its application to small amounts of material. Thus, I here modify TAIL-seq to increase the sensitivity. The new method ("mTAIL-seq") allows us to investigate poly(A) tail regulation in *Drosophila* oocytes and eggs where poly(A) tail length has not been accurately measured yet. I discover a major phase of polyadenylation during late oogenesis and a modulation of poly(A) tail upon egg activation. By comparing mTAIL-seq data to ribosome profiling data, I further find a strong coupling between poly(A) regulation and translational activation in fly eggs.

3.2 Results

3.2.1 mTAIL-seq: a solution for limited materials

For the original version of TAIL-seq, a large amount of total RNA (~100 ug) was needed to achieve enough sequencing depth for mRNA (Figure 3.1, left) (Chang et al., 2014b). In order to improve the sensitivity, I decided to use splint ligation which allowed us to capture RNAs with a specific type of terminus. Note that I did not use oligo(dT) affinity purification so as to avoid a potential bias towards long poly(A) tails. Splint ligation has been used to generate various cDNA libraries, and it has been shown that splint ligation does not cause a significant bias over a wide range of poly(A) tails except for very short A

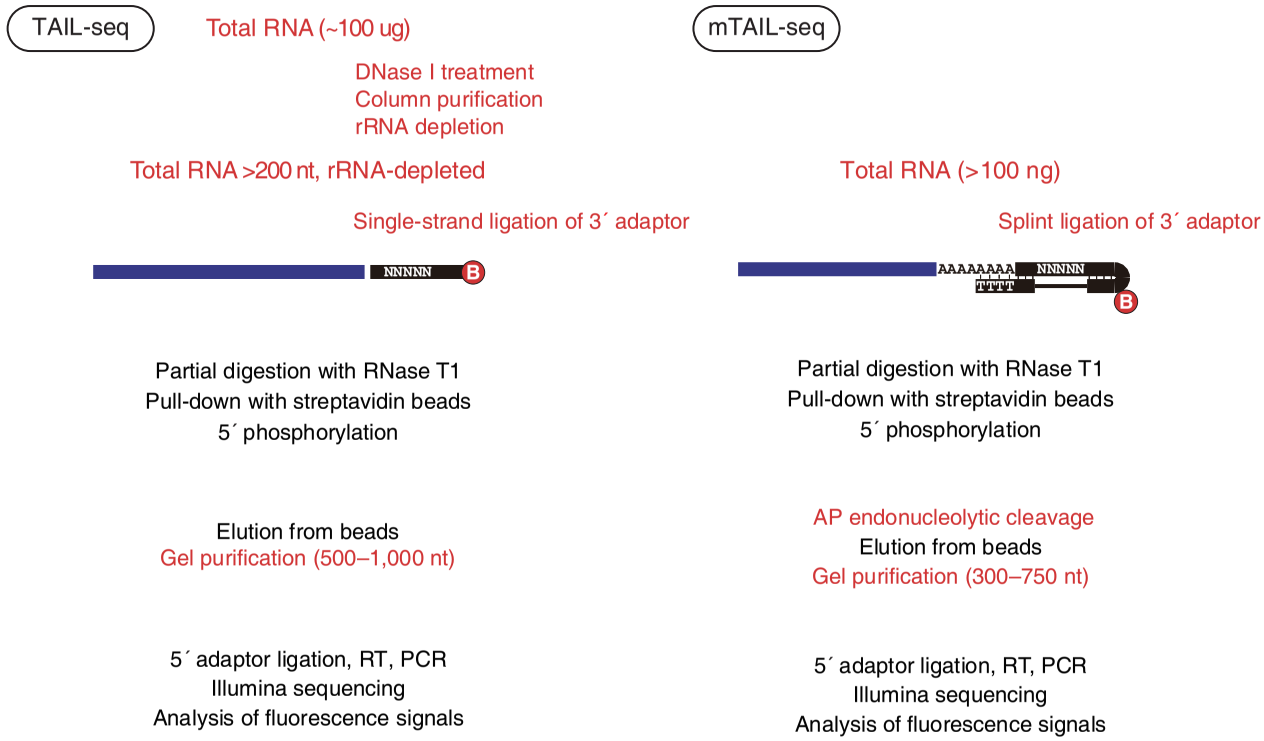

Figure 3.1 Schematic of experimental procedures. (left) TAIL-seq, (right) mTAIL-seq. Common steps are shown in black color while red indicates method-specific procedures. Blue bars and black bars represent mRNAs and 3′ adpators, respectively. N (random sequence) and T (thymine) shown in 3′ adaptors are abbreviated proportional to the original length. B refers to a biotin.

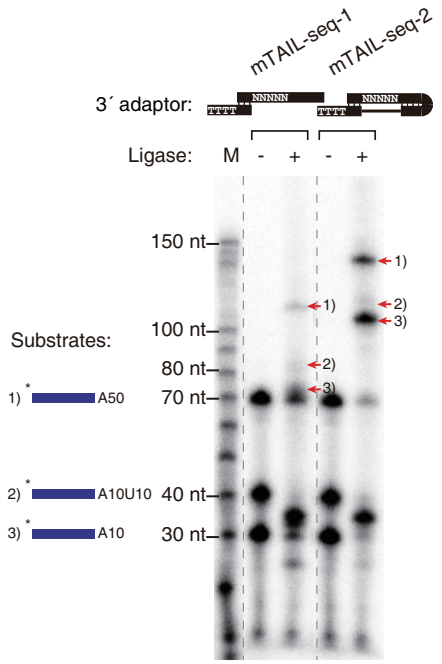

Figure 3.2 Ligation efficiency test. 5′ labeled substrates which have various tails (A10, A10U10, and A50) are ligated with denoted 3′ adaptor (mTAIL-seq-1 and mTAIL-seq-2). Blue bar refers to 20 nt heterogenous sequences (5′-UUUAUUACAGCUCUACCUAG-3′). Black bar represents the 3′ adpator. N (random sequence) and T (thymine) shown in adaptors are abbreviated to the original length. Red arrows indicate the ligated products. Dashed line marks discontinuous lanes from the same gel.

tails (below ~8 nt) (Subtelny et al., 2014).

For splint ligation, stable annealing of the bridge oligo and the 3′ adaptor was a major issue because the TAIL-seq 3′ adaptor contains degenerate sequences that is used to improve sequencing performance and monitor uneven amplification (Chang et al., 2014b). Initially, I employed splint ligation in a conventional way which uses a bridge oligo between 3′ adaptor and target RNA (Figure 3.2, mTAIL-seq-1); however, ligation efficiency was poor due to weak base pairing between the 3′ adaptor and bridge. To stably anchor the bridge to the 3′ adaptor, I designed a hairpin adaptor instead of using two single stranded oligos (Figures 3.2 and 3.3, mTAIL-seq-2)[1]. The intervening random sequences are bypassed by

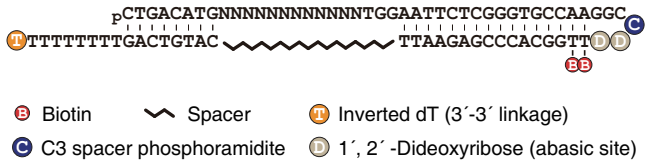

Figure 3.3 Design of the 3′ hairpin adaptor. N refers to a random sequence.

an ethylene glycol spacer. I confirmed that ligation was efficient and specific to A-tailed substrates (Figure 3.2).

mTAIL-seq has several distinct features in library construction procedure (Figures 3.1 and 3.4, see Methods and Materials). First, the 3′ hairpin adaptor specifically captures poly(A)$^+$ RNA so I omit the rRNA depletion step which is expensive and time-consuming. Second, the 3′ hairpin adaptor has two abasic sites which can easily be cut by apurinic/apyrimidinic endonuclease 1 (APE1). The cleavage helps elution of the ligated RNA from the bead and allows reverse transcription by releasing the opposite strand. Third, I changed the range of size fractionation from 500–1,000 nt to 300–750 nt to increase gel elution efficiency. Remaining steps of library preparation and data analysis are similar to the previous version, with minor changes (see detailed information in Methods and Materials). I validated the performance of mTAIL-seq analysis pipeline by using spike-ins of known poly(A) tail length (Figure 3.5)[2].

Compared with TAIL-seq, mTAIL-seq provided significantly more mRNA reads that are mapped to coding sequence (CDS) and 3′ untranslated region (UTR) (Figure 3.6). Expectedly, the tags were mainly derived from near the annotated 3′ ends (Figure 3.7). In terms of sensitivity, mTAIL-seq detected ~1,250 genes per million reads on average, which is approximately 5 times greater than the original TAIL-seq (Figure 3.8). It allowed us to analyze thousands of genes even from a small scale run on Illumina MiSeq, which reduces the cost of sequencing. It is noteworthy that mTAIL-seq detected 643 genes with at least 50 poly(A)$^+$ tags even from 33 ng total RNA which corresponds to ~1,000 HeLa cells. Four experiments covering a broad dynamic range of input RNA showed reproducible results, indicating that mTAIL-seq is a robust technique (Figures 3.9 and 3.10).

[1]The adaptor was designed in collaboration with Dr. Hyeshik Chang.

[2]mTAIL-seq analyses in this study were done by Dr. Hyeshik Chang's pipeline.

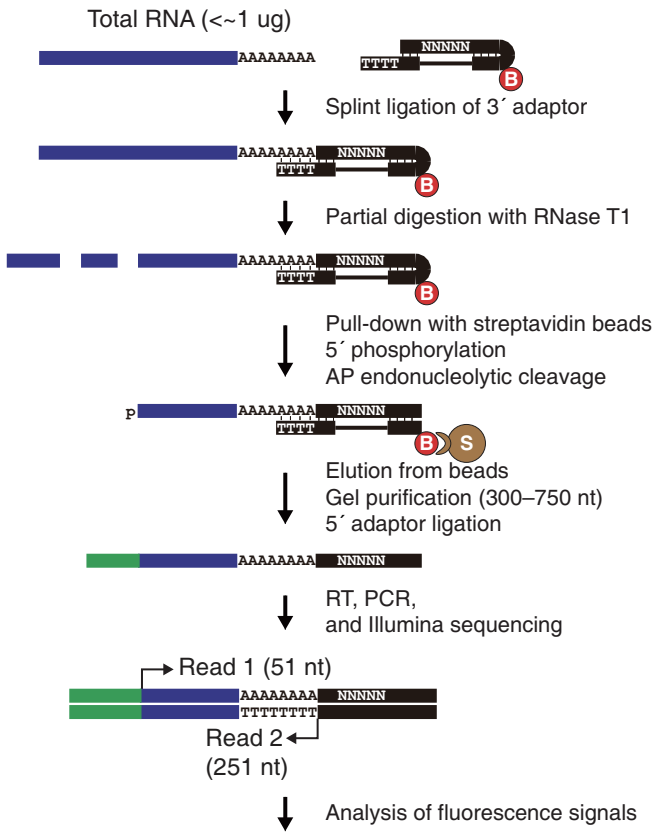

Figure 3.4 Schematic description of experimental procedure.

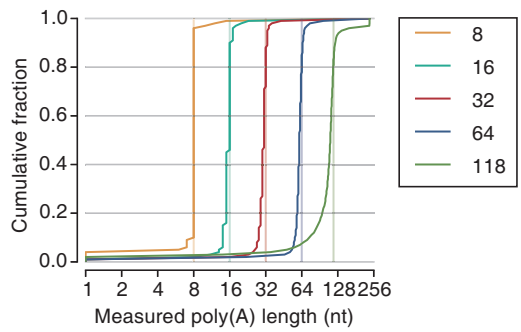

Figure 3.5 A cumulative graph of poly(A) tail length of chemically synthesized spike-ins (A8, A16, A32, A64, A118) measured by TAIL-seq algorithm.

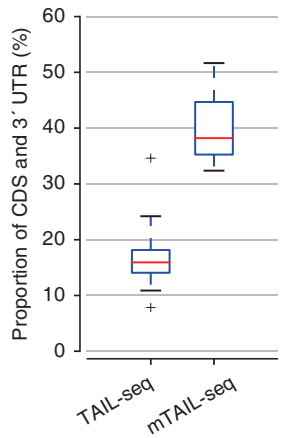

Figure 3.6 A box plot showing read proportion of CDS and 3′ UTR in TAIL-seq and mTAIL-seq. For comparison, 12 libraries of TAIL-seq and 13 libraries of mTAIL-seq made from HeLa cells are used. Box indicates the first and third quartiles and the internal bar refers to the median. Whiskers denote the lowest and highest values within 1.5 times the interquartile range of the first and third quartiles, respectively.

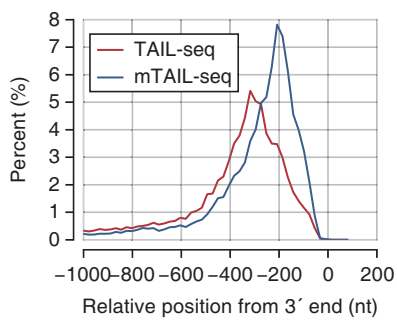

Figure 3.7 TAIL-seq reads are enriched in the 3′ part of genes. X-axis shows a relative distance between the 5′ end of read 1 and the annotated 3′ end.

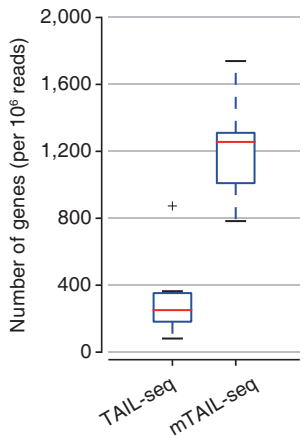

Figure 3.8 A box plot showing the number of detected genes which are normalized by one million reads in TAIL-seq and mTAIL-seq. Box and whisker plots are shown as in Figure 3.6.

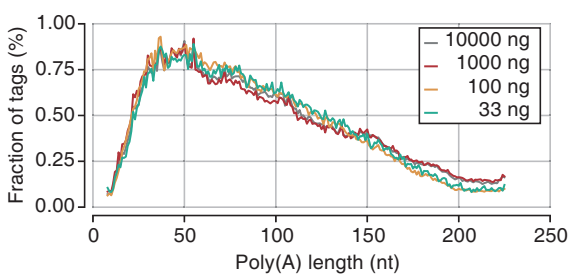

Figure 3.9 Global distributions of poly(A) tails (8–225 nt) from 4 different amounts of HeLa RNA.

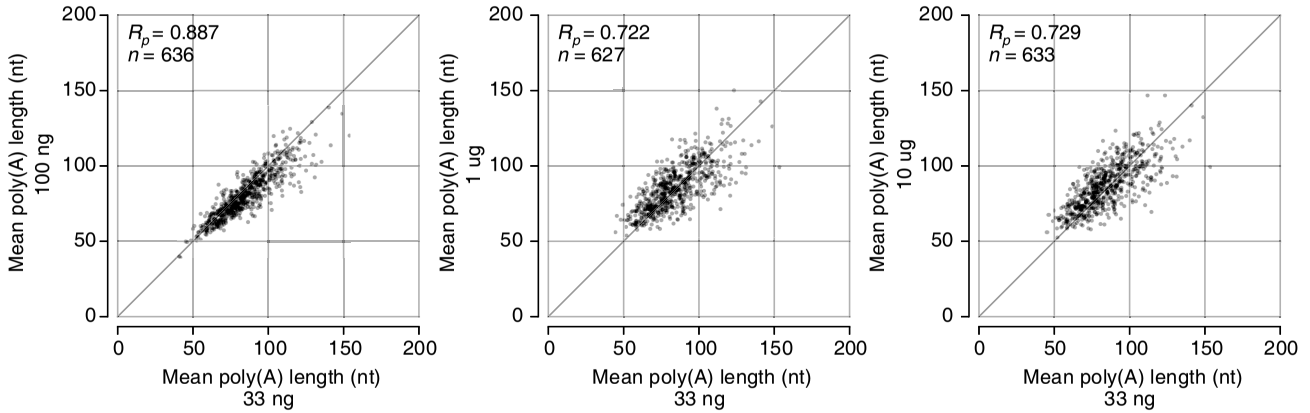

Figure 3.10 Scatter plots showing the correlation between poly(A) tail lengths measured with four different amounts of input RNA from HeLa. R_p refers to Pearson correlation coefficient.

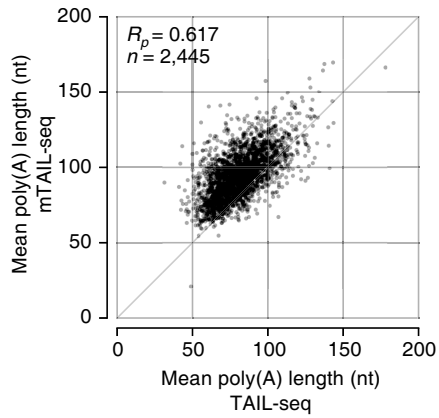

Figure 3.11 Comparison of poly(A) tail lengths estimated by TAIL-seq and mTAIL-seq. R_p refers to Pearson correlation coefficient.

As expected, mTAIL-seq provides longer median lengths than TAIL-seq does (Figure 3.11) because the splint ligation used in mTAIL-seq cannot capture certain types of tails such as very short A-tails (below 8 nt) or those with 3′ modifications. Uridylation is the most frequent modification of poly(A) tail, and is found mainly on short tails less than 25 nt (Chang et al., 2014b; Lim et al., 2014). Mono- and di-uridylation are the most prevalent uridylation types. Since uridylated tails are not efficiently ligated to the adaptor with 8 Ts (Figure 3.12, mTAIL-seq-T8), I sought to capture uridylated tails by synthesizing and mixing two additional hairpin adaptors which carry one or two adenosines at the overhang (Figure 3.12, mTAIL-seq-T7A1 and mTAIL-seq-T6A2). With the mixture of adaptors, I could detect uridylated tails, albeit at a lower frequency as compared to original TAIL-seq (Figure 3.12). Thus, mTAIL-seq is adjustable to enrich a specific type of terminus, by changing the design of adaptors with different sequences.

In conclusion, both TAIL-seq and mTAIL-seq have unique strengths suitable for particular purposes. TAIL-seq offers a comprehensive view of 3′ terminome which covers all types of RNA termini. On the other hand, mTAIL-seq can be more practical if one is interested in a specific type of RNA terminus, such as poly(A)$^+$ mRNAs. For its enhanced sensitivity and reduced cost and time, mTAIL-seq is useful especially when only a small amount of biological sample is available and/or when many samples need to be analyzed

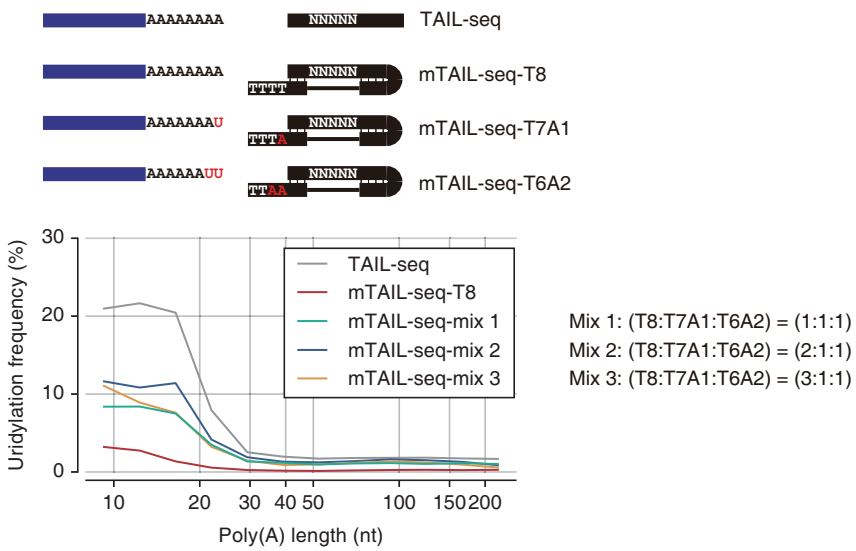

Figure 3.12 Detection of U-tails by mTAIL-seq. (Top) 3′ adaptors used in TAIL-seq and mTAIL-seq are shown in black bars. The nucleotide composition of overhang is denoted in the name (T8, T7A1, and T6A2). Blue bar refers to 3′ end of transcript. (Bottom) Poly(A) tail lengths from 8 nt to 231 nt are pooled in equal-width bins in the logarithmic scale (base 2) (x-axis). The left sides of bins (inclusive) are 8, 11, 15, 20, 26, 34, 46, 61, 81, 108, 144, 192 nt. Uridylation frequency (y-axis) indicates the percentage of mono-U and di-U tails within each length range.

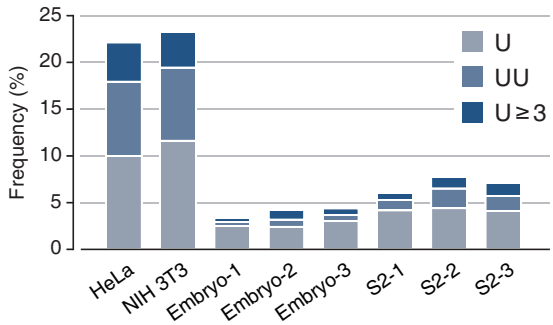

Figure 3.13 3′ uridylation frequency of mRNAs with short poly(A) tail (5–25 nt) detected by TAIL-seq. Three independent biological replicates from embryos (0–2 hr) and S2 cells are shown along with HeLa and NIH 3T3 (Chang et al., 2014b).

and compared.

3.2.2 Global poly(A) tail length measurement in *Drosophila*

Previous studies on cytoplasmic polyadenylation focused on specific individual mRNAs with critical roles in developmental processes. To gain a transcriptomic landscape of cytoplasmic polyadenylation, I applied mTAIL-seq on *Drosophila* oocytes and embryos. Of note, the original TAIL-seq protocol was initially used for *Drosophila* early embryos (0–2 hr after egg laying [AEL]) and S2 cells which are relatively easy to get a large amount of samples. I found that uridylation frequency in these samples is far lower than that in HeLa and NIH 3T3 cells, which implies that uridylation may play a limited role in flies (Figure 3.13)[3].

Using mTAIL-seq, I monitored poly(A) tail length at six different time points during early embryo development, ranging from 0 hr to 4.5 hr AEL (Figure 3.14)[4]. Because major activation of zygotic transcription occurs around 2 hr AEL, the samples up to 2 hr AEL represent an early stage of development where transcription is silenced (Tadros & Lipshitz, 2009). I expected that poly(A) tail length would increase globally as described in fertilized

[3] TAIL-seq data from fly samples were made by Dr. Mihye Lee.

[4] Fly embryos were collected by Dr. Mihye Lee.

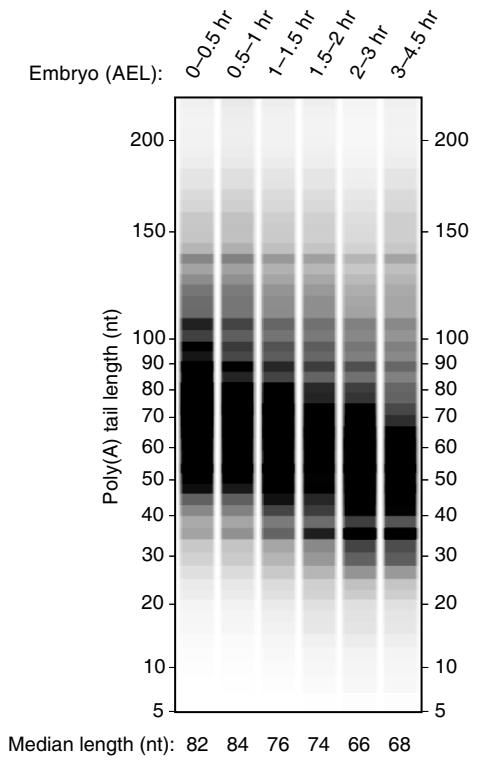

Figure 3.14 Virtual gel image of poly(A) tail length distribution from *Drosophila* early embryos. The total intensity of each bin (intensity multiplied by area) is proportional to read counts and normalized by each lane.

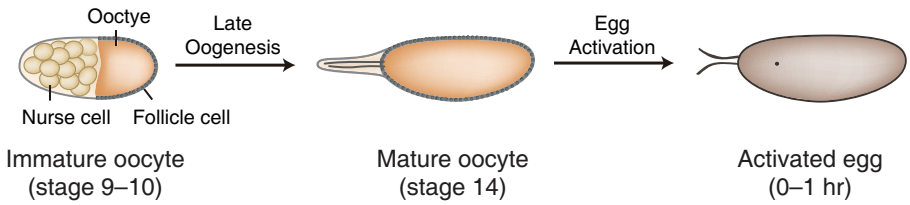

Figure 3.15 Schematic illustration of late oogenesis and egg activation in *Drosophila*. Global poly(A) tail lengths are addressed at three different stages: immature oocyte, mature oocyte and activated egg. 'Stage 9–10 egg chamber', 'stage 14 egg chamber', and 'unfertilized, but activated egg' are indicated as immature oocyte, mature oocyte, and activated egg, respectively. These terms are used throughout the thesis.

eggs of *Xenopus* and zebrafish (Subtelny et al., 2014), but surprisingly, the median length of poly(A) tail was not significantly increased in 0–1 hr period in fly embryos, and indeed decreased after 1 hr (Figure 3.14).

To determine the developmental stage where cytoplasmic polyadenylation takes place, I decided to examine earlier stages of female gametes: immature oocyte (stage 9–10 egg chamber), mature oocyte (stage 14 egg chamber), and activated egg (0–1 hr AEL) (Figure 3.15)[5] (Bastock & St Johnston, 2008; He et al., 2011). *Drosophila* ovarian development comprises 14 distinct stages. Two critical events, oocyte maturation and egg activation, are required for the production of functional embryos. Around stage 12–13, immature oocytes undergo maturation to yield metaphase I-arrested mature oocytes (stage 14) (Laver et al., 2015; Resnick et al., 2009; Von Stetina & Orr-Weaver, 2011). Mature oocytes are ovulated from the ovary and pass through the reproductive tract which triggers egg activation and exit from meiosis. In *Drosophila*, egg activation is induced by mechanical pressure, independent of fertilization (Heifetz et al., 2001; Horner & Wolfner, 2008). Thus, Dr. Mihyee Lee collected activated but unfertilized eggs for one hour after they were laid, instead of fertilized embryos. This allowed us to examine maternal mRNAs upon egg activation, avoiding the compounding effects from zygotic transcription. From small amounts (less than 5 ug of total RNA) of oocyte and egg samples, I performed mTAIL-seq

[5] Fly samples were collected by Dr. Mihye Lee.

with MiSeq and measured the poly(A) tail length of 3,664 genes (with at least 50 poly(A)$^+$ tags in all three samples). Two biological replicates at each stage showed a high degree of reproducibility (Figure 3.16)[6].

Interestingly, I observed a drastic difference in poly(A) length distribution between immature oocytes and mature oocytes while only a minor change was seen between mature oocytes and activated eggs (Figures 3.17 and 3.18). The median length in global profile increased from 60 nt in immature oocytes to 75 nt in mature oocytes (Figure 3.17). At the gene level, most genes (3,365 out of 3,940 genes, 85.4%) were polyadenylated during late oogenesis (Figure 3.19, left). The median of mean increased from 56 nt to 76 nt. However, upon egg activation, the median length of poly(A) tail did not increase at the global level (Figures 3.17 and 3.19, the median: 73 nt, the median of mean: 70 nt), although there were some gene-specific modulations (Figure 3.19, right). To confirm that this dramatic change of poly(A) tail during late oogenesis is not due to transcription, RNA-seq was carried out on the same samples used for mTAIL-seq and found that individual mRNA abundance is largely unchanged during late oogenesis and egg activation (Figure 3.20)[7]. Additionally, there was no substantial correlation between mRNA abundance change and poly(A) length change (Figure 3.21). Taken together, these analyses indicate that the changes of poly(A) tail length may be caused by cytoplasmic polyadenylation, not by nascent transcription.

For validation, I next examined several individual genes that were previously studied (Figure 3.22) (Benoit et al., 2005, 2008; Salles et al., 1994; Vardy & Orr-Weaver, 2007; Vardy et al., 2009). The mTAIL-seq results were validated by high-resolution poly(A) tail assay (Hire-PAT) (Figure 3.23)[8]. As expected, cell cycle regulators, such as *cycB*, as well as embryo patterning related genes, like *Tl* and *bcd*, showed dramatic increase of poly(A) tail length during late oogenesis and egg activation, whereas *sop* (ribosomal protein S2) remained nearly unchanged. In the case of embryo posterior determinant *osk*, the poly(A) tail is relatively long in immature oocytes and mature oocytes, which differs from the previous report showing elongation in this stage (Benoit et al., 2005). But, given the earlier studies reporting the presence of Osk protein in immature oocytes (Kim-Ha et al., 1995; Yoshida

[6] All analyese of mTAIL-seq were carried out in collaboration with Ahyeon Son.

[7] RNA-seq analysis was done by Ahyeon Son.

[8] In collaboration with Dr. Mihye Lee.

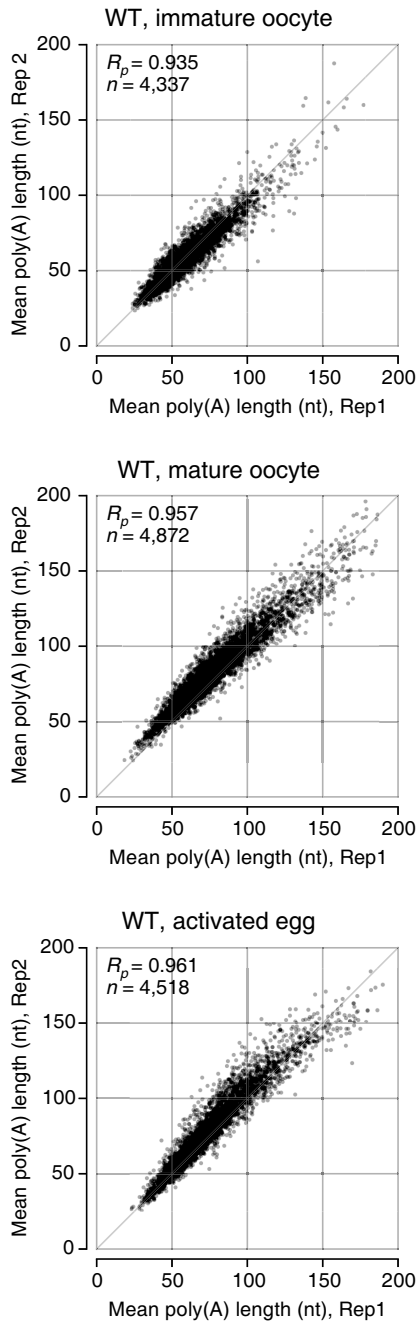

Figure 3.16 Reproducibility between two biological replicates of mTAIL-seq. R_p refers to Pearson correlation coefficient.

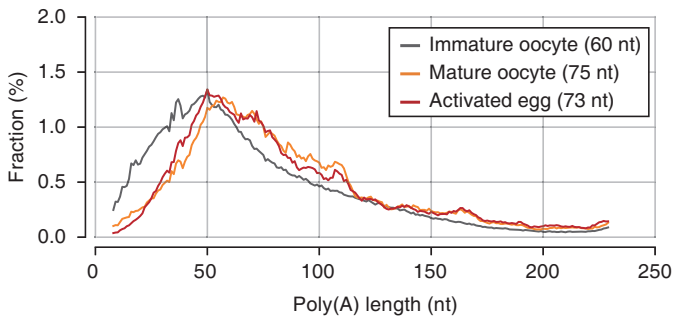

Figure 3.17 Global distributions of poly(A) tails at three stages. The median poly(A) tail lengths is 60 nt in immature oocytes, 75 nt in mature oocytes, and 73 nt in activated eggs. The result from biological replicates is shown in Figure 3.18.

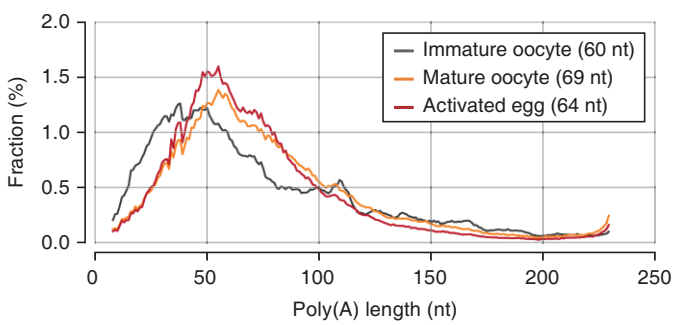

Figure 3.18 Global distributions of poly(A) tails at three stages in biological replicates. The median poly(A) tail lengths is 60 nt in immature oocytes, 69 nt in mature oocytes, and 66 nt in activated eggs.

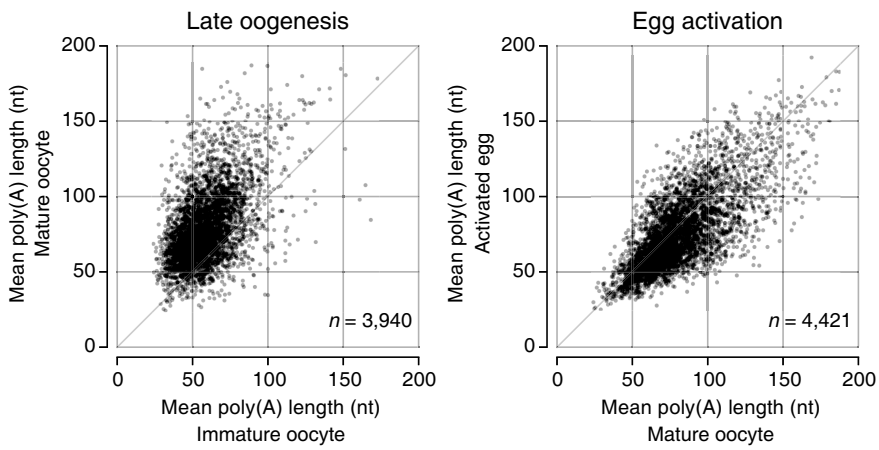

Figure 3.19 Scatter plots showing the changes of poly(A) tail length upon late oogenesis and egg activation, respectively. The mean poly(A) tail lengths from two biological replicates are averaged (n=2). The median of mean poly(A) tail lengths is 58 nt in immature oocytes, 76 nt in mature oocytes, and 70 nt in activated eggs.

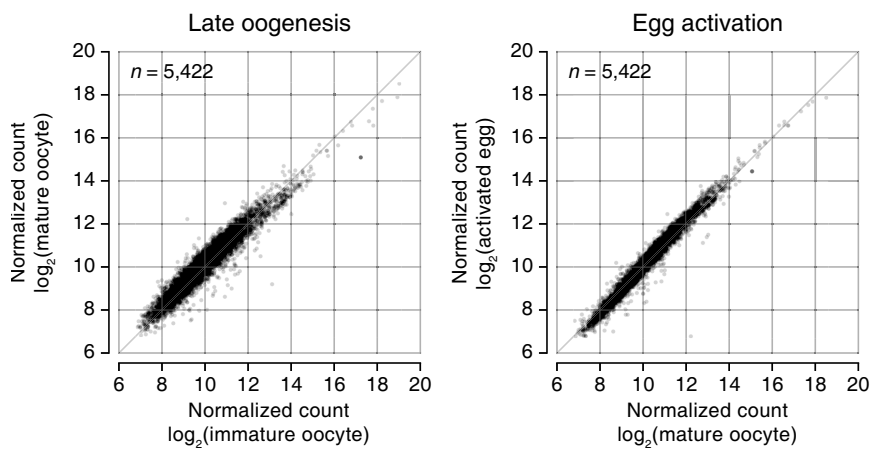

Figure 3.20 Changes of mRNA abundance upon late oogenesis and egg activation measured by RNA-seq.

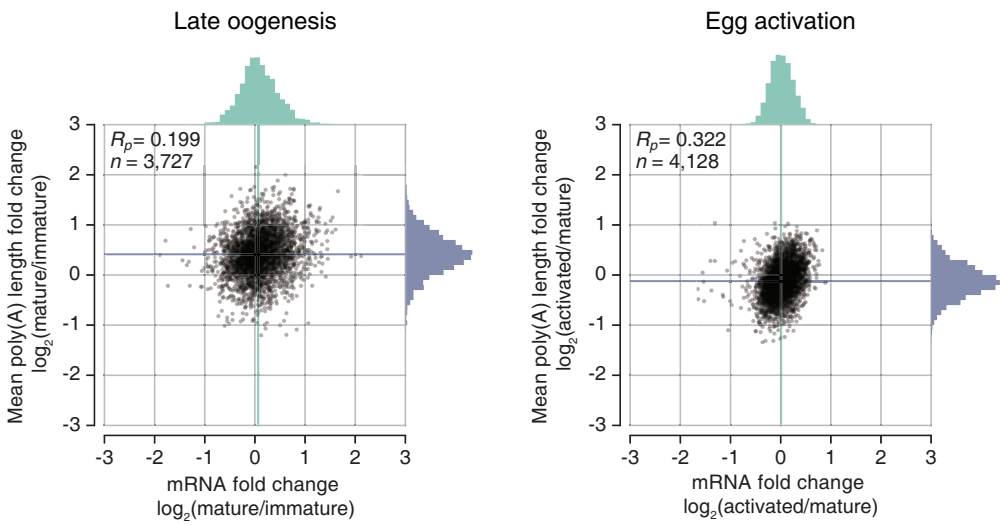

Figure 3.21 Scatter plots showing the correlation between mRNA abundance change and mean poly(A) length change during late oogenesis and egg activation, respectively. For each stage transition, densities of mRNA abundance change and mean poly(A) length change are plotted in upper and right sides of the scatter plot, respectively. R_p refers to Pearson correlation coefficient.

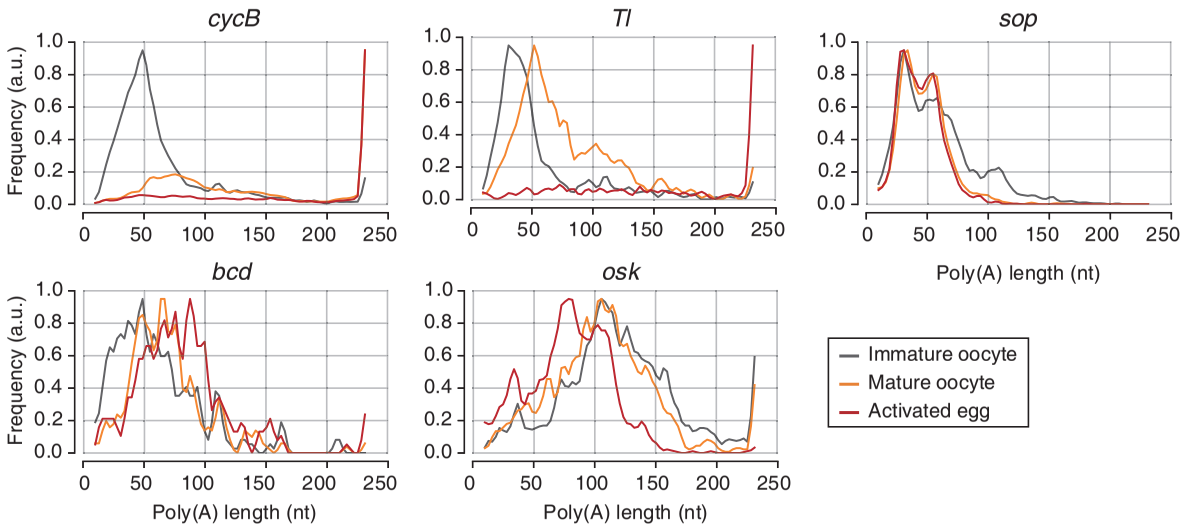

Figure 3.22 Examples of individual genes. mTAIL-seq tags are plotted in 3 nt wide bins, then smoothened with Hanning window (width=5). The frequency along the y-axis is normalized by the maximum value at each stage.

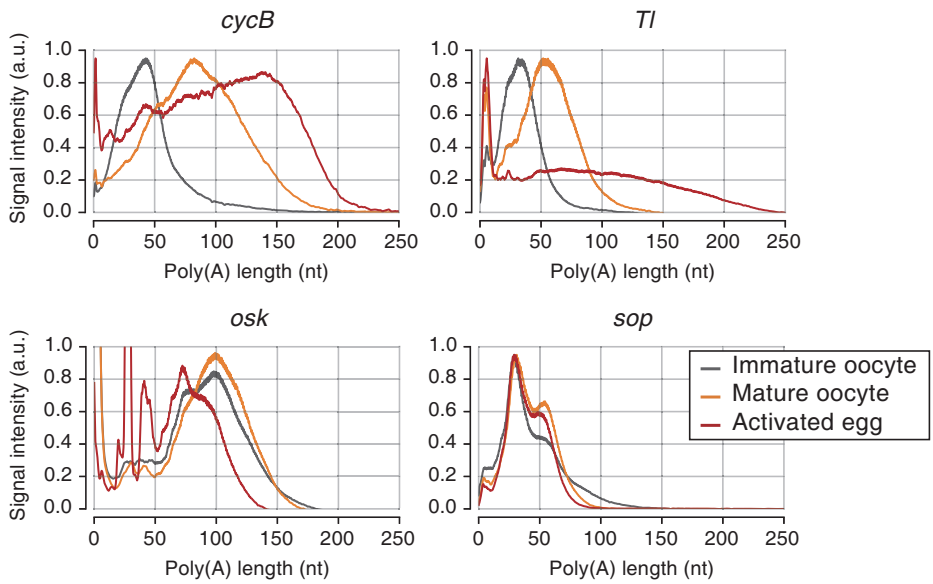

Figure 3.23 Results of high-resolution poly(A) tail assay (Hire-PAT). The signal intensity is normalized to maximum value at each stage, except for osk, the signal of which is fitted into the immature oocyte stage.

et al., 2004) and the enhancement of osk translation by cytoplasmic polyadenylation at the posterior pole before late oogenesis (Castagnetti & Ephrussi, 2003), it is likely that the osk mRNA indeed has a long tail and is actively translated in immature oocytes. Therefore, adenylation of some mRNAs may occur prior to stage 9–10.

In conclusion, my mTAIL-seq experiments provide an accurate profile of poly(A) length at the genomic level, revealing dynamic regulation of poly(A) tail during *Drosophila* oogenesis and egg activation.

3.2.3 Distinct patterns of poly(A) tail regulation

Although poly(A) tail length increases during late oogenesis and is maintained during egg activation at the global level, many individual genes show interesting temporal regulation patterns. Based on these dynamic changes, I classified 3,664 genes into 8 groups (Figures 3.24, 3.25, 3.26, and Table 3.1, see 3.4)[9]. Groups 1, 2, and 3 show an increase throughout late oogenesis and egg activation. Transcripts in these groups have considerably shorter poly(A) tails at the immature oocyte stage than other transcripts. Specifically, group 1 contains 441 transcripts whose poly(A) tail increases continuously throughout late oogenesis and egg activation. The median length of poly(A) tail changed from 49 nt to 105 nt. This group includes several well-known targets of cytoplasmic polyadenylation such as *cycB*, *Tl*, and *bcd*, which is consistent with previous studies (Benoit et al., 2005, 2008; Salles et al., 1994; Vardy & Orr-Weaver, 2007; Vardy et al., 2009). Interestingly, gene ontology analysis of group 1 reveals enrichment for terms such as "regionalization", "wing disc development", "zinc ion binding", and "regulation of RNA metabolic processes" (Figure 3.27). It is tempting to speculate that group 1 may include some unknown developmental regulators that are poised to act in early embryo through cytoplasmic polyadenylation.

Next, groups 4 and 5 show fluctuating patterns: lengthening during late oogenesis and shortening during egg activation. Thus, transcripts in these groups are polyadenylated specifically during late oogenesis and undergo deadenylation afterwards. What stops their polyadenylation and triggers deadenylation upon egg activation is interesting, but unclear at this point. Genes in groups 4 and 5 consists of functionally diverse genes, but contains

[9] Analyses in this section were done by Ahyeon Son.

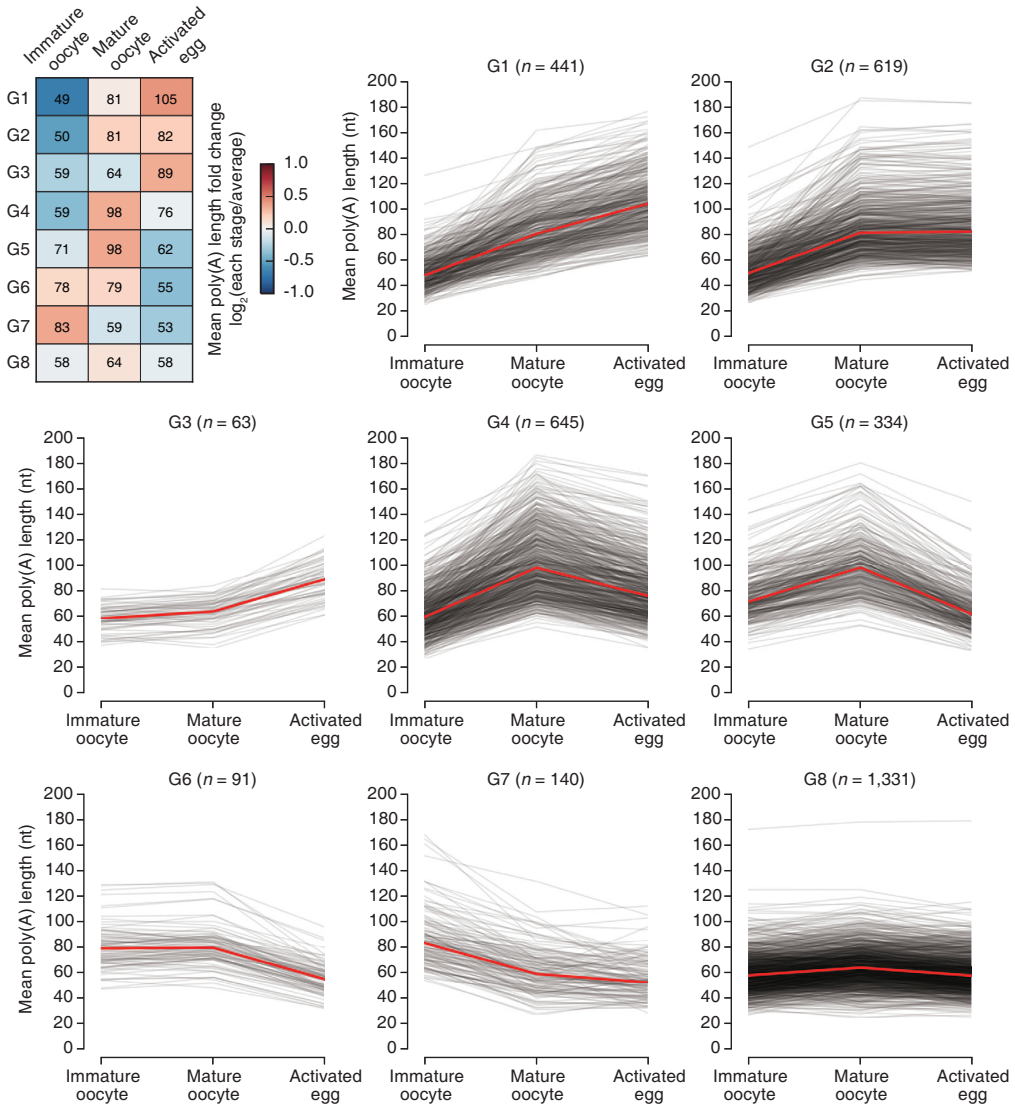

Figure 3.24 Classification of transcripts according to the changes of poly(A) tail length into 8 groups. Fold changes from the average to poly(A) length of each stage are shown in heat map (left top). The median of mean poly(A) length of each group is presented in heat map. Patterns of poly(A) length changes at individual gene level are presented in line graphs. Red lines indicate the median. See Methods and Materials for classification method and Table 3.1 for the full list.

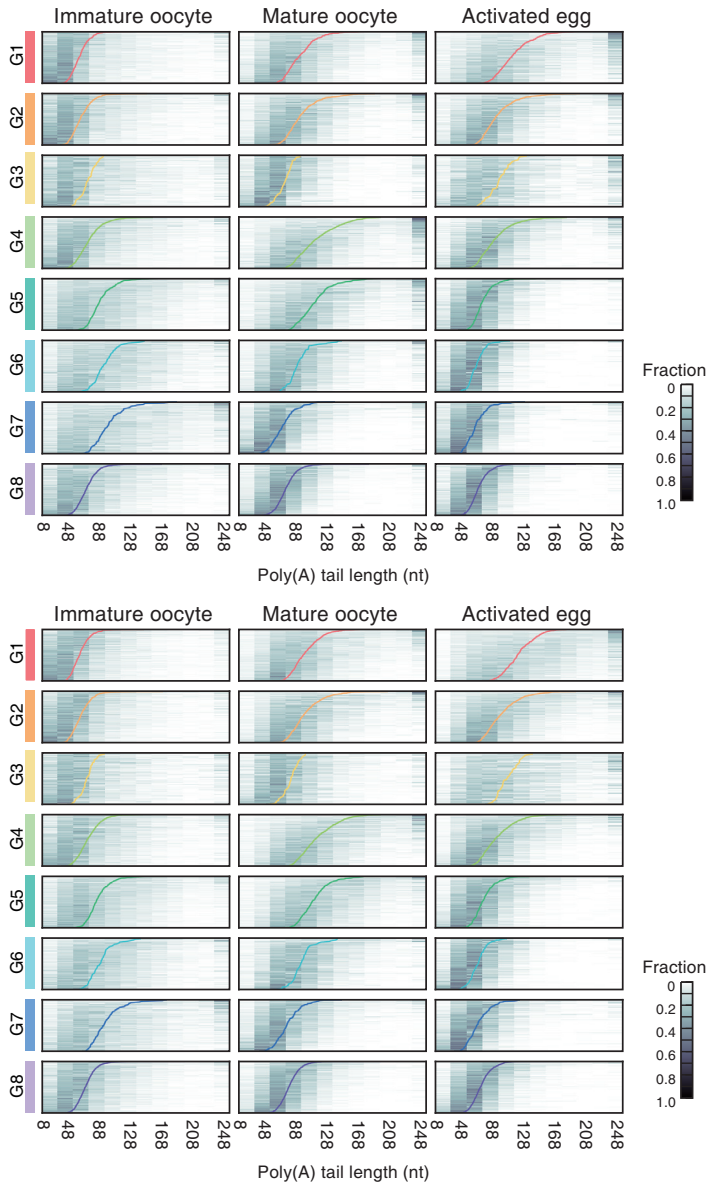

Figure 3.25 Heat maps showing the distributions of intragenic poly(A) tail lengths in each group. Poly(A) length is discretized with 20 nt wide bins, and the color intensity indicates the fraction of poly(A) tags for the gene. For each heat map, genes are sorted and reordered by geometric mean of poly(A) length (colored line).

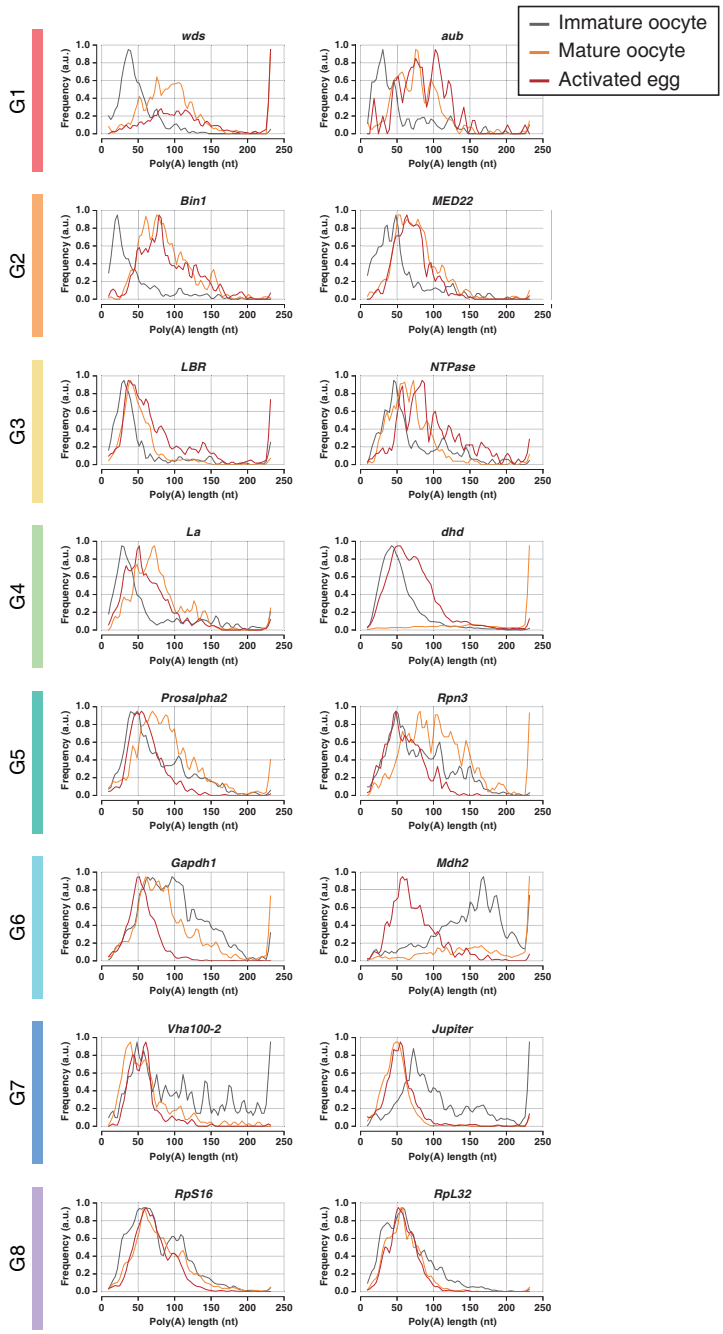

Figure 3.26 Poly(A) tail distribution of two representative genes from each group is presented as in Figure 3.22.

		Gene ontology groups
G1		regionalization wing disc development zinc ion binding regulation of RNA metabolic process
G2		regulation of transcription
G3		gamete generation
G4		-
G5		proteasome complex lipid particle proteolysis oxidative phosphorylation chaperonin-containing T-complex
G6		generation of precursor metabolites and energy
G7		-
G8		ribosome ribonucleoprotein complex structural molecule activity translation

Figure 3.27 Functional categorization of genes in each group by gene ontology analysis (FDR <0.1). For overlapping terms, a representative term is selectively shown.

many genes involved in proteolysis and oxidative phosphorylation. These genes may need to be transiently translated in mature oocytes and silenced in early embryos immediately following egg activation.

Groups 6 and 7 show descending patterns (Figure 3.24). Transcripts in these groups have relatively long poly(A) tails in immature oocytes (78 nt and 83 nt for G6 and G7, respectively) as compared with those in other groups (58 nt for all detected genes). It is possible that these transcripts are cytoplasmically adenylated earlier (before and at the stage 9–10) than other transcripts are. Alternatively, but not mutually exclusively, the transcripts in G6 and G7 may retain their long tails by resisting deadenylation in immature oocytes. Like group 5, group 6 is enriched with genes related to generation of precursor metabolites and energy. Rapid deadenylation of these metabolic genes suggests that metabolic pathways may need to be reprogrammed at the onset of animal development.

Group 8 shows little changes in poly(A) tail length profile (less than 20 nt difference across three stages). This group is enriched with genes with constitutive functions such as ribosomal subunits and translation (Figure 3.27).

To understand the mechanism underlying the selectivity of cytoplasmic polyadenylation, I searched for sequence motifs enriched in each group. However, the analysis did not reveal any known motifs, such as CPE (cytoplasmic polyadenylation element) (data not shown). While vertebrate CPE is well-known to play a central role in coordinating cytoplasmic polyadenylation, the role of *Drosophila* CPE remains unclear. Although a fly homolog of CPEB (CPE binding protein), Orb, was reported to physically and genetically interact with a homolog of GLD-2, Wispy, during oogenesis (Benoit et al., 2008), CPE sequences have not been found commonly in Wispy target mRNAs (Coll et al., 2010; Cui et al., 2013). I suspect that the control of poly(A) tail length may be governed by multiple sequence motifs working in combination, as opposed to one master regulatory element, such as CPE.

Cytoplasmic polyadenylation by Wispy

To verify the global cytoplasmic polyadenylation that I observed in late oogenesis, I carried out mTAIL-seq on *wisp* mutants at the same stages as those where wild type samples were collected (Figure 3.28). Wispy is a non-canonical poly(A) polymerase that is exclusively expressed in maturing oocytes and early embryos (Benoit et al., 2008; Cui et al., 2008; Lee et al., 2014a). Wispy acts on mRNAs and miRNAs, but its specificity on individual transcripts remains unclear. In immature oocytes, poly(A) tail lengths in *wisp* mutant were similar to those in wild type (the median of mean length, 56 nt vs 58 nt), indicating that the activity of Wispy may be limited until this stage (Figure 3.29, left panel).

In stark contrast, mature oocytes displayed a marked difference between wild type and *wisp* mutant (Figure 3.29, middle panel). The mutant had substantially shorter poly(A) tails than wild type (the median of mean length, 34 nt and 76 nt, respectively). I also observed a comparable difference in activated eggs (the median of mean length, 32 nt and 70 nt in mutant and wild type, respectively) (Figure 3.29, right panel). Gene-level analyses revealed that most mRNA species have shorter poly(A) tails in *wisp* mutant (98.9% and 97.8% of detected genes in mature oocytes and activated eggs, respectively). Moreover, when examining those genes that displayed changes in poly(A) length of more than 1.5 fold (Figure 3.29, indicated by dashed lines), 89.2% and 82.4% of genes carried shorter poly(A) tails in mature oocytes and activated eggs of the mutant, respectively. Thus, Wispy is responsible for most, if not all, polyadenylation events at these developmental stages. These results also confirm that cytoplasmic polyadenylation takes place mainly during late oogenesis, although Wispy may act either before stage 9 or after egg activation on some select transcripts. I also noticed that mRNA abundance is modestly reduced in activated eggs of *wisp* mutant as compared with those of wild type (Figure 3.30), suggesting that Wispy may increase the stability of maternal mRNAs during embryogenesis.

I identified a group of genes that are refractory to Wispy (Figure 3.29, shown in red dots). This group includes 191 genes (10.8%) and 196 genes (17.6%) detected in mature oocytes and activated eggs, respectively (Figure 3.31). Notably, most of them encode ribosomal proteins (Figure 3.31). Consistently, these mRNA species belong to "group 8" whose poly(A) tails do not change in length during both late oogenesis and egg activation

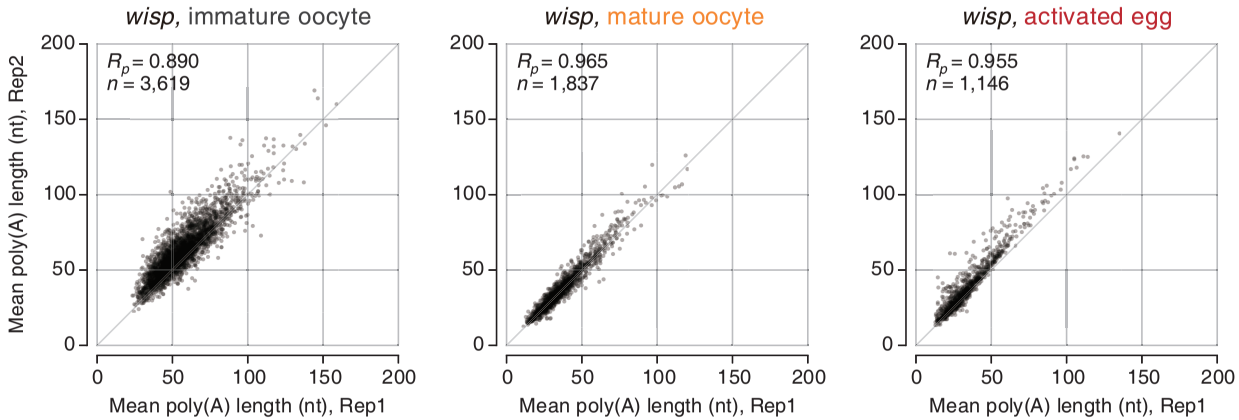

Figure 3.28 Reproducibility between two biological replicates of *wisp* mutant.

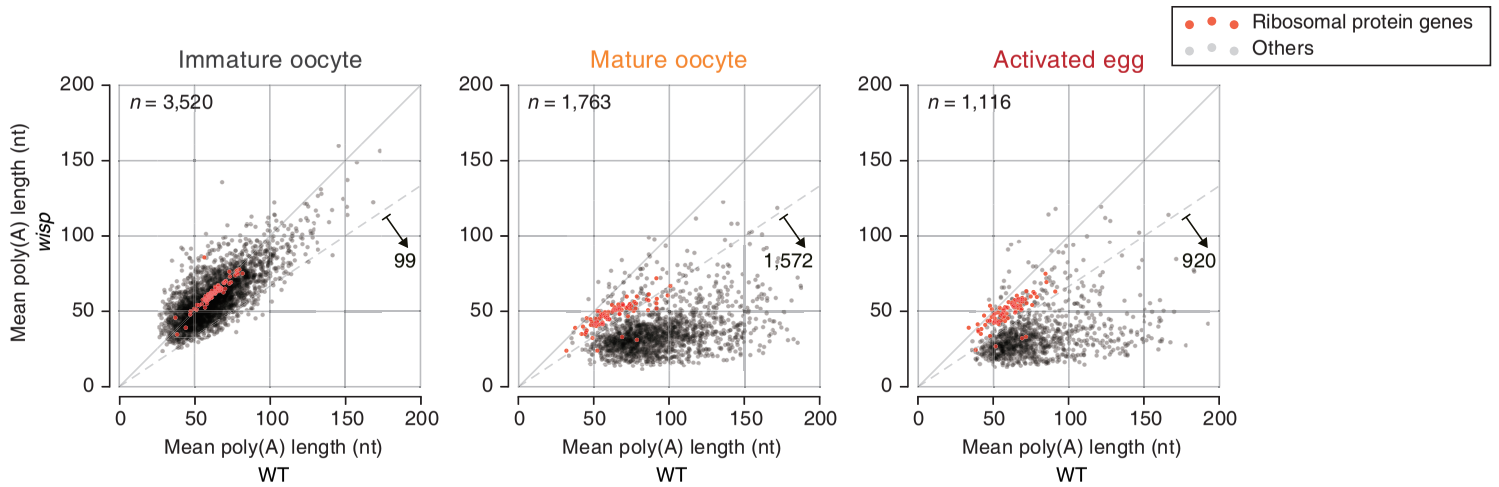

Figure 3.29 Comparison of poly(A) tail lengths between wild type and *wisp* mutant in each stage. The mean poly(A) tail lengths from two biological replicates are averaged (n=2). The median of mean poly(A) tail lengths of *wisp* mutants is 56 nt in immature oocytes, 34 nt in mature oocytes and 32 nt in activated eggs. Dashed line marks 1.5-fold reduction. Red dots represent ribosomal protein genes.

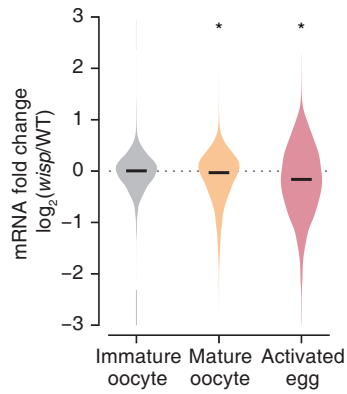

Figure 3.30 Violin plots showing the changes of mRNA abundance in *wisp* mutant at three different stages (*P $<2.2 \times 10^{-16}$, two-sided Kolmogorov-Smirnov test). Black line refers to the median.

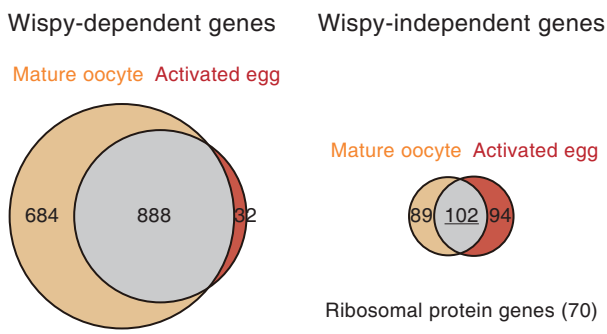

Figure 3.31 Wispy-dependent groups in mature oocytes and activated eggs are defined as in Figure 3.29 and are presented in Venn diagram (left). Gray region contains genes which have dependency on both stages. Orange and red color refer to stage-specific genes in mature oocytes and activated eggs, respectively. Genes independent of Wispy are depicted similarly in the Venn diagram on the right.

in wild type (Figures 3.24 and 3.27). These data suggest that the transcripts encoding ribosomal proteins may specifically escape from cytoplasmic polyadenylation.

Of note, it was previously reported that genes involved in mitochondrial function are independent of Wispy (Cui et al., 2013); however, I found that such genes displayed changes in poly(A) tail length in a Wispy-dependent manner (Figure 3.32, shown as green dots). The apparent discrepancy between the studies are likely because the previous approach relied on oligo(dT) column which captures mRNAs with long A-tail (>~40 nt) indiscriminately (Cui et al., 2013).

My analysis also revealed that, in the absence of wisp, poly(A) length continues to decrease instead of staying at the same length (Figure 3.33). The median length changed from 56 nt (at stage 9–10) to 34 nt (at stage 14) (Figure 3.33). This result implies that Wispy may be required not only for polyadenylation, but also for protection against deadenylation during late oogenesis.

3.2.4 Correlation between poly(A) tail length and translational efficiency

To understand the functional consequences of cytoplasmic polyadenylation, I compared poly(A) tail length with translational efficiency (TE). It was shown recently that poly(A) length correlates with TE in zebrafish and frog embryos before zygotic transcription, while there is no such correlation in somatic cells (Subtelny et al., 2014). It remains unknown whether invertebrate embryos have comparable regulatory mechanism at the genomic scale.

Terry Orr-Weaver and colleagues previously measured TE by ribosome profiling in mature oocytes and activated eggs (0–2 hr). To match the developmental stage, I generated poly(A) tail profile of the 0–2 hr activated eggs in addition to the 0–1 hr activated eggs (Figures 3.34 and 3.35)[10]. The comparison of poly(A) profile and ribosome profile showed a clear correlation between poly(A) tail length and TE in activated eggs (Figure 3.34, right panel, R_s=0.638). Thus, like in vertebrates, protein synthesis is mainly and globally dictated by poly(A) tail in early embryos of *Drosophila*. This result confirms earlier studies on

[10] Analyses in this section were done by Ahyeon Son.

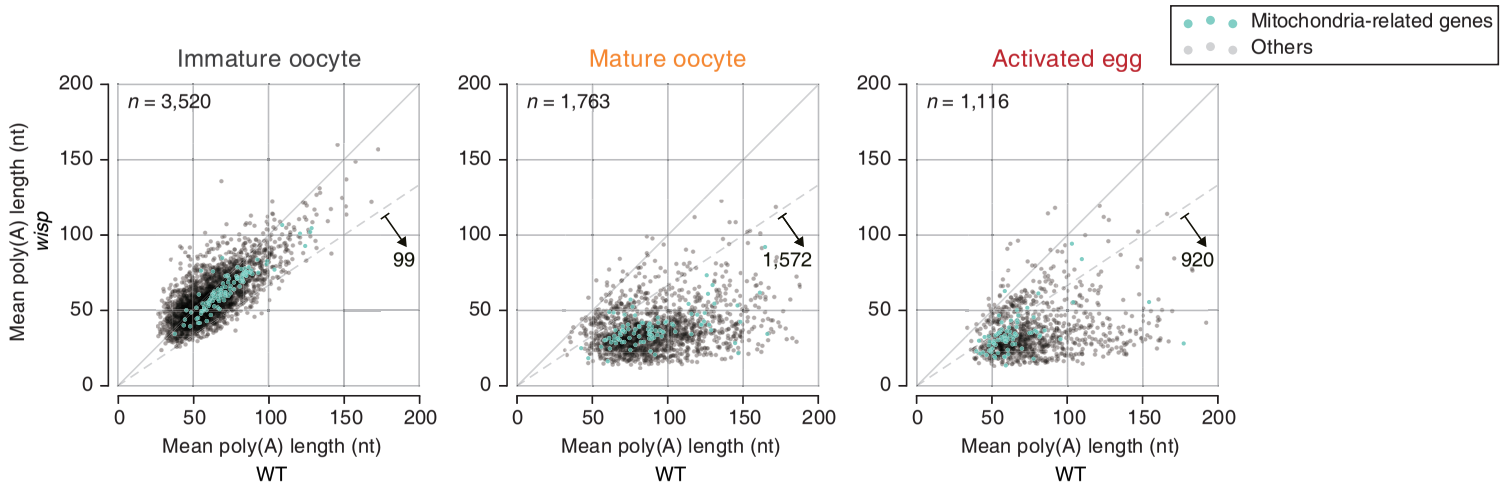

Figure 3.32 Comparison of poly(A) tail lengths between wild type and *wisp* mutant in each stage as in Figure 3.29. Dashed line marks 1.5-fold reduction. Turquoise dots indicate mitochondria-related genes.

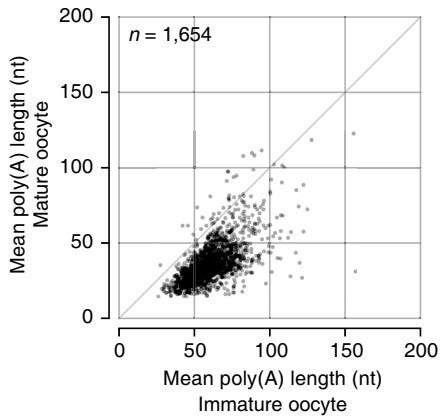

Figure 3.33 A scatter plot showing the changes of poly(A) tail length in *wisp* mutants upon late oogenesis.

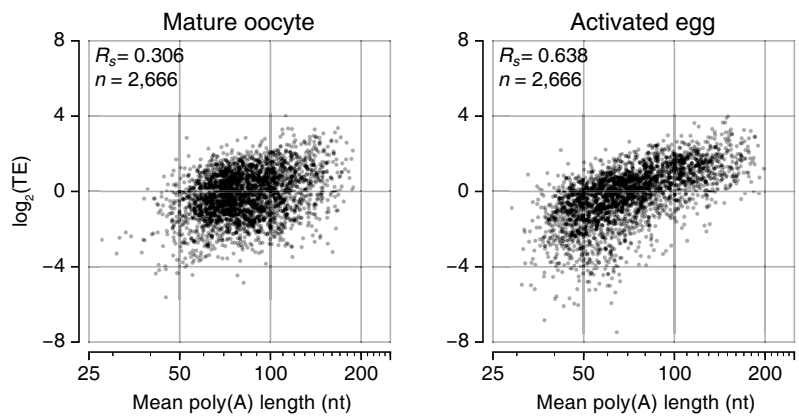

Figure 3.34 Comparison of poly(A) tail length with translational efficiency (TE) which was estimated by Kronja et al. (Kronja et al., 2014). TE is calculated by dividing ribosome density over RNA abundance from two biological replicates. The median of TE at each stage is adjusted to 0. R_s refers to Spearman correlation coefficient.

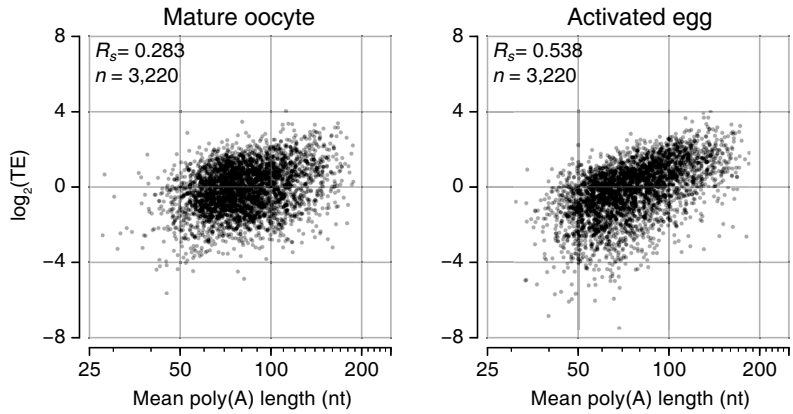

Figure 3.35 Poly(A) tail lengths of mature oocytes and activted eggs (0–1 hr) are compared to translational efficiency as in Figure 3.34.

individual genes (Benoit et al., 2008; Coll et al., 2010), and further suggests that animals have a highly conserved mechanism for the regulation of the earliest translation events.

A notable observation from this analysis is that the correlation is modest in mature oocytes (Figure 3.34, left panel, R_s=0.306). This was unexpected because the global poly(A) distribution does not change substantially during egg activation (Figure 3.17). Nevertheless, it is noteworthy that many individual genes are modulated in poly(A) tails during egg activation (Figure 3.19, right). The changes in poly(A) tail length during egg activation correlate well to the changes in TE (Figures 3.36 and 3.37). These results suggest that while global elongation occurs during late oogenesis, the additional modulation of poly(A) tail length during egg activation may be important for translational control. The polysome/-monosome ratio in activated eggs is 5 fold higher than that in mature oocytes, indicating that translation is globally up-regulated during egg activation (Kronja et al., 2014). Thus, in flies, polyadenylation and translational activation appear to be partly separated. Polyadenylation begins during late oogenesis while translational activation occurs later during egg activation.

I next compared TEs of different groups of transcripts that show distinct patterns of poly(A) tail length (Figures 3.24 and 3.38). Transcripts in groups 1, 2, and 3 whose poly(A) tails are continuously elongated showed dramatic increase of TE upon egg acti-

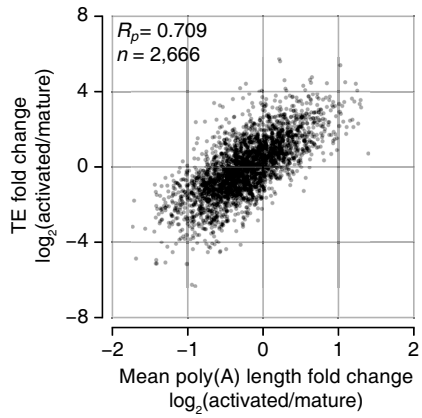

Figure 3.36 A scatter plot showing the correlation between mean poly(A) length changes and TE changes upon egg activation. R_p refers to Pearson correlation coefficient.

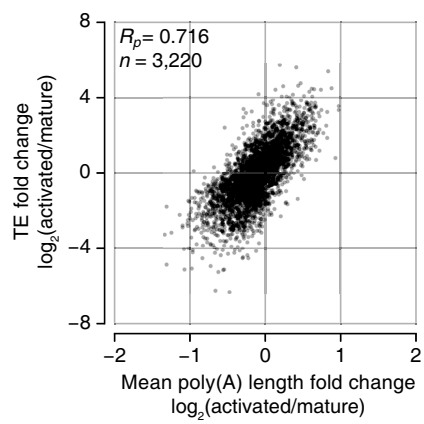

Figure 3.37 A scatter plot showing the correlation between mean poly(A) length changes (from mature oocytes to activated eggs [0–1 hr]) and TE changes as in Figure 3.36.

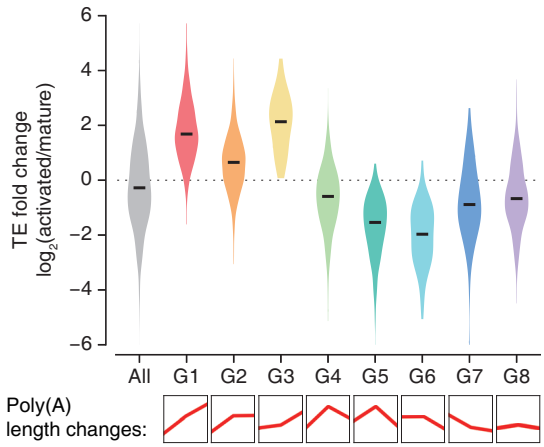

Figure 3.38 Violin plots showing the differences in TE changes between 8 groups which were defined in Figure 3.24. Poly(A) length changes of each group are simplified in the bottom panel. Black line represents the median.

vation (Figure 3.38). In contrast, genes in groups 5 and 6, which include many energy metabolism related genes, are translationally suppressed. Poly(A) tails continue to be modified during egg activation, presumably by concurrent polyadenylation and deadenylation. For instance, transcripts encoding vacuolar H^+ ATPase subunit, cytochrome C oxidase subunit, and some enzymes involved in metabolism are deadenylated during egg activation, and translationally suppressed. Transcripts in group 8 with little changes in poly(A) tail tend to be translated at constant rates. I obtained similar results when another index for translation rate was applied, the ribosome occupancy, which is the ratio of RNA associated with polysome over monosome (Figure 3.39). Taken together, my analyses demonstrate that the regulation of poly(A) tail shapes the translational landscape in early embryos.

3.3 Discussion

In conclusion, mTAIL-seq is a potent tool for investigating poly(A) tail. This method costs substantially less, takes less time than the original version (TAIL-seq), and can be applied to diverse species as it omits the affinity-based rRNA depletion step and it runs on

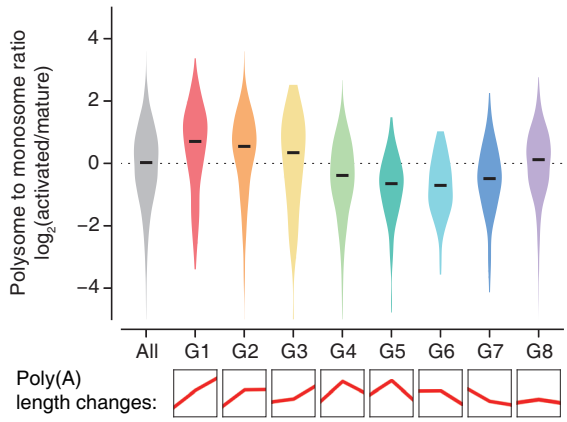

Figure 3.39 Violin plots showing the changes in ratio of polysome fractions (≥5 ribosomes) to monosome fractions (40S, 60S, and 80S) between activated eggs and mature oocytes. Polysome profiling and RNA-seq were adopted from Kronja et al. (Kronja et al., 2014). Each color indicates a corresponding group defined in Figure 3.24, and poly(A) length changes of each group are simplified in the bottom panel. Black line represents the median.

MiSeq. mTAIL-seq is improved markedly in sensitivity (by ~1000 fold) so that one can now analyze small amounts of biological samples (as little as ~33 ng of total RNA).

Applying mTAIL-seq, I here determine the accurate poly(A) tail length of maternal transcripts in *Drosophila* oocytes and eggs for the first time. Previous global analysis was performed by microarray combined with enrichment of long poly(A) tails (>40 nt) in wild type and *wisp* mutant (Cui et al., 2013), but was limited in resolution and accuracy. My current study using mTAIL-seq allows us to accurately document dynamic and temporal regulation of poly(A) tail length during oogenesis and egg activation. Specifically, I confirm that Wispy-deficient oocytes fail to induce global elongation of poly(A) tail during late oogenesis, indicating that lengthening of poly(A) tails at this stage is fully dependent on cytoplasmic polyadenylation. During egg activation, I further find a modest yet significant modulation of poly(A) tail length. These changes correlate strongly with the changes in translation efficiency, implying that poly(A) tail length may function as a critical factor for translation at this developmental stage.

Based on stage-specific changes of poly(A) tail length, maternal transcripts can be

classified into 8 groups. Notably, I identified groups 1, 2, and 3, which include transcripts that continue to be polyadenylated through two consecutive stages and are translated efficiently in activated eggs. Known targets of cytoplasmic polyadenylation that are associated with cell cycle (*cycB* and *cycA*) and embryonic patterning (*bcd* and *Tl*) are enriched in groups 1 and 2 (Table 3.1) (Benoit et al., 2005, 2008; Salles et al., 1994; Vardy & Orr-Weaver, 2007; Vardy et al., 2009). In addition, many genes related to RNA metabolism belong to these groups. Genes in the small RNA pathway such as *AGO1*, *AGO2*, *aub*, and *gw* (a homolog of *GW182*) are found in group 1. Genes associated with RNA degradation and translational repression (such as smg, pum, and brat) and the components of deadenylase complex (*twin* (a homolog of *CCR4*), *Not1*, *PAN2*, and *CG11486* (*PAN3*)) also belong to groups 1 or 2. Thus, many key factors involved in mRNA destabilization are maternally inherited and are induced post-transcriptionally by cytoplasmic polyadenylation during late oogenesis and egg activation.

Using *wisp* mutant, I confirmed that global poly(A) lengthening is dependent on Wispy. Furthermore, in *wisp* mutants, I found that poly(A) tail lengths are not fixed, but get shortened during late oogenesis, suggesting that Wispy may protect poly(A) tails from deadenylation. In *Xenopus* oocytes and mouse neurons, the CPEB-associated complex contains a deadenylase, PARN, as well as poly(A) polymerase, Gld2, which balance out the poly(A) tail lengths in the absence of cellular signals (Kim & Richter, 2006; Udagawa et al., 2012). Upon induction of CPEB phosphorylation by meiotic maturation or synaptic stimulation, deadenylase is released from the complex, leading to poly(A) tail elongation. Likewise, the dynamic balance between Wispy and deadenylase may determine poly(A) tail length during *Drosophila* oogenesis and in egg activation. It is interesting that although there is no homolog of PARN in flies, the regulatory principle that polyadenylation and deadenylation work together to shape poly(A) tail appears to be conserved. In future studies, it will be necessary to identify a deadenylase/exonuclease that is responsible for trimming poly(A) tails in *Drosophila* oocytes and embryos.

The data show that the dynamic adjustment of poly(A) tail length shapes the translatome in early embryo. In contrast, mature oocytes do not show a strong correlation even though the global poly(A) tail lengths are similar in those two stages. Then, what makes activated eggs so special? One possible hypothesis is the dispersion of repressive complexes

such as P bodies upon egg activation. Recently, super-resolution imaging unveiled that mature oocytes contain electron-dense bodies which are composed of various mRNPs including translational repressors such as Me31B and CUP (Weil et al., 2012). Egg activation, also known as oocyte-to-embryo transition, disassembles the complex and facilitates remodelling of specialized ribonucleoprotein particles, which may trigger subsequent translational activation (Krauchunas et al., 2012; Kronja et al., 2014; Weil et al., 2012). Additionally, PAN GU (PNG) kinase complex which relieves PUM dependent translational repression of *cycA*, *cycB*, and *smg* at egg activation (Kronja et al., 2014; Tadros et al., 2007; Vardy & Orr-Weaver, 2007; Vardy et al., 2009), may has a role in the global translational activation. It remains to be investigated how the poly(A) tail length is fine-tuned and is mechanistically coupled to translation at this interesting developmental stage. Additional studies using various tissues such as neurons and other species will help to reveal the mechanisms as well as the conserved features in the regulation of poly(A) tails. By virtue of high sensitivity, low cost, technical robustness, and broad accessibility, mTAIL-seq will be a potent tool to improve our understanding of mRNA tailing and translational control.

3.4 Methods and Materials

Construction of mTAIL-seq library

Total RNAs were extracted from HeLa cells or *Drosophila* samples by TRIzol reagent (Invitrogen, 15596-018). Total RNA (~1–5 ug) was ligated to 3′ hairpin adaptor using T4 RNA ligase 2 (NEB, M0239) for overnight. 3′ ligated RNA was partially digested by RNase T1 (Ambion, AM2283) and subject to streptavidin beads (Invitrogen, 11206D). 5′ phosphorylation by PNK reaction (Takara, 2021B) and endonucleolytic cleavage by APE1 reaction (NEB, M0282) were performed on beads. Subsequently, RNA was eluted by 2X RNA loading dye and gel purified by 6% Urea-PAGE gel in the range of 300–750 nucleotides. The purified RNAs were ligated to 5′ adaptor, subjected to reverse-transcription (Invitrogen, 18080-085) and amplified by PCR using Phusion DNA polymerase (Thermo, F-530L). PCR products were purified by AMPure XP beads (Beckman, A63881). The library was sequenced on Illumina MiSeq (51×251 paired end run) with 50% of the PhiX control library (Illumina, FC-

110-3001) and 10% of the spike-in mixture. The spike-ins were prepared and mixed as previously described (Chang et al., 2014b). The 3′ hairpin adaptor sequence for mTAIL-seq is /5Phos/CTGACATGNNNNNNNNNNNNTGGAATTCTCGGGTGCCAAGGC/iSpC3/-/idSp//idSp//iBiodT//iBiodT/GGCACCCGAGAATT/iSp18/CATGTCAGTTTTTTTT/3-InvdT/. N refers to random sequence. /5Phos/ 5′ phosphorylation; /iSpC3/ internal C3 phosphoramidite; /idSp/ internal 1′,2′-Dideoxyribose; /iBioT/ internal biotinylated deoxythymine; /iSp18/ internal 18-atom hexa-ethyleneglycol spacer; /3InvdT/ 3′ inverted deoxythynime.

mTAIL-seq analysis

The detailed procedure of poly(A) length measurement is identical to that of TAIL-seq (Chang et al., 2014b) except for variations in usage of 3′ hairpin adaptor. Genes with ≥50 poly(A) tags were analyzed. A geometric mean of poly(A) lengths was used as a representative value and referred as 'Mean poly(A) length' because a distribution of intragenic poly(A) lengths is a lognormal-like distribution. For replicates, the average of geometric mean lengths was used in analyses.

Drosophila Stocks and Oocyte/Egg Collection

Fly lines of w^{1118} and $wisp^{KG5287}$ were obtained from Bloomington stock center and tud^{1} was from Kyoto stock center. w^{1118} was used as wild type control. $wisp^{KG5287}$ was previously described as a null allele of *wisp* (Benoit et al., 2008). Immature (stage 9–10) and mature (stage 14) egg chambers were collected by hand dissection in Grace′s Unsupplemented Insect Media (Gibco, 11595-030) from 3 or 4 day old female flies. Unfertilized activated eggs were produced from w^{1118} virgin females mated to sterile males (son of tud^{1} mothers) (Boswell & Mahowald, 1985). Fly eggs and embryos were collected on grape juice plates for the designated time frame at 25°C.

RNA-seq analysis

Total RNA was extracted with TRIzol (Invitrogen, 15596-018), and the quality was checked by Agilent 2100 Bioanalyzer. rRNA was depleted from total RNA using Ribo-Zero kit (Epicentre, MRZH11124). RNA-seq libraries were constructed by Macrogen Inc. using Illumina TruSeq RNA sample preparation kit v2. Sequencing reads derived from cDNA libraries described above were processed by using FASTX-Toolkit (http://hannonlab.cshl.edu/fastx_toolkit). First, the 3′ adaptor sequence was removed, and trimmed reads were filtered by Phred quality score (fastq_quality_filter -Q 33 -p 30 -q 90). The sequence reads were aligned to ERCC RNA spike-ins using STAR version 2.4.2a (Dobin et al., 2013) with options (–alignIntronMin 99999 –alignEndsType EndToEnd). Reads that do not match to any spike-in were aligned to UCSC (the University of California, Santa Cruz) dm6 genome assembly using RSEM version 1.2.25 with STAR (Dobin et al., 2013; Li & Dewey, 2011) and splicing junction annotations generated from the NCBI RefSeq (downloaded from UCSC Genome Browser on Dec 12, 2014). The reduced RefSeq transcript set for non-overlapping representation was prepared as previously described (Chang et al., 2014b). The reads mapped to ERCC spike-ins were counted by using htseq-count (Anders et al., 2015). Then, the expected counts from RSEM (Li & Dewey, 2011) were normalized with spike-ins by using RUVg (k=1) in R package RUVSeq (Risso et al., 2014). For analysis, transcripts with insufficient reads (<100 normalized reads in any library) were removed.

Classification and functional categorization of genes

Classification of genes was based on the difference of poly(A) tail length between consecutive developmental stages. First, genes with less than 20 nt difference across three stages were regarded as an unchanged group (group 8). Then, 10 nt difference between adjacent two stages was set as a criteria to discriminate changes of poly(A) tail length: elongated or shortened (≥10 nt difference), or unchanged (<10 nt difference). A group showing elongation of poly(A) tail in late oogenesis and shortening in egg activation was further subdivided into two groups depending on the the value of sgn (elongated length - shortened length). Additionally, 3 groups with shortened poly(A) tails in late oogenesis were merged since each group had the small number of members. The gene list of each

group is shown in Table 3.1. Functional annotation was done for each gene group using DAVID bioinformatics tools (Huang da et al., 2009). For the background population, members of all groups (3,664 genes) were used, and gene ontology (GO) terms with FDR <0.1 were selected.

Ribosome profiling analysis

RPF (ribosome profiling) and RNA-seq data were downloaded from publicly available database (GSE52799) (Kronja et al., 2014). Sequencing reads were trimmed into 27 nt-long sequences, then were filtered with Phred quality score. RPF and RNA-seq tags were counted and normalized by using RSEM (Li & Dewey, 2011). To minimize a tendency from ribosome accumulating near the start codon, reads with 5′ ends mapping within the first 50 nucleotides of each ORF (open reading frame) were disregarded (Ingolia et al., 2009; Subtelny et al., 2014). Translational efficiency (TE) was calculated by the TPM ratio of RPF to RNA-seq, then the median of $\log_2$(TE) was adjusted to zero. Genes with ≥10 TPM (transcripts per million) in both RPF and RNA-seq libraries were included in the analysis.

High-resolution poly(A) tail assay (Hire-PAT)

To validate the poly(A) tail length measured by mTAIL-seq, Hire-PAT was carried out as previously described (Chang et al., 2014b). Primers used in Hire-PAT are *cycB* forward 5′-GCTGGCCGAACACATCGGCG-3′; *Tl* forward 5′-CTATGTGTATATCGTCTAAGC-3′; *osk* forward 5′-GTAGCACAGTGTAGAATTCTG-3′; *sop* forward 5′-GGATTGCTACACC-TCGGCCCGT-3′.

Polysome profiling analysis

As in the ribosome profiling analysis, deposited libraries were used for analysis (GSE52799) (Kronja et al., 2014). Sequencing reads were trimmed into 27 nt-long sequences, then filtered with Phred quality score. The *Drosophila* dm6 genome and the Saccharomyces

cerevisiae genome (Ensembl assembly R64-1-1 release 82) were combined, and gene annotation file was made by merging reduced fly RefSeq and yeast GTF file as previously described (Kronja et al., 2014). Sequencing reads were mapped to the merged genome using RSEM (Li & Dewey, 2011). The top 20 highly expressed yeast genes which were sorted by the highest abundance in the RNP fraction were regarded as an exogenous control group, and fly transcript levels were normalized with RUVg (k=1, [Risso et al., 2014]). To reduce noises, transcripts with <100 normalized reads in fraction which corresponds to ≥10 ribosomes were excluded. For each fly transcript, a percentage in each fraction was calculated by dividing normalized reads by total reads. Percentage recruitment to polysomes (≥5 ribosomes) and monosomes (40S, 60S, and 80S) were calculated and used for comparing a degree of translational activation.

Gene Name	Group Number	Gene Name	Group Number	Gene Name	Group Number	Gene Name	Group Number	Gene Name	Group Number
RpII215	1	borr	1	Cp190	1	CG1463	1	pre-mod(mdg4)-T	1
Inx2	1	CG8545	1	CG3847	1	CG14194	1	Pax	1
crok	1	pic	1	CG3918	1	x16	1	MTA1-like	1
CG16972	1	Hrb98DE	1	CG14438	1	Wee1	1	Ext2	1
IntS6	1	Pect	1	lack	1	cdm	1	bmm	1
CG31729	1	Mst85C	1	CG4615	1	CG12200	1	aub	1
CG31650	1	pea	1	Dek	1	arm	1	smg	1
raptor	1	CycE	1	Ref1	1	Psn	1	CG6650	1
pcx	1	CG2310	1	Spred	1	Hel25E	1	CG9425	1
l(2)34Fd	1	tej	1	Rcd1	1	Taf2	1	MEP-1	1
EloA	1	Ncoa6	1	CG2926	1	cic	1	Non2	1
Brf	1	wap	1	Nnp-1	1	Stat92E	1	CG3797	1
twin	1	CG8617	1	Mtor	1	CG8108	1	CG10600	1
BRWD3	1	CycD	1	CG6422	1	CG1812	1	CG8389	1
CG31195	1	for	1	Topors	1	CG6961	1	Atg18a	1
CG42240	1	nonA	1	CG1888	1	02-Sep	1	Poc1	1
CG1677	1	Trn	1	bcd	1	Dab	1	CG10139	1
CG10492	1	CG14722	1	Alh	1	CG3876	1	kis	1
crb	1	CG8949	1	Sap130	1	CG10880	1	velo	1
Rab30	1	CG4768	1	CG1603	1	Chd1	1	Ras85D	1
lilli	1	Srp54	1	CG1344	1	insv	1	CG32699	1
SF2	1	Stim	1	dalao	1	fax	1	CG2023	1
Src42A	1	ebi	1	CG12121	1	aph-1	1	Patronin	1
su(Hw)	1	HP1b	1	tgo	1	Spt5	1	RhoGAP5A	1
pyd	1	pod1	1	l(1)G0289	1	CG3542	1	nst	1
CG2698	1	wds	1	Hmr	1	Rox8	1	su(s)	1
Bap170	1	fray	1	D1	1	Rpb7	1	l(3)72Ab	1
Rm62	1	CG6398	1	Trf4-2	1	CycB3	1	CG6983	1
geminin	1	krimp	1	pum	1	CG3744	1	CG33095	1
dos	1	CG6962	1	Tl	1	MED15	1	Dp1	1
CG4119	1	CG13192	1	Liprin-beta	1	fu2	1	CG7728	1
CG4165	1	ix	1	cno	1	Fas1	1	CG33695	1
CG12081	1	fu	1	mod	1	Acer	1	svr	1
U2af38	1	dome	1	CG32425	1	Acn	1	eIF4AIII	1
Mon1	1	CycA	1	Hip14	1	CG5789	1	CycB	1
Tbc1d15-17	1	CG11123	1	l(2)35Df	1	Set2	1	CG11266	1
dco	1	mbt	1	Pep	1	osa	1	Mio	1
CG32521	1	Gug	1	CG6951	1	Tpr2	1	kdn	1
sip3	1	CG1737	1	Mgat1	1	CG9941	1	thr	1
RNaseX25	1	Src64B	1	MESR6	1	CG5728	1	CG32732	1
slam	1	CG30499	1	CG1523	1	B4	1	CG4101	1
DLP	1	dah	1	pygo	1	GC1	1	CG14478	1
e(y)3	1	Kdm4A	1	msk	1	CG5787	1	CG12207	1
NAA20	1	Bap60	1	lolal	1	mor	1	CG8379	1
l(2)k09022	1	LIMK1	1	Cbp80	1	CG12608	1	CG3662	1
HP4	1	CG14749	1	CG1815	1	CG5854	1	Ptp4E	1
CG3038	1	CG6498	1	disp	1	CG7872	1	pzg	1
CG6013	1	dsh	1	Vps26	1	CG8944	1	N	1
Neos	1	Pmm45A	1	CG11563	1	Nup98-96	1	hang	1
CG43867	1	dx	1	RAF2	1	TfIIB	1	Map60	1
CG4364	1	AGO1	1	brm	1	CG10375	1	CG6479	1
ago	1	Spx	1	Nopp140	1	pim	1	Gcn5	1
wapl	1	mof	1	CG4281	1	His4r	1	Chd64	1
DnaJ-1	1	Pal1	1	AGO2	1	CG5004	1	CG14650	1
CG2924	1	CG7530	1	Ptp61F	1	CG8289	1	MESR4	1
CG2186	1	Sce	1	CG6330	1	Rsf1	1	Patr-1	1
BTBD9	1	CG30020	1	CG32479	1	put	1	CG11811	1
CG12299	1	Tango2	1	CG5447	1	Su(var)3-7	1	ph-d	1
CG2938	1	CG2691	1	CG13900	1	CG8173	1	CG17931	1
CG4751	1	CG11164	1	Spt6	1	CG6506	1	CG11970	1
ZnT63C	1	Galphai	1	CG16721	1	CG6179	1	cg	1
Ced-12	1	fzy	1	CG31523	1	CG17829	1	CG3638	1
01-Sep	1	ash1	1	CdGAPr	1	r-l	1	CG45050	1
His2Av	1	CG8311	1	CG42726	1	GalNAc-T2	1	Rs1	1
ldgf4	1	aux	1	MBD-like	1	fbl	1	Syx6	1

hyd	1	Tango10	1	CG7686	2	ric8a	2	CG18004	2
kibra	1	Cul1	1	tamo	2	CG31908	2	CG6420	2
Cdc6	1	Cpr	1	CG18749	2	emb	2	mod(mdg4)	2
Jarid2	1	CG42336	1	Sin3A	2	ced-6	2	CG5746	2
SelD	1	CG6701	1	lin	2	pen	2	Pi3K68D	2
CG34159	1	Tctp	1	mei-S332	2	cactin	2	Arpc2	2
Btk29A	1	CG9849	1	CG1307	2	Cbs	2	dgt1	2
Camta	1	rump	1	bip2	2	CG1637	2	Tak1	2
CG9776	1	nct	1	CG32095	2	Taf8	2	dsd	2
Nup153	1	CG3925	1	CG10903	2	Hlc	2	zf30C	2
Cbl	1	CG30344	1	CG11007	2	Taf11	2	CG2224	2
Fit1	1	MAPk-Ak2	1	CG14463	2	Trip1	2	Yeti	2
CG4266	1	nej	1	CG5210	2	CG10555	2	vtd	2
CG7737	1	CG30122	1	CG2126	2	Hsc70-5	2	CycG	2
CG10413	1	CG6406	1	Klp98A	2	U2af50	2	Zip102B	2
DUBAI	1	sbb	1	Hdac3	2	14-3-3zeta	2	CG11873	2
CG1311	1	CG5482	1	CG7564	2	CG9107	2	ghi	2
Rpd3	1	cin	1	CG1024	2	Lac	2	CG3021	2
CG7133	1	Sema-1b	1	Ice	2	wdn	2	spas	2
meigo	1	lid	1	nero	2	MED14	2	Invadolysin	2
CG31731	1	CdsA	1	Sry-delta	2	CG31643	2	Aps	2
barr	1	grp	1	CG10866	2	Taf5	2	Atu	2
CG11523	1	Not1	1	CG10732	2	Incenp	2	RpII15	2
CG10590	1	l(1)G0193	1	Klp67A	2	Tsp39D	2	alt	2
CG31705	1	whd	1	eIF3-S8	2	GIIIspla2	2	blp	2
scny	1	ref(2)P	1	CG31550	2	Psa	2	Rab8	2
Abl	1	CG8004	1	Mcr	2	CG1636	2	dnk	2
Psc	1	D19B	1	pen-2	2	CG43736	2	nes	2
PEK	1	Ubc-E2H	1	ptip	2	CG15435	2	CG6145	2
Plod	1	RhoBTB	1	Arf102F	2	Su(var)2-10	2	NAT1	2
Plc21C	1	CG15111	1	chb	2	Phax	2	Atpalpha	2
EDTP	1	CG4049	1	CG14562	2	Fpps	2	pre-mod(mdg4)-K	2
gro	1	CG17680	1	Ada2b	2	Ubqn	2	pit	2
ens	1	tub	1	ssh	2	csul	2	c12.1	2
pck	1	CG33116	1	bon	2	Dlc90F	2	CG8841	2
Rif1	1	Dp	1	mars	2	CG9940	2	Taf12	2
trr	1	pUf68	1	asun	2	crl	2	mago	2
CG5104	1	Gadd34	1	CG42724	2	CG10188	2	Oda	2
gw	1	wech	1	Indy	2	dwg	2	Adk2	2
Doa	1	Gk	1	TAF1B	2	d4	2	sina	2
CG9304	1	CG14764	1	Cbp20	2	Parg	2	CG11444	2
Amun	1	l(1)G0232	1	H	2	CG8915	2	CG31694	2
prod	1	CG5199	1	Opa1	2	CG5445	2	Tbp	2
Mi-2	1	CG5033	1	CG32147	2	dbe	2	spn-E	2
Pp4-19C	1	M1BP	1	CG9393	2	bin3	2	gek	2
sax	1	pdgy	1	alpha-Man-II	2	Rrp45	2	Prp19	2
dikar	1	Bre1	1	Hph	2	Tsc1	2	nmd	2
scra	1	Magi	1	CG12025	2	CG4949	2	CG5708	2
DAAM	1	CG42797	1	CstF-50	2	CG6712	2	Hrb87F	2
Cdk9	1	CG3313	2	CG4300	2	Chrac-16	2	CG32276	2
CG17514	1	L	2	CG9821	2	Traf6	2	CG31961	2
CG7611	1	TMS1	2	eIF-3p66	2	sws	2	CG9062	2
Chi	1	l(2)06496	2	TfIIA-S	2	KdelR	2	aur	2
Bgb	1	RpII140	2	Chro	2	crn	2	Pof	2
CG8420	1	l(3)05822	2	CG7324	2	fz4	2	Eap	2
MED21	1	gwl	2	pita	2	Ggamma1	2	Cypl	2
Cyt-c-p	1	Taspase1	2	Su(Tpl)	2	pnut	2	ics	2
bora	1	RYBP	2	CG11753	2	Pex19	2	CG16989	2
CG11474	1	ClC-c	2	Bin1	2	CG1622	2	CG12773	2
CG3732	1	CG9945	2	Nxf3	2	xmas-2	2	Sse	2
CG9399	1	CG6597	2	Mcm7	2	tth	2	pst	2
SNF4Agamma	1	CG1542	2	jumu	2	Klp10A	2	lark	2
Atg8a	1	DNApol-iota	2	Rbm13	2	Clp	2	inc	2
nito	1	l(3)07882	2	pll	2	CG2371	2	Srp54k	2
Tango11	1	CycT	2	Spp	2	CG13096	2	CG6565	2
CG4747	1	fwd	2	dock	2	RpI1	2	Ubi-p63E	2
qkr58E-2	1	Nup214	2	TfIIA-L	2	CG11486	2	spoon	2

pfk	2	Tab2	2	CG14100	2	CG8602	2	CG1951	2
CG32409	2	mahj	2	CG9132	2	CG10103	2	Su(fu)	2
Rab6	2	PAN2	2	CG9300	2	CG13298	2	CG15817	2
CG8298	2	MrgBP	2	Fur2	2	bc10	2	Hrs	2
Ent1	2	CG4338	2	U3-55K	2	MED27	2	rb	2
BCL7-like	2	Pbp49	2	eIF5	2	CHMP2B	2	Rbf	2
CG13605	2	CG31301	2	CG11577	2	brat	2	dbo	2
dup	2	CG6171	2	CG8481	2	coro	2	skd	2
CG6758	2	l(2)dtl	2	CG6843	2	Tsp97E	2	krz	2
CG8273	2	Ccm3	2	Gbeta13F	2	phtf	2	CG15514	2
Moca-cyp	2	CG11107	2	phl	2	Tim9a	2	CG11504	2
Snp	2	CG17002	2	CG7441	2	BicD	2	scat	2
PMCA	2	RpS15Ab	2	Nedd4	2	CG42258	2	CG7946	2
CoRest	2	CG12391	2	CG5541	2	Tango4	2	Atox1	2
Med	2	btz	2	CG42271	2	polybromo	2	Nop56	2
Art1	2	Mob4	2	CG7603	2	swm	2	CG14805	2
DMAP1	2	CG8388	2	Papst2	2	CG7006	2	CG14806	2
ZnT86D	2	CG8370	2	Fit2	2	feo	2	CG2260	2
CG9143	2	Axn	2	CG11399	2	dia	2	CG10425	2
CG42678	2	CG8366	2	Dyb	2	MED7	2	CG11807	2
CG11906	2	mud	2	CG3634	2	cad	2	CG2059	2
CG15087	2	CG30467	2	CG3680	2	hb	2	Nf-YC	2
Sec6	2	GalNAc-T1	2	CG17163	2	l(2)09851	2	wuho	2
sub	2	CG8155	2	Ald	2	Eb1	2	CG10543	2
Ns2	2	Ciao1	2	CG8009	2	Arfrp1	2	jigr1	2
CG9646	2	CG3281	2	Vps24	2	mim	2	CG3499	2
pre-mod(mdg4)-U	2	Sgt1	2	CG11586	2	CG30497	2	CG3149	2
NiPp1	2	Arc2	2	Alg-2	2	CG7246	2	Pdk1	2
CG7747	2	Hrb27C	2	Rcd5	2	Caf1-180	2	CG3309	2
p53	2	milt	2	Hpr1	2	Es2	2	CG3527	2
east	2	Cka	2	YT521-B	2	CG2202	2	Snr1	2
CG8199	2	tum	2	CG11505	2	Dis3	2	CG11436	2
B52	2	CG5850	2	gry	2	Rbp1	2	CG6428	2
cue	2	fand	2	slmo	2	TfIIS	2	CG3071	2
CG2199	2	spt4	2	CG2162	2	Ssu72	2	CG3587	2
vlc	2	larp	2	CG7504	2	CG3887	2	drpr	2
CG8726	2	lok	2	CG9004	2	CG14215	2	mip130	2
Rabex-5	2	CG17018	2	CG1317	2	CG15237	2	eIF3-S10	2
CG13907	2	Lam	2	CG9666	2	CG11030	2	CG11526	2
rgr	2	CG11148	2	ecd	2	homer	2	PSR	2
Cdc5	2	Pex10	2	CG9018	2	HP1c	2	CG12788	2
CG32344	2	metl	2	CG1227	2	CG7288	2	cold	2
MCPH1	2	elgi	2	CG3223	2	CG7101	2	CG7357	2
CG9773	2	CG7519	2	grau	2	Ublcp1	2	Unc-76	2
CG13876	2	CG13484	2	CG10435	2	Rassf	2	CG31457	2
Eps-15	2	MED1	2	CG7967	2	Arp8	2	CG9302	2
CG11982	2	CG11583	2	ovo	2	IntS2	2	CG2875	2
CG11984	2	Pdxk	2	ash2	2	CG5800	2	Arp5	2
CG10809	2	Abp1	2	woc	2	CalpC	2	CG16812	2
beag	2	CG7407	2	CG4360	2	CG10217	2	TFAM	2
Akap200	2	CG4069	2	Aats-leu	2	lp259	2	Tom40	2
lbf2	2	Ubp64E	2	Lis-1	2	CG5991	2	fs(1)h	2
CG5543	2	CG7130	2	Nf-YA	2	MAN1	2	ncm	2
l(2)k09913	2	Rich	2	CG9791	2	mRNA-cap	2	CG6583	2
RnpS1	2	CG17486	2	CG4495	2	CG16865	2	CG6766	2
CG8435	2	conu	2	RpL7-like	2	Rpb5	2	CG4538	2
spn-A	2	Ube3a	2	Cont	2	E(Pc)	2	Csl4	2
Got1	2	AGO3	2	CG1074	2	tou	2	CG6230	2
CG9925	2	CG11367	2	CG7185	2	CG2129	2	PPP4R2r	2
CG12909	2	CG7839	2	CG12128	2	mino	2	CG7705	2
Nup93-2	2	CG6321	2	lig	2	CG11417	2	Non3	2
Cam	2	CG7369	2	CG14641	2	mus81	2	CG6015	2
CG6654	2	CG34133	2	CG7197	2	CG11307	2	Dpy-30L1	2
CG8026	2	mon2	2	Fip1	2	MED22	2	CG7456	2
Prp38	2	Yippee	2	CG8042	2	Hmt4-20	2	Bx42	2
Mys45A	2	CG10584	2	Sec63	2	CG18273	2	bif	2
CG8229	2	cp309	2	CG11999	2	CG7927	2	G9a	2

CG15160	2	caz	3	CG12499	4	SpdS	4	CG34200	4
CG15908	2	Mms19	3	CG5028	4	Usp7	4	CG4042	4
Pitslre	2	CG17068	3	CG2091	4	CG8892	4	Uba2	4
CG10565	2	spin	3	asl	4	CG12721	4	CG1792	4
sced	2	Nab2	3	CG34261	4	CG14200	4	TER94	4
jing	2	CG1275	3	CG14232	4	eca	4	NitFhit	4
Tbce	2	CG18259	3	CG1785	4	CG11593	4	eco	4
Abi	2	par-6	3	CG6927	4	CG6454	4	chic	4
CG10465	2	CG8552	3	Zpr1	4	CG42389	4	CG32442	4
CG9246	2	CTPsyn	3	CG1309	4	kra	4	fal	4
CG7713	2	CG12006	3	Lst8	4	CG6937	4	WASp	4
Rad23	2	fifl	3	CG3651	4	CG3558	4	Ubc12	4
CG9253	2	tank	3	Aats-val	4	CG14985	4	CG34394	4
CG31357	2	Arp3	3	lsn	4	Nup133	4	Rok	4
CG5516	2	CG14182	3	RIOK2	4	CG5776	4	Cdc27	4
Ns4	2	CG5934	3	CG4769	4	CG4332	4	Gp93	4
CG2614	2	lace	3	CG3446	4	CG12163	4	CG18586	4
mask	2	ifc	3	CG14618	4	srl	4	CDC45L	4
CG17556	2	fws	3	Rpt6	4	Rac1	4	CG11418	4
Nup358	2	Sam-S	3	Cchl	4	CG8878	4	CG10075	4
mib2	2	pr	3	l(2)k05819	4	CG8032	4	CG7970	4
Tango6	2	Sfmbt	3	Marf	4	Gdh	4	Sgf11	4
CG10428	2	mael	3	Pcl	4	Aats-glupro	4	CG3630	4
cdi	2	CG8405	3	Ate1	4	Rab7	4	CG13917	4
CG5343	2	CG9727	3	CG6439	4	KrT95D	4	CG12091	4
koko	2	CG4670	3	CG2976	4	Syx18	4	Seipin	4
Smr	2	Csp	3	CG14442	4	asp	4	CG2694	4
lwr	2	kuk	3	CG30389	4	Mkk4	4	Snm1	4
CG2807	2	fwe	3	CG31549	4	CG6638	4	RnrS	4
Atg4a	2	ssx	3	olf186-F	4	CSN6	4	CG5484	4
Atx2	2	Tor	3	CG3040	4	Ets97D	4	CG7601	4
Elp3	2	Nc73EF	3	CG17841	4	Lk6	4	Klp3A	4
CG5466	2	tkv	3	CG8300	4	CG10979	4	mtrm	4
Art3	2	CG13185	3	CG1109	4	Sap-r	4	san	4
AdSS	2	CG7510	3	CG34409	4	CG10171	4	HipHop	4
ATP7	2	retn	3	alien	4	atms	4	Larp7	4
CG10874	2	Saf-B	3	CG9323	4	MED20	4	Smn	4
Sec15	2	CG32767	3	CG15011	4	CG11077	4	CG5098	4
Ice2	2	tlk	3	SMC1	4	CG11576	4	beta'COP	4
CG5862	2	Pdk	3	CG5446	4	Xbp1	4	lds	4
Bacc	2	Aef1	3	Tpc1	4	Glg1	4	Zn72D	4
Cwc25	2	smid	3	CG9215	4	CG1943	4	CG30118	4
Elba2	2	ttk	3	CG9281	4	T-cp1	4	Fer1HCH	4
Hexim	2	CG8176	3	rictor	4	CG6455	4	CG9238	4
Saf6	2	CG5537	3	CG14977	4	glec	4	Hsc70Cb	4
Atxn7	2	Spn	3	Ndc1	4	CSN3	4	RpII18	4
CG15439	2	CG9005	3	Droj2	4	Rpn10	4	Catsup	4
Nxt1	2	CG9086	3	CG5510	4	CycH	4	CG7911	4
Wdr82	2	rno	3	Cand1	4	CG32066	4	Pp1-87B	4
CG3679	2	Ptpmeg	3	CG5045	4	TfIIFalpha	4	Syx13	4
CG3008	2	upSET	3	CG5384	4	mRpS9	4	CG8209	4
CG7818	2	glo	3	snRNP-U1-70K	4	dmt	4	CG33303	4
RhoGAPp190	2	tay	3	CG34401	4	CG15387	4	Spn88Ea	4
CG13097	2	sqd	3	PGAP5	4	Mcm5	4	CG7457	4
CG7154	2	dom	3	CG13822	4	CG14894	4	CG7492	4
Ns1	2	out	3	MBD-R2	4	mbo	4	l(3)01239	4
CG4936	2	NTPase	3	CG4408	4	CG5194	4	CG7987	4
CG14005	2	CG44243	3	CG9586	4	140up	4	CG32441	4
CG9915	2	psq	3	CG9723	4	Caf1	4	CG12400	4
Marcal1	2	Cpsf160	3	step	4	mRpS10	4	rdx	4
mtDNA-helicase	2	LBR	3	PDZ-GEF	4	CG9922	4	CG18659	4
CG7706	2	CG15107	4	Syx5	4	Sply	4	CG43340	4
Gos28	2	CG10674	4	CG15047	4	Art4	4	CG9926	4
l(2)SH0834	2	Aats-asp	4	CG9318	4	cathD	4	Fs(2)Ket	4
Pdcd4	2	hoe1	4	CG2247	4	Crc	4	Mes-4	4
CG34422	3	CG11851	4	p24-1	4	CG5026	4	S2P	4
Ars2	3	CG6567	4	Rpb10	4	slmb	4	CG15012	4

CG8860	4	CG9471	4	CG14341	4	CG7110	4	CaBP1	4
ana3	4	NC2alpha	4	CG17660	4	Prx5	4	CG17768	4
Nup54	4	CG41378	4	vnc	4	CG32803	4	ade2	4
CG9796	4	CG42487	4	CG15356	4	CG18012	4	mts	4
ApepP	4	CG3295	4	CG3353	4	CG5861	4	CG6115	4
muskelin	4	Trax	4	CG3605	4	CG5823	4	Iswi	4
Idgf2	4	CG7414	4	CG3077	4	sds22	4	Sos	4
CG16974	4	OstDelta	4	CG5734	4	Rpb11	4	ctp	4
Fsn	4	scu	4	Duox	4	CG6453	4	Khc	4
mip120	4	CG7206	4	Sas-4	4	CG12321	4	CG14446	4
CG5946	4	SRPK	4	CG7044	4	CG33181	4	Ucrh	4
trus	4	CG8204	4	AIF	4	CG10344	4	stc	4
CG13344	4	CG8207	4	CG7730	4	Atg12	4	Fancd2	4
CG18549	4	CG14712	4	CG17271	4	CG12125	4	Tim8	4
CG13016	4	ben	4	cpb	4	Aats-thr	4	mRpL3	4
Mat1	4	Ice1	4	morgue	4	Cas	4	Tap42	4
twf	4	Art7	4	CG17078	4	Nup154	4	Nat1	4
CG17765	4	casp	4	CG12576	4	Df31	4	PGAP3	4
Drep-2	4	CG8116	4	Hel89B	4	stau	4	CG32103	4
CG6236	4	cutlet	4	Taf4	4	bun	4	CG16838	4
CSN7	4	Crk	4	CG9641	4	Su(var)205	4	Manf	4
CG4065	4	Nup62	4	eEF1delta	4	alphaTub84B	4	CG7172	4
CG13751	4	RpS3A	4	14-3-3epsilon	4	tud	4	CG32625	4
CG30349	4	ste24a	4	Tgs1	4	l(1)G0020	4	Cul3	4
CG8243	4	Ef1gamma	4	Jwa	4	Axs	4	CG7332	4
Set	4	CG8135	4	faf	4	ast	4	Rad1	4
CG5174	4	CG42668	4	Mal-A5	4	CSN8	4	Orc1	4
DNApol-alpha73	4	CG6568	4	CG5220	4	crc	4	Taz	4
E(var)3-9	4	Bap55	4	mld	4	thoc7	4	Prp31	4
chn	4	nsl1	4	EfTuM	4	cdc2	4	RanBPM	4
CG5641	4	CG3800	4	bru	4	CG4658	4	CG42684	4
CG12241	4	skap	4	Spase22-23	4	ERp60	4	rnh1	4
wdb	4	Arl4	4	Mapmodulin	4	raw	4	Grasp65	4
CG8027	4	CG9662	4	ATPsyn-Cf6	4	BicC	4	fbp	4
CG8771	4	CG3394	4	Pomp	4	CG14476	4	scf	4
GlyS	4	az2	4	Sac1	4	dod	4	eIF-2alpha	4
GstT1	4	CG44001	4	Mtp	4	Pfk	4	gnu	4
CG3817	4	CG14040	4	msps	4	por	4	CG12316	4
pds5	4	CG13807	4	kune	4	l(1)G0148	4	Surf4	4
CG1418	4	CG7239	4	CG17734	4	sofe	4	smt3	4
BigH1	4	CG9140	4	CG8223	4	CG13025	4	UbcD10	4
CG1371	4	Arpc4	4	CG3548	4	Cks30A	4	wus	4
CG11980	4	Rcd-1	4	CG17266	4	Arf79F	4	mop	4
Tif-IA	4	CG42232	4	CG3303	4	vih	4	polo	4
CG8531	4	Tango1	4	Hmt-1	4	mRpS18B	4	Taf10b	4
alph	4	CG7326	4	nudC	4	Mpp6	4	Orc6	4
CG6923	4	Nuf2	4	Mpcp	4	plu	4	CG2201	4
CG3501	4	Herp	4	Hsp23	4	CG17746	4	CG31689	4
CG5190	4	SmE	4	Lamp1	4	E2f	4	colt	4
aralar1	4	Socs16D	4	CG12042	4	Br140	4	CG8184	4
GCC88	4	CG8460	4	Atac2	4	Sec13	4	Spase25	4
CG15100	4	wol	4	CG6412	4	dhd	4	ppan	4
CG7744	4	Ostgamma	4	CG4972	4	RpS3	4	pelo	4
TBCB	4	CG8001	4	CG5355	4	ZnT49B	4	nod	4
CG10444	4	l(2)k12914	4	prtp	4	mtTFB1	4	CG33276	4
CASK	4	CG14286	4	Lint-1	4	otu	4	spd-2	4
CG44242	4	GlcAT-S	4	CG7168	4	CG30051	4	poe	4
rig	4	CtsB1	4	CG32676	4	CG5805	4	wisp	4
Mvl	4	CG31249	4	nocte	4	Act5C	4	Sec61alpha	4
Hydr1	4	CG31917	4	dgt2	4	Acon	4	La	4
cpa	4	CG8891	4	CG33156	4	E2f2	4	ND75	4
crq	4	Gmd	4	Rab1	4	Bub3	4	CG32537	4
Rbpn-5	4	CG2469	4	A16	4	ncd	4	Mcm6	4
LSm1	4	CG4552	4	Sec22	4	spir	4	GABPI	4
Vps20	4	CG10068	4	CG9426	4	Act42A	4	Rel	4
CG9467	4	Tango14	4	Ski6	4	Ote	4	CG15743	4
CG8507	4	IntS14	4	CG10803	4	TM9SF4	4	PDCD-5	4

Rca1	4	TRAM	4	Rpn3	5	cype	5	CG2118	5
CG8134	4	CSN1b	4	CG1746	5	CG11964	5	CG14711	5
CG11178	4	CG4562	4	CG5126	5	UGP	5	Pp2A-29B	5
CG12304	4	Uev1A	4	CG10527	5	CG6020	5	Pxt	5
CG7650	4	Akt1	4	CG5010	5	dpa	5	CG8498	5
Nop17l	4	wls	4	CG5359	5	NUCB1	5	CG9705	5
boca	4	betaTub56D	4	CG9125	5	CG6726	5	PCNA	5
lic	4	CG13364	4	CG2789	5	ATPsyn-d	5	Uch	5
toc	4	CG9376	4	CG5532	5	CG5110	5	CG9306	5
Dlic	4	CG32267	4	CG4610	5	Adam	5	CG8397	5
tos	4	Tim17b	4	Hop	5	Etf-QO	5	janA	5
jub	4	CG7218	4	rngo	5	Rpt2	5	Aldh	5
sesB	4	CG31224	4	CG17737	5	eIF-1A	5	Ipk2	5
CG33977	4	Tsf2	4	Dip-B	5	Cht2	5	Rpn1	5
Hsc70-3	4	asf1	4	CG9577	5	CG1671	5	FK506-bp2	5
Asap	4	Tal	4	Rpn7	5	CG34293	5	mRpS35	5
ari-2	4	CG6023	4	CG10576	5	awd	5	CG11699	5
CG11137	4	CG32250	4	barc	5	Nedd8	5	ColV	5
CG8112	4	Mtap	4	CG3609	5	CG8258	5	Dhfr	5
APP-BP1	4	Ugt	4	blw	5	GstE12	5	Dph5	5
mats	4	Snap29	4	porin	5	NKAIN	5	CG7770	5
boi	4	loj	4	GstE6	5	CG8818	5	O-fut2	5
CG10424	4	CG1407	4	CG3792	5	CG40042	5	CG42575	5
CG7182	4	blot	4	Gint3	5	RagC-D	5	CG9265	5
CG7484	4	CG17896	4	CG2246	5	CG42813	5	Ost48	5
mus210	4	CG33229	4	CG8993	5	CG6543	5	Ikb1	5
CG13366	4	rasp	4	Gnf1	5	stil	5	RfC4	5
egl	4	CG16952	4	CG16985	5	Prosalpha6	5	beta4GalT7	5
CG8180	4	CG3776	4	sktl	5	Tapdelta	5	me31B	5
pre-lola-G	4	bl	4	CG5721	5	CG6180	5	CG12582	5
Txl	4	CG3335	4	CG15099	5	CG5525	5	Rpt5	5
eRF1	4	AMPKalpha	4	wts	5	wal	5	mbf1	5
CG2852	4	CG9330	4	CG3214	5	CG2004	5	FucT6	5
hay	4	Ssrp	4	PIG-U	5	CG6770	5	Ufd1-like	5
Idh	4	CG17168	4	CG3731	5	CG34310	5	CG1218	5
Chd3	4	CG8963	4	Drp1	5	Neb-cGP	5	CG15717	5
PIG-V	4	CG33123	5	Pgk	5	dUTPase	5	CG6293	5
HmgD	4	Hsp26	5	eff	5	Sod2	5	Jafrac1	5
CG3376	4	Sptr	5	Eip55E	5	26-29-p	5	VhaSFD	5
CG14814	4	Arc42	5	Eogt	5	CG12404	5	CG9147	5
Klp68D	4	Ntf-2	5	CG18190	5	Nup107	5	CG40045	5
CG32452	4	Ssb-c31a	5	CG17259	5	CG4169	5	CG3430	5
Bl-1	4	CG2918	5	CG30159	5	mtacp1	5	Pop2	5
CkIIalpha	4	Hsp27	5	RnrL	5	Cpsf73	5	deltaCOP	5
ATPsyn-b	4	CG3011	5	CG4679	5	CG13551	5	Aats-asn	5
Atg3	4	Cctgamma	5	eIF5B	5	CG5676	5	CG34439	5
Uch-L5	4	Plap	5	Cp1	5	Mlh1	5	Prosbeta2	5
O-fut1	4	Prosalpha5	5	p47	5	CG11134	5	Prosbeta7	5
CG2943	4	CG3773	5	CG1707	5	CG5885	5	gammaTub37C	5
CG14483	4	Rpn12	5	yps	5	Etl1	5	CG12096	5
eIF3-S9	4	CG42376	5	CG11876	5	CG9135	5	CG9953	5
cindr	4	Aats-his	5	CG9836	5	CG30415	5	CG10932	5
wibg	4	poly	5	RpL34a	5	Sar1	5	PyK	5
Gie	4	CG10638	5	CG3940	5	CG1516	5	CG14103	5
Myb	4	Nup44A	5	dre4	5	CG7950	5	yip2	5
wash	4	Roc1a	5	ubl	5	ATPsyn-gamma	5	l(3)04053	5
Arl1	4	CoVb	5	CG14516	5	Tango9	5	CG7033	5
TfIIEalpha	4	epsilonCOP	5	Tcp-1eta	5	CG7834	5	CG2076	5
SH3PX1	4	CG2915	5	l(1)G0334	5	CG10166	5	mRpL22	5
Nmt	4	Pen	5	Aos1	5	CG8036	5	Aats-gly	5
RhoGDI	4	capt	5	Sec23	5	ebd1	5	wac	5
pont	4	CG6907	5	CG8503	5	pch2	5	CG3192	5
Rpn2	4	Prosbeta3	5	sol	5	Ef1alpha48D	5	Ctr1A	5
Pdi	4	Rpn11	5	CG33129	5	CG10602	5	Dak1	5
AdenoK	4	Npc2a	5	Nbr	5	FKBP59	5	betaCOP	5
CG13887	4	CG15093	5	CG11396	5	Gdi	5	APC7	5
CG45068	4	CG8331	5	Prosalpha3	5	CG33155	5	l(1)G0320	5

Ran	5	mod(r)	5	Gip	6	CG3689	7	CG4686	7
Mtpalpha	5	Sod	5	CG5270	6	Zw10	7	yin	7
l(1)G0230	5	Sem1	5	CG10960	6	Irp-1B	7	Mcm3	7
Rga	5	Iva	5	CG31717	6	CG7600	7	Adhr	7
CG32230	5	Fen1	5	CG10254	6	Ucp4A	7	CG2556	7
Rpn8	5	Rpt1	5	dgt3	6	Tsp74F	7	CG13865	7
Rpt4	5	CG5941	5	l(1)G0156	6	MRP	7	CG10585	7
Rpt3	5	CG9865	5	Capr	6	Acph-1	7	CG2767	7
CG4593	5	Ahcy13	5	Rpn5	6	icln	7	pgant5	7
lost	5	png	5	CG18624	6	CG11208	7	CG14036	7
Cyp1	5	Aats-gln	5	GstD3	6	Gs1	7	Vav	7
Vha36-1	5	beta4GalNAcTB	5	SelG	6	VhaM8.9	7	tsr	7
CG2051	5	RecQ4	5	CG34150	6	RpL13A	7	Trxr-1	7
E(z)	5	Men	5	CG5214	6	COQ7	7	Dsor1	7
CG7712	5	DNApol-alpha180	5	Vha44	6	Pp2B-14D	7	Elf	7
RPA3	5	CG14931	5	CG3321	6	Men-b	7	Hsp60	7
CG1703	5	CG6084	5	CG6463	6	Dhpr	7	CG5604	7
Hr96	5	Sec61beta	5	Grip84	6	Vha26	7	MED9	7
tral	5	RhoGEF2	5	Prosbeta5	6	Wnk	7	Ent2	7
UK114	5	Prosbeta6	5	Fmr1	6	ND23	7	DppIII	7
pes	5	mus301	5	flr	6	Dip-C	7	VhaAC39-1	7
CG2263	5	Prosalpha2	5	CG9344	6	CG7433	7	nesd	7
CG42514	5	CG7656	5	Nup75	6	CG11880	7	Lsd-2	7
yl	5	SsRbeta	5	CG10219	6	Arp1	7	Gapdh2	7
tefu	5	CG1458	5	GstE11	6	bel	7	path	7
CG1890	5	CG11686	5	Hsc70-4	6	CG6512	7	slik	7
Eno	5	Tcp-1zeta	5	l(3)neo18	6	Scsalpha	7	Nhe3	7
mRpS25	5	Vha100-1	5	Jabba	6	CG4627	7	Inos	7
CG4603	5	CG12173	5	GstD1	6	CG5339	7	CG4022	7
CG5590	5	wkd	5	CG4991	6	CycJ	7	Uba1	7
CG5548	5	CG9911	5	CG2862	6	CG8778	7	Pgi	7
CG13623	5	Ho	5	osk	6	CG30185	7	CG14434	7
CG5706	5	CG17327	5	CoVa	6	Cdc42	7	fs(1)N	7
Alg10	5	Prosbeta1	5	CG6340	6	Mtch	7	ACC	7
CG6540	5	Bruce	5	Pcd	6	CG5009	7	Nap1	7
l(2)35Di	5	CG6903	6	Trx-2	6	pix	7	alpha-Man-Ib	7
CG4449	5	CG17202	6	CG12203	6	RpL10Ab	7	Jafrac2	7
CG8206	5	CG8735	6	Pglym78	6	CG15098	7	Gasz	7
CG6950	5	Den1	6	CG4586	6	CG3902	7	debcl	7
CG10157	5	CG9588	6	CG14482	6	AP-2mu	7	Nipsnap	7
CG4598	5	CG1598	6	Desat1	6	RpS5b	7	trx	7
iPLA2-VIA	5	CG7777	6	Rpn9	6	CG6707	7	Nurf-38	7
CG5703	5	sut1	6	RpA-70	6	Actn	7	CG5068	7
endos	5	U2A	6	CG12082	6	CG13603	7	Ts	7
CG9099	5	CG4692	6	Hcs	6	AGBE	7	ORMDL	7
CG4476	5	dj-1beta	6	yata	6	didum	7	frj	7
Su(z)12	5	Got2	6	elm	6	CG6509	7	tra2	7
Cct5	5	CG12384	6	Ssadh	6	mei-41	7	VhaAC45	7
CG4789	5	eIF-4E	6	alphaTub67C	6	stet	7	l(2)06225	7
SmG	5	CG7091	6	Tpi	6	CG5044	7	CG2604	7
Aats-ala	5	CG11790	6	Mdh2	6	SdhA	7	rost	7
sqh	5	GlyP	6	RfC3	6	HDAC6	7	wake	7
grsm	5	CG5903	6	Pdp	6	Snx1	7	robl	7
twr	5	RPA2	6	LSm7	6	CG9149	7	Mdh1	7
CG17059	5	CG9034	6	Kap3	6	Jupiter	7	exu	7
CG7054	5	CG6045	6	Nup43	6	CG5039	7	SMSr	7
slim	5	CG31648	6	Nup37	6	fs(1)M3	7	rin	7
AdipoR	5	mfrn	6	CG12264	6	CG13005	7	CG8270	7
Thiolase	5	CG7920	6	l(1)G0255	6	GAA1	7	CG17337	7
EloC	5	trsn	6	CG34348	7	CG31075	7	CG33228	7
RhoGAP68F	5	Roc2	6	vsg	7	psidin	7	CG2034	7
CG9603	5	CG15771	6	Acyp2	7	CG13384	7	sun	7
Pdsw	5	ATPsyn-beta	6	CG16817	7	Ork1	7	rpk	7
Tdrd3	5	Gapdh1	6	CG8516	7	Vha100-2	7	rod	7
CG12204	5	CG8230	6	CG3209	7	Hmu	7	Ipp	7
CG12262	5	Prosalpha7	6	CanB2	7	babo	7	CG7158	8
alphaTub84D	5	Xpac	6	Cirl	7	EndoGI	7	CG33170	8

CG2656	8	RpS9	8	crm	8	CG44254	8	CG11771	8
Hr78	8	Argk	8	ptr	8	pad	8	CG11781	8
CG16790	8	mRpL36	8	CG4199	8	CG17565	8	mRpS18A	8
CG5969	8	CG18809	8	Pex5	8	CG14898	8	Smg6	8
Cap-G	8	CG3267	8	Dgkepsilon	8	Der-2	8	CG31472	8
CG1105	8	eIF6	8	Nmda1	8	CG31126	8	godzilla	8
Dpck	8	MED8	8	TppII	8	CG3534	8	jagn	8
CG10098	8	Skp2	8	bbc	8	CG16941	8	bai	8
CG33169	8	CG32069	8	CG11412	8	AdSL	8	Mocs2	8
CG7338	8	CG32364	8	Jra	8	atl	8	Sec8	8
CG10286	8	QC	8	CG5273	8	GckIII	8	RpS27	8
Fibp	8	CG10671	8	CG13585	8	CLS	8	CG11857	8
CG11739	8	PHGPx	8	RpL12	8	p38a	8	CG11858	8
SmD2	8	Su(dx)	8	Upf3	8	CG7208	8	Kap-alpha3	8
CG12007	8	Rab5	8	RpS15	8	CG5382	8	MED28	8
mRpL47	8	RpL28	8	GstS1	8	CG5191	8	CG5112	8
CG33172	8	CG32278	8	l(2)k01209	8	CG4390	8	Npl4	8
p	8	pgant6	8	Rab4	8	mTerf5	8	CG5886	8
CG12746	8	RpL8	8	pAbp	8	gukh	8	CG5913	8
mRpL44	8	ABCB7	8	Synj	8	CG31229	8	CG14543	8
RpL35A	8	CG7115	8	RpS18	8	CG12333	8	Cerk	8
CG13741	8	CG8475	8	Tim10	8	Mekk1	8	IntS12	8
CG8043	8	CG8372	8	CG30291	8	snRNP-U1-C	8	ball	8
CG8202	8	mri	8	CG4050	8	NP15.6	8	CG5500	8
l(2)k10201	8	mus312	8	Xpd	8	CG31360	8	BCAS2	8
CG8611	8	CG1486	8	RpL36	8	gatA	8	CG1116	8
hd	8	Pgant35A	8	CG12134	8	CREG	8	slif	8
ArfGAP3	8	CG11899	8	CG32736	8	CG7379	8	Aats-ile	8
su(w[a])	8	CG11837	8	RpS6	8	Lnk	8	CG5514	8
eIF2B-epsilon	8	dgt6	8	pico	8	CG5205	8	CG5116	8
CG2658	8	CG11897	8	Myo31DF	8	CG5815	8	CG13630	8
CG3566	8	CG1907	8	crol	8	gammaCOP	8	Ppox	8
Chc	8	Cap-D2	8	Tom70	8	CG6693	8	CG6695	8
l(2)tid	8	CG7593	8	l(1)G0222	8	CG17726	8	CG4572	8
Bx	8	CG7598	8	Vha68-2	8	CG14701	8	Mhcl	8
Rtnl1	8	IntS11	8	DnaJ-H	8	Arfip	8	mdlc	8
enc	8	CG7789	8	mRpS23	8	Fer2LCH	8	CG5180	8
CG11737	8	CG9391	8	Smg5	8	RpS7	8	CG5412	8
MAGE	8	Vps16B	8	ZnT35C	8	mgr	8	CG16953	8
CG5196	8	RpS8	8	glu	8	Ranbp9	8	Srp72	8
CG2846	8	CG42557	8	CG3632	8	RpL24-like	8	Arpc3A	8
Rpb8	8	CG4365	8	kat80	8	CG5276	8	CG17272	8
CG2046	8	l(2)k14710	8	Hakai	8	CG7943	8	Ubpy	8
Cf2	8	CG2218	8	Pis	8	CG6744	8	CG3337	8
CG7878	8	l(3)03670	8	EF2	8	RpL32	8	AP-2sigma	8
CG14647	8	HLH106	8	opm	8	CG10898	8	CG5919	8
sav	8	Bet1	8	GstT2	8	Zip99C	8	Orc2	8
Spase12	8	CG5535	8	RpS14a	8	ca	8	CG3308	8
CG9769	8	RpL6	8	e(r)	8	Atg4b	8	CG6353	8
RpL34b	8	Eip71CD	8	Aats-lys	8	CG6276	8	CG6028	8
Ranbp11	8	RpS12	8	CG1354	8	Zip88E	8	RpS29	8
CG8121	8	CG3719	8	CG14767	8	CG31344	8	CG6607	8
CG7148	8	Ady43A	8	CG9986	8	CG5938	8	Spps	8
CG1236	8	DNApol-alpha60	8	CG15312	8	CG8066	8	CG5515	8
CG2182	8	VhaPPA1-1	8	PhKgamma	8	Ppcs	8	CG5902	8
Vps16A	8	Ccs	8	CG10347	8	CG3061	8	RpL3	8
Coq2	8	CG11652	8	CG1640	8	CG9799	8	CG6195	8
CG11109	8	RIOK1	8	Aldh-III	8	CG8031	8	Plip	8
Madm	8	CG5498	8	Vha16-1	8	CG12279	8	Csk	8
RpL29	8	Hnf4	8	Pld	8	Not10	8	CG12360	8
CG3909	8	CG31715	8	Evi5	8	CG5844	8	CG8449	8
CG17508	8	Nup205	8	Noa36	8	CG4860	8	rumi	8
CG14545	8	Syb	8	CG12413	8	omd	8	mRpL45	8
CG15386	8	Pl31	8	Gfat2	8	P58IPK	8	CG13850	8
CG7630	8	RpL35	8	vig2	8	Nup58	8	RanBP3	8
ksh	8	SmD3	8	veli	8	CG11447	8	CG6178	8
CG8336	8	RpS11	8	CG4287	8	CG11089	8	PNUTS	8

CG15881	8	ald	8	ox	8	CG4646	8	Rrp1	8
Arp10	8	m-cup	8	sgl	8	rho-7	8	CG30183	8
Sec61gamma	8	cher	8	Vha14-1	8	CG7220	8	CG42239	8
Tyler	8	CG14882	8	Vha55	8	CoVIIc	8	ATPCL	8
CG7556	8	Aats-ser	8	lat	8	oys	8	Rpn13	8
Vps4	8	ea	8	msl-1	8	Sec24AB	8	Fis1	8
RpS5a	8	mRpS21	8	Arl2	8	Vamp7	8	CG17691	8
RpS19a	8	Elp1	8	bic	8	wun2	8	CG4951	8
CG9947	8	SdhC	8	AP-2alpha	8	Non1	8	CG42542	8
vap	8	FBX011	8	Klp61F	8	Tom7	8	LpR2	8
CG9172	8	CG11975	8	neb	8	gcl	8	cdc2c	8
CG15602	8	CD98hc	8	usp	8	Cyp4e2	8	LSm3	8
mRpS30	8	CG1091	8	sta	8	CG30373	8	cnn	8
CG8128	8	CG14671	8	RanGAP	8	CG4882	8	CG3358	8
Gmap	8	Pcmt	8	nos	8	eIF4G2	8	qua	8
CG1662	8	Kat60	8	RpL19	8	CG10904	8	Sgt	8
CG1764	8	CG9855	8	hk	8	HSPC300	8	SC35	8
CG2200	8	RpL10	8	grk	8	RpS30	8	l(2)gd1	8
CG4645	8	CG14450	8	RpL22	8	att-ORFA	8	CG7627	8
mRpL49	8	RpLP0	8	zyd	8	Sirt2	8	Snx6	8
Sec16	8	CG14561	8	Srp19	8	RhoGAP92B	8	eIF-4a	8
CG1578	8	P5CDh1	8	Cnx99A	8	Vha13	8	CoVIb	8
Psf3	8	CG11306	8	Slbp	8	CG5916	8	CG14231	8
CG2972	8	Synd	8	Sps2	8	Nsf2	8	CG14220	8
RpS28b	8	Smox	8	Taf10	8	Dic1	8	Pfrx	8
c11.1	8	AnxB9	8	CstF-64	8	CAHbeta	8	CG9240	8
CG16892	8	wge	8	Dnz1	8	CG31460	8	AP-1gamma	8
CG11284	8	RpL7A	8	CSN4	8	CG11309	8	CG7766	8
Mer	8	Top3beta	8	CSN5	8	CG9231	8	lawc	8
CG1440	8	Ubi-p5E	8	Trap1	8	mRpL21	8	cib	8
Rpp20	8	CG5966	8	esc	8	Chmp1	8	tko	8
CG12702	8	lin-52	8	RpII33	8	CG10222	8	CG32856	8
CG10383	8	Tre1	8	nop5	8	RpS4	8	ctrip	8
RpS26	8	CG15465	8	JTBR	8	UbcD4	8	CG14184	8
CG7200	8	Pp2C1	8	Int6	8	CG5660	8	CG7580	8
RpL24	8	Torsin	8	CG4585	8	foi	8	Fdxh	8
CG9305	8	CHOp24	8	und	8	Oseg1	8	pigeon	8
RfC38	8	tyf	8	ial	8	CG45186	8	RpL37A	8
RpL9	8	CG2941	8	Nmd3	8	Aprt	8	RpL27A	8
RpL7	8	CG18508	8	RpL39	8	HBS1	8	CG7048	8
CG17292	8	CG2662	8	D19A	8	Cct1	8	BEAF-32	8
RpS13	8	CG3457	8	dor	8	Mkp	8	CG12945	8
RpL36A	8	CG17776	8	Osbp	8	CG3608	8	CG34242	8
Coprox	8	CG3621	8	SA	8	Fcp1	8	Tina-1	8
CG13766	8	CG14817	8	kraken	8	CG3860	8	CG4622	8
mmy	8	Mur2B	8	Gs1l	8	CoVIII	8	Sod3	8
mtm	8	rush	8	Nacalpha	8	CG5664	8	CG10462	8
CG8680	8	Ns3	8	Cdk4	8	CG4825	8	CG6144	8
CG9643	8	RhoGAP1A	8	nrv1	8	CG2100	8	CG34015	8
CG3436	8	CG40160	8	dare	8	Sin	8	skpA	8
Cp110	8	RpL27	8	CycK	8	Clc	8	CG4293	8
CG14621	8	jar	8	CG6000	8	CG5021	8	CG33785	8
mst	8	Hrd3	8	Calx	8	Nop60B	8	CG33774	8
Mgstl	8	orb	8	RpS16	8	eIF2B-delta	8	CG33635	8
CG1532	8	Gclm	8	Ppcdc	8	CG10320	8	primo-1	8
GstT3	8	VhaM9.7-b	8	CG18870	8	SP2637	8	sea	8
mal	8	CG31673	8	CG30152	8	Cul4	8	PGRP-LD	8
CG11710	8	Cyp6u1	8	maf-S	8	l(2)37Cc	8	bbx	8
CG15456	8	Pi3K59F	8	RpL11	8	fu12	8	CG33714	8
parvin	8	Orc5	8	CG7461	8	drongo	8	Pink1	8
Faf	8	lap2	8	CG10915	8	pcm	8	CG40002	8
sni	8	Mcm2	8	cnk	8	MED18	8	CG41128	8
snz	8	SdhB	8	Ef1beta	8	yrt	8	CG40191	8
CG15922	8	CG4038	8	CG8399	8	Best1	8	RpL15	8
Mpc1	8	oaf	8	Cyp6a19	8	Wbp2	8	Top1	8
CG31122	8	pav	8	Cyp6a22	8	mRpL23	8	RpL41	8
CG44009	8	Cdc37	8	CG17385	8	capu	8	CG33506	8

stmA	8	CG12848	8	His3.3A	8	adp	8	msb1l	8
Acsl	8	mRpL17	8	mRpL28	8	P32	8	l(2)37Ce	8
CG9967	8	CG5262	8	mRpL27	8	APC10	8	CG17343	8
CG7255	8	Tom20	8	RpL40	8	Tes	8	CG10470	8
CG9853	8	CG8334	8	CG17593	8	CG6805	8	CG15168	8
CG33969	8	trc	8	CG31950	8	clu	8	CG10336	8
CG42259	8	RpL26	8	RpS21	8	CG8386	8	CG15141	8
CG32068	8	CG4753	8	Arpc5	8	Pex11	8	CG17996	8
CG10274	8	roq	8	Sec24CD	8	CG8314	8	CG4278	8
CG15019	8	MED10	8	CG11723	8	CG8297	8	CG4935	8
CG11537	8	th	8	fs(1)Ya	8	mRpL41	8	Ku80	8
CG34213	8	GXIVsPLA2	8	CG4238	8	GPHR	8	NC2beta	8
Sesn	8	NHP2	8	RFeSP	8	SMC2	8	l(2)35Be	8
wmd	8	CG6928	8	Pino	8	Trs31	8	mTTF	8
pgc	8	CG7394	8	RpLP1	8	CG12859	8	CG6523	8
CG15118	8	CG8003	8	CG14613	8	CG12863	8	CG5705	8
Phb2	8	SrpRbeta	8	CG1518	8	Arc1	8	CG30392	8
CG34191	8	RpL18	8	Phf7	8	CG8494	8	CG9752	8
mute	8	zpg	8	Pmp70	8	RpS23	8	CG10795	8
CG9003	8	lama	8	CG43658	8	Tango7	8	scramb1	8
Pkn	8	Dhc64C	8	CG9921	8	CG16935	8	pall	8
CG12795	8	Rop	8	CG32579	8	mRpL54	8	CG3437	8
CrebB	8	mge	8	CG11151	8	CG8728	8	CG4452	8
Arp2	8	Hsp83	8	REG	8	CG12107	8	Use1	8
CG13373	8	Asciz	8	ade5	8	CG6750	8	Srp68	8
CG34117	8	CG12104	8	Der-1	8	CG5168	8	CG5989	8
yki	8	CG2277	8	snf	8	CG5037	8	Nelf-E	8
Hsf	8	CG13901	8	Rnp4F	8	CG4968	8	GstO1	8
mRpL34	8	RhoGEF3	8	swa	8	CG4953	8	Exo70	8
RpL5	8	Tudor-SN	8	Pex13	8	Mob3	8	cert	8
CG43345	8	CG13392	8	CG17019	8	CG4619	8	CG8038	8
CG34132	8	baf	8	mRpL18	8	C1GalTA	8	Srp9	8
CG34125	8	Rack1	8	mos	8	Trs23	8	CG8111	8
Rab21	8	mei-P26	8	dgt5	8	mRpL51	8	CG7506	8
CG12877	8	His3.3B	8	garz	8	Rcd4	8	CTCF	8
CG8950	8	fh	8	CG8321	8	CG7787	8	CG43780	8
CG3760	8	CG1885	8	CG7745	8	CG7840	8	mRpL50	8
BtbVII	8	CG4617	8	CG9067	8	SLC5A11	8	BHD	8
Khc-73	8	cm	8	mms4	8	Rbsn-5	8	CG8549	8
CG17574	8	CG3842	8	CG7637	8	Wwox	8	CG6610	8
CG13220	8	CG4078	8	CG12935	8	r2d2	8	Pole2	8
prel	8	dgt4	8	Git	8	CG5261	8	mad2	8
CG8080	8	PI4KIIIalpha	8	RpLP0-like	8	CG9548	8	Myt1	8
Vps28	8	mRpL16	8	sel	8	CG9536	8	Ppat-Dpck	8
koi	8	CG14818	8	CG12129	8	CG9175	8	CG10635	8
RpL38	8	a6	8	CG18446	8	CG13993	8	Membrin	8
CG40127	8	CG11448	8	Ntmt	8	CG13994	8	CG6418	8
RpL21	8	CG1970	8	RpL31	8	CG7382	8	Prpk	8
CG3262	8	mrt	8	Updo	8	CG14043	8	CG6404	8
l(2)k14505	8	CG6364	8	alc	8	Scox	8	GlcAT-P	8
Top2	8	CG5380	8	tsu	8	jet	8	CG6841	8
CG10237	8	PP2A-B'	8	CG8235	8	CG6729	8	CG5147	8
RpL30	8	sll	8	CG8272	8	CG12159	8	CG7430	8
CG31739	8	stck	8	CG8635	8	CG6746	8	CG5567	8
Prosbeta4	8	Prat	8	beta3GalTII	8	Uvrag	8	U4-U6-60K	8
cni	8	CG17233	8	Nup50	8	CG1620	8	CG32174	8
aret	8	CG6852	8	Roe1	8	Hsepi	8	CG9715	8
Lrr47	8	CG4729	8	CG11210	8	CG9436	8	CG9669	8
CG6094	8	CG5114	8	Uba3	8	CG3420	8	CG9706	8
pie	8	Vap-33B	8	Ctf4	8	CG9422	8	Baldspot	8
mRpS7	8	spri	8	Fem-1	8	CG1416	8	CG4842	8
RpL13	8	ras	8	CG11110	8	CG9257	8	CG4933	8
CG4592	8	Tango5	8	CG8929	8	CG12050	8	Trs20	8
RpS2	8	CG2061	8	CG8920	8	CG9272	8	CG7427	8
hoip	8	Liprin-alpha	8	CG7137	8	ik2	8	CG7011	8
CG5757	8	Gpdh	8	CG15083	8	CG10463	8	CG6878	8
CG13090	8	cl	8	CG10914	8	CG10631	8	CG6833	8

stmA	8	CG12848	8	His3.3A	8	adp	8	msb1l	8
Acsl	8	mRpL17	8	mRpL28	8	P32	8	l(2)37Ce	8
CG9967	8	CG5262	8	mRpL27	8	APC10	8	CG17343	8
CG7255	8	Tom20	8	RpL40	8	Tes	8	CG10470	8
CG9853	8	CG8334	8	CG17593	8	CG6805	8	CG15168	8
CG33969	8	trc	8	CG31950	8	clu	8	CG10336	8
CG42259	8	RpL26	8	RpS21	8	CG8386	8	CG15141	8
CG32068	8	CG4753	8	Arpc5	8	Pex11	8	CG17996	8
CG10274	8	roq	8	Sec24CD	8	CG8314	8	CG4278	8
CG15019	8	MED10	8	CG11723	8	CG8297	8	CG4935	8
CG11537	8	th	8	fs(1)Ya	8	mRpL41	8	Ku80	8
CG34213	8	GXIVsPLA2	8	CG4238	8	GPHR	8	NC2beta	8
Sesn	8	NHP2	8	RFeSP	8	SMC2	8	l(2)35Be	8
wmd	8	CG6928	8	Pino	8	Trs31	8	mTTF	8
pgc	8	CG7394	8	RpLP1	8	CG12859	8	CG6523	8
CG15118	8	CG8003	8	CG14613	8	CG12863	8	CG5705	8
Phb2	8	SrpRbeta	8	CG1518	8	Arc1	8	CG30392	8
CG34191	8	RpL18	8	Phf7	8	CG8494	8	CG9752	8
mute	8	zpg	8	Pmp70	8	RpS23	8	CG10795	8
CG9003	8	lama	8	CG43658	8	Tango7	8	scramb1	8
Pkn	8	Dhc64C	8	CG9921	8	CG16935	8	pall	8
CG12795	8	Rop	8	CG32579	8	mRpL54	8	CG3437	8
CrebB	8	mge	8	CG11151	8	CG8728	8	CG4452	8
Arp2	8	Hsp83	8	REG	8	CG12107	8	Use1	8
CG13373	8	Asciz	8	ade5	8	CG6750	8	Srp68	8
CG34117	8	CG12104	8	Der-1	8	CG5168	8	CG5989	8
yki	8	CG2277	8	snf	8	CG5037	8	Nelf-E	8
Hsf	8	CG13901	8	Rnp4F	8	CG4968	8	GstO1	8
mRpL34	8	RhoGEF3	8	swa	8	CG4953	8	Exo70	8
RpL5	8	Tudor-SN	8	Pex13	8	Mob3	8	cert	8
CG43345	8	CG13392	8	CG17019	8	CG4619	8	CG8038	8
CG34132	8	baf	8	mRpL18	8	C1GalTA	8	Srp9	8
CG34125	8	Rack1	8	mos	8	Trs23	8	CG8111	8
Rab21	8	mei-P26	8	dgt5	8	mRpL51	8	CG7506	8
CG12877	8	His3.3B	8	garz	8	Rcd4	8	CTCF	8
CG8950	8	fh	8	CG8321	8	CG7787	8	CG43780	8
CG3760	8	CG1885	8	CG7745	8	CG7840	8	mRpL50	8
BtbVII	8	CG4617	8	CG9067	8	SLC5A11	8	BHD	8
Khc-73	8	cm	8	mms4	8	Rbsn-5	8	CG8549	8
CG17574	8	CG3842	8	CG7637	8	Wwox	8	CG6610	8
CG13220	8	CG4078	8	CG12935	8	r2d2	8	Pole2	8
prel	8	dgt4	8	Git	8	CG5261	8	mad2	8
CG8080	8	PI4KIIIalpha	8	RpLP0-like	8	CG9548	8	Myt1	8
Vps28	8	mRpL16	8	sel	8	CG9536	8	Ppat-Dpck	8
koi	8	CG14818	8	CG12129	8	CG9175	8	CG10635	8
RpL38	8	a6	8	CG18446	8	CG13993	8	Membrin	8
CG40127	8	CG11448	8	Ntmt	8	CG13994	8	CG6418	8
RpL21	8	CG1970	8	RpL31	8	CG7382	8	Prpk	8
CG3262	8	mrt	8	Updo	8	CG14043	8	CG6404	8
l(2)k14505	8	CG6364	8	alc	8	Scox	8	GlcAT-P	8
Top2	8	CG5380	8	tsu	8	jet	8	CG6841	8
CG10237	8	PP2A-B'	8	CG8235	8	CG6729	8	CG5147	8
RpL30	8	sll	8	CG8272	8	CG12159	8	CG7430	8
CG31739	8	stck	8	CG8635	8	CG6746	8	CG5567	8
Prosbeta4	8	Prat	8	beta3GalTII	8	Uvrag	8	U4-U6-60K	8
cni	8	CG17233	8	Nup50	8	CG1620	8	CG32174	8
aret	8	CG6852	8	Roe1	8	Hsepi	8	CG9715	8
Lrr47	8	CG4729	8	CG11210	8	CG9436	8	CG9669	8
CG6094	8	CG5114	8	Uba3	8	CG3420	8	CG9706	8
pie	8	Vap-33B	8	Ctf4	8	CG9422	8	Baldspot	8
mRpS7	8	spri	8	Fem-1	8	CG1416	8	CG4842	8
RpL13	8	ras	8	CG11110	8	CG9257	8	CG4933	8
CG4592	8	Tango5	8	CG8929	8	CG12050	8	Trs20	8
RpS2	8	CG2061	8	CG8920	8	CG9272	8	CG7427	8
hoip	8	Liprin-alpha	8	CG7137	8	ik2	8	CG7011	8
CG5757	8	Gpdh	8	CG15083	8	CG10463	8	CG6878	8
CG13090	8	cl	8	CG10914	8	CG10631	8	CG6833	8

CG8783	8	l(3)02640	8	Shc	8	Ggt-1	8	eIF2B-beta	8
CG10133	8	msd1	8	trbl	8	CG7192	8	CG8636	8
ste14	8	CG9186	8	mRpL30	8	CG7772	8	CG13760	8
CG11267	8	CG13890	8	mRpL1	8	CG15814	8	CG4045	8
CG10688	8	MED30	8	Hem	8	CG8142	8	Pgam5	8
CG10418	8	CG16940	8	Acox57D-p	8	CG8675	8	CG14803	8
thoc6	8	mv	8	POSH	8	CG9104	8	CG3704	8
CG5642	8	Prp3	8	RpL18A	8	CG9917	8	CG3711	8
Bmcp	8	Dim1	8	cyp33	8	CG3560	8	CG13367	8
crim	8	Cep97	8	RpLP2	8	CG8931	8	CG13365	8
CG7638	8	mRpL32	8	mRpS16	8	CG15916	8	CG3156	8
CG10672	8	mRpS18C	8	SmF	8	Aats-arg	8	rhi	8
CG1319	8	Nlp	8	mRpL42	8	CG8974	8	or	8
CG1316	8	RpL4	8	Socs44A	8	CG9203	8	l(2)37Bb	8
CG3511	8	mRpS22	8	Tsp42Ef	8	Grip128	8	cv	8
CG11414	8	mRpS24	8	bsf	8	shtd	8	Irbp	8
CG3356	8	DNApol-epsilon	8	mre11	8	CG9114	8	mtSSB	8
eIF-5A	8	CenB1A	8	cort	8	RpL37a	8	Acf1	8
mr	8	Rpl12	8	Kr-h2	8	CG5599	8	128up	8
CG3065	8	rtet	8	mRpS2	8	CG9065	8	Cat	8
CG16787	8	RpS20	8	Ptpa	8	CG14407	8	RpS14b	8
CG3803	8	EloB	8	S	8	Fbxl4	8	mRpS17	8
DNA-ligI	8	P5cr	8	smo	8	CG11674	8	CG4041	8
Dcp1	8	Prx3	8	mRpL10	8	CG11590	8	l(1)G0045	8
CG5569	8	mRpS11	8	Syx16	8	CG11095	8	CG3160	8
ytr	8	mRpS33	8	Rab10	8	Rtc1	8	CG3016	8
Rrp4	8	ldlCp	8	AP-1-2beta	8	BthD	8	CG2540	8
levy	8	FK506-bp1	8	dik	8	CG6617	8	CG15735	8
CG3500	8	mRpL9	8	r	8	Ndc80	8	Upf1	8
CG9890	8	Oscp	8	mRpL38	8	CG7453	8	CG11802	8
CG3831	8	mRpL11	8	bys	8	Rho1	8	CG1847	8
Gmer	8	timeout	8	PpV	8	CG2818	8	CG1749	8
asrij	8	Past1	8	mRpS29	8	Cog3	8	CG11752	8
RpS24	8	mRpL40	8	Karybeta3	8	E23	8	CG1657	8
bonsai	8	RpS25	8	RpL23	8	alpha4GT1	8	CG17333	8
GlcT-1	8	Fdh	8	mRpL43	8	CG3165	8	CG15317	8
CG2921	8	mRpL37	8	Ddx1	8	CG8814	8	sIgA	8
CG10306	8	SF1	8	ppl	8	CG15362	8	APC4	8
Rae1	8	mRpL19	8	alphaSnap	8	CG17712	8	CG12123	8
CG10321	8	spag	8	cyc	8	CG31937	8	Psf2	8
CG10494	8	Pgm	8	Kap-alpha1	8	Vps29	8	CG11190	8
CG3570	8	pon	8	mRpS26	8	CG11885	8	CG2116	8
CG3663	8	mRpL14	8	Su(P)	8	CG11562	8	CG1575	8
NDUFA8	8	Ilk	8	nxf2	8	CG11454	8	CG42593	8
CG3894	8	bor	8	mRpS34	8	Nhe1	8	CG10777	8
VhaM9.7-c	8	mRpL33	8	mRpS31	8	galectin	8	Ykt6	8
Ero1L	8	PpD3	8	DNApol-delta	8	CG1529	8	CG1444	8
Ack	8	l(3)87Df	8	mRpL39	8	Cyp6v1	8	NELF-B	8
CG10863	8	mRpL4	8	mnd	8	l(1)G0004	8	RpL17	8
Sc2	8	CIAPIN1	8	Gl	8	CG9578	8	CG3224	8
armi	8	l(3)73Ah	8	mRpL20	8	CG9581	8	CG3226	8
CG14969	8	mus101	8	eIF-2beta	8	Alr	8	CG3815	8
CG12016	8	mus205	8	ArfGAP1	8	CG14230	8	Rbcn-3A	8
PIG-C	8	Bka	8	Nrx-IV	8	CG12237	8	Efr	8
NDUFS3	8	e(y)2	8	viaf	8	CG14210	8	CG2147	8
Sk2	8	eIF-3p40	8	Nc	8	RpS10b	8	CR43685	8
scramb2	8	Aats-trp	8	RpS17	8	Dhod	8		
CG12093	8	abo	8	Cp15	8	Rab11	8		
CG15440	8	SmD1	8	RpL14	8	CG7889	8		
CG9977	8	Surf1	8	pbl	8	CG1673	8		
CG12024	8	shark	8	Rcc1	8	CG4404	8		
mRpL46	8	mRpL12	8	RpL23A	8	CG4407	8		
CG2021	8	Sara	8	ken	8	CG2982	8		
CG12018	8	ScpX	8	Fib	8	Tip60	8		
CG13933	8	Hmgs	8	Prosalpha4	8	CG10802	8		
CG13926	8	RpS15Aa	8	flil	8	CG3939	8		
dmGlut	8	bgm	8	ltd	8	ttm50	8		

Table 3.1 The list of genes belong to 8 groups.

4. Conclusion

Adding extra nucleotides which were not encoded in the genome gives cells a chance to control the fate of transcripts. It has been shown that one uridine addition to pre-miRNA is capable of modulating its processing (Heo et al., 2012). In this study, I investigated two types of nontemplated nucleotide addition, uridylation and adenylation in human cells and *Drosophila*, respectively. With the techniques based on high-throughput sequencing, I sought to examine how widespread the modifications take place, which enzyme catalyzes them, and what the functional consequences are.

In this thesis work, I found that TUT4 and TUT7 redundantly uridylate deadenylated mRNAs, and that the uridylated mRNAs are targeted by multiple decay factors for rapid degradation. Because U-tail may serve as a general decay signal, it would be important to uridylate only authentic targets which must be eliminated. I suggest the molecular mechanism how U-tails are strictly found on short poly(A) tails (<~25 nt); first, two enzymes have an intrinsic property to act preferentially on short poly(A) tails and second, PABP cooperatively inhibits uridylation of long poly(A) tails (>25 nt) as a fail safe mechanism. By doing so, uridylation leads deadenylated mRNAs to decay pathways as a fast track. I expect that the current model of uridylation-dependent decay that I propose here would be applied to biological contexts where rapid clearance of mRNA is required.

Next, I improved TAIL-seq to increase sensitivity for poly(A)$^+$ mRNAs in order to apply to minute amounts of samples (<5 ug). Using highly sensitive mTAIL-seq, I discovered that cytoplasmic polyadenylation mainly occurs in late oogenesis of *Drosophila* and is largely carried out by Wispy, a noncanonical PAP. Furthermore, I addressed the biological impact of cytoplasmic polyadenylation during *Drosophila* late oogenesis and egg activation. I was able to profile and define a group of genes that gets polyadenylated, which contributes to translational activation depending on the length of poly(A) tail. In the future, it will be interesting to find the mechanism how specific transcripts are subject to cytoplasmic polyadenylation and translation.

In conclusion, I developed TAIL-seq and mTAIL-seq based on high-throughput sequencing and unveiled the characteristics of two distinct post-transcriptional modifications. Deep sequencing allowed me to investigate mRNA tails at transcriptome-scale with high-resolution, which was infeasible with traditional biochemical methods. I expect that the observations made in this study will expand into the research on other types of RNA tailing, which would ultimately inform us a better understanding of post-transcriptional modifications.

국문초록

진핵생물의 전령RNA 꼬리에 관한 전사체 수준의 연구

진핵생물의 전령RNA는 안정성과 번역 능력에 중대한 영향을 미치는 수 많은 전사 후 변형 과정을 겪는다. 새로 합성된 전령RNA는 5′ 말단에 7-메틸구아닌 모자와 3′ 말단에 긴 아데닌 꼬리를 얻는다. 그런 정규적인 변형 이외에도, 최근 연구들은 유리딘화, 구아닌화 같은 비주형 핵산 추가, N6-메틸아데노신, 슈도유리딘화와 같은 리보핵산의 염기 변형, 아데닌-이노신 교정 등 다양한 종류의 변형을 전령RNA의 전사체후 표식으로 밝혀내었다.

RNA 꼬리를 유전체 전체 수준에서 연구하기 위해, 나는 긴 아데닌 꼬리 길이와 3′ 말단 변형을 정밀하게 측정하는 꼬리서열 분석법(TAIL-seq)을 개발하였다. 신기하게도, 나는 포유동물 세포의 긴 아데닌 꼬리 길이가 평균적으로 50–100 nt 이며, 그 끝에 광범위한 유리딘화와 구아닌화가 일어난다는 것을 발견했다. 그리고 유리딘 꼬리는 주로 짧은 아데닌 꼬리(<~25 nt)에 존재한 것으로 보아 전령RNA의 분해에 관여할 것으로 생각되었다.

유리딘화는 다양한 종의 전령RNA에서 발견되어 왔는데, 그 기작과 중요성은 아직 알려지지 않았다. 나는 최근 개발한 꼬리서열분석법을 적용해서 TUT4와 TUT7(TUT4/7, 또는 ZCCHC11/6)효소가 포유류의 전령RNA 유리딘화를 담당한다는 것을 알아내었다. 유리딘화는 짧은 아데닌 꼬리를 가지는 전령RNA에 일어나는데, 시험관에서 정제된 TUT4/7도 선택적으로 짧은 아데닌 꼬리를 인지하고 유리딘 꼬리를 붙이는 것이 관찰되었다. 게다가, PABPC1은 긴 아데닌 꼬리를 가지는 전령RNA의 유리딘화를 억제해서 짧은 아데닌 꼬리에만 유리딘화가 일어나도록 도와주었다. 이 두 개의 효소를 실험적으로 제거한 세포에서는 전령RNA의 유리딘 꼬리가 사라지면서 분해가 느려지는 것이 확인되었고, 전령RNA의 분해를 담당하는 단백질을 억제하면 유리딘 꼬리가 축척되었다. 이와 일치하게, 마이크로RNA는 그 표적의 유리딘화를 촉진하며, 표적의 효과적인 분해를 위해 TUT4/7이 필요하다는 것을 발견되었다. 나는 이번 연구를 통해 짧은 아데닌 꼬리에 선택적인 유리딘화가 일어나는 기작을 밝히고, 전령RNA분해의 일반적인

표지로서 유리딘화의 중요성을 제시한다.

두 번째로, 나는 이전 버전보다 전령RNA를 약 1,000배 효율적으로 서열분석할 수 있는 새로운 버전의 꼬리서열분석법 (전령RNA 꼬리서열분석법 또는 m꼬리서열분석법)을 보고한다. 기존 꼬리서열분석법은 다양한 종류의 3′ 말단 정보를 줄 수 있지만, 전령RNA에 대한 민감도는 떨어져서 적은 양의 생물학적 시료에는 적용하기 어려웠다. 나는 개선된 방법으로 초파리 난자와 배아에서 긴 아데닌 꼬리가 조절되는 현상을 최초로 연구했다. 나는 모체로부터 전달된 전령RNA의 아데닌화가 대부분 수정 전, 후기 난자발생과정 중에 일어나며, 난자 활성화 이후 더 조절되는 것을 발견했다. 또한 이 과정에서 Wispy 효소가 리보좀 단백질을 만드는 RNA를 제외한 대부분의 전령RNA를 아데닐화 시킨다는 것을 알아내었다. 나는 이번 데이터를 리보좀 프로필 분석 자료와 비교해서 난자 활성화 과정중에 아데닌 꼬리의 길이와 번역 효율 사이에 강한 상관관계가 생긴다는 것을 발견하였다. 이번 연구는 난자에서 일어나는 긴 아데닌 꼬리 조절이 이후 배아의 번역 환경을 형성하는데 중요하며, 동물 발생의 시작을 결정한다는 점을 제시한다. 높은 민감도, 적은 비용, 기술적 견고함, 넓은 적용성 등의 장점으로, m꼬리서열분석법은 앞으로 전령RNA 꼬리를 연구하는데 유용한 도구가 될 것으로 기대한다.

종합적으로, 나는 이번 연구에서 내가 개발한 서열분석 방법인 꼬리서열분석법과 m꼬리서열분석법을 이용해, 진핵 생물의 전령RNA 꼬리를 연구하였고, 그것이 전령RNA 안정성과 번역에 미치는 역할을 보고하였다.

Bibliography

Ameres, S. L. & Zamore, P. D. (2013). Diversifying microrna sequence and function. *Nat Rev Mol Cell Biol*, 14(8), 475–88.

Anders, S., Pyl, P. T., & Huber, W. (2015). Htseq–a python framework to work with high-throughput sequencing data. *Bioinformatics*, 31(2), 166–9.

Aravind, L. & Koonin, E. V. (1999). Dna polymerase beta-like nucleotidyltransferase superfamily: identification of three new families, classification and evolutionary history. *Nucleic Acids Res*, 27(7), 1609–18.

Baer, B. W. & Kornberg, R. D. (1983). The protein responsible for the repeating structure of cytoplasmic poly(a)-ribonucleoprotein. *J Cell Biol*, 96(3), 717–21.

Barckmann, B. & Simonelig, M. (2013). Control of maternal mrna stability in germ cells and early embryos. *Biochim Biophys Acta*, 1829(6-7), 714–24.

Bastock, R. & St Johnston, D. (2008). Drosophila oogenesis. *Curr Biol*, 18(23), R1082–7.

Belasco, J. G. (2010). All things must pass: contrasts and commonalities in eukaryotic and bacterial mrna decay. *Nat Rev Mol Cell Biol*, 11(7), 467–78.

Benoit, B., Mitou, G., Chartier, A., Temme, C., Zaessinger, S., Wahle, E., Busseau, I., & Simonelig, M. (2005). An essential cytoplasmic function for the nuclear poly(a) binding protein, pabp2, in poly(a) tail length control and early development in drosophila. *Dev Cell*, 9(4), 511–22.

Benoit, P., Papin, C., Kwak, J. E., Wickens, M., & Simonelig, M. (2008). Pap- and gld-2-type poly(a) polymerases are required sequentially in cytoplasmic polyadenylation and oogenesis in drosophila. *Development*, 135(11), 1969–79.

Boswell, R. E. & Mahowald, A. P. (1985). tudor, a gene required for assembly of the germ plasm in drosophila melanogaster. *Cell*, 43(1), 97–104.

Bragg, L. M., Stone, G., Butler, M. K., Hugenholtz, P., & Tyson, G. W. (2013). Shining a light on dark sequencing: characterising errors in ion torrent pgm data. *PLoS Comput Biol*, 9(4), e1003031.

Castagnetti, S. & Ephrussi, A. (2003). Orb and a long poly(a) tail are required for efficient oskar translation at the posterior pole of the drosophila oocyte. *Development*, 130(5), 835–43.

Chang, C. T., Bercovich, N., Loh, B., Jonas, S., & Izaurralde, E. (2014a). The activation of the decapping enzyme dcp2 by dcp1 occurs on the edc4 scaffold and involves a conserved loop in dcp1. *Nucleic Acids Res*, 42(8), 5217–5233.

Chang, H., Lim, J., Ha, M., & Kim, V. N. (2014b). Tail-seq: Genome-wide determination of poly(a) tail length and 3' end modifications. *Mol Cell*, 53(6), 1044–52.

Chang, H. M., Triboulet, R., Thornton, J. E., & Gregory, R. I. (2013). A role for the perlman syndrome exonuclease dis3l2 in the lin28-let-7 pathway. *Nature*, 497(7448), 244–8.

Chowdhury, A., Mukhopadhyay, J., & Tharun, S. (2007). The decapping activator lsm1p-7p-pat1p complex has the intrinsic ability to distinguish between oligoadenylated and polyadenylated rnas. *RNA*, 13(7), 998–1016.

Coll, O., Villalba, A., Bussotti, G., Notredame, C., & Gebauer, F. (2010). A novel, noncanonical mechanism of cytoplasmic polyadenylation operates in drosophila embryogenesis. *Genes Dev*, 24(2), 129–34.

Cui, J., Sackton, K. L., Horner, V. L., Kumar, K. E., & Wolfner, M. F. (2008). Wispy, the drosophila homolog of gld-2, is required during oogenesis and egg activation. *Genetics*, 178(4), 2017–29.

Cui, J., Sartain, C. V., Pleiss, J. A., & Wolfner, M. F. (2013). Cytoplasmic polyadenylation is a major mrna regulator during oogenesis and egg activation in drosophila. *Dev Biol*, 383(1), 121–31.

D'Ambrogio, A., Nagaoka, K., & Richter, J. D. (2013). Translational control of cell growth and malignancy by the cpebs. *Nat Rev Cancer*, 13(4), 283–90.

Djuranovic, S., Nahvi, A., & Green, R. (2011). A parsimonious model for gene regulation by mirnas. *Science*, 331(6017), 550–3.

Dobin, A., Davis, C. A., Schlesinger, F., Drenkow, J., Zaleski, C., Jha, S., Batut, P., Chaisson, M., & Gingeras, T. R. (2013). Star: ultrafast universal rna-seq aligner. *Bioinformatics*, 29(1), 15–21.

Dreyfus, M. & Regnier, P. (2002). The poly(a) tail of mrnas: bodyguard in eukaryotes, scavenger in bacteria. *Cell*, 111(5), 611–3.

Du, L. & Richter, J. D. (2005). Activity-dependent polyadenylation in neurons. *RNA*, 11(9), 1340–7.

Eliseeva, I. A., Lyabin, D. N., & Ovchinnikov, L. P. (2013). Poly(a)-binding proteins: structure, domain organization, and activity regulation. *Biochemistry (Mosc)*, 78(13), 1377–91.

Faehnle, C. R., Walleshauser, J., & Joshua-Tor, L. (2014). Mechanism of dis3l2 substrate recognition in the lin28-let-7 pathway. *Nature*.

Garneau, N. L., Wilusz, J., & Wilusz, C. J. (2007). The highways and byways of mrna decay. *Nat Rev Mol Cell Biol*, 8(2), 113–26.

Guo, H., Ingolia, N. T., Weissman, J. S., & Bartel, D. P. (2010). Mammalian microrna predominantly act to decrease target mrna levels. *Nature*, 466(7308), 835–40.

He, L., Wang, X. B., & Montell, D. J. (2011). Shining light on drosophila oogenesis: live imaging of egg development. *Current Opinion in Genetics & Development*, 21(5), 612–619.

Heifetz, Y., Tram, U., & Wolfner, M. F. (2001). Male contributions to egg production: the role of accessory gland products and sperm in drosophila melanogaster. *Proceedings of the Royal Society B-Biological Sciences*, 268(1463), 175–180.

Heo, I., Ha, M., Lim, J., Yoon, M. J., Park, J. E., Kwon, S. C., Chang, H., & Kim, V. N. (2012). Mono-uridylation of pre-microrna as a key step in the biogenesis of group ii let-7 microrna. *Cell*, 151(3), 521–32.

Hoefig, K. P., Rath, N., Heinz, G. A., Wolf, C., Dameris, J., Schepers, A., Kremmer, E., Ansel, K. M., & Heissmeyer, V. (2013). Eri1 degrades the stem-loop of oligouridylated histone mrnas to induce replication-dependent decay. *Nat Struct Mol Biol*, 20(1), 73–81.

Horner, V. L. & Wolfner, M. F. (2008). Transitioning from egg to embryo: Triggers and mechanisms of egg activation. *Developmental Dynamics*, 237(3), 527–544.

Houseley, J., LaCava, J., & Tollervey, D. (2006). Rna-quality control by the exosome. *Nat Rev Mol Cell Biol*, 7(7), 529–39.

Houseley, J. & Tollervey, D. (2009). The many pathways of rna degradation. *Cell*, 136(4), 763–76.

Huang da, W., Sherman, B. T., & Lempicki, R. A. (2009). Systematic and integrative analysis of large gene lists using david bioinformatics resources. *Nat Protoc*, 4(1), 44–57.

Huntzinger, E. & Izaurralde, E. (2011). Gene silencing by micrornas: contributions of translational repression and mrna decay. *Nat Rev Genet*, 12(2), 99–110.

Ingolia, N. T., Ghaemmaghami, S., Newman, J. R., & Weissman, J. S. (2009). Genome-wide analysis in vivo of translation with nucleotide resolution using ribosome profiling. *Science*, 324(5924), 218–23.

Khanam, T., Muddashetty, R. S., Kahvejian, A., Sonenberg, N., & Brosius, J. (2006). Poly(a)-binding protein binds to a-rich sequences via rna-binding domains 1+2 and 3+4. *RNA Biol*, 3(4), 170–7.

Kim, J. H. & Richter, J. D. (2006). Opposing polymerase-deadenylase activities regulate cytoplasmic polyadenylation. *Mol Cell*, 24(2), 173–83.

Kim-Ha, J., Kerr, K., & Macdonald, P. M. (1995). Translational regulation of oskar mrna by bruno, an ovarian rna-binding protein, is essential. *Cell*, 81(3), 403–12.

Krauchunas, A. R., Horner, V. L., & Wolfner, M. F. (2012). Protein phosphorylation changes reveal new candidates in the regulation of egg activation and early embryogenesis in d. melanogaster. *Dev Biol*, 370(1), 125–34.

Krol, J., Loedige, I., & Filipowicz, W. (2010). The widespread regulation of microrna biogenesis, function and decay. *Nat Rev Genet*, 11(9), 597–610.

Kronja, I., Yuan, B., Eichhorn, S. W., Dzeyk, K., Krijgsveld, J., Bartel, D. P., & Orr-Weaver, T. L. (2014). Widespread changes in the posttranscriptional landscape at the drosophila oocyte-to-embryo transition. *Cell Rep*, 7(5), 1495–508.

Kuhn, U. & Pieler, T. (1996). Xenopus poly(a) binding protein: functional domains in rna binding and protein-protein interaction. *J Mol Biol*, 256(1), 20–30.

Kwak, J. E., Wang, L., Ballantyne, S., Kimble, J., & Wickens, M. (2004). Mammalian gld-2 homologs are poly(a) polymerases. *Proc Natl Acad Sci U S A*, 101(13), 4407–12.

Lapointe, C. P. & Wickens, M. (2013). The nucleic acid-binding domain and translational repression activity of a xenopus terminal uridylyl transferase. *J Biol Chem*, 288(28), 20723–33.

Laver, J. D., Marsolais, A. J., Smibert, C. A., & Lipshitz, H. D. (2015). Regulation and function of maternal gene products during the maternal-to-zygotic transition in drosophila. *Curr Top Dev Biol*, 113, 43–84.

Ledergerber, C. & Dessimoz, C. (2011). Base-calling for next-generation sequencing platforms. *Brief Bioinform*, 12(5), 489–97.

Lee, M., Choi, Y., Kim, K., Jin, H., Lim, J., Nguyen, T. A., Yang, J., Jeong, M., Giraldez, A. J., Yang, H., Patel, D. J., & Kim, V. N. (2014a). Adenylation of maternally inherited micrornas by wispy. *Mol Cell*, 56(5), 696–707.

Lee, M., Kim, B., & Kim, V. N. (2014b). Emerging roles of rna modification: ma and u-tail. *Cell*, 158(5), 980–987.

Li, B. & Dewey, C. N. (2011). Rsem: accurate transcript quantification from rna-seq data with or without a reference genome. *BMC Bioinformatics*, 12, 323.

Lim, J., Ha, M., Chang, H., Kwon, S. C., Simanshu, D. K., Patel, D. J., & Kim, V. N. (2014). Uridylation by tut4 and tut7 marks mrna for degradation. *Cell*, 159(6), 1365–76.

Liu, X., Zheng, Q., Vrettos, N., Maragkakis, M., Alexiou, P., Gregory, B. D., & Mourelatos, Z. (2014). A microrna precursor surveillance system in quality control of microrna synthesis. *Mol Cell*, 55(6), 868–79.

Lubas, M., Damgaard, C. K., Tomecki, R., Cysewski, D., Jensen, T. H., & Dziembowski, A. (2013). Exonuclease hdis3l2 specifies an exosome-independent 3'-5' degradation pathway of human cytoplasmic mrna. *EMBO J*, 32(13), 1855–68.

Malecki, M., Viegas, S. C., Carneiro, T., Golik, P., Dressaire, C., Ferreira, M. G., & Arraiano, C. M. (2013). The exoribonuclease dis3l2 defines a novel eukaryotic rna degradation pathway. *EMBO J*, 32(13), 1842–54.

Marnef, A. & Standart, N. (2010). Pat1 proteins: a life in translation, translation repression and mrna decay. *Biochem Soc Trans*, 38(6), 1602–7.

Martin, G. & Keller, W. (2007). Rna-specific ribonucleotidyl transferases. *RNA*, 13(11), 1834–49.

Meijer, H. A., Bushell, M., Hill, K., Gant, T. W., Willis, A. E., Jones, P., & de Moor, C. H. (2007). A novel method for poly(a) fractionation reveals a large population of mrnas with a short poly(a) tail in mammalian cells. *Nucleic Acids Res*, 35(19), e132.

Mendez, R. & Richter, J. D. (2001). Translational control by cpeb: a means to the end. *Nat Rev Mol Cell Biol*, 2(7), 521–9.

Morozov, I. Y., Jones, M. G., Gould, P. D., Crome, V., Wilson, J. B., Hall, A. J., Rigden, D. J., & Caddick, M. X. (2012). mrna 3' tagging is induced by nonsense-mediated decay and promotes ribosome dissociation. *Mol Cell Biol*, 32(13), 2585–95.

Morozov, I. Y., Jones, M. G., Razak, A. A., Rigden, D. J., & Caddick, M. X. (2010). Cucu modification of mrna promotes decapping and transcript degradation in aspergillus nidulans. *Mol Cell Biol*, 30(2), 460–9.

Mullen, T. E. & Marzluff, W. F. (2008). Degradation of histone mrna requires oligouridylation followed by decapping and simultaneous degradation of the mrna both 5' to 3' and 3' to 5'. *Genes Dev*, 22(1), 50–65.

Norbury, C. J. (2013). Cytoplasmic rna: a case of the tail wagging the dog. *Nat Rev Mol Cell Biol*, 14(10), 643–53.

Novoa, I., Gallego, J., Ferreira, P. G., & Mendez, R. (2010). Mitotic cell-cycle progression is regulated by cpeb1 and cpeb4-dependent translational control. *Nat Cell Biol*, 12(5), 447–56.

Parker, R. & Song, H. (2004). The enzymes and control of eukaryotic mrna turnover. *Nat Struct Mol Biol*, 11(2), 121–7.

Pillai, R. S., Artus, C. G., & Filipowicz, W. (2004). Tethering of human ago proteins to mrna mimics the mirna-mediated repression of protein synthesis. *RNA*, 10(10), 1518–25.

Pique, M., Lopez, J. M., Foissac, S., Guigo, R., & Mendez, R. (2008). A combinatorial code for cpe-mediated translational control. *Cell*, 132(3), 434–48.

Quinlan, A. R. & Hall, I. M. (2010). Bedtools: a flexible suite of utilities for comparing genomic features. *Bioinformatics*, 26(6), 841–2.

Ren, G., Xie, M., Zhang, S., Vinovskis, C., Chen, X., & Yu, B. (2014). Methylation protects microrna from an ago1-associated activity that uridylates 5' rna fragments generated by ago1 cleavage. *Proc Natl Acad Sci U S A*, 111(17), 6365–70.

Resnick, T. D., Dej, K. J., Xiang, Y., Hawley, R. S., Ahn, C., & Orr-Weaver, T. L. (2009). Mutations in the chromosomal passenger complex and the condensin complex differentially affect synaptonemal complex disassembly and metaphase i configuration in drosophila female meiosis. *Genetics*, 181(3), 875–87.

Richter, J. D. (2007). Cpeb: a life in translation. *Trends Biochem Sci*, 32(6), 279–85.

Rissland, O. S., Mikulasova, A., & Norbury, C. J. (2007). Efficient rna polyuridylation by noncanonical poly(a) polymerases. *Mol Cell Biol*, 27(10), 3612–24.

Rissland, O. S. & Norbury, C. J. (2009). Decapping is preceded by 3' uridylation in a novel pathway of bulk mrna turnover. *Nat Struct Mol Biol*, 16(6), 616–23.

Risso, D., Ngai, J., Speed, T. P., & Dudoit, S. (2014). Normalization of rna-seq data using factor analysis of control genes or samples. *Nat Biotechnol*, 32(9), 896–902.

Robinson, M. D. & Oshlack, A. (2010). A scaling normalization method for differential expression analysis of rna-seq data. *Genome Biol*, 11(3), R25.

Sachs, A. B., Davis, R. W., & Kornberg, R. D. (1987). A single domain of yeast poly(a)-binding protein is necessary and sufficient for rna binding and cell viability. *Mol Cell Biol*, 7(9), 3268–76.

Salles, F. J., Lieberfarb, M. E., Wreden, C., Gergen, J. P., & Strickland, S. (1994). Coordinate initiation of drosophila development by regulated polyadenylation of maternal messenger rnas. *Science*, 266(5193), 1996–9.

Salles, F. J., Richards, W. G., & Strickland, S. (1999). Assaying the polyadenylation state of mrnas. *Methods*, 17(1), 38–45.

Schmidt, M. J., West, S., & Norbury, C. J. (2011). The human cytoplasmic rna terminal u-transferase zcchc11 targets histone mrnas for degradation. *RNA*, 17(1), 39–44.

Schoenberg, D. R. & Maquat, L. E. (2012). Regulation of cytoplasmic mrna decay. *Nat Rev Genet*, 13(4), 246–59.

Sement, F. M., Ferrier, E., Zuber, H., Merret, R., Alioua, M., Deragon, J. M., Bousquet-Antonelli, C., Lange, H., & Gagliardi, D. (2013). Uridylation prevents 3' trimming of oligoadenylated mrnas. *Nucleic Acids Res*, 41(14), 7115–27.

Sharif, H. & Conti, E. (2013). Architecture of the lsm1-7-pat1 complex: a conserved assembly in eukaryotic mrna turnover. *Cell Rep*, 5(2), 283–91.

Shen, B. & Goodman, H. M. (2004). Uridine addition after microrna-directed cleavage. *Science*, 306(5698), 997.

Slevin, M. K., Meaux, S., Welch, J. D., Bigler, R., Miliani de Marval, P. L., Su, W., Rhoads, R. E., Prins, J. F., & Marzluff, W. F. (2014). Deep sequencing shows multiple oligouridylations are required for 3' to 5' degradation of histone mrnas on polyribosomes. *Mol Cell*, 53(6), 1020–30.

Song, M. G. & Kiledjian, M. (2007). 3' terminal oligo u-tract-mediated stimulation of decapping. *RNA*, 13(12), 2356–65.

Su, W., Slepenkov, S. V., Slevin, M. K., Lyons, S. M., Ziemniak, M., Kowalska, J., Darzynkiewicz, E., Jemielity, J., Marzluff, W. F., & Rhoads, R. E. (2013). mrnas containing the histone 3' stem-loop are degraded primarily by decapping mediated by oligouridylation of the 3' end. *RNA*, 19(1), 1–16.

Subtelny, A. O., Eichhorn, S. W., Chen, G. R., Sive, H., & Bartel, D. P. (2014). Poly(a)-tail profiling reveals an embryonic switch in translational control. *Nature*, 508(7494), 66–71.

Tadros, W., Goldman, A. L., Babak, T., Menzies, F., Vardy, L., Orr-Weaver, T., Hughes, T. R., Westwood, J. T., Smibert, C. A., & Lipshitz, H. D. (2007). Smaug is a major regulator of maternal mrna destabilization in drosophila and its translation is activated by the pan gu kinase. *Dev Cell*, 12(1), 143–55.

Tadros, W. & Lipshitz, H. D. (2009). The maternal-to-zygotic transition: a play in two acts. *Development*, 136(18), 3033–42.

Thornton, J. E., Chang, H. M., Piskounova, E., & Gregory, R. I. (2012). Lin28-mediated control of let-7 microrna expression by alternative tutases zcchc11 (tut4) and zcchc6 (tut7). *RNA*, 18(10), 1875–85.

Udagawa, T., Swanger, S. A., Takeuchi, K., Kim, J. H., Nalavadi, V., Shin, J., Lorenz, L. J., Zukin, R. S., Bassell, G. J., & Richter, J. D. (2012). Bidirectional control of mrna translation and synaptic plasticity by the cytoplasmic polyadenylation complex. *Mol Cell*, 47(2), 253–66.

Ustianenko, D., Hrossova, D., Potesil, D., Chalupnikova, K., Hrazdilova, K., Pachernik, J., Cetkovska, K., Uldrijan, S., Zdrahal, Z., & Vanacova, S. (2013). Mammalian dis3l2 exoribonuclease targets the uridylated precursors of let-7 mirnas. *RNA*, 19(12), 1632–8.

Vardy, L. & Orr-Weaver, T. L. (2007). The drosophila png kinase complex regulates the translation of cyclin b. *Dev Cell*, 12(1), 157–66.

Vardy, L., Pesin, J. A., & Orr-Weaver, T. L. (2009). Regulation of cyclin a protein in meiosis and early embryogenesis. *Proc Natl Acad Sci U S A*, 106(6), 1838–43.

Von Stetina, J. R. & Orr-Weaver, T. L. (2011). Developmental control of oocyte maturation and egg activation in metazoan models. *Cold Spring Harb Perspect Biol*, 3(10), a005553.

Wahle, E. & Keller, W. (1996). The biochemistry of polyadenylation. *Trends Biochem Sci*, 21(7), 247–50.

Weil, T. T., Parton, R. M., Herpers, B., Soetaert, J., Veenendaal, T., Xanthakis, D., Dobbie, I. M., Halstead, J. M., Hayashi, R., Rabouille, C., & Davis, I. (2012). Drosophila patterning is established by differential association of mrnas with p bodies. *Nat Cell Biol*, 14(12), 1305–13.

Weill, L., Belloc, E., Bava, F. A., & Mendez, R. (2012). Translational control by changes in poly(a) tail length: recycling mrnas. *Nat Struct Mol Biol*, 19(6), 577–85.

Wilusz, C. J. & Wilusz, J. (2013). Lsm proteins and hfq: Life at the 3' end. *RNA Biol*, 10(4), 592–601.

Wu, T. D. & Nacu, S. (2010). Fast and snp-tolerant detection of complex variants and splicing in short reads. *Bioinformatics*, 26(7), 873–81.

Yoshida, S., Muller, H. A., Wodarz, A., & Ephrussi, A. (2004). Pka-r1 spatially restricts oskar expression for drosophila embryonic patterning. *Development*, 131(6), 1401–10.

Zheng, D. & Tian, B. (2014). Sizing up the poly(a) tail: insights from deep sequencing. *Trends Biochem Sci*, 39(6), 255–7.

Zhou, L., Zhou, Y., Hang, J., Wan, R., Lu, G., Yan, C., & Shi, Y. (2014). Crystal structure and biochemical analysis of the heptameric lsm1-7 complex. *Cell Res*, 24(4), 497–500.